The University of Manchester

DECARBONISED POLYGENERATION FROM FOSSIL AND BIOMASS RESOURCES

A thesis submitted to The University of Manchester for the degree of
Doctor of Philosophy
in the Faculty of Engineering and Physical Sciences

2011

KOK SIEW NG

Centre for Process Integration
School of Chemical Engineering and Analytical Science

Table of Contents

Abstract **5**

Declaration **6**

Copyright Statement **8**

Acknowledgements **9**

Rationale for Submitting the Thesis in an Alternative Format **12**

List of Published Research Papers **13**

List of Submitted Research Papers **13**

Chapter 1 Introduction **14**

1.1 Background and Motivation 14

1.2 Contribution of Research 21

Chapter 2 Discussion of the Nature of Bio-oil based Biorefinery Concept **24**

2.1 PUBLICATION 1: Ng, K.S., Sadhukhan, J., Techno-economic performance analysis of bio-oil based Fischer-Tropsch and CHP synthesis platform. *Biomass & Bioenergy*. **35** (7): 3218-3234 (2011) 24

2.2 PUBLICATION 2: Ng, K.S., Sadhukhan, J., Process integration and economic analysis of bio-oil platform for the production of methanol and combined heat and power. *Biomass & Bioenergy*. **35** (3): 1153-1169 (2011). 25

Chapter 3 Discussion of the Nature of Decarbonised Coal Polygeneration Systems **27**

3.1 PUBLICATION 3: Ng, K.S., Zhang, N., Sadhukhan, J., CO_2 abatement strategies for polygeneration systems: Process integration and analysis. *Chemical Engineering Research and Design.* Submitted (2011). 27

3.2 PUBLICATION 4: Ng, K.S., Zhang, N., Sadhukhan, J., A graphical CO_2 emission treatment intensity assessment for energetic and economic analyses of integrated decarbonised energy systems. *Computers & Chemical Engineering.* Submitted (2011). 28

Chapter 4 Conclusions and Future Work.....30

4.1 Conclusions.....30

4.2 Future Work.....35

References.....36

The Published Research Paper…….38

The Submitted Research Paper……41

Appendix 1……..44

List of Figures

Figure 1.1: Timeline for transition of primary resources to biomass resources.....17

Figure 1.2: Distributed processing of biomass into bio-oil and centralised processing of bio-oil into fuels and power. 19

Figure 1.3: Distributed pyrolysis plant. 19

Figure 1.4: Polygeneration concept using gasification as the processing route.....20

List of Tables

Table 4.1: Performances of bio-oil integrated gasification systems for the production of FT liquid / methanol and electricity. 31

Table 4.2: Performance analyses of various decarbonised coal cogeneration and polygeneration systems. 33

Abstract

Utilisation of biomass resources and CO_2 abatement systems in currently exploited fossil resource based energy systems are the key strategies in resolving energy sustainability issue and combating against global climate change. These strategies are affected by high energy penalty and high investment. Therefore, it is imperative to assess the viability of these energy systems and further identify niche problem areas associated with energy efficiency and economic performance improvement.

The current research work has two parts. The first part presents techno-economic investigation of thermochemical conversion of biomass into the production of fuels (Fischer-Tropsch liquid or methanol) and electricity. The work encompasses centralised bio-oil integrated gasification plant, assuming that the bio-oil is supplied from distributed pyrolysis plant. Bio-oil is a high energy density liquid derived from biomass fast pyrolysis process, providing advantages in transport and storage. Various bio-oil based integrated gasification system configurations were studied. The configurations were varied based on oxygen supply units, once-through and full conversion configurations and a range of capacities from small to large scale. The second part of this thesis considers integration of various CO_2 abatement strategies in coal integrated gasification systems. The CO_2 abatement strategies under consideration include CO_2 capture and storage, CO_2 capture and reuse as well as CO_2 reuse from flue gas. These facilities are integrated into cogeneration or polygeneration systems. The cogeneration concept refers to the production of combined heat and power while polygeneration concept is an integrated system converting one or more feedstocks into three or more products. Polygeneration is advocated in this work attributed to its high efficiency and lower emission. Furthermore, it can generate a balanced set of products consisting of fuels, electricity and chemicals. It is regarded as a promising way of addressing the future rapidly growing energy demands.

A holistic approach using systematic analytical frameworks comprising simulation modelling, process integration and economic analysis has been developed and adopted consistently throughout the study for the techno-economic performance evaluation of decarbonised fossil and bio-oil based systems. Important design methodology, sensitivity analysis of process parameters and process system modifications are proposed. These are to enhance the efficiency as well as lower the economic and environmental impacts of polygeneration systems. A shortcut methodology has also been developed as a decision-making tool for effective selection from a portfolio of CO_2 abatement options and integrated systems. Critical and comprehensive analyses of all the systems under considerations are presented. These embrace the impact of carbon tax, product price evaluation and recommendations for sustainability of low carbon energy systems.

University of Manchester

PhD by Published Work Candidate Declaration

Candidate Name: **Kok Siew Ng**

Faculty: **Engineering and Physical Sciences**

Thesis Title: **Decarbonised Polygeneration from Fossil and Biomass Resources**

Declaration

I declare that no portion of the work referred to in the thesis has been submitted in support of an application for another degree or qualification of this or any other university or other institute of learning.

The thesis contains original papers published in peer-reviewed journals [Publication 1 and 2] and unpublished / submitted papers [Publication 3 and 4]. I confirm that the materials covered in Publication 1 to 4 in the thesis, including simulation models, data, calculation and analyses are the results of my own original contribution. These studies were carried out under the supervision of the co-authors of the research papers, Dr. Jhuma Sadhukhan (principal supervisor) and Dr. Nan Zhang (co-supervisor). The contribution of the co-authors was through the provision of technical guidance and language corrections. I certify that I have obtained permission from the co-authors for incorporating the published materials in my thesis.

I declare that, to the best of my knowledge, my thesis does not infringe upon anyone's copyright nor violate any proprietary rights and that any ideas, techniques, quotations, or any other material from the work of other people included in my thesis, published or otherwise, are fully acknowledged in accordance with the standard referencing practices.

All the work presented in this thesis has been completed whilst a registered student at The University of Manchester.

I confirm that this is a true statement and that, subject to any comments above, the submission is my own original work.

Kok Siew Ng

Copyright Statement

(i) The author of this thesis (including any appendices and/or schedules to this thesis) owns certain copyright or related rights in it (the "Copyright") and s/he has given The University of Manchester certain rights to use such Copyright, including for administrative purposes.

(ii) Copies of this thesis, either in full or in extracts and whether in hard or electronic copy, may be made only in accordance with the Copyright, Designs and Patents Act 1988 (as amended) and regulations issued under it or, where appropriate, in accordance with licensing agreements which the University has from time to time. This page must form part of any such copies made.

(iii) The ownership of certain Copyright, patents, designs, trademarks and other intellectual property (the "Intellectual Property") and any reproductions of copyright works in the thesis, for example graphs and tables ("Reproductions"), which may be described in this thesis, may not be owned by the author and may be owned by third parties. Such Intellectual Property and Reproductions cannot and must not be made available for use without the prior written permission of the owner(s) of the relevant Intellectual Property and/or Reproductions.

(iv) Further information on the conditions under which disclosure, publication and exploitation of this thesis, the Copyright and any Intellectual Property Rights and/or Reproductions described in it may take place is available from the Head of School of Chemical Engineering & Analytical Science.

Acknowledgements

Stepping into the 20th year of my student life, it is inevitable that my emotion is deeply stirred especially when it is approaching the end of my student days and soon I am about to enter a new stage of life. As part of the learning process, there were, of course, ups and down during the three years of my PhD education − a period that is a mix bag of confusion, struggle yet in a challenging and rewarding way. It is an unforgettable journey in my life. I feel that I am a lucky person to have so many wonderful people around me, giving me an abundance of inspiration, courage, support and enlightenment that I always need. It would not have been possible to complete this thesis without the contribution from these people. Seizing this opportunity while my memory is still fresh, I must acknowledge these people with my greatest sincerity.

First and foremost, I would like to express my deepest gratitude to my supervisor, Dr. Jhuma Sadhukhan. Jhuma's professional acquaintance with me started since my undergraduate days. She was my personal tutor, course tutor as well as supervisor for my MEng research. It is not an overstatement to say that my interest and enthusiasm in research was evoked by Jhuma. She brought me into the world of research leading me all the way through my PhD studies. It is my honour to work with her as she has given me a wealth of encouragement, motivation, guidance, freedom and a comfortable environment to develop my own ideas. I pay my highest respect to Jhuma for being a very kind, helpful, patient, thoughtful, friendly, caring and supportive teacher. I would like to convey my strongest appreciation to Jhuma for all the efforts she has put on me throughout these seven years in this university. I also faithfully acknowledge Dr. Nan Zhang, who serves as my co-supervisor for my PhD. He had

provided me with lots of valuable advices and useful guidance while Jhuma was taking her sabbatical leave.

For financial support I would like to thank the following bodies: Overseas Research Scholarship (ORS), The University of Manchester Alumni Fund, Process Integration Research Consortium (PIRC) and School of Chemical Engineering and Analytical Science.

I am indebted to Dr. Grant Campbell for his insights on research originality and professional academic research writing. I also wish to express my appreciation to Prof. Robin Smith, Dr. Megan Jobson and Mr. Simon Perry for their warm concerns and kind helps during my studies in the Centre for Process Integration.

My heartfelt thanks to my awesome colleagues for creating a fun and exciting work environment over these few years: Nan Jia and his wife Liz, Li, Xuesong, Sonia, Yadira, Zixin, Yongwen, Lu, Yufei, Michael, Elias, Thomas Davison, Anestis and Yuhang and other fellow colleagues in the Centre for Process Integration.

A balanced social-learning life is always the key to achieving success. There are countless special moments with my best friends, and those precious memories cannot be easily erased. It is my pleasure to thank my best friends Way Sheong, Thomas Lau, Enn Swan, Yet Th'ng, Andy, Wei Ning, Tzyy Shyang, Yi Pei, Danny, Tom, Pasika, Siang Sen, Fion, Seong Keat, Seong Chuin, Yi Hao and Tze Howe.

Last but not least, I owe my greatest gratitude to my father Kweng Chuan Ng and my mother Eng Tho Woo for their love, support, care and understanding. I am grateful to my sister Chui Mei Ng for being a patient listener when I was in low spirits. I

also thank her for being a good companion when I attended an international conference in Italy. Special thanks to my cousins Chui Lim, Kok Chuan and Alice for their warm and generous hospitality during my holiday stay in Hong Kong and Penang.

Kok Siew Ng

Rationale for Submitting the Thesis in an Alternative Format

The thesis is given in an alternative format which represents a new option for PhD students in the University of Manchester. This option allows students to present their work in a publishable format which can be accessed easily from scientific databases. The alternative format is expected to be widely accepted and adopted by many students and institutions in the future. Furthermore, the main reason for submitting in this format here is due to the fast-moving nature of the area under investigation, so that the corresponding articles can be published as soon as possible.

This thesis consists of two peer-reviewed archived journal publications and two submitted manuscripts for publication, conforming to the standard of an alternative format thesis at The University of Manchester. This implies that a major portion of the work including the methodology and results presented in this thesis has been validated and recognised through a rigorous peer-review process, further proving the value of the research. Thus, a higher level of confidence on the results has been achieved and the methodology has been consolidated, by high profile publications.

List of Published Research Papers

1. Ng, K.S., Sadhukhan, J., Techno-economic performance analysis of bio-oil based Fischer-Tropsch and CHP synthesis platform. *Biomass & Bioenergy*. **35** (7): 3218-3234 (2011).

2. Ng, K.S., Sadhukhan, J., Process integration and economic analysis of bio-oil platform for the production of methanol and combined heat and power. *Biomass & Bioenergy*. **35** (3): 1153-1169 (2011).

List of Submitted Research Papers

1. Ng, K.S., Zhang, N., Sadhukhan, J., CO_2 abatement strategies for polygeneration systems: Process integration and analysis. *Chemical Engineering Research and Design.* Submitted (2011).

2. Ng, K.S., Zhang, N., Sadhukhan, J., A graphical CO_2 emission treatment intensity assessment for energetic and economic analyses of integrated decarbonised energy systems. *Computers & Chemical Engineering.* Submitted (2011).

Chapter 1 Introduction

1.1 Background and Motivation

The soaring global energy demand has led to severe environmental issue, such as rapid depletion of fossil fuels into substantial CO_2 emission to the atmosphere. Furthermore, energy security issues which attributed to political factors and monopolisation of the petroleum industry by certain countries in the world have resulted in unstable oil prices. Rapidly rising oil prices pose significant impact on the prices of commodity, electricity and transportation fuels, and thus the well-being of every individual in the world today is affected. Driven by these causes, an exigent approach to the evaluation of alternative energy feedstock in terms of energy efficiency enhancement, economics and CO_2 emission mitigation has been called upon. The desirable energy system for the future should fulfil several criteria: high efficiency, high economic potential, low environmental impact, and flexibility in feedstock and product selection through polygeneration.

Utilisation of renewable energy provides a sustainable solution to encounter the exhausting crude oil problems and environmental issues. Wind, solar and hydro are amongst the cleaner energy options, however the employment of these technologies is decided by geological factors and capital cost. Biomass is the only low carbon energy resource containing carbon, providing backbone for large scale production of fuels, chemicals and electricity. Energy transition takes time. It took centuries from wood to coal and decades from coal to oil, natural gas and nuclear (Rhodes, 2007). The substitution of crude oil by biomass is expected to take another few decades. The long

transition period is primarily attributed to the economic competitiveness between biorefinery and the conventional oil refinery, the cost of feedstock and supply chain, the advancement in technology and uncertainties in governmental policies (Smith, 2007). It is thus imperative to investigate the future potential of large scale deployment of biomass infrastructure. During the interim period, a blend of biomass and coal or other fossil fuel as the feedstock will be the possible strategy (ScottishPower, 2008), before bioenergy feedstock can fully replace fossil fuels.

Based on the reserves to production ratio, the proven reserves of coal can last for about 120 years, longer than the proven reserves of oil of approximately 50 years (BP, 2010). Coal is expected to play a major role during this transition period from crude oil to biomass. Coal is versatile and can be used for the production of fuels, chemicals and electricity. The coal based energy system has been a favourable option in faster developing economy such as China and India, due to their abundant indigenous sources. However, coal is not a clean fuel and it releases considerable amount of CO_2, NO_x, SO_x etc. to the atmosphere during the conversion process. Mitigating CO_2 in clean coal utilisation constitutes a major research effort. Carbon capture and storage (CCS) is a state-of-the-art demonstration technology in mitigating CO_2 level in clean coal energy system (ScottishPower, 2008). However, the capturing process results in high penalty in efficiency. A power plant with CCS, for example requires 10-40% more energy than a plant without CCS (IPCC, 2005). This also implies that more energy thus more fuel is needed to compensate for the efficiency loss. CO_2 reuse into chemicals is a viable and an alternative route to CCS, in the interim phase. CO_2 reuse prevents the direct emission from a plant and prolongs the CO_2 lifetime after being converted into other forms of products.

More stringent environmental regulations are being implemented and higher emission reduction target is set from year to year. The UK emission reduction target is 50% by 2025 compared to 1990 level (ITN, 2011). The EU Renewable Energy Directive has imposed a mandate where countries in EU are required to meet a target of 20% share of energy from renewable sources by 2020 (The European Parliament and The Council of the European Union, 2009). It is thus inevitable that the research into carbon reduction and renewable energy will attract resurgence of interest. However, it will be a long-run shifting from fossil energy era into renewable energy era. A timeline for the replacement of fossil fuel energy by biomass is depicted in Figure 1.1 (Rhodes, 2007; Smith, 2007). Current biofuel technologies include biodiesel and bioethanol production from food crops; 2nd generation biofuel comprises of lignocellulosic ethanol and biomass to liquid (BTL) plants which utilise the lignocellulosic crops such as miscanthus, wood etc. rather than food crops as the feedstock; advanced biorefinery can be lignocellulosic, whole crop, green and two-platform biorefineries (Kamm et al., 2006). It is expected that renewable energy would widely and commercially be available in large scale within next few decades. During the interim period, before renewable energy can fully replace fossil energy, carbon reduction strategy is of utmost importance to combat against the global warming. These constitute the overall motivation and the whole rationale for this research, embodied in this thesis.

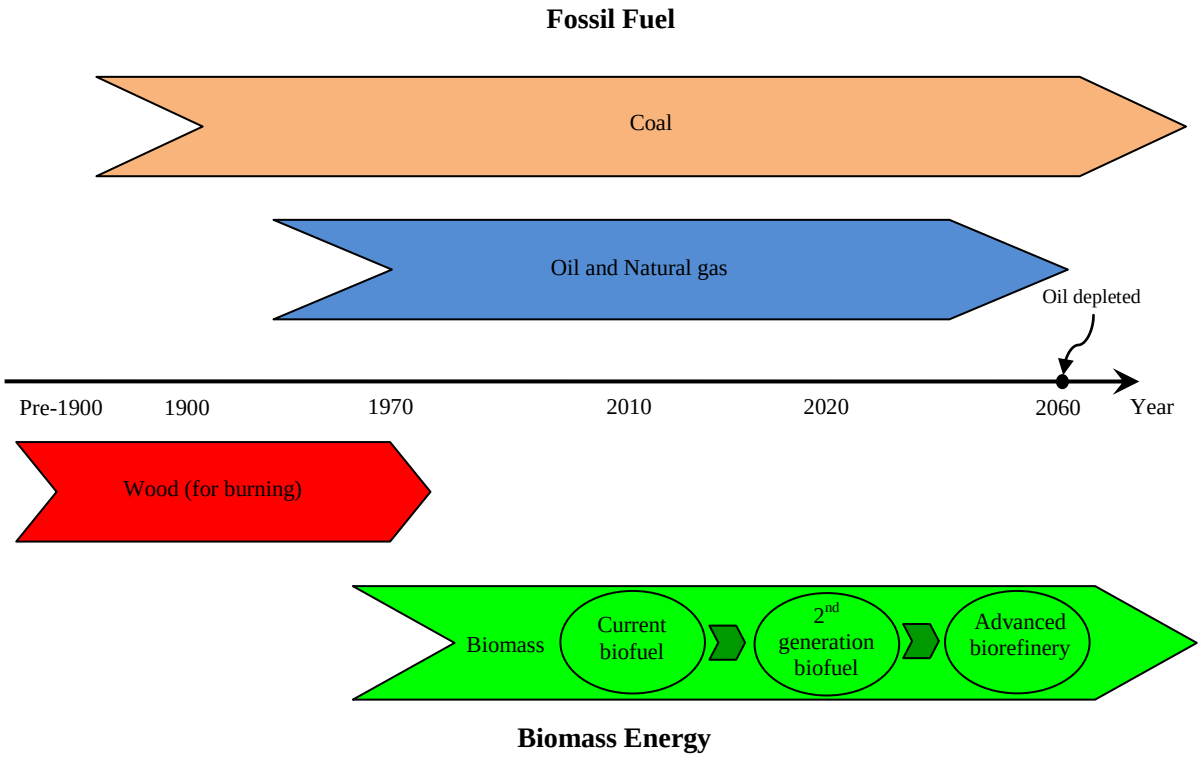

Figure 1.1: Timeline for transition of primary resources to biomass resources.

The development of biofuel production system and carbon abatement system is often hampered by their high capital and operating costs as well as loss in efficiency. The application of process integration techniques is thus extremely crucial in order to attain higher system efficiency at a lower economic impact. Heat integration, one of the prominent process integration techniques has been applied substantially in this work. Process-to-process material integration has also been adopted for the design and modelling of the systems under consideration. Economic analysis using discounted cash flow method has been performed in order to assess the feasibility of proposed integrated systems. A wide range of product portfolios, market price scenarios and carbon tax is taken into account to provide insights into ways of CO_2 emission mitigation.

The study undertaken can be divided into two parts: biofuel (Fischer-Tropsch liquid and methanol) production from bio-oil and decarbonised (CCS and CO_2 reuse)

coal polygeneration system. Bio-oil is a high energy density (energy per unit volume) liquid derived from biomass through fast pyrolysis process. Bio-oil is advantageous in term of transportation and storage. Biomass sources are collected and converted into bio-oil in pyrolysis at distributed sites. Subsequently, bio-oil is transported to centralised gasification sites for further conversion into fuels, chemicals or electricity. The integrated strategy is depicted in Figure 1.2 (Sadhukhan, 2009). The bio-oil yield model from wood pyrolysis not detailed in this thesis is based on NREL study (Ringer et al., 2006). A comprehensive mass and energy balance diagram showing the yield of bio-oil has been obtained from 200 t/d of biomass throughput, demonstrated in Figure 1.3 (Ringer et al., 2006). The yields of bio-oil, char and gas obtained from the pyrolysis process are 75%, 12% and 13% (by weight), respectively (Bridgwater, 2004). The rates of electricity generation and air consumption are estimated based on the study by Ringer et al. (2006).

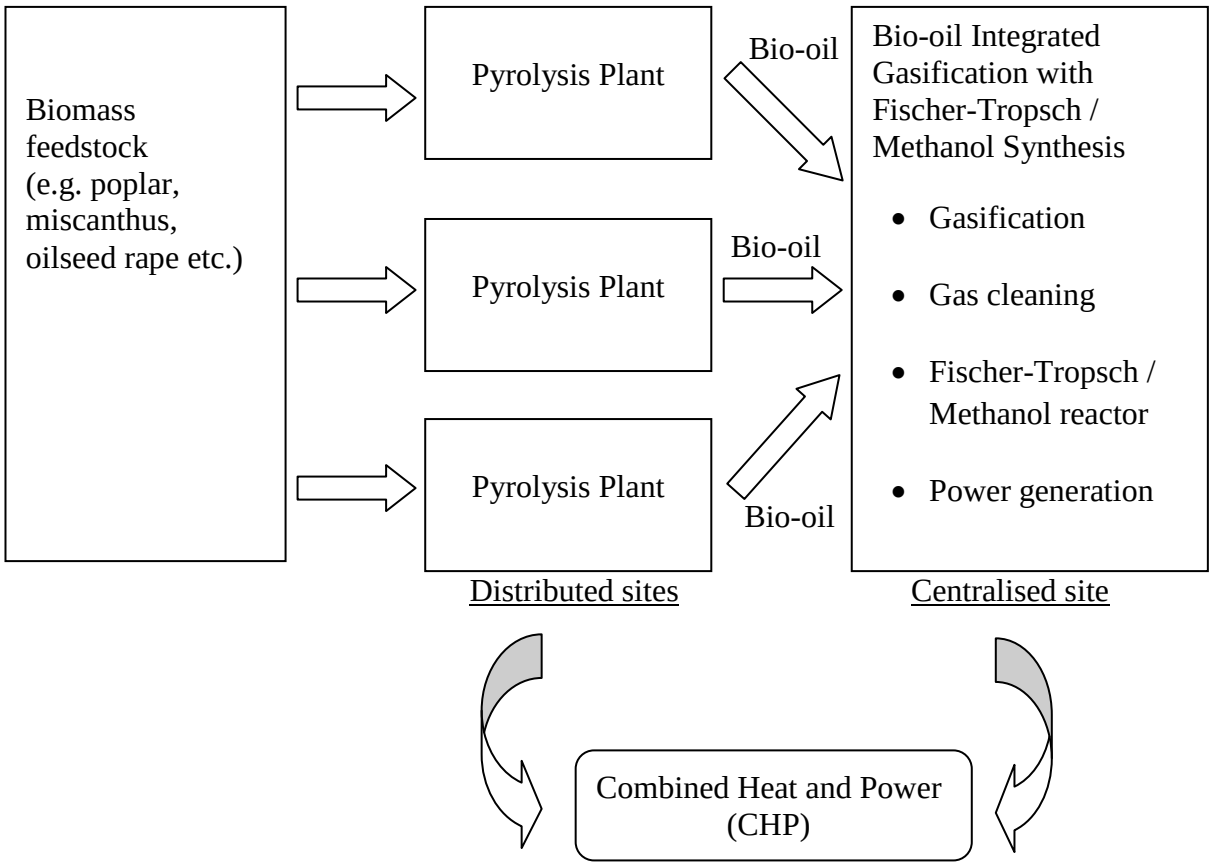

Figure 1.2: Distributed processing of biomass into bio-oil and centralised processing of bio-oil into fuels and power.

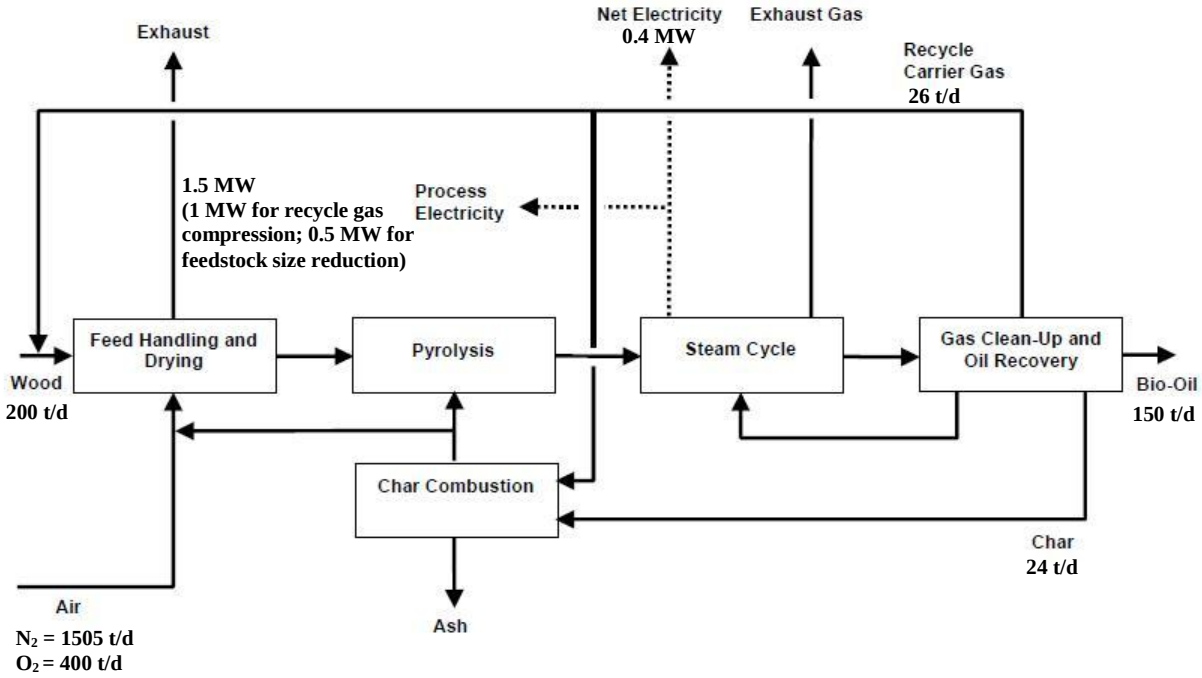

Figure 1.3: Distributed pyrolysis plant.

Polygeneration (Liu et al., 2007; POLYSMART, 2008; Adams and Barton, 2011) into multiple products from one or more resources utilising integrated systems is regarded as a promising solution in meeting the future energy demand while mitigating the environmental pollution. A polygeneration concept using gasification route is illustrated in Figure 1.4. Feedstocks can be coal, natural gas, biomass, bio-oil etc, whereas products can be primarily fuels, chemicals, electricity. Polygeneration system provides flexibility in production suitable for the contemporary market needs. In addition, it offers a self-satisfied environment by on-site generation of heating and cooling requirements. This reduces the costs of transportation and trading of the utilities.

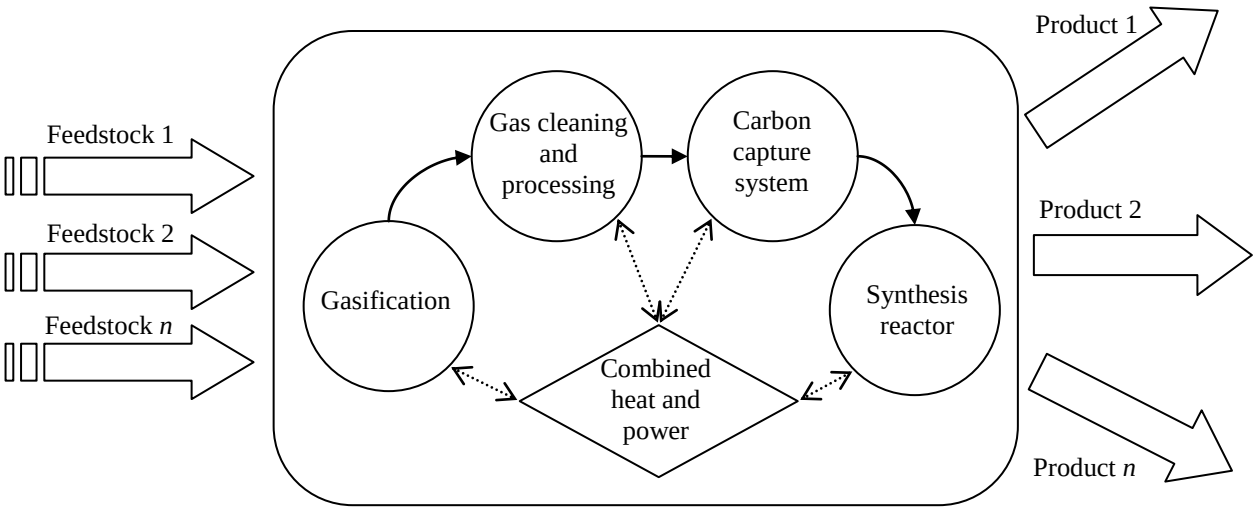

Figure 1.4: Polygeneration concept using gasification as the processing route.

1.2 Contribution of Research

The main contribution of this work is the techno-economic analyses of various process schemes, e.g. thermochemical conversion of bio-oil and fossil based feedstock into energy products, e.g. fuels, chemicals, heat and power. A holistic approach using systematic analytical frameworks comprising simulation modelling, process integration and economic analysis was developed and adopted consistently throughout the study. Performance analyses of all the process schemes under consideration were evaluated with respect to energetic efficiency and economic performances. The energetic efficiency is based on the first law of thermodynamics. The economic evaluation was carried out using the correlations given in the literatures. The results from the performance analyses are sensible and valid for preliminary conceptual design studies undertaken in this work. The contribution of this work is elucidated in two parts, as follows:

<u>Bio-oil based biorefinery:</u>

(1) Simulation frameworks for bio-oil integrated gasification and synthesis of Fischer-Tropsch liquid and methanol are established. Bio-oil is a complex mixture made up of hundreds of components. Research contribution in the modelling of bio-oil includes representation with three components, justified using statistical approach. The bio-oil representative model has further facilitated estimation of product gas composition from bio-oil gasification using Gibbs free energy minimisation reaction model in Aspen Plus. Statistically reliable results in terms of product gas composition from bio-oil gasification are generated aligned with literature data (Burgt, 2005). This provides a

comprehensive platform for the simulation of integrated conversion processes from bio-oil to liquid fuel. With this, variation in syngas composition under different gasifier operating conditions can be captured. In addition, bio-oil from other sources of biomass can also be conveniently modelled using the proposed bio-oil model.

(2) A whole biorefinery process simulation with respect to energy integration and process-to-process material integration can be explored substantially, using the proposed simulation-analysis frameworks. The energy value of bio-oil is less than that of a fossil fuel such as coal. Systematic heuristic-based heat integration strategies can improve an overall site efficiency to a maximum extent based on energy available from bio-oil that may help in identifying market conditions, subsidies and credits required for cost-competitive solutions against state-of-the-art fossil based processes. An appropriate level of recovery and utilisation of heat and power within an overall site has also been demonstrated.

(3) Comprehensive economic analyses using discounted cash flow method have been carried out to evaluate netback (maximum acceptable price of a feedstock) of bio-oil utilised in various biofuel centred biorefinery schemes. The viability of biorefinery systems is highly dependent upon associated costs. Therefore, transportation costs are examined for two scenarios: transporting bio-oil from local pyrolysis plant (biomass from indigenous resources) and importing bio-oil from other countries abundant in biomass resources.

(4) The variation of cost of production of the main products (FT liquids or methanol) with cost of feedstock (bio-oil) and cost of by-product (electricity) is

investigated to identify viable market scenarios for the production of biofuel at a competitive price.

Decarbonised coal polygeneration:

(1) Various polygeneration system designs in relation to different decarbonisation strategies are proposed (see Appendix 1), giving more options for future decarbonisation solutions. These embrace CCS, CO_2 capture and reuse and CO_2 reuse from post-combustion exhaust gas. The modification of a cogeneration system into a polygeneration by the utilisation of CO_2 is also considered.

(2) A systematic conceptual design methodology for polygeneration system consisting of extensive process integration, thermodynamic efficiency, economic risk assessment and economic potential analysis is proposed. The performances of various integrated decarbonised polygeneration systems with respect to the above criteria are evaluated and compared for tradeoffs.

(3) A methodology is developed for effective selection of CO_2 reuse pathways and analysing the impact of CO_2 abatement system (CCS and reuse) integration into the gasification system.

Chapters 2 and 3 highlight the contents of each research paper, either published or submitted (with decision pending) in peer-reviewed archived journals.

Chapter 2 Discussion of the Nature of Bio-oil based Biorefinery Concept

2.1 PUBLICATION 1: Ng, K.S., Sadhukhan, J., Techno-economic performance analysis of bio-oil based Fischer-Tropsch and CHP synthesis platform. *Biomass & Bioenergy*. **35** (7): 3218-3234 (2011).

This paper investigates bio-oil derived from fast pyrolysis process of biomass (i.e. poplar wood) utilisation into the production of Fischer-Tropsch (FT) liquid. FT liquid can be upgraded into synthetic fuel such as diesel. This study provides an insight into an integrated bio-oil gasification FT synthesis (BOIG-FT) system, expected to be economically incentivised beyond 2020 (Smith, 2007). The work has focused on techno-economic performances of once-through and full conversion of centralised BOIG-FT system. A bio-oil composition model comprising of acetic acid, acetol and guaiacol, has been developed, sufficiently capable of representing bio-oil and bio-oil gasification process performance in the product gas generation. Heat integration strategy including heat recovery and usage at various levels through combined heat and power (CHP) network diagram has been formalised. The conceptual design of CHP network is highly relevant for biorefinery system. Finally, the economies of scales of the BOIG-FT system for capacities of 1 MW, 675 MW and 1350 MW based on LHV of bio-oil are assessed using netback of bio-oil. The import economy of bio-oil from other countries (e.g. Malaysia in this context) abundant in oil palm is also considered. Dr. Jhuma Sadhukhan is responsible for providing technical guidance, correction and checking the appropriateness and originality of this paper.

2.2 PUBLICATION 2: Ng, K.S., Sadhukhan, J., Process integration and economic analysis of bio-oil platform for the production of methanol and combined heat and power. *Biomass & Bioenergy*. **35** (3): 1153-1169 (2011).

This paper further explores the techno-economic feasibility of bio-oil refining into the production of methanol, an important chemical and liquid fuel. The economies of scales of 1 MW, 675 MW and 1350 MW based on LHV of bio-oil are considered for the integrated bio-oil gasification and methanol synthesis (BOIG-MeOH) system. The methodology in this paper is analogous to PUBLICATION 1 with respect to heat integration and economic analysis. A heuristic-based heat integration approach instead of total site pinch analysis has been employed in this work. Both approaches generally give similar results, however the former approach provides a clearer view and better control of the utilisation of sensible heat from process units into steam generation. The theory of pinch analysis is not provided in this publication since this fundamental knowledge can be found in the relevant published literature. The scope has been extended to impact analysis of integration of oxygen supply unit (air separation unit and water electrolysis unit) to the overall system and sensitivity analysis of syngas conditioning on the performance of methanol synthesis reactor. The reported stoichiometric ratio $(H_2-CO_2)/(CO+CO_2) = 2.0$ should be satisfied as a suitable syngas condition for methanol synthesis (Katofsky, 1993). However, it has been analysed that this ratio is not sufficient to guarantee a high yield of methanol production. Further, this work has identified that the water content in the syngas is also an important criterion to include and that water removal is a vital procedure prior to methanol synthesis reaction.

This work also explores the performances of the BOIG-MeOH systems under consideration, with bio-oil from various indigenous biomass resources, e.g. miscanthus and oilseed rape, and further compares the performance with respect to bio-oil from poplar wood. Furthermore, the transportation cost of bio-oil from distributed pyrolysis site to centralised gasification site has also been estimated, as part of the economic analysis. Dr. Jhuma Sadhukhan is responsible for providing technical guidance, correction, and checking the appropriateness and originality of the contents of this paper.

Chapter 3 Discussion of the Nature of Decarbonised Coal Polygeneration Systems

3.1 PUBLICATION 3: Ng, K.S., Zhang, N., Sadhukhan, J., CO_2 abatement strategies for polygeneration systems: Process integration and analysis. *Chemical Engineering Research and Design.* Submitted (2011).

CO_2 reduction approach is imperative due to tightened environmental legislation and global warming. This paper studies the deployment of polygeneration concept advantageous in extracting maximum energy content from clean coal. Various designs of coal polygeneration system, comprising of different CO_2 abatement options are proposed. CO_2 reuse, a potential alternative to carbon capture and storage (CCS) is particularly highlighted in this paper. Direct and indirect routes of converting CO_2 are proposed. Additionally, modification on conventional IGCC configuration is made, transforming it into a polygeneration system by the utilisation of CO_2 from the exhaust gas of gas turbine. Air separation unit (ASU) is considered in all the cases for providing the oxygen supply into the systems. These systems under consideration are analysed in terms of thermodynamic efficiency, economic potential and environmental impact. Heat integration strategy is elucidated and exemplified through the case studies. The design methodology proposed in this paper also includes an economic risk assessment, relevant and vital for a polygeneration system. Finally, the impact of carbon tax is also studied and the relevance of decarbonised polygeneration options is discussed. Two main conclusions can be derived from this paper: (a) adding more production lines to a polygeneration system may not necessarily improve the overall performances; (b)

revamping a cogeneration system into a polygeneration system can enhance the overall performances significantly. Dr. Jhuma Sadhukhan and Dr. Nan Zhang are responsible for providing advices, correction and checking the appropriateness and originality of the contents of this paper.

3.2 PUBLICATION 4: Ng, K.S., Zhang, N., Sadhukhan, J., A graphical CO_2 emission treatment intensity assessment for energetic and economic analyses of integrated decarbonised energy systems. *Computers & Chemical Engineering.* Submitted (2011).

The abundance of choices in CO_2 reuse pathways and integrated configurations has led to complexity in process system network design and integration. A methodology for selecting thermodynamically, economically and environmentally efficient integrated system designs has been developed in this paper. A shortcut two-step methodology comprising of thermodynamic feasibility assessment on the selection of CO_2 conversion pathways using Gibbs energy method, and performance analysis using graphical approach has been presented. An index coined as emission treatment intensity index (ETII) is proposed, derived from a CO_2 emission balance diagram (EBD). CO_2 EBD consists of graphical representation of CO_2 generation and removal processes from all process units in a system. ETII is defined as the ratio between the area under the generation profile and the area under the removal profile. It has been found that ETII is strongly correlated with the energy and cost intensities of integrated gasification with CO_2 abatement systems, under different categories of CO_2 disposal method. This has been proven through a series of energy and economic evaluation on integrated coal gasification systems with various CO_2 abatement strategies, through using Block and

Boundary concept. Processes in a flowsheet are grouped into key blocks of similar functionality through Block and Boundary concept, enhancing the scoping analysis between different flowsheets with similar plant types. Shortcut energy auditing and economic evaluation suggest that the exclusion of same process units can simplify the comparison analyses between two or more flowsheets. It also implies that heat integration is not taken into account for shortcut energy auditing while only equipment cost and variable operating costs are taken into consideration. The general observation of the empirical studies suggests that higher ETII in reuse case and lower ETII in storage case are desirable, in order to attain lower cost and energy intensities of a system. The proposed method can be thus conveniently adopted for effective comparison and selection between flowsheets during a preliminary design or retrofitting stage. Dr. Jhuma Sadhukhan and Dr. Nan Zhang are responsible for providing technical inputs, correction and checking the appropriateness and originality of the contents of this paper.

Chapter 4 Conclusions and Future Work

4.1 Conclusions

Comprehensive techno-economic analyses of bio-oil based biorefinery systems for the production of Fischer-Tropsch (FT) liquid methanol, with co-production of electricity were carried out. Their performance analyses were established using process simulation, heat integration and economic analysis. Various bio-oil integrated gasification and FT synthesis (BOIG-FT) systems embracing once-through and recycle configurations for a range of capacities from 1 MW, through 675 MW to 1350 MW were explored. The integration of air separation unit (ASU) and electrolyser was considered for bio-oil integrated gasification and methanol synthesis (BOIG-MeOH) system. Capacities of 1 MW, through 675 MW to 1350 MW were investigated for once-through mode, and 1350 MW for recycle mode, respectively. The performances of these systems in terms of efficiency and netback of bio-oil are summarised in Table 4.1. Larger scale with recycle configuration of a system achieves higher efficiency and netback of bio-oil. The integration of electrolyser into the bio-oil integrated gasification system is not economically viable for any capacities under consideration, however achieves higher efficiency compared to the systems with ASU configuration. The performance of the BOIG-MeOH system is generally more compelling compared to BOIG-FT system with respect to both efficiency and economics. Importing bio-oil from other countries may not be economically viable at present. Considering a supply of 2.43 million tonne/year of bio-oil from Malaysia to a 1350 MW biorefinery system in the UK, a shipping cost of 5.2 Euro/GJ was estimated, resulting in 4 times the original operating cost. The transportation cost of bio-oil within a radius 100 km from the

distributed pyrolysis plant to 1350 MW centralised gasification plant was estimated to be 4.3-8.9 Euro/t, reducing the netback of bio-oil from 45.2 Euro/t to 40.9-36.3 Euro/t. The transportation cost analysis hence suggests that the reliance on imported bio-oil may not be possible until the shipping cost is further reduced to a great extent and that priority should be given to indigenously grown biomass feedstock pyrolysis into bio-oil.

Table 4.1: Performances of bio-oil integrated gasification systems for the production of FT liquid / methanol and electricity.

Configuration	Capacity	Product	Efficiency [a] (%)	Netback of bio-oil [b] (Euro/t)
Once-through	1 MW	FT liquid Electricity	36.2	−198.9
	675 MW	FT liquid Electricity	38.7	11.4
	1350 MW	FT liquid Electricity	38.8	12.7
Recycle	1 MW	FT liquid Electricity	37.2	−201.5
	675 MW	FT liquid Electricity	38.8	15.4
	1350 MW	FT liquid Electricity	38.9	20.9
Once-through ASU	1 MW	Methanol Electricity	44.8	−287.5
	675 MW	Methanol Electricity	46.8	−3.2
	1350 MW	Methanol Electricity	48.3	6.65
Recycle ASU	1350 MW	Methanol Electricity	56.6	45.2
Once-through Electrolyser	1 MW	Methanol	38.7	−367.8
	675 MW	Methanol	41.8	−121.9
	1350 MW	Methanol	41.9	−122.6
Recycle Electrolyser	1350 MW	Methanol	54.6	−83.4

[a] Efficiency = (LHV of products / LHV of feedstock) × 100%

[b] Climate Change Levy is excluded.

Several polygeneration systems consisting of different decarbonisation strategies, such as capture and store, capture and reuse and reuse without capture, have been proposed. Essential design considerations for polygeneration systems have been presented. These comprise of product shifting and economic risk analysis. Further, the performances of ploygeneration systems under consideration with respect to thermodynamic efficiency, economic potential and CO_2 emission are compiled in Table 4.2. It has been recognised that introducing more production pathways into a polygeneration system by utilising the captured CO_2 may not improve the overall performance of the system, primarily due to considerable hydrogen requirement in the CO_2 conversion reaction. However, transforming a cogeneration system into a polygeneration system by reusing CO_2 in the flue gas of a gas turbine can enhance the overall performance of the system significantly. Product value analyses were also performed for the realisation of economically viable systems. Furthermore, the impact of carbon tax on the coal polygeneration systems was studied. Higher CO_2 emission rate from a system results in higher sensitivity of the system to carbon tax. Lower economic potential of a system also results in higher vulnerability to carbon tax.

Table 4.2: Performance analyses of various decarbonised coal cogeneration and polygeneration systems.

Type of decarbonised system	Capacity [a]	Main product	Efficiency [b] (%)	Economic potential (Euro/GJ)	CO_2 emission per unit product (t CO_2/GWh)
Cogeneration; capture and store	648 MW	Electricity	36.6	−1.9	127.8
Polygeneration; capture and store	648 MW	Electricity Hydrogen Acetic acid Methanol	78.4	9.5	7.7
Polygeneration; capture and reuse	1268 MW	Electricity Acetic acid Methanol Methane	74.2	0.6	8.3
Polygeneration; reuse without capture	3451 MW	Electricity Methanol	86.3	3.6	16.9

[a] Capacity refers to the total LHV of feed input to the system.

[b] Efficiency = (LHV of products / LHV of feedstock) × 100%

A shortcut methodology has been developed to facilitate the decision-making process on the selection of appropriate CO_2 abatement route to be integrated into a coal gasification system. The proposed methodology comprises of two steps: thermodynamic feasibility assessment using Gibbs energy method and quantification of energy and cost intensities of integrated decarbonised energy systems using graphical approach, i.e. emission balance diagram (EBD) followed by emission treatment intensity index (ETII). ETII has found to be strongly correlated with the energy and cost intensities of integrated decarbonised gasification based energy systems. This has been justified through shortcut energy and economic evaluation of a range of coal gasification

configurations integrated with various CO_2 abatement systems using the proposed Block and Boundary concept.

The energetic efficiency evaluated for all the case studies in this work is based on the first law of thermodynamics, which accounts for all thermal energy transformation into work. This is only sensible and valid for preliminary conceptual design undertaken in this work. In reality, thermal energy cannot be converted into useful work with 100% efficiency, and thus the actual efficiency will be lower than that estimated using first law based efficiency. Therefore, second law based efficiency would be a more realistic indicator for evaluating the energetic performance of a system during detailed design stage.

The capital cost estimation described in this work uses the correlations applicable within a certain limit of capacity. Larger capacity of the system may lead to over / underestimation of the value estimated from the correlation. This is reasonable at the preliminary design cost estimation, however one should be cautious on treating the absolute cost figures reported in this work.

4.2 Future Work

There are still various challenges to overcome for biorefinery deployment. The integration between distributed pyrolysis plants and centralised gasification sites requires in-depth exploration and optimisation. It has been estimated that the total land to be used in poplar wood plantation for supplying through distributed fast pyrolysis plants to 648 MW centralised bio-oil polygeneration plant is 0.01 ha/GJ. Life cycle analysis of whole systems, including forestry and transportation is an essential study in promoting sustainable energy production and competing against fossil fuels. The replacement of coal based polygeneration system by bio-oil would require 1.5 times more energy from bio-oil, assuming that the LHV of bio-oil and coal are 18 MJ/kg and 28 MJ/kg, respectively and that the estimated overall efficiency of the bio-oil and coal polygeneration systems are 52% and 78.4%, respectively. On the other hand, CO_2 mitigation studies can be extended into more reuse options, such as converting CO_2 into polymers, which can retain the life cycle of carbon for longer period of time while meeting the market demand. Research into the integration of CO_2 abatement system into crude oil refinery site is also desirable since the refinery site constitutes vast amount of CO_2 emission.

References

Adams, T.A. II, Barton, P.I., Combining coal gasification and natural gas reforming for efficient polygeneration. *Fuel Processing Technology*, **92**(3): 639-655 (2011).

BP, BP statistical review of world energy June 2010 (2010). [cited 19 May 2011]. Available from: www.bp.com/statisticalreview.

Bridgwater, A.V., Biomass Fast Pyrolysis. *Thermal Science*, **8**(2): 21-49 (2004).

Burgt, M.J.v.d., Chapter 12: Entrained-flow gasification. In: Knoef, H.A.M, editors. Handbook biomass gasification, Netherlands: BTG Biomass Technology Group, pp. 248-258 (2005).

Intergovernmental Panel on Climate Change (IPCC), IPCC special report on carbon dioxide capture and storage. (2005).

ITN, Pollution targets to be announced, 17 May (2011). [cited 27 May 2011]. Available from: http://itn.co.uk/uk/19000/pollution.

Kamm, B., Gruber, P.R., Kamm, M., Biorefineries - Industrial processes and products: status quo and future directions Volume 1. Wiley-VCH (2006).

Katofsky, R.E., The production of fluid fuels from biomass. Princeton University (1993).

Liu, P., Gerogiorgis, D.I., Pistikopoulos, E.N., Modeling and optimization of polygeneration energy systems. *Catalysis Today*, **127**(1-4): 347-359 (2007).

POLYSMART, Polygeneration in Europe - A technical report. Contract/Proposal No. 019988 (2008). [cited 19 May 2011]. Available from: http://www.polygeneration.org/.

Rhodes, R., Energy transitions: A curious history. Center for International Security and Cooperation, Stanford University (2007).

Ringer, M., Putsche, V., Scahill, J., Large-scale pyrolysis oil production: A technology assessment and economic analyses. NREL/TP-510-37779. National Renewable Energy Laboratory (NREL) (2006).

Sadhukhan, J., Modified integrated biorefinery schematic, obtained from personal communication, The University of Manchester (2009).

ScottishPower, ScottishPower announces major coal contract with Scottish coal, 3 July (2008). [cited 6 June 2011].
Available from: http://www.scottishpower.com/PressReleases_1725.htm.

Smith, W., Mapping the development of UK biorefinery complexes. NFC 07/008. Tamutech Consultancy (2007).

The European Parliament and The Council of The European Union. Directive 2009/28/EC of the European Parliament and of the Council of 23 April 2009 on the promotion of the use of energy from renewable sources and amending and subsequently repealing Directives 2001/77/EC and 2003/30/EC Official Journal of the European Union (2009).

The Published Research Papers

PUBLICATION 1: Ng, K.S., Sadhukhan, J., Techno-economic performance analysis of bio-oil based Fischer-Tropsch and CHP synthesis platform. *Biomass & Bioenergy*. **35** (7): 3218-3234 (2011).

Available at www.sciencedirect.com

ScienceDirect

http://www.elsevier.com/locate/biombioe

Techno-economic performance analysis of bio-oil based Fischer-Tropsch and CHP synthesis platform

*Kok Siew Ng, Jhuma Sadhukhan**

Centre for Process Integration, Chemical Engineering, The University of Manchester, Manchester M13 9PL, UK

ARTICLE INFO

Article history:
Received 4 December 2010
Received in revised form
18 April 2011
Accepted 22 April 2011
Available online 23 May 2011

Keywords:
Gasification
Fischer-Tropsch
Polygeneration
Bio-oil
Energy efficiency
Biorefinery

ABSTRACT

The techno-economic potential of the UK poplar wood and imported oil palm empty fruit bunch derived bio-oil integrated gasification and Fischer-Tropsch (BOIG-FT) systems for the generation of transportation fuels and combined heat and power (CHP) was investigated. The bio-oil was represented in terms of main chemical constituents, i.e. acetic acid, acetol and guaiacol. The compositional model of bio-oil was validated based on its performance through a gasification process. Given the availability of large scale gasification and FT technologies and logistic constraints in transporting biomass in large quantities, distributed bio-oil generations using biomass pyrolysis and centralised bio-oil processing in BOIG-FT system are technically more feasible. Heat integration heuristics and composite curve analysis were employed for once-through and full conversion configurations, and for a range of economies of scale, 1 MW, 675 MW and 1350 MW LHV of bio-oil. The economic competitiveness increases with increasing scale. A cost of production of FT liquids of 78.7 Euro/MWh was obtained based on 80.12 Euro/MWh of electricity, 75 Euro/t of bio-oil and 116.3 million Euro/y of annualised capital cost.

1. Introduction

The UK's biofuel supply accounted for 3.33% of the total road transport fuel in the past year that exceeded the Government's target of 3.25% [1]. However, this is way below the EU Renewable Energy Directive's mandates of 20% renewable energy targets, including 10% biofuel mix by 2020 [2]. The UK is obliged to meet a target of 15% share of energy from renewable sources by 2020 [2]. At present, the biofuel resources are largely the first generation arable crops that supply majority of bioethanol and waste oils and oily crops that supply biodiesel. The contribution of biomass towards the world's future energy supply can be in the range of 20–50% from currently exploited less than 10% of the total energy supply in the industrialised countries [3]. This implies moving towards energy integrated and efficient lignocellulosic biorefinery systems.

Gasification followed by Fischer-Tropsch (FT) is a promising route for producing transportation fuel and CHP from lignocellulosic biomass, in a biorefinery fashion. Integrated biomass gasification FT systems were analysed for technical feasibility and economics, alternative process configurations and prioritising R&D activities for their commercialisation [4–7]. Studies have demonstrated up to 50% overall energy efficiency and economic acceptability achievable due to reduction in capital investment and learning effect. However, transportation, handling, storage, availability and supply in bulk and low bulk energy density of biomass remain a major obstacle in the development of large scale biomass based processing. For these logistic reasons, biomass can be processed into more convenient, cleaner (without tar, char and ashes) and transportable forms such as liquid bio-oils, through fast pyrolysis or liquefaction process. Liquid bio-oil has a higher energy density compared to solid biomass by up to 7 times. This reduces logistics and transportation difficulties, and storage space requirement associated with biomass [8]. Fast pyrolysis involves thermal

* *Corresponding author.*
E-mail address: jhumasadhukhan@gmail.com (J. Sadhukhan).
0961-9534/$ – see front matter © 2011 Elsevier Ltd. All rights reserved.
doi:10.1016/j.biombioe.2011.04.037

decomposition reactions that occur in a few seconds, at modest temperature conditions and in the absence of oxygen or in oxygen lean environment. Aston University, UK and Dynamotive undertakes extensive research and development of biomass pyrolysis technologies for the production of bio-oil [9–11]. The Energy research Centre of the Netherlands (ECN) focuses on the thermochemical production routes from biomass to syngas and FT diesel production [7,12]. Other specialist biomass gasification and pyrolysis research centres include BTG [13,14] and Indian Institute of Petroleum [15]. Gasification of bio-oil [16] and bio-oil/char (bio-slurry) [17,18] have received considerable interest, and research has been carried out extensively by FZK, Dynamotive, Future Energy and BTG.

The reference bio-oil used is from the UK poplar wood and oil palm empty fruit bunch produced elsewhere. The area available for growing UK poplar wood is ~0.8 million ha [19]. Indonesia (7 million ha) and Malaysia (4.5 million ha) are the major producers of oil palm [20]. Oil palm empty fruit bunch can also be processed into bio-oil [21] that can be imported to the UK. Bio-oil can be collected from various distributed biomass pyrolysis plants and imported and subsequently processed in centralised BOIG-FT plants [11]. In a large centralised BOIG-FT plant, similar to a petro-refinery accepting oils from different locations within specifications, the bio-oil can be converted into different products through a series of processing operation. Even though gasification and FT technologies are available at centralised scale, bio-oil is a premature energy commodity and overall BOIG-FT systems for various biomass resources must be energy integrated and analysed using energy and process integration tools, which are the main aims of this study.

The creation of an advanced biorefinery framework utilising bio-oils into biofuels is potentially a very effective way to lower our dependency on crude oil based refinery [22]. However, there are techno-economic barriers to overcome for the commercial deployment of such biorefining technologies. The main objective of this paper is to achieve competitive process efficiency using heat integration and CHP network design strategies and enhance economic feasibility by the employment of full conversion configurations (in addition to once-through configurations) and economies of scale ranging from 1 MW, through 675 MW to 1350 MW. The study presents systematic modelling and operability studies of BOIG-FT processes based on their impacts on overall system performance. The viability of importing bio-oil from other countries using shipping cost analysis has also been assessed.

2. Modelling and simulation

2.1. *Process description*

The BOIG-FT system under consideration can be divided into four main sections: gasification, gas cleaning and processing, FT synthesis reactor and power generation, as depicted in Fig. 1. The process models used in ASPEN Plus simulation are presented in Table 1.

Bio-oil (stream 2 in Fig. 1) is converted into product gas through the high-temperature gasification (~1100 °C), GASIFIER (modelled using Gibbs free energy minimisation method in ASPEN Plus), using oxygen (stream 1). Entrained flow gasifier (technology developers including GE, Shell, E-Gas etc.) can be employed for gasifying bio-oil [13]. An oxygen-blown gasifier is opted since air will lower the heating value of the resulting product gas. Oxygen is assumed to be supplied from oxygen plant, the cost of which was included in the economic analysis. Oxygen was preheated to 480 °C using high pressure (HP) steam generated on site. In addition to the reduction in the operating temperature of the gasifier, preheating oxygen can also achieve thermally neutral condition in the gasifier. It is not necessary to preheat bio-oil since it will degrade and promote char formation at high temperature. Product gas (stream 4) from the gasifier contains significant amount of CO and H_2 which are the main reactants for the FT process, and it has been assumed to be free from nitrogen, sulphur, tar and ash. Subsequently, the product gas passes through a series of cleaning and processing units, in order to meet the stringent conditions required by the FT synthesis process. These include water removal columns, H2OREM1 and H2OREM2. H2OREM1 was used to manipulate the steam required by the water-gas shift reaction whilst H2OREM2 was used to reduce the amount of water content in syngas which may influence the conversion of FT reaction. The water removed can be sent to a wastewater treatment plant, e.g. physical, chemical or biological processes, the cost of which has been considered in this study. A water-gas shift reactor (WGS) was used for adjusting the H_2/CO molar ratio to about 2, detailed in section 2.4. A Sulfinol unit (a combined physical and chemical solvent process) [4], represented as a CO_2 separator (CO2SEP) was needed to remove CO_2 by 99% on molar basis. The Sulfinol unit can also be used for co-capturing H_2S and COS. Subsequently, the CO_2 captured was compressed in CO2COMP to 80 bar for storage.

The clean syngas is sent to the FT reactor (FTREACT) for producing hydrocarbon liquids. The type of FT reactor configuration is highly dependent on the desired product distribution [23]. The low temperature Fischer-Tropsch (LTFT) was employed for higher diesel range production (C_{12}–C_{18}). An LTFT tubular fixed bed reactor with cobalt-based catalyst available from Shell, Malaysia can be employed [24]. The operating temperature of FT reactor is 240 °C and the pressure is 25 bar, within typical ranges of 200–250 °C and 25–60 bar, respectively. Cobalt catalyst is active at lower temperature operations and for high diesel and wax yields. A flash column (VLFLASH) was used to separate the gaseous stream 20 and liquid product stream 21 which were cooled to 40 °C.

The offgas containing light gases such as CH_4, C_2H_6 etc. (stream 23) are fed to gas turbine (GASTURB) for power generation. To enable a stable combustion, Wobbe Index of the gas turbine was validated to ensure that it was within ±10% compared to the base case provided by Shah et al. [25]. The Wobbe Index is a measure of interchangeability of fuel gases and for comparing the combustion energy among fuel gases with different compositions. Co-firing with trace amount of natural gas was further undertaken in the gas turbine to increase the Wobbe Index of the feed gas to the gas turbine. Co-firing was advantageous since it could eliminate any need for modifying the gas turbine and combustor for low heating value syngas [26]. Air containing 79 mol% N_2 and 21 mol% O_2 was compressed to 14 bar through AIRCOMP and supplied to the gas turbine combustion chamber (GTCOMB) to assist the combustion reaction of FT offgas. Since the LHV of

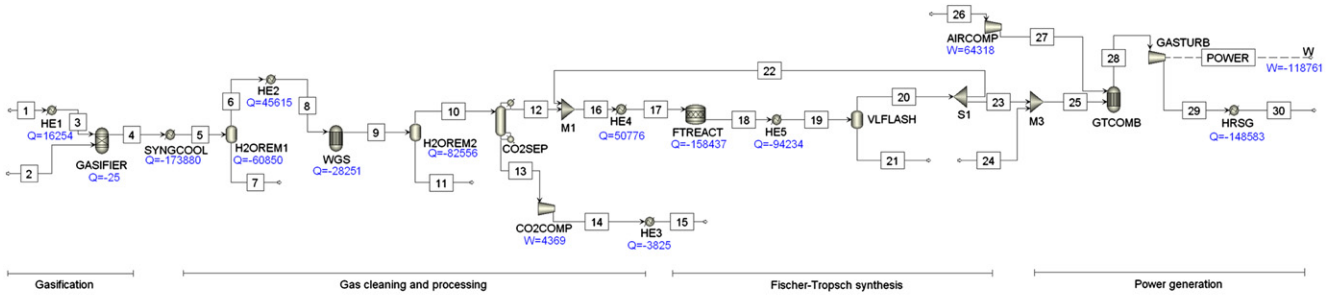

Q: Heat (kW)
W: Power (kW)

Component's mole fraction	Stream No.															
	1	2	4	7	11	12	15	17	18	20	21	22	23	24	26	30
Acetic acid		0.109														
Acetol		0.109														
Guaiacol		0.109														
H_2			0.307	0.001	0.001	0.679		0.618	0.459	0.561	0.002	0.561	0.561			
H_2O		0.673	0.251	0.986	0.864	0.001		0.002	0.161	0.003	0.866	0.003	0.003			0.189
CO			0.318	0.005	0.007	0.314		0.301	0.237	0.288	0.014	0.288	0.288			
CO_2			0.124	0.008	0.128	0.004	1.000	0.007	0.009	0.010	0.006	0.010	0.010			0.110
O_2	1.000														0.210	
N_2															0.790	0.700
Natural gas (CH_4)														1.000		
C_1-C_4 paraffins								0.050	0.092	0.095		0.095	0.095			
C_{5+} paraffins								0.022	0.042	0.043	0.113	0.043	0.043			
Molar flow rates (kmol/s)	1.14	2.10	6.20	0.56	0.30	3.89	1.45	8.06	6.13	5.00	1.12	4.18	0.83	0.20	6.00	3.60
Mass flow rates (kg/s)	36.48	84.38	120.86	10.20	23.13	40.36	63.88	104.66	104.66	77.00	27.65	64.30	12.70	3.21	173.10	102.42

Note: All the results above vary accordingly for different capacities and configuration. Stream 22 is omitted for all once-through cases.

Fig. 1 – Simulation of BOIG-FT flowsheet in ASPEN Plus. The values of heat duties and power shown are for 1350 MW case with full conversion configuration. This flowsheet can be applied to once-through configuration where there is no offgas recycle stream.

the syngas into the combustor was greater than 6 MJ/m^3, de-rating (reduction in burning temperature and compressor power ratio to allow stable combustion) of the gas turbine combustor was not required for an operating condition of 1200 °C and 14 bar in the combustor. The exit temperature and pressure of the exhaust gas from the gas turbine (stream 29 in Fig. 1) are 744 °C and 2 bar respectively. An enthalpy of -2.3×10^3 kJ/kg and entropy of 1.2 kJ/kg-K (with respect to the reference temperature and pressure of 25 °C and 1.013 bar) were available with this exhaust gas. The heat content in the exhaust gas from the gas turbine was recovered into the generation of high pressure superheated steam using heat recovery steam generator (HRSG). The carbon balance across the centralised BOIG-FT system (Fig. 1) shows 0.19 kmol/GW of net carbon removal from the site. This is a net result of CO_2 capture, which has a carbon negative impact, and addition of natural gas, which has a carbon positive impact.

2.2. *Selection of model components for bio-oil*

The model component of bio-oil was represented by validating its gasification performance. The bio-oil represented using one (dextrose), two (acetic acid and guaiacol), three (acetic acid, acetol and guaiacol) and four (acetic acid, acetol, guaiacol and furfural, $C_5H_4O_2$) chemical components was assessed. These models were tested by comparing the syngas composition obtained from simulation of bio-oil gasification, against industrial reference cases [27]. The feed and product composition and gasification process operating conditions are presented in Table 2. The composition of bio-oil, represented by different sets of model components, was estimated by balancing the C, H and O elements in the product gas component. The combinations were selected systematically by taking into consideration that the aqueous phase comprises acetic acid and acetol (soluble in water), while guaiacol and furfural (insoluble in water) are present in the lignin phase of bio-oil. The rationale was to distribute the masses of C, H and O according to the atomic ratio, e.g. for 3-component model, acetic acid ($C_2H_4O_2$) carries 2/12 of the mass of C, whilst acetol ($C_3H_6O_2$) and guaiacol ($C_7H_8O_2$) carry 3/12 and 7/12 of the mass of C, respectively. An example of the mass balance in relation to C, H and O elements for 3-component model (acetic acid, acetol and guaiacol) is presented in Table 3.

The chi-square (χ^2) test was performed for justifying statistical significance of bio-oil representation. The statistical significance gives an indication of how likely the hypothesis is wrong. In the present context, the null hypothesis is defined as "the selected model component(s) is (are) acceptable for representing bio-oil". Firstly, χ^2 for each model was calculated, using equation (1), and is summarised in Table 2. $y_{i,S}$ and $y_{i,R}$ denote the mole fraction of component i (components in product gas) obtained from simulation and reference cases, respectively.

$$\chi^2 = \sum_{i=1}^{N} \frac{\left(y_{i,S} - y_{i,R}\right)^2}{y_{i,R}} \quad (1)$$

By assuming a significance level (the probability of rejecting the hypothesis) of 0.05, and taking into account that there are 4 degrees of freedom, the critical value was determined to be 9.49 from chi-square distribution table [28]. As can be seen from Table 2, the χ^2 for each model falls below the critical

Table 1 – ASPEN Plus model description of BOIG-FT system.

Unit	ASPEN plus model	Outlet temperature (°C)	Pressure (bar)	Other specification
AIRCOMP	Compr		14	Isentropic efficiency = 0.9
CO2COMP	Compr		80	Isentropic efficiency = 0.9
CO2SEP	Sep			CO_2 split fraction = 0.99
FTREACT	RStoic	240	25	
GASIFIER	RGibbs	1111	30	
GASTURB	Compr		2	Isentropic efficiency = 0.9
GTCOMB	REquil	1200	14	
H2OREM1	Flash2	155	30	
H2OREM2	Flash2	25	30	
HE1	Heater	480	30	
HE2	Heater	400	30	
HE3	Heater	35	80	
HE4	Heater	220	25	
HE5	Heater	40	25	
HRSG	Heater	100	1.013	
M1	Mixer		25	
M2	Mixer		14	
S1	FSplit			Split fraction = 0.835 (full conversion); (stream 22)
SYNGCOOL	Heater	155	30	
VLFLASH	Flash2	40	25	
WGS	REquil	400	30	

'Compr' = Compressor/turbine; 'Sep' = Component separator; 'RStoic' = Stoichiometric reactor; 'RGibbs' = Gibbs reactor; 'REquil' = Equilibrium reactor; 'Flash2' = Two-outlet flash; 'Heater' = Heater; 'Mixer' = Stream mixer; 'FSplit' = Stream splitter.

value of 9.49. Therefore, it can be concluded that there is no sufficient evidence to reject the hypothesis.

The lower χ^2 value obtained for the 3-component model presented in Table 2, signifies that the 3-component model is more acceptable compared to the others. The residual sum of square (RSS) statistical method demonstrated in equation (2) was also applied to describe the degree of discrepancy between the simulation and the reference results in terms of compositions of syngas obtained from bio-oil gasification. The RSS obtained for each model is presented in Table 2.

$$\text{Residual sum of square (RSS)} = \sum_{i=1}^{N}\left(y_{i,S} - y_{i,R}\right)^2 \quad (2)$$

The 3-component model (acetic acid, acetol and guaiacol) with the lowest χ^2 value (0.018) and the least RSS value (0.41) can thus adequately represent bio-oil for its performance through the gasification process under consideration.

2.3. *Sensitivity studies of gasification*

The sensitivity studies in terms of the effect of the gasifier temperature, pressure and oxygen-to-feed (O_2/F) molar ratio on H_2 and CO concentration in the product gas, were studied. Fig. 2(a) presents changes in the composition of the product gas with the gasification temperature, for a constant pressure of 30 bar and O_2/F molar ratio of 0.54. It can be seen that H_2 and CO contents in the product gas rise substantially from 500 °C to 1000 °C. H_2 starts declining and CO increases at a lower rate, above 1000 °C. It is thus proposed that the gasifier temperature should be kept above 1000 °C. Also, the concentration of CH_4 is less than 1 vol% at this temperature [13]. A relatively higher proportion of CH_4 is advantageous if the gas is used into power generation, however it is undesirable for an application into FT synthesis reaction [13]. Lower CO_2 composition can also be observed when the temperature increases. FT synthesis imposes a stringent condition on H_2/CO molar ratio of 2. The impact of the gasifier temperature on H_2/CO molar ratio in the product gas is depicted in Fig. 2(b). The H_2/CO molar ratio in the gas from the gasifier normally falls below 2. Hence, the ratio needs to be adjusted using water-gas shift reactor in between the gasifier and the FT reactor.

The pressure has a negligible impact on the product gas composition due to the equimolar stoichiometric gasification reactions, where pressure has less effect on changing the equilibrium composition. However, in order to avoid any compression work for the subsequent FT reaction at 25 bar, the gasifier was operated at a higher pressure (Table 1). The gas composition is highly sensitive to the changes in O_2/F molar ratio, as shown in Fig. 3(a). It is intended to keep the O_2/F molar ratio as low as possible (e.g. less than 0.5) primarily to maintain increasing H_2 and CO contents in the product gas. As illustrated in Fig. 3(b), lower O_2/F molar ratio results in higher H_2/CO molar ratio in the product gas.

2.4. *Modelling and sensitivity studies of FT synthesis*

The H_2/CO molar ratio in the syngas feed to the FT reactor is a highly influential parameter for dictating the reaction rate. Higher H_2/CO molar ratio results in a higher selectivity for lighter hydrocarbons due to higher probability of chain termination. Water gas-shift reactor should be used prior to FT reactor to adjust H_2/CO molar ratio since cobalt catalyst has negligible water-gas shift activity. Ideally, the required H_2/CO

Table 2 – Results of validation of bio-oil gasification process, and bio-oil modelling using Chi-square test and residual sum of square analysis.

Gasifier operating condition

Temperature	1300 °C
Pressure	30 bar
Bio-oil	1 kmol/s (29.6 mol% oil and 70.4 mol% water/moisture)
Oxygen	0.57 kmol/s

Product gas composition

Component	Mole fraction (Reference case), $y_{i,R}$ (%)
H_2	29.4
H_2O	26.3
CO	33.8
CO_2	10.5
CH_4	0.01

Component	Mole fraction (Simulation case), $y_{i,S}$ (%)			
	1-component model	2-component model	3-component model	4-component model
H_2	26.9	29.8	29.1	28.2
H_2O	31.3	23.8	26.7	25.2
CO	29.7	36.3	33.5	35.6
CO_2	12.0	10.0	10.7	11.0
CH_4	0.003	0.007	0.005	0.005

Component	$\chi^2 = \frac{(y_{i,S} - y_{i,R})^2}{y_{i,R}}$			
	1-component model	2-component model	3-component model	4-component model
H_2	0.21	0.0065	0.0031	0.047
H_2O	0.96	0.23	0.0073	0.049
CO	0.49	0.18	0.0029	0.095
CO_2	0.21	0.019	0.0028	0.025
CH_4	0.0047	0.0010	0.0023	0.0021
χ^2	**1.88**	**0.44**	**0.018**	**0.22**

Component	RSS $= (y_{i,S} - y_{i,R})^2$			
	1-component model	2-component model	3-component model	4-component model
H_2	6.08	0.19	0.09	1.37
H_2O	25.35	6.13	0.19	1.29
CO	16.56	6.17	0.10	3.22
CO_2	2.24	0.20	0.03	0.26
CH_4	4.7×10^{-5}	1.0×10^{-5}	2.3×10^{-5}	2.1×10^{-5}
RSS	**50.24**	**12.69**	**0.41**	**6.14**

Note: 1-component model refers to dextrose only. 2-component model consists of acetic acid and guaiacol (1 aqueous and 1 lignin fractions). 3-component model includes acetic acid, acetol and guaiacol (2 aqueous and 1 lignin fractions). 4-component model encompasses acetic acid, acetol, guaiacol and furfural (2 aqueous and 2 lignin fractions).

molar ratio is 2 (practically is about 2.15) when cobalt catalyst is used [29].

The FT synthesis reactions are highly exothermic. The main reactions involve the production of paraffin (equation (3)) and olefin. The production of straight-chain paraffins from C_1 to C_{30} was modelled using equation (3) in a stoichiometric reactor (RStoic in Table 1) in ASPEN Plus.

Table 3 – Mass balance in terms of C, H and O elements present in bio-oil for 3-component bio-oil model.

Element	Acetic acid ($C_2H_4O_2$)	Acetol ($C_3H_6O_2$)	Guaiacol ($C_7H_8O_2$)	Total
C	2.76	4.14	9.65	**16.55**
H	0.46	0.69	0.92	**2.06**
O	3.63	3.63	3.63	**10.88**
Total	**6.84**	**8.45**	**14.20**	**29.49**

Note: The last column indicates the mass of bio-oil in terms of C, H and O (without moisture and ash), and the last row represents the masses of each representative component present in bio-oil. All values indicate the mass in kg.

$$n\,CO + (2n + 1)\,H_2 \rightarrow C_nH_{2n+2} + n\,H_2O \quad (3)$$

The fractional conversion of each reaction was estimated based on the weight distribution of each FT product obtained via Anderson-Schulz-Flory (ASF) distribution model [30,31], in Excel spreadsheet. This model assumes a constant chain growth probability, α. Thus, $(1-\alpha)$ equals to the probability of termination of the carbon chain. In general, FT reaction involves two principal mechanisms (excluding chain initiation step):

- Chain growth by absorbing CO and H_2 (stepwise addition of CH_2) to form longer carbon chain length.
- Termination by desorption from the catalyst to form paraffin or olefin.

The ASF model which relates the weight fraction of the FT product, w with the chain growth probability α, is described in equation (4). n denotes the carbon number.

$$w_n = \alpha^{n-1}(1-\alpha)^2\, n \quad (4)$$

Typical values of α fall between 0.7–0.9 [31]. An empirical equation (5), in which α can respond to changes in temperature,

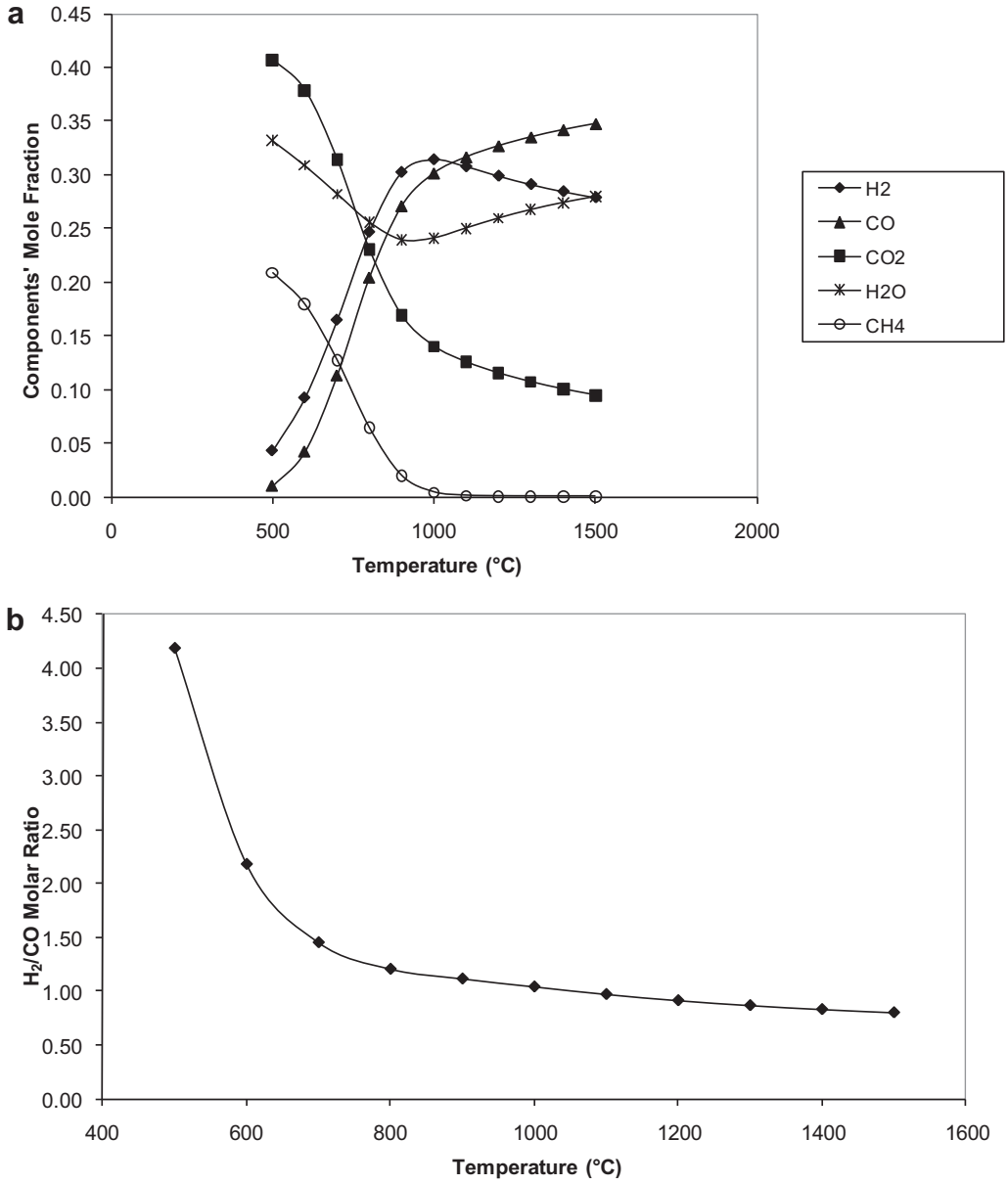

Fig. 2 – (a) Effect of gasifier temperature on the product gas composition. (b) Effect of gasifier temperature on H_2/CO molar ratio. Pressure of the gasifier was set at 30 bar and O_2/F molar ratio at 0.54.

by Song et al. [32], was adopted. A value of α of 0.76 at an FT reactor operating temperature of 240 °C is used in the simulation.

$$\alpha = \left(A \frac{y_{CO}}{y_{H_2} + y_{CO}} + B \right) [1 - 0.0039(T - 533)] \quad (5)$$

A and B are the parameters with values of 0.2332 ± 0.0740 and 0.6330 ± 0.0420, respectively [32]. y_{CO} and y_{H_2} denote the mole fractions of CO and H_2, respectively in the feed stream to the FT reactor. T is the operating temperature of the FT reactor, K.

By applying ASF relation in equation (4), the weight and molar distributions of each FT product were obtained. An overall conversion of 80% of the syngas (by taking CO as the limiting reactant) was assumed. The fractional conversion of CO in each reaction was determined by solving equation (6) in the spreadsheet environment integrated to the Aspen simulation framework.

$$\text{Total CO converted} = \sum_{n=1}^{n=30} y_{p,n} \times F_p \times n \quad (6)$$

$y_{p,n}$ is the mole fraction of paraffin with carbon number n produced. F_p is the total molar flow rate of paraffin produced, kmol/s.

The simulation results in terms of the weight and molar distribution are featured in Fig. 4(a) and (b), respectively. By adopting equation (5), a sensitivity analysis in terms of the effect of temperature on the product distribution can be evaluated, in Fig. 5. It implies that a higher diesel range product can be attained at a lower temperature.

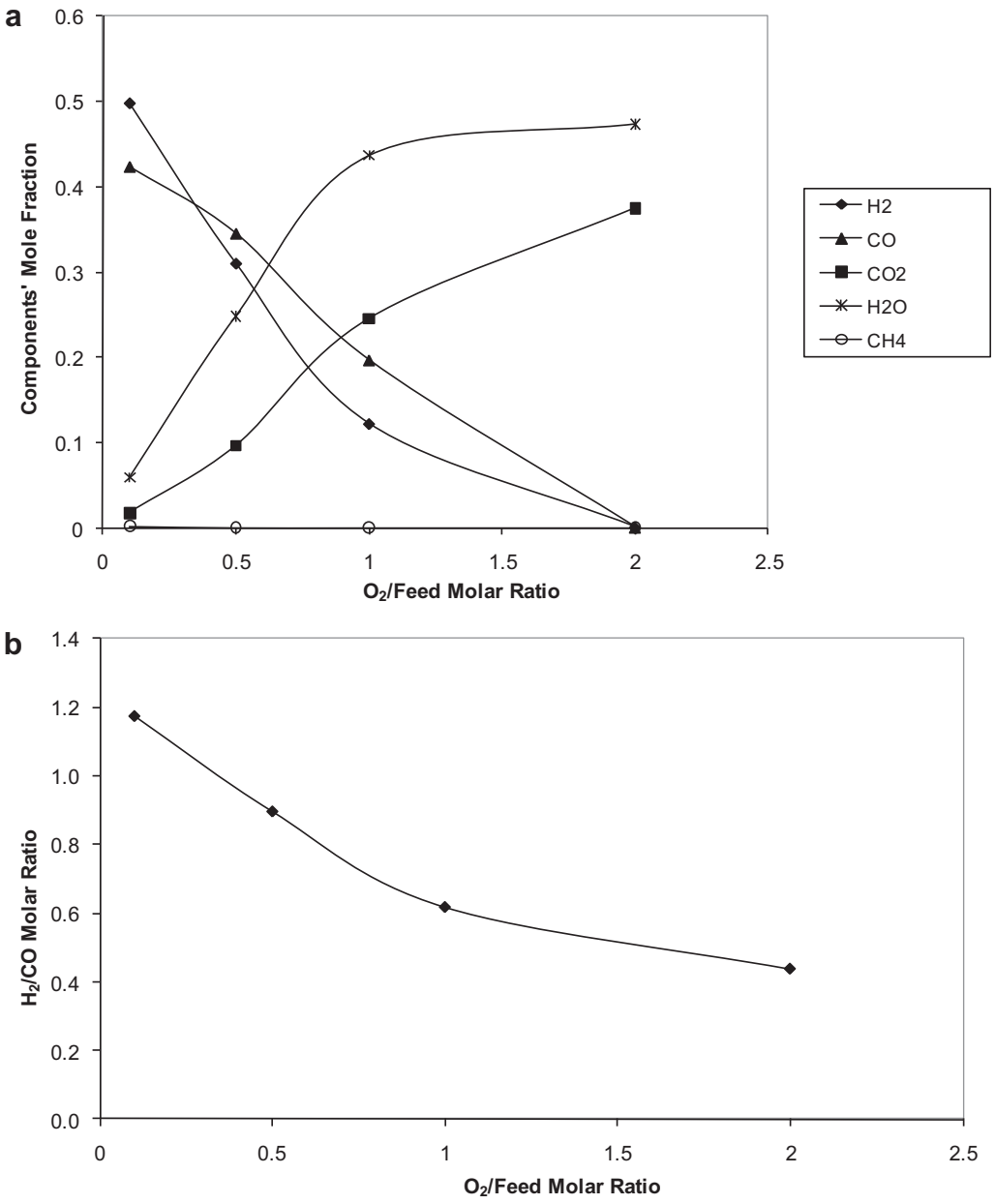

Fig. 3 – (a) Effect of O_2/F molar ratio to gasification on the product gas composition. (b) Effect of O_2/F molar ratio to gasification on H_2/CO molar ratio in the product gas. Pressure of the gasifier was set at 30 bar and temperature at 1300 °C.

3. Performance analysis of BOIG-FT system of various capacities

The BOIG-FT systems with various capacities were considered for 80% conversion of CO in the FT feedstock. In addition, the 675 MW case was studied for 60% CO conversion. For full conversion FT reactor configuration, CO conversion of 40% per pass was assumed, so that an overall 80% CO conversion can be obtained.

3.1. *Combined heat and power (CHP) integration and energy efficiency*

Strategies for overall heat integration of the BOIG-FT system under consideration have been proposed, in order to maximise energy recovery within the site and thereby improve cost-effectiveness of the system. The sensible heat from the site can be graded based on the temperature level and the heat content. The high grade surplus heat from processes can be used into process heating and the generation of high pressure steam to be used for other processes. The low grade surplus heat from the site can be utilised into low level process-to-process heating. The CHP integration strategy was demonstrated for an integrated coal gasification combined cycle study by Ng et al. [33]. The process heat supply and demand are listed in Table 4.

Three levels of steam can be generated from the site, i.e. high pressure (HP) steam at 40 bar and superheated to 500 °C, medium pressure (MP) steam at 15 bar and slightly above the saturated temperature at 200 °C and low pressure (LP) steam at 5 bar and 152 °C, respectively. The high grade heat from

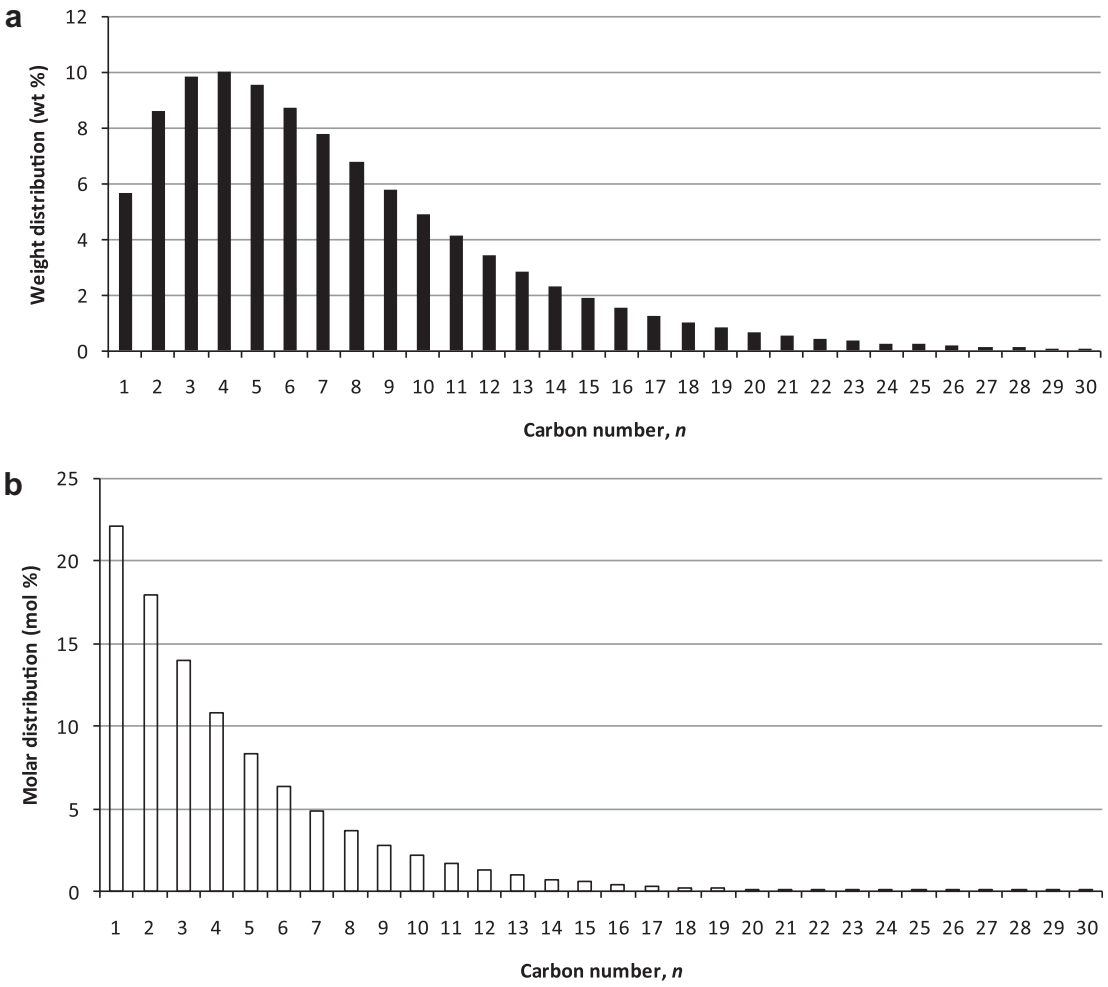

Fig. 4 – (a) Weight distribution of FT products predicted using ASF model. (b) Molar distribution of FT products predicted using ASF model. Operating condition of FT reactor: $T = 240\ ^{\circ}C$ which corresponds to $\alpha = 0.76$.

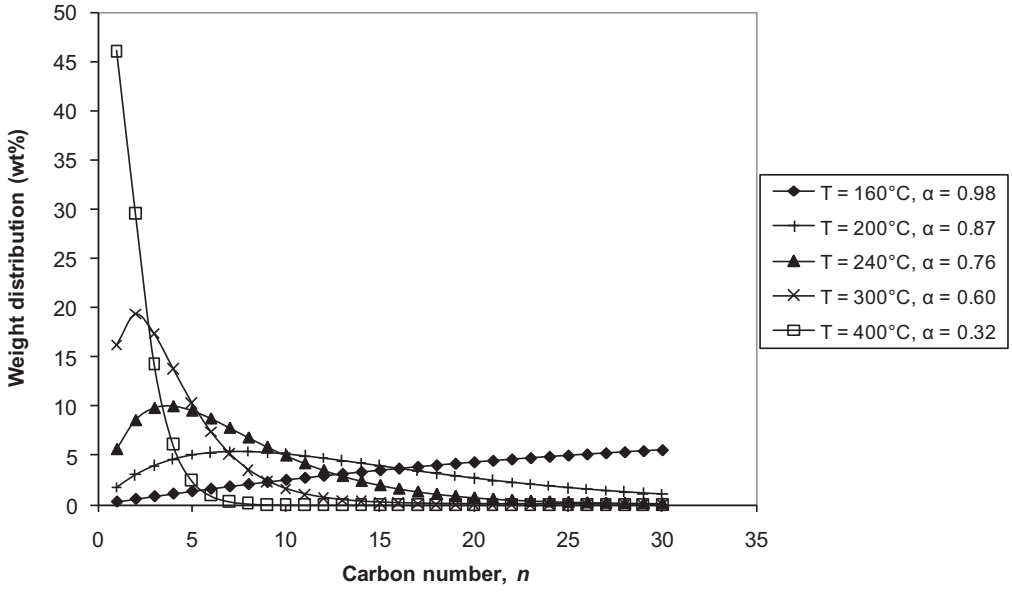

Fig. 5 – Variation of product distribution with temperature, with constant H_2/CO molar ratio of approximately 2.1.

Table 4 – Classification of heat supply and demand on site (heat duties shown for 1350 MW case with full conversion configuration).

Heat Supply/ Demand	Types of Heat Recovery/Utilisation	Process Unit	Temperature Level (°C)	Heat Duty (MW)
Heat Supply	High Level Heat	SYNGCOOL + H2OREM1	1111–155	234.7
		HRSG	743.9–100	148.8
		FTREACT	240	158.4
	Low Level Heat	WGS	400	28.3
		H2OREM2	400–25	82.6
		HE3	102–35	3.8
		HE5	240–40	94.2
Heat Demand	Steam Heating	HE1	25–480	16.3
		HE2	155–400	45.6
		HE4	40.7–220	50.8
		Sulfinol unit (reboiler)	151.8	312.0

SYNGCOOL + H2OREM1 and HRSG was used in the generation of HP steam, whilst the exothermic heat from FTREACT was utilised into the production of MP steam. The excess HP and MP steam was let down to generate low pressure (LP) steam and additional power.

The hot and cold composite curves [34] were analysed for estimating the maximum amount of steam generation from SYNGCOOL + H2OREM1 and HRSG, presented in Fig. 6(a) and (b), respectively. In each of these figures, the cold composite curve was shifted horizontally towards the hot composite

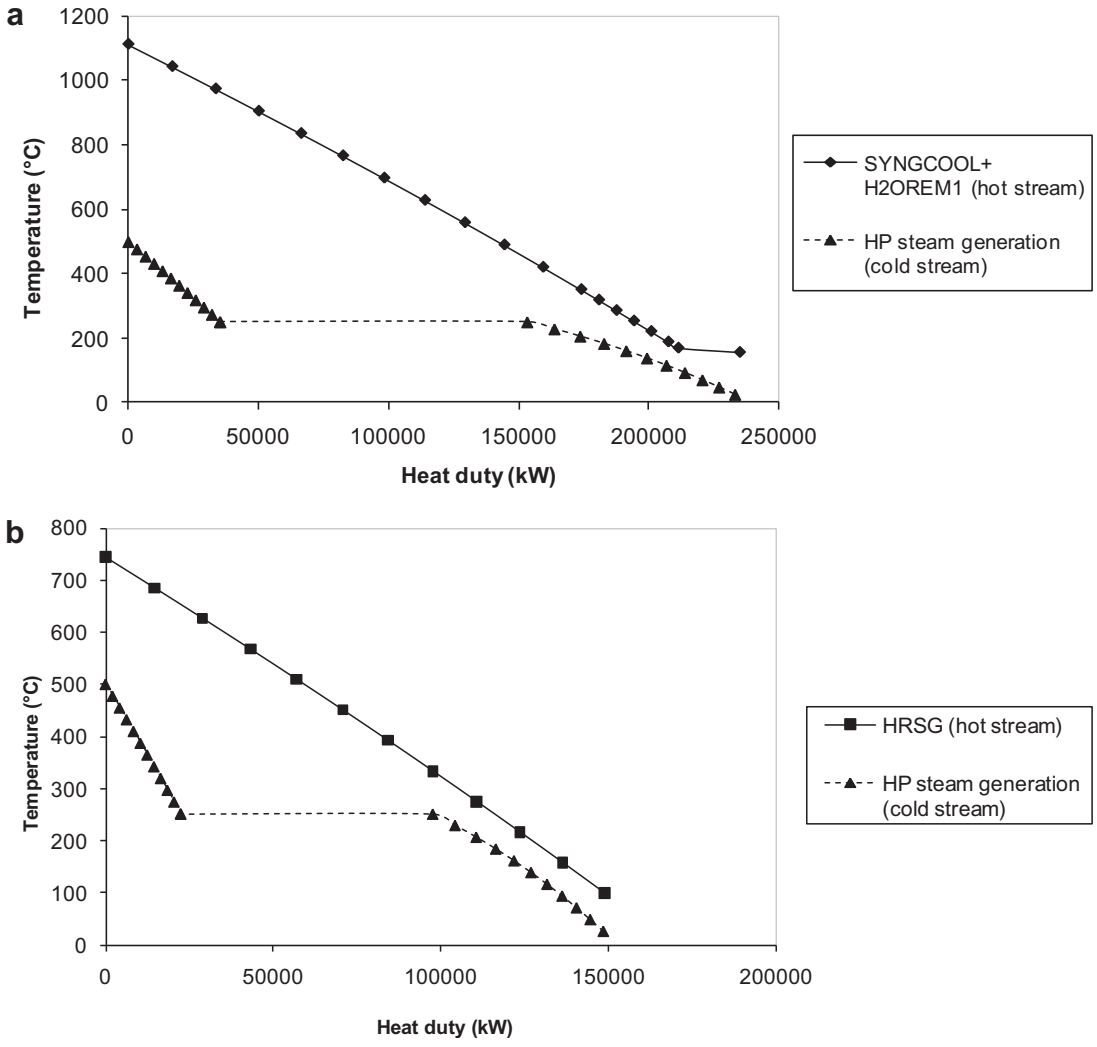

Fig. 6 – (a) Composite curves showing the heat recovery from SYNGCOOL and H2OREM1 into HP steam generation. (b) Composite curves showing the heat recovery from HRSG into HP steam generation. Both figures are for 1350 MW case with full conversion configuration.

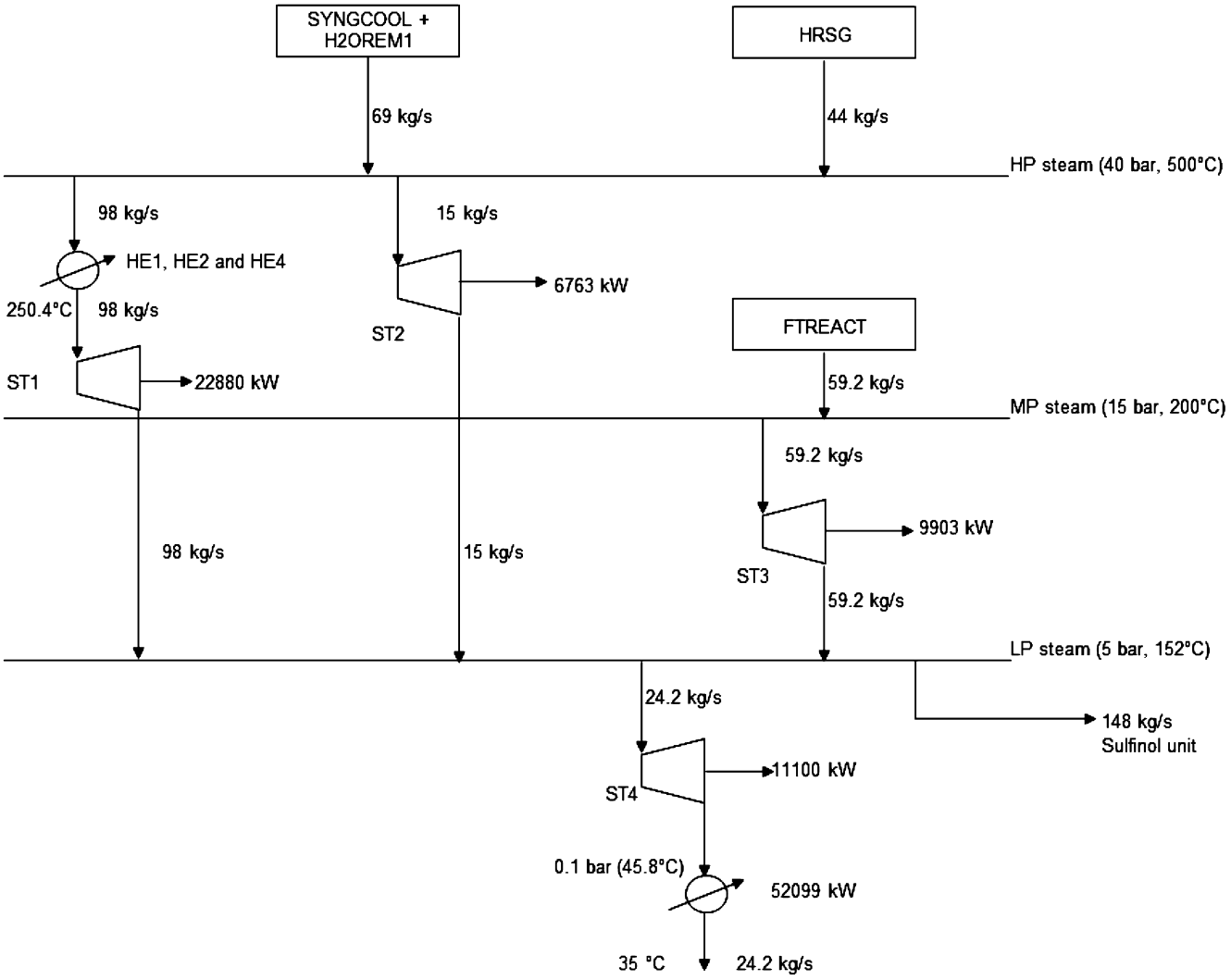

Fig. 7 – Steam and power network for 1350 MW case with full conversion configuration.

curve (i.e. by increasing the mass flow rate of steam) in order to reach a minimum approach temperature of 20 °C. The shifting of composite curves ensures a maximum heat recovery that can be attained from a site. The SYNGCOOL and H2OREM1 can physically be one unit. The temperatures and heat duties of the hot streams (SYNGCOOL + H2OREM1 and HRSG) and the cold streams (steam generation) were obtained from ASPEN Plus simulation. For the HP steam generation, water at 25 °C was heated to the saturated temperature of 250.4 °C at 40 bar, and then superheated to 500 °C. The amount of steam generation from FTREACT was estimated from its heat of reaction at isothermal condition and the enthalpy of vaporisation of MP steam at 200 °C at 15 bar.

The heat demands by HE1, HE2 and HE4 were satisfied by the HP steam, and the remaining steam was sent to a steam turbine ST1 for power generation. The composite curves for these heat balances were analysed to determine the amount of HP steam needed. The steam required by the preheaters and reboilers in Sulfinol unit for solvent regeneration was evaluated based on 1.42 kg/kg of LP steam to acid gas [35]. The remaining HP and MP steam was let down through the steam turbines ST2 and ST3 (back pressure turbines) generating additional power. The excess LP steam from the exit of the steam turbines after fulfilling the heat requirement by the Sulfinol unit was utilised in condensing turbine ST4 for power generation. The site-wide steam and power network is depicted in Fig. 7. The steam turbines were assumed to perform at 80% isentropic efficiency and 95% mechanical efficiency. The low grade heat surplus from WGS, H2OREM2, HE3, HE5 and condenser can be used for generating hot water for domestic heating systems and small-scale industrial plants.

Energy balances performed for different capacities of the BOIG-FT system (1 MW, 675 MW and 1350 MW) are summarised in Table 5 for once-through configuration and Table 6 for full conversion configuration, respectively. The LHV of FT liquids was assumed to be 45 MJ/kg. The net heat generation accounts for the entire low grade heat surplus from the site that does not involve steam generation. The C_{5+} liquid yield and selectivity between various BOIG-FT system cases under consideration were analysed and compared. Additionally, a comparison of energy efficiency based on the lower heating values (LHV) of the resulting FT liquids and the amount of heat and power generation is also presented.

Table 5 – Energy balances for 1 MW, 675 MW and 1350 MW cases with once-through configuration (all cases are based on 80% conversion unless otherwise stated).

System capacity	1 MW		675 MW		675 MW (60%)		1350 MW	
	kW	kg/s	kW	kg/s	kW	kg/s	kW	kg/s
Heat recovery into steam generation	**402.0**	**0.128**	**269025.1**	**85.9**	**258996.8**	**81.4**	**541458.2**	**172.8**
SYNGCOOL and H2OREM1 (HP, 40 bar)	168.8	0.050	114814.4	34.0	114814.4	34.0	233005.8	69.0
HRSG (HP, 40 bar)	118.2	0.035	74291.7	22.0	84422.4	25.0	148583.4	44.0
FTREACT (MP, 15 bar)	115.0	0.043	79919.0	29.9	59760.0	22.4	159869.0	59.8
Heat supplied to process units using generated steam	**291.6**	**0.17**	**197722.6**	**123.9**	**197722.6**	**123.9**	**396109.9**	**248.0**
HE1, HE2 and HE4	59.0	0.06	42023.0	50.0	42023.0	50.0	84097.0	100.0
Sulfinol unit	232.6	0.11	155699.6	73.9	155699.6	73.9	312012.9	148.0
Surplus LP steam into condensing turbine ST4	**37.9**	**0.018**	**25253.8**	**12.0**	**15704.6**	**7.5**	**52236.2**	**24.8**
Low grade heat surplus from the site	**166**		**113987**		**99127**		**229842**	
WGS	22		14119		14119		28248	
H2OREM2	57		41244		41244		82556	
HE3	3		1911		1911		3825	
HE5	45		30922		25814		61865	
Condenser	39		25791		16039		53348	
Net heat generation	**166**		**113987**		**99127**		**229842**	
Power generation from gas turbine	**62**		**59506**		**62721**		**119033**	
Power generation from steam turbine	**41**		**27080**		**25096**		**54986**	
ST1	15		13882		13882		27758	
ST2	11		2705		4058		5862	
ST3	7		4998		3739		10000	
ST4	8		5495		3417		11366	
Power requirement on site	**30**		**34342**		**34342**		**68687**	
CO2COMP	3		2183		2183		4369	
AIRCOMP	27		32159		32159		64318	
Net power generation	**73**		**52244**		**53475**		**105332**	
C_{5+} liquid selectivity/yield (%)	63.9/50.9		66.3/52.9		51.3/30.7		66.3/52.8	
Production of FT liquid	289	0.0064	209500	4.65	121300	2.70	418700	9.31
Efficiency based on LHV (FT liquid + electricity/bio-oil) (%)	**36.2**		**38.7**		**25.8**		**38.8**	
Efficiency based on LHV (FT liquid + electricity + heat/bio-oil) (%)	**52.8**		**55.6**		**40.5**		**55.8**	

The 675 MW BOIG-FT system with once-through configuration was studied for 80% and 60% conversions respectively. The lower conversion case has the advantage of generating more power, e.g. approximately 2.4% higher than the system with 80% conversion. This is due to higher amount of offgas produced from the FT reaction that is utilised in the gas turbine. However, the BOIG-FT system with 60% conversion has efficiency 15% lower than the system with 80% conversion (Table 5). This is due to a much lower C_{5+} liquid yield, approximately 22.2% lower than the system with 80% conversion. Therefore, higher conversion of the FT reaction is more favourable for obtaining higher efficiency. Further, it can be concluded that higher efficiency can be achieved at higher capacity of the BOIG-FT system, while the full conversion configuration is generally more efficient than the once-through configuration. The efficiency which includes the net heat is higher than the efficiency without the net heat, suggesting that the recovery of the low grade heat into useful by-products such as hot water can be beneficial.

The proximate and ultimate analyses of bio-oils obtained from poplar and oil palm empty fruit bunch are presented in Table 7(a). The performance of BOIG-FT system using bio-oils from poplar and oil palm empty fruit bunch is compared in terms of energy efficiency, defined as the LHV of FT liquid, electricity with/without heat with respect to the LHV of bio-oil, summarised in Table 7(b). The LHV of FT liquid was assumed to be 45 MJ/kg. The efficiency of FT liquid and CHP generated using bio-oil from oil palm empty fruit bunch is higher than using poplar, i.e. 50.5% compared to 38.9%, respectively. This is due to the lower moisture content in the oil, i.e. 30% and 18.6% for bio-oils from poplar and oil palm empty fruit bunch, respectively. The FT liquid, low grade heat and electricity contributed to 54–66%, 22.5–33.2% and 11.6–12.8% of the total output energy, for the 1350 MW case using either poplar or oil palm empty fruit bunch as feedstocks. The surplus low grade heat from the site can be recovered into hot water generation, which is highly essential in the UK energy scenario. The energy efficiency of biomass gasification with FT synthesis has been reported to be 42–50% [5], which in turn reflects that the bio-oil system is competitive against the biomass system.

3.2. *Economic analysis*

Detailed capital cost, operating cost and discounted cash flow (DCF) analyses performed for 1 MW, 675 MW and 1350 MW LHV cases with once-through and full conversion

Table 6 – Energy balances for 1 MW, 675 MW and 1350 MW cases with full conversion configuration.

System capacity	1 MW		675 MW		1350 MW	
	kW	kg/s	kW	kg/s	kW	kg/s
Heat recovery into steam generation	**398.0**	**0.125**	**168311.1**	**85.6**	**540026.1**	**172.2**
SYNGCOOL and H2OREM1 (HP, 40 bar)	168.8	0.050	114814.4	34.0	233005.8	69.0
HRSG (HP, 40 bar)	118.2	0.035	74291.7	22.0	148583.4	44.0
FTREACT (MP, 15 bar)	111.0	0.040	79205.0	29.6	158437.0	59.2
Heat supplied to process units using generated steam	**316.4**	**0.17**	**211961.6**	**121.9**	**424666.9**	**246.0**
HE1, HE2 and HE4	82.0	0.06	56262.0	48.0	112654.0	98.0
Sulfinol unit	234.4	0.11	155699.6	73.9	312012.9	148.0
Surplus LP steam into condensing turbine ST4	**37.9**	**0.018**	**24663.6**	**11.7**	**51013.6**	**24.2**
Low grade heat surplus from the site	**183**		**129528**		**260965**	
WGS	23		14119		28251	
H2OREM2	53		41244		82556	
HE3	3		1911		3825	
HE5	72		47066		94234	
Condenser	32		25188		52099	
Net heat generation	**183**		**129528**		**260965**	
Power generation from gas turbine	**82**		**59370**		**118761**	
Power generation from steam turbine	**38**		**24985**		**50646**	
ST1	10		11060		22880	
ST2	14		3607		6763	
ST3	7		4951		9903	
ST4	7		5367		11100	
Power requirement on site	**41**		**34342**		**68687**	
CO2COMP	3		2183		4369	
AIRCOMP	38		32159		64318	
Net power generation	**79**		**50013**		**100720**	
C_{5+} liquid selectivity/yield (%)	65.5/53.0		66.4/53.5		66.4/53.5	
Production of FT liquid	293	0.0065	212200	4.72	424300	9.43
Efficiency based on LHV (FT liquid + electricity/bio-oil) (%)	**37.2**		**38.8**		**38.9**	
Efficiency based on LHV (FT liquid + electricity + heat/bio-oil) (%)	**55.5**		**58.0**		**58.2**	

configurations are presented. The economic analysis also includes an analysis of the netback of bio-oil. In addition, the import economics of bio-oil derived from oil palm empty fruit bunch was evaluated for viability in the UK context.

3.2.1. *Capital costs*

The capital costs of a BOIG-FT system include the direct (ISBL and OSBL) and indirect capital (design and installation costs for constructing a site as well as the costs forecasted for some

Table 7 – (a) Proximate and ultimate analyses of bio-oils from various sources. (b) Comparison of performance analysis of full conversion, 1350 MW BOIG-FT, using poplar wood and oil palm empty fruit bunch as feedstocks. .

(a)

Source of bio-oil	Heating value (MJ/kg)	Proximate Analysis (wt%)		Ultimate Analysis (wt %)		
		Fixed carbon and volatiles	Moisture	C	H	O
Poplar	23.3	70.0	30.0	56.0	7.0	37.0
Oil palm empty fruit bunch	21.2	81.4	18.6	54.5	8.9	36.6

(b)

Type of bio-oil	Poplar	Oil palm empty fruit bunch
Net heat generation (MW)	261.0	197.8
Net power generation (MW)	100.7	101.9
C_{5+} liquid selectivity (%)	66.4	72.0
C_{5+} liquid yield (%)	53.5	57.6
FT liquid (kg/s)	9.4	12.9
LHV of FT liquid (MW)	424.3	580.5
Efficiency based on LHV, (FT liquid + electricity)/bio-oil (%)	38.9	50.5
Efficiency based on LHV, (FT liquid + electricity + net heat)/bio-oil (%)	58.2	65.2

Table 8 – Input data for capital cost evaluation.

Direct capital cost				
ISBL				
Item No.	Process unit	Base Cost (million Euro, 1999)	Scale factor, R	Base scale
1	Gasifier	25.5	0.7	400 MW HHV
2	Water-gas shift reactor	0.38	0.6	2400 kmol/h CO + H_2
3	FT reactor	14.2	1.0	100 MW FT liquid
4	Gas turbine	6.55	0.7	25 MW
5	Steam turbine (inc. condenser)	3.81	0.7	12.3 MW
6	HRSG	2.87	0.8	47.5 t/h
7	SYNGCOOL	2.87	0.8	47.5 t/h
8	Oxygen plant	19.6	0.75	24 t/h
9	Compressor	10.2	0.85	13.2 MW
OSBL				
Item No.	Specification	Cost estimation (% of ISBL)		
10	Instrumentation and control	5.0		
11	Buildings	1.5		
12	Grid connections	5.0		
13	Site preparation	0.5		
14	Civil works (inc. waste water treatment)	10.0		
15	Electronics	7.0		
16	Piping	4.0		
	Total Direct Capital (TDC)	**ISBL + OSBL**		
Indirect Capital Cost				
Item No.	Specification	Cost estimation (% of TDC)		
17	Engineering	15		
18	Contingency	10		
19	Fees/overheads/profits	10		
20	Start-up	5		
	Total Indirect capital (TIC)			
	Total Capital Costs	**TDC + TIC**		

unforeseen circumstances). The cost data, base costs, scale factors and base scales of major process units in ISBL were adapted from Tijmensen et al. [5], summarised in Table 8. A scale factor *R* was applied for different sizes in the cost and size relationship, in equation (7). Maximum size of a gasifier is 400 MW HHV. Thus, multiple units were taken into account for the gasification capacity exceeding its maximum size. The cost of Sulfinol unit is generally proprietary information and has been assumed to account for 10% of the total capital cost [4]. The cost of SYNGCOOL was estimated the same way as for the HRSG. This also includes the base cost, scale factor, base scale and progress ratio.

$$\frac{\mathrm{COST}_{\mathrm{size2}}}{\mathrm{COST}_{\mathrm{size1}}} = \left(\frac{\mathrm{SIZE}_2}{\mathrm{SIZE}_1}\right)^R \quad (7)$$

SIZE_1 and $\mathrm{COST}_{\mathrm{size1}}$ represent the capacity and the cost of the base system, whilst SIZE_2 and $\mathrm{COST}_{\mathrm{size2}}$ represent the capacity of the system after scaling up/down and its corresponding cost, respectively. *R* is the scaling factor.

Cost index method was applied, as given in equation (8), for levelising the cost taken from to the recent year 2009. The cost index adopted is from Chemical Engineering Plant Cost Index (CEPCI) [36]. The CEPCI for the years 1999 and 2009 are reported at 390.6 and 524.2, respectively.

$$\text{Present cost} = \text{Original cost} \times \left(\frac{\text{Index at present}}{\text{Index when original cost was obtained}}\right) \quad (8)$$

3.2.2. *Operating costs*

The operating costs of the BOIG-FT system were evaluated by considering the fixed and variable operating costs and other miscellaneous costs such as sales expense. Fixed operating costs are independent of the production rate, and estimated based on percentage of total indirect capital costs (TIC) [37], given in Table 9. The cost allocated for personnel is based on the work by Tijmensen et al. [5].

3.2.3. *Discounted cash flow and netback of bio-oil analysis*

The discounted cash flow (DCF) analysis was performed to estimate the annual capital charges. The cumulative discounted cash flow is expressed as the net present value (NPV) in a DCF analysis. A discount rate of 10% for 15 operating years has been assumed. The construction/start-up period was assumed to be 2 years, where 25% and 75% of the total capital cost were distributed in the −1 and 0th year (0th year indicates plant start-up year) [5]. An annualised capital charge of 13.1% can be incurred, for the conditions specified above.

The netback indicates the value of a feedstock obtained from selling its products at market price after the deduction of associated costs. The netback thus sets the maximum acceptable cost (market price) of a feedstock. The cost/market price of a feedstock needs to be less than its netback in order to make profits from its processing. The netback of bio-oil was calculated by applying equation (9).

Table 9 – Input data for operating cost evaluation.

Item No.	Specification	Cost Estimation
Fixed operating cost		
1	Maintenance	10% of TIC
2	Personnel	0.595 million Euro/100 MW LHV
3	Laboratory costs	20% of (2)
4	Supervision	20% of (2)
5	Plant overheads	50% of (2)
6	Capital Charges	10% of TIC
7	Insurance	1% of TIC
8	Local taxes	2% of TIC
9	Royalties	1% of TIC
	Total Fixed Operating Cost (TFO)	
	Total Fixed Operating Cost per year	
Variable operating cost		
10	Natural gas	0.021 Euro/kWh
	Total Variable Operating Cost (TVO)	
	Direct Production Cost (DPC) per year	**TFO + TVO**
Miscellaneous		
11	Sales expense, General overheads, Research and development	30% of DPC
	Total Operating Costs Per Year	**DPC + Miscellaneous**

$$\text{Netback} = \text{Value from products} - (\text{Annualised capital cost} + \text{Annual operating cost}) \quad (9)$$

The products from the BOIG-FT system are the FT liquids and electricity. It has been assumed that the system operates for 8000 h per year. The value of the FT liquids was assumed to be 42.6 Euro/MWh, which is its cost of production from wood [38]. The price of electricity was adopted from DECC, reported at 7.284 pence/kWh in the year 2009 (equivalent to 80.12 Euro/MWh, assuming 1 GBP = 1.1 Euro), and excluding Climate Change Levy (CCL) [39]. CCL only applies to industrial sector where taxable supplies such as electricity, coal and petroleum are charged. The full rate of CCL for electricity is reported at 0.47 pence/kWh (equivalent to 5.17 Euro/MWh). A comparison of costs, i.e. annualised capital charge, annual operating cost, value from products and thus the netback of bio-oil (with and without CCL) for 1 MW, 675 MW and 1350 MW cases with once-through and full conversion configurations is presented in Table 10.

The netback of bio-oil is an effective way for examining the economy of scale. The BOIG-FT system is economically competitive for larger capacities, i.e. the netback of bio-oil ranges from 11.4–20.9 Euro/t (excluding CCL) for 675 MW and 1350 MW capacities for both configurations. The full conversion configuration is more attractive than the once-through configuration. In addition, lower conversion is not desirable, as demonstrated in 675 MW case with 60% conversion, which has a negative netback of bio-oil of −7.96 Euro/t (excluding CCL).

3.2.4. *Import economics of bio-oil*

Secured and ample supply of bio-oil is required for a large scale BOIG-FT system. Import of bio-oil from other countries at an acceptable cost may be an option to fulfil the rising demand for biofuels in the UK. Limited cost information on importing bio-oil from other countries to the UK is available, mainly due to the fact that bio-oil is yet to be established as an energy commodity in the UK and European countries. Hence,

Table 10 – Summary of economic analysis and estimated netback of bio-oil.

Configuration	Once through				Full conversion		
Capacity (MW LHV)	1	675	675 (60%)	1350	1	675	1350
Annualised capital charge (million Euro/y)	0.447	64.1	60.1	116.3	0.458	64.1	116.3
Annual operating cost (million Euro/y)	0.072	26.9	26.6	52.8	0.073	26.9	52.8
Value of products, exc. CCL (million Euro/y)	0.161	104.8	77.0	199.9	0.169	109.7	219.8
Value of products, inc. CCL (million Euro/y)	0.164	107.0	79.2	203.6	0.172	111.8	223.9
a. Electricity, without CCL (million Euro/y)	0.047	33.5	34.3	57.3	0.051	32.1	64.6
b. CCL for electricity (million Euro/y)	0.003	2.16	2.21	3.70	0.003	2.07	4.17
c. FT liquids (million Euro/y)	0.114	71.3	42.8	142.5	0.118	77.7	155.2
Bio-oil consumption (t/y)	1800	1214496	1214496	2430000	1800	1214496	2430000
Netback of bio-oil, exc. CCL (million Euro/y)	**−0.358**	**13.8**	**−9.67**	**30.9**	**−0.363**	**18.7**	**50.8**
Netback of bio-oil, exc. CCL (Euro/t)	**−198.9**	**11.4**	**−7.96**	**12.7**	**−201.5**	**15.4**	**20.9**
Netback of bio-oil, inc. CCL (million Euro/y)	**−0.355**	**16.0**	**−7.46**	**34.6**	**−0.359**	**20.8**	**54.9**
Netback of bio-oil, inc. CCL (Euro/t)	**−197.2**	**13.2**	**−6.14**	**14.2**	**−199.7**	**17.1**	**22.6**

the total delivered cost of bio-oil that depends on various aspects, such as loading and discharging, rail and road transportation, labour, taxes, shipping etc., is yet not fully estimated. The delivered cost of bio-oil to Rotterdam, The Netherlands from Canada, Brazil, South Africa, Ukraine and Baltic was studied by Bradley [40]. This cost was 6–10.6 Euro/GJ, using 4700 t tankers (ship) and without return trip.

Shipping cost is the major component of the delivered cost of bio-oil, especially when the distance between the countries is significant. This study estimates the shipping cost of bio-oil derived from oil palm empty fruit bunches, from Malaysia to the UK. Previous study provided an estimation of the shipping cost of bio-oil from Vancouver to Rotterdam to be 4.96 Euro/GJ, for a distance of 14400 km [40]. Thus a shipping cost of 5.2 Euro/GJ (equivalent to 83.2 Euro/t) is incurred for transporting bio-oil from Port Kelang, Malaysia to Port of Immingham, UK, over a distance of 15000 km, assuming a linear relationship between the distance and the shipping cost. For 2.43 million t/y of bio-oil import to the 1350 MW BOIG-FT system, 202.2 million Euro/y are incurred from shipping of bio-oil that is 4 times the original operating cost of 52.8 million Euro/y (Table 10). The high cost of shipping of bio-oil from other countries rich in biomass resources such as South East Asia is not economically viable at present. However, this cost can be reduced considerably (e.g. by approximately half) by introducing larger tanker for shipment, i.e. 61 Euro/t to 30 Euro/t [40]. Correspondingly, 41.6 Euro/t of shipping cost indicates a total cost of 101 million Euro/y for 1350 MW system.

By incorporating shipping costs of 83.2 Euro/t and 41.6 Euro/t, the netback of bio-oil for 1350 MW case with full conversion is further reduced to −62.3 Euro/t and −20.7 Euro/t, respectively, from 20.9 Euro/t in Table 10. Furthermore, a maximum shipping cost of 20.8 Euro/t for the 1350 MW full conversion case is estimated, (based on zero netback of bio-oil) implying a maximum locus of radius within 3774 km from the UK. It is not cost-effective to ship bio-oil across a long distance under the current economic scenario, albeit bio-oil from oil palm empty fruit bunch achieves higher efficiency than poplar (Table 7(b)).

3.3. *Analysis of performances*

A lower temperature FT reaction at 200 °C which corresponds to a higher chain growth probability, α of 0.87 (determined using equation (5)) was also studied, in addition to the base case with FT reaction temperature at 240 °C and α at 0.76. Higher C_{5+} selectivity of 79.4% and yield of 63.5% can be achieved from lower temperature FT reaction, compared to the selectivity of 66.3% and yield of 52.9% from 675 MW BOIG-FT system with once-through configuration (Table 5). This suggests that the lower temperature FT reaction can have higher yields of diesel, which is consistent with the observation mentioned in section 2.4.

The best case with 1350 MW capacity and full conversion configuration was taken as the basis for further economic sensitivity studies. The relationship between the costs of production of FT liquids and bio-oil is illustrated in Fig. 8, by taking the prices of electricity of 46.61 Euro/MWh and 80.12 Euro/MWh for the years 2005 and 2009, respectively, as the basis [39]. The cost of production of FT liquids was predicted by subtracting the value of electricity from the total unit annualised cost of 169.1 million Euro/y (Table 10) incurred by the 1350 MW BOIG-FT system with full conversion configuration, including the following costs of bio-oil, (i) 0 Euro/t, (ii) 9.8 Euro/t (2005) and 20.9 Euro/t (2009) for a given cost of production of FT liquid from wood-based FT plant: 42.6 Euro/MWh [38], (iii) 75 Euro/t and (iv) 150 Euro/t. The reported cost of production of bio-oil is between 75-300 Euro/t [41]. Even for a minimum reported cost of bio-oil of 75 Euro/MWh and an electricity price of 80.12 Euro/MWh in 2009, the cost of production of FT liquids is expected to be at 78.7 Euro/MWh, which is higher than that currently produced from coal and

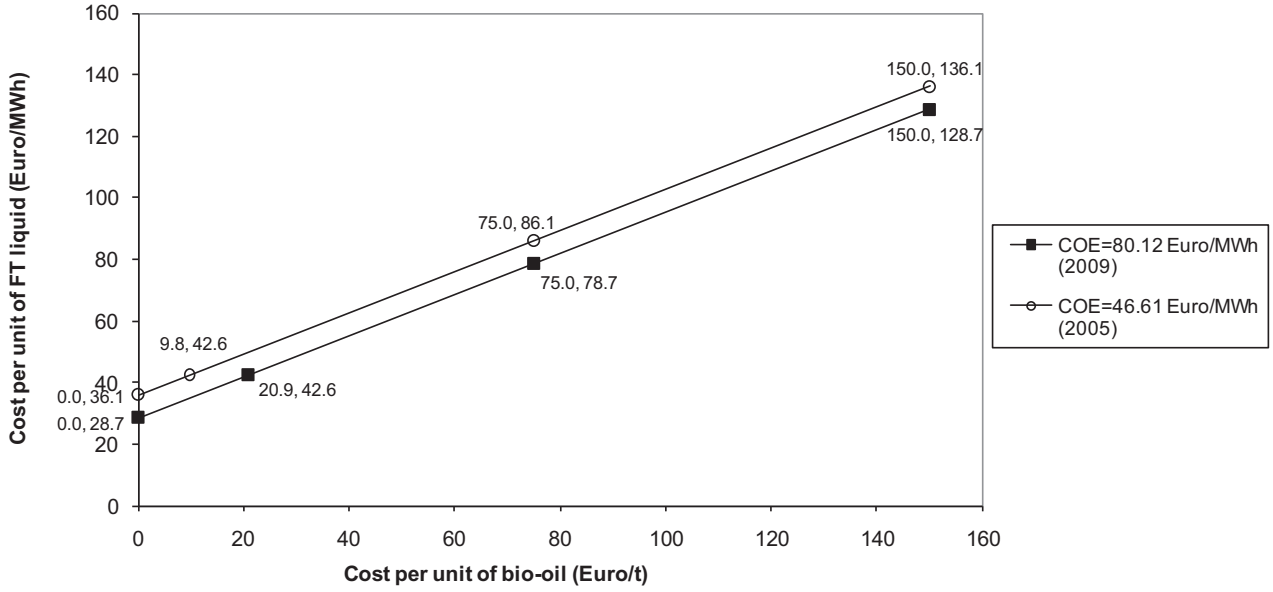

Fig. 8 – Sensitivity analysis on the cost of FT liquid with variation in cost of bio-oil, for 1350 MW BOIG-FT system with full conversion configuration.

biomass, i.e. 29.2–43.15 Euro/MWh and 46 Euro/MWh, respectively [5,42]. A lower electricity price, e.g. 46.6 Euro/MWh in 2005 further enhances the cost of FT liquids to 86.1 Euro/MWh for the same cost of bio-oil of 75 Euro/MWh. If the operating cost of BOIG-FT system can be reduced by 5–20% due to higher energy saving and infrastructure sharing, the COP of FT liquid can be reduced by 0.9–3.7%. 2–8% reduction in COP of FT liquid can be achieved by 5–20% reduction in capital cost. It has also been projected that a reduction in capital by 69% can be achieved after 100th is built, due to technological learning, based on the progress ratio of individual units given by Faaij et al. [43]. Also, economic incentives may be created by versatile price structure for energy commodities through the UK Renewable Obligation Certification, which currently offers a single electricity price from all renewable resources.

4. Conclusions

This paper presents simulation based techno-economic analysis of centralised scale BOIG-FT systems, using bio-oil as feedstock. Bio-oil has been modelled generically and adequately, using three representative chemical components, i.e. acetic acid, acetol and guaiacol, based on its performance through gasification. A comprehensive study has been followed thereafter for deciding on operating conditions for individual processes as well as overall system. Site-wide heat integration was applied for improving the efficiency of the overall system while achieving cost savings through CHP generation. Case studies were performed for 1 MW, 675 MW and 1350 MW, with once-through and full conversion FT reactor configurations. Higher FT conversion was preferable for obtaining higher C_{5+} liquid selectivity. This way, higher efficiency and also lower cost of production of FT liquid can be attained. The 1350 MW BOIG-FT system with full conversion configuration was found to result into the lowest cost of production of FT liquid amongst all the cases studied. The import of bio-oil from other countries by shipping to the UK adds 2–4 times more than the operating cost. This is therefore not feasible under the current economic climate. The BOIG-FT system under research is considered to be a very effective lignocellulosic biorefinery system and commercially deployable within the next 10 years. The capital cost of the BOIG-FT system is thus expected to decrease according to the learning curve effect. It is envisaged that a more competitive cost of production of biofuels from bio-oil can be realised in the future, in the light of increasing value of electricity and reduction in capital and operating costs.

Acknowledgement

The authors would like to express their gratitude to The University of Manchester Alumni Fund and Process Integration Research Consortium for financial aid to support this research.

Nomenclature

A	parameter in equation (5), with values of 0.2332 ± 0.0740
B	parameter in equation (5), with values of 0.6330 ± 0.0420
F_p	total molar flow rate of paraffin produced (kmol/s)
N	carbon number
T	temperature (K)
w_n	weight fraction of Fischer-Tropsch product with carbon number n
$y_{i,S}$	mole fraction of component i (components in product gas) obtained from simulation
$y_{i,R}$	mole fraction of component i (components in product gas) from reference case
$y_{p,n}$	mole fraction of paraffin with carbon number n produced
y_{CO}	mole fraction of CO in Fischer-Tropsch feed stream
y_{H_2}	mole fraction of H_2 in Fischer-Tropsch feed stream
A	probability chain growth

REFERENCES

[1] Goodall NRenewable fuels Agency. RTFO: year two (provisional data), low carbon vehicle partnership, Annual Conference. 15 July 2010 [cited 21 July 2010]. available at: http://www.renewablefuelsagency.gov.uk/sites/rfa/files/LowCVP_Yr2_provisional_results_presentation.pdf; 2010.
[2] Directive 2009/28/EC of the European Parliament and of the Council of 23 April 2009 on the promotion of the use of energy from renewable sources and amending and subsequently repealing Directives 2001/77/EC and 2003/30/EC Official Journal of the European Union 2009. The European Parliament and the Council of the European Union.
[3] Tustin J, Brown A. Potential contribution of bioenergy to the world's future energy demand. IEA Bioenergy; 2007.
[4] Tijmensen MJ, Faaij AP, Hamelinck CN, Hardeveid MV. The production of Fischer-Tropsch liquids and power through biomass gasification. Utrecht, Netherlands: Universiteit Utrecht, Science Technology Society; 2000.
[5] Tijmensen MJA, Faaij APC, Hamelinck CN, van Hardeveld MRM. Exploration of the possibilities for production of Fischer Tropsch liquids and power via biomass gasification. Biomass Bioenerg 2002;23(2):129–52.
[6] Hamelinck CN, Faaij APC, den Uil H, Boerrigter H. Production of FT transportation fuels from biomass; technical options, process analysis and optimisation, and development potential. Energy 2004;29(11):1743–71.
[7] Boerrigter H, Uil HD. Green diesel from biomass via Fischer-Tropsch Synthesis: new insights in gas cleaning and process design. In: Pyrolysis and gasification of biomass and waste, Expert Meeting; 2002. 30th September-1st October. Strasbourg, France.
[8] Bridgwater AV. Renewable transport fuels from biomass. In: International biofuels Opportunities. London: Royal Society; 2007.
[9] Bridgwater AV. Biomass fast pyrolysis. Therm Sci 2004;8(2):21–49.
[10] Bridgwater AV, Peacocke GVC. Fast pyrolysis processes for biomass. Renew Sust Energ Rev 2000;4(1):1–73.
[11] Bridgwater AV. Technical and economic assessment of thermal processes for biofuels. Life cycle and techno-

economic assessment of the Northeast biomass to liquid projects NNFCC project 08/018. COPE Ltd; 2009.
[12] Boerrigter H, Calis HP, Slort DJ, Bodenstaff H, Kaandorp AJ, Uil HD, et al. Gas cleaning for integrated biomass gasification (BG) and Fischer-Tropsch (FT) systems: experimental demonstration of two BG-FT systems ("Proof-of-Principle"). Energy research Centre of the Netherlands (ECN); 2004.
[13] Venderbosch RH, Beld LVD, Prins W. Entrained flow gasification of bio-oil for synthesis gas. Amsterdam, The Netherlands. In: 12th European Conference and technology Exhibition on biomass for energy, Industry and Climate Protection; 2002. p. 556–9.
[14] Knoef HAM. Handbook biomass gasification. Netherlands: BTG Biomass Technology Group; 2005.
[15] Goyal HB, Seal D, Saxena RC. Bio-fuels from thermochemical conversion of renewable resources: a review. Renew Sust Energ Rev 2008;12(2):504–17.
[16] van Rossum G, Kersten SRA, van Swaaij WPM. Catalytic and noncatalytic gasification of pyrolysis oil. Ind Eng Chem Res 2007;46(12):3959–67.
[17] Raffelt K, Henrich E, Koegel A, Stahl R, Steinhardt J, Weirich F. The BTL2 process of biomass utilization entrained-flow gasification of pyrolyzed biomass slurries. In: Twenty-seventh symposium on biotechnology for fuels and chemicals; 2006. p. 153–64.
[18] Edmund H, Nicolaus D, Eckhard D. Cost estimate for biosynfuel production via biosyncrude gasification. Biofuel Bioprod Bior 2009;3(1):28–41.
[19] Poplars, willows and peoples's wellbeings. synthesis of country progress reports - activities related to poplar and willow cultivation and utilization, 2004 through 2007. Working, Paper IPC/6. In: International poplar Commission. Beijing, China: Food and Agriculture Organization of the United Nations (FAO); 2008.
[20] World Growth. Palm oil – The Sustainable oil, 2009. [cited 29 June 2009]. available at: http://www.worldgrowth.org
[21] Abdullah N, Gerhauser H. Bio-oil derived from empty fruit bunches. Fuel 2008;87(12):2606–13.
[22] Smith W. Mapping the development of UK biorefinery Complexes NFC 07/008. Tamutech Consultancy; 2007.
[23] Steynberg AP, Dry ME, Davis BH, Breman BB. Chapter 2 Fischer-Tropsch reactors. In: Steynberg AP, Dry ME, editors. Fischer-Tropsch technology, studies in Surface Science and Catalysis. Elsevier; 2004. p. 64–195.
[24] Sudiro M, Bertucco A. Production of synthetic gasoline and diesel fuel by alternative processes using natural gas and coal: process simulation and optimization. Energy; 2009. doi:10.1016/j.energy.2008.12.009.
[25] Shah M, Raybold T, Jamal A, Drnevich R, Bonaquist D, Jones RIGCC. CO_2 capture ready?. In: Gasification technology Conference; 2005. San Francisco.
[26] Rodrigues M, Walter A, Faaij A. Co-firing of natural gas and biomass gas in biomass integrated gasification/combined cycle systems. Energy 2003;28(11):1115–31.
[27] Burgt MJVD. Chapter 12: Entrained-flow gasification. In: Knoef HAM, editor. Handbook biomass gasification. Netherlands: BTG Biomass Technology Group; 2005. p. 248–58.
[28] Kreyszig E. Advanced Engineering Mathematics. 8th ed. , New York: John Wiley & Sons, Inc; 1999.
[29] Dry ME. The Fischer-Tropsch process: 1950–2000. Catal Today 2002;71(3–4):227–41.
[30] Schulz H. Short history and present trends of Fischer-Tropsch synthesis. Appl Catal A: Gen 1999;186(1–2):3–12.
[31] Vessia Ø. Biofuels from lignocellulosic material in the Norwegian context 2010 –Technology, potential and costs. Trondheim: NTNU; 2005. Norwegian University of Science and Technology, Faculty of information technology, mathematics and electrical engineering, Department of electrical engineering.
[32] Song H-S, Ramkrishna D, Trinh S, Wright H. Operating strategies for Fischer-Tropsch reactors: a model-directed study. Kor J Chem Eng 2004;21(2):308–17.
[33] Ng KS, Lopez Y, Campbell GM, Sadhukhan J. Heat integration and analysis of decarbonised IGCC sites. Chem Eng Res Des 2010;88(2):170–88.
[34] Smith R. Chemical process design and integration. Chichester, U.K: John Wiley and Sons Ltd; 2005.
[35] Kohl AL, Nielsen RB. Gas Purification. 5th ed. Elsevier; 1997.
[36] Lozowski D. Economic Indicators. Chem Eng 2010;117(3):63–4.
[37] Sinnott RK. Coulson & Richardson's chemical Engineering design Volume 6. 4th ed. , Oxford: Elsevier: Butterworth-Heinemann; 2006.
[38] McKeough P, Kurkela E. Process evaluations and design studies in the UCG project 2004–2007. ESPOO; 2008. Research Notes 2434 2008. VTT Tiedotteita.
[39] DECC. Quarterly energy prices: March 2010. Department of Energy and Climate Change (DECC); 2010.
[40] Bradley D. European market study for BioOil (Pyrolysis oil). Clim Change Solution; 2006.
[41] Bridgwater AV. An introduction to fast pyrolysis of biomass for fuels and chemicals. In: Bridgwater AV, Czernik S, Diebold J, Meier DO A, Peacocke C, Piskorz J, et al., editors. Fast pyrolysis of biomass: a Handbook Volume 1. CPL Press; 1999. p. 1–13.
[42] Williams RH, Larson ED, Jin H. F-T liquids production from coal and coal + biomass with CO2 capture and alternative storage options: aquifer CO_2 storage vs CO2-enhanced oil recovery. Review draft; 13 January 2006. 2006.
[43] Faaij A, Meuleman B, Ree RV. Long term perspectives of biomass integrated gasification/combined cycle (BIG/CC) technology: cost and electrical efficiency. Netherlands: Utrecht; 1998.

PUBLICATION 2: Ng, K.S., Sadhukhan, J., Process integration and economic analysis of bio-oil platform for the production of methanol and combined heat and power. *Biomass & Bioenergy*. **35** (3): 1153-1169 (2011).

Available at www.sciencedirect.com

ScienceDirect

http://www.elsevier.com/locate/biombioe

Process integration and economic analysis of bio-oil platform for the production of methanol and combined heat and power

*Kok Siew Ng, Jhuma Sadhukhan**

Centre for Process Integration, School of Chemical Engineering and Analytical Science, University of Manchester, Manchester, M13 9PL, UK

ARTICLE INFO

Article history:
Received 13 July 2010
Received in revised form
22 November 2010
Accepted 1 December 2010
Available online 13 January 2011

Keywords:
Gasification
Methanol
Polygeneration
Bio-oil
Low grade heat
Biorefinery

ABSTRACT

Process to process material and heat integration strategies for bio-oil integrated gasification and methanol synthesis (BOIG-MeOH) systems were developed to assess their technological and economic feasibility. Distributed bio-oil generations and centralised processing enhance resource flexibility and technological feasibility. Economic performance depends on the integration of centralised BOIG-MeOH processes, investigated for cryogenic air separation unit (ASU) and water electrolyser configurations. Design and operating variables of gasification, heat recovery from gases, water and carbon dioxide removal units, water-gas shift and methanol synthesis reactors and CHP network were analysed to improve the overall efficiency and economics. The efficiency of BOIG-MeOH system using bio-oil from various feedstocks was investigated. The system efficiency primarily attributed by the moisture content of the raw material decreases from oilseed rape through miscanthus to poplar wood. Increasing capacity and recycle enhances feasibility, e.g.1350 MW BOIG-MeOH with ASU and 90% recycle configuration achieves an efficiency of 61.5% (methanol, low grade heat and electricity contributions by 89%, 7.9% and 3% respectively) based on poplar wood and the cost of production (COP) of methanol of 318.1 Euro/t for the prices of bio-oil of 75 Euro/t and electricity of 80.12 Euro/MWh, respectively. An additional transportation cost of 4.28–8.89 Euro/t based on 100 km distance between distributed and centralised plants reduces the netback of bio-oil to 40.9–36.3 Euro/t.

1. Introduction

Methanol is globally one of the most important chemicals as well as energy carrier with application to fuel cell vehicles, flexible fuel vehicles and biodiesel production. In recent times, the global demand for methanol has increased by over 43% from 31.4 million tonne in year 2001 [1]. Methanol is produced from syngas using a range of resources, including currently exploited natural gas [2–4], and also other resources such as coal [5,6] and biomass [7–9]. Comparative studies undertaken by Williams et al. [7], Katofsky [8] and Hamelinck and Faaij [9–11] have demonstrated lower energy efficiencies of 54–58% and higher COP of methanol of 14–17 USD/GJ based on biomass feedstock, compared to 67.5% and 6–14.5 USD/GJ from natural gas, respectively. With rapidly growing interest in the development and demonstration of biomass pyrolysis processes, bio-oil or pyrolysis oil can become a promising infrastructure-compatible intermediate for the production of methanol [12–15]. Fast pyrolysis process involves thermal decomposition reactions that occur in a few seconds, at modest temperature conditions (~500 °C) and in the absence of oxygen or oxygen-deficient environment. The capital and operating costs of a biomass fast pyrolysis plant have been estimated to be 48.3 million USD and 9.6 million USD, respectively for producing 426

* *Corresponding author*. Tel.: +44 161 306 4396; fax: +44 161 236 7439.
E-mail address: Jhuma.Sadhukhan@manchester.ac.uk (J. Sadhukhan).
0961-9534/$ – see front matter © 2010 Elsevier Ltd. All rights reserved.
doi:10.1016/j.biombioe.2010.12.003

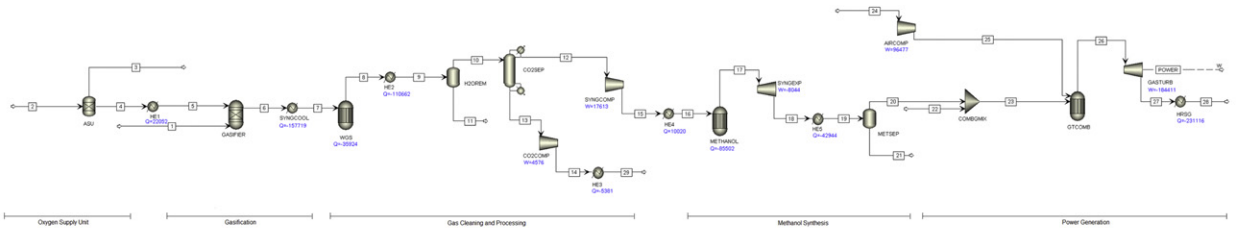

Q: Heat (kW)

W: Power (kW)

Component Mole Fraction	Stream No.																
	1	2	3	4	6	8	10	11	12	16	17	20	21	22	24	28	29
Acetic acid	0.109																
Acetol	0.109																
Guaiacol	0.109																
H_2					0.305	0.459	0.513	0.001	0.687	0.687	0.473	0.734	0.001				
H_2O	0.673				0.253	0.099	0.004	0.912	0.005	0.005	0.007		0.020			0.225	
CO					0.320	0.166	0.185	0.005	0.248	0.248	0.073	0.112	0.003				
CO_2					0.122	0.276	0.298	0.082	0.060	0.060	0.102	0.138	0.037			0.095	1.000
CH_3OH											0.343	0.014	0.938				
O_2		0.210		1.000													
N_2		0.790	1.000												0.210	0.676	
Natural gas / CH_4											0.001	0.002		1.000	0.790		
Molar flow rates (kmol/s)	2.10	5.43	4.29	1.14	6.20	6.20	5.55	0.65	4.14	4.14	2.46	1.58	0.88	0.60	9.00	10.51	1.41
Mass flow rates (t/h)	303.76	563.82	432.50	131.32	435.08	435.08	387.87	47.22	164.92	164.92	164.92	63.64	101.28	34.65	934.75	1033.04	222.95

Fig. 1 – Simulation of BOIG-MeOH flowsheet in ASPEN Plus. The values of heat duties and power shown are for once-through 1350 MW case with ASU configuration.

tons/day of bio-oil from 550 dry tons/day of wood chip [16]. A number of significant advantages exist in fast pyrolysis as a pretreatment step for converting biomass into liquids, ~8–12 times more bulk density; removal of char along with alkali metals; lower tar content; ease and lower cost in handling, storing and transporting liquids to the production as well as reception sites [12]. In addition, bio-oil has an advantage over crude oil during transportation, due to its inert and non-toxic properties and separation into heavy organic fractions that will sink, instead of spreading over the water surface [17]. Consequently, this will not cause severe environmental pollution during a spill or pipeline leakage, as in the incident of Gulf of Mexico oil spill in 2010 [18].

Alongside all these advantages, there exist flexibility in biomass selection for distributed generations of bio-oil and opportunities for industrial scale processing of bio-oil in centralised chemical or fuel production plants, such as, methanol synthesis [12,19]. Brammer et al. [15] and Bridgwater

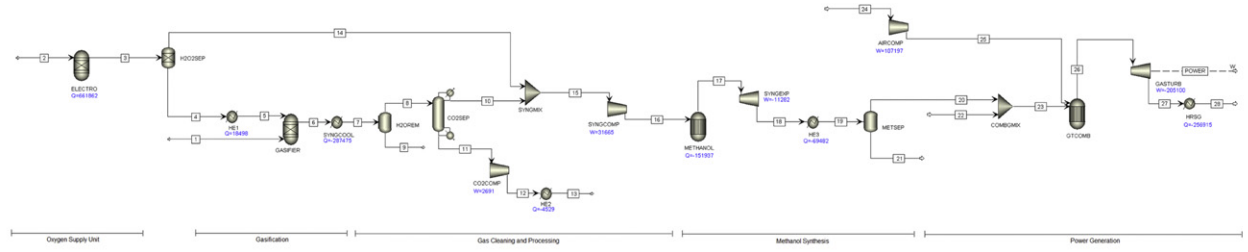

Q: Heat (kW)

W: Power (kW)

Component Mole Fraction	Stream No.															
	1	2	4	6	8	9	10	13	14	16	17	20	21	22	24	28
Acetic acid	0.109															
Acetol	0.109															
Guaiacol	0.109															
H_2				0.305	0.398		0.469		1.000	0.661	0.421	0.727	0.001			
H_2O	0.673	1.000		0.253	0.033	0.973	0.039			0.025	0.002		0.004			0.225
CO				0.320	0.415	0.008	0.49			0.313	0.113	0.191	0.004			
CO_2				0.122	0.153	0.018	0.002	1.000		0.001	0.046	0.066	0.018			0.094
CH_3OH											0.418	0.014	0.972			
O_2			1.000												0.210	
N_2															0.790	0.676
Natural gas / CH_4												0.001		1.000		
Molar flow rates (kmol/s)	2.10	2.28	1.14	6.20	4.75	1.45	4.03	0.72	2.28	6.31	3.43	1.99	1.45	0.60	10.00	11.69
Mass flow rates (t/h)	303.76	147.87	131.32	435.08	338.12	96.96	224.00	114.12	16.55	240.55	240.55	73.03	167.52	34.65	1038.61	1146.29

Fig. 2 – Simulation of BOIG-MeOH flowsheet in ASPEN Plus. The values of heat duties and power shown are for once-through 1350 MW case with electrolyser configuration.

Table 1 – BOIG-MeOH process specification in Aspen simulation.

Unit	ASPEN Plus model	Outlet temperature (°C)	Pressure (bar)	Other specification
AIRCOMP	Compr		14	Isentropic efficiency = 0.9
ASU	Sep			O_2 split fraction = 1.0
CO2COMP	Compr		80	Isentropic efficiency = 0.9
CO2SEP	Sep			CO_2 split fraction = 0.85[A], 0.99[E]
COMBGMIX	Mixer		14	
ELECTRO [E]	RGibbs	130	30	
GASIFIER	RGibbs	1132	30	
GASTURB	Compr		2	Isentropic efficiency = 0.9
GTCOMB	REquil	1200	14	
H2O2SEP	Sep			O_2 split fraction = 1.0
H2OREM	Flash2	50[A], 100[E]	30	
HE1	Heater	630	30	
HE2	Heater	50[A], 35[E]	30[A], 80[E]	
HE3	Heater	35[A], 40[E]	80[A], 24[E]	
HE4 [A]	Heater	270	100	
HE5 [A]	Heater	40	24	
HRSG	Heater	100	1.013	
SYNGCOMP	Compr		100	Isentropic efficiency = 0.9
SYNGCOOL	Heater	450[A], 100[E]	30	
SYNGEXP	Compr		40	Isentropic efficiency = 0.9
SYNGMIX [E]	Mixer		30	
METHANOL	REquil	250	100	
METSEP	Flash2	40	24	
WGS [A]	REquil	450	30	

'Compr' = Compressor/turbine; 'Sep' = Component separator; 'RGibbs' = Gibbs reactor; 'REquil' = Equilibrium reactor; 'Flash2' = Two-outlet flash; 'Heater' = Heater; 'Mixer' = Stream mixer. [A] denotes ASU configuration while [E] denotes electrolyser configuration.

et al. [13] investigated into the commercial competitiveness of bio-oil systems for a range of applications, heat, power and CHP. The economic attractiveness depends on many factors, including the scale, the location and its associated economic and logistic factors, e.g. availability and price against competitive fossil resources and industrial practices etc. It is clear from their studies that the centralised applications of bio-oil enhance economic competitiveness. Building upon these concepts [12–15], this study explores process integration opportunities for the conversion of bio-oil from distributed pyrolysis plants as a commodity through a centralised methanol synthesis plant. The evaluation of commercial opportunities is undertaken by quantitative assessment of the number of commercial/demonstrated process units required. These include gasification, methanol synthesis and oxygen supply units that may be exploited in distributed and centralised scales respectively. The approach here was also to use a range of scales, 1 MW through 675 MW–1350 MW based on thermal input of bio-oil to a specific application and carry out economic assessment and sensitivity to important cost factors, such as the price of electricity and the transportation cost of bio-oil (in the context of the UK and EU) [13,14,20] which determine the acceptable buy-in price of bio-oil for conversion.

Bio-oil can be resourced from wood such as poplar. The UK has a total poplar plantation area of approximately 11337 ha (0.01% of global): England (88.2%), Wales (4.8%), Scotland (4.3%) and Northern Ireland (2.7%), with mean yield of 7.3 odt/ha per year [21–23]. Due to the limited local supply of poplar wood, indigenous resources such as miscanthus and oilseed rape can be used. The plantation area of miscanthus in the UK has been reported to be 12700 ha, with yield of 9–10 odt/ha per year [24]. Oilseed rape has a plantation area of 85711 ha, with yield of 2.5–3.3 t/ha [24]. The process under consideration was based on poplar wood and further established for the above energy crop and agricultural waste.

Table 2 – Technology developers and capacities of the major process units.

Process Unit	Technology Developer	Capacity for single unit	Type of process unit selected
Gasifier	Shell, GE, E-Gas, Koppers Totzek, Destec, Prenflo, etc.	up to 2000 t/d of coal [30]	Entrained flow
Methanol synthesis reactor	Lurgi, ICI, Air Products, etc.	5000 t/d of methanol [31]	Fixed bed, gas phase, isothermal
Electrolyser	Proton Energy Systems, Hydrogenics, Norsk Hydro Electrolysers AS, etc.	10–60 Nm^3/h of hydrogen [32]	Pressurised alkaline electrolysis process
Cryogenic ASU	Air Products, Universal Industrial Gases, etc.	90–820 t/d of oxygen [33]	Oxygen production

Table 3 – Validation of gasification model based on the proximate and ultimate analyses of bio-oil, under given input and operating conditions [34].

Gasifier operating condition			
Temperature	1300 °C		
Pressure	30 bar		
Bio-oil	1 kmol/s (29.6 mol% oil and 70.4 mol% water/moisture)		
Oxygen	0.57 kmol/s		
Proximate Analysis, as received (mass %)		Ultimate Analysis, moisture and ash free (mass %)	
Fixed carbon and volatile matter	70	C	56
Moisture	30	O	37
Ash	0	H	7
LHV, as received (MJ/kg)	15.6		
LHV, moisture and ash free (MJ/kg)	23.3		

Component	Mole fraction (%)		Residual sum of square = (Reference − Simulation)^2
	Reference	Simulation	
Product gas composition			
H_2	29.4	29.1	0.09
H_2O	26.3	26.7	0.19
CO	33.8	33.5	0.10
CO_2	10.5	10.7	0.03
CH_4	0.01	0.005	2.3×10^{-5}
			0.41

The process-related elements in this work include facilitation of partial oxidation within bio-oil gasification to achieve thermally efficient performance in fluidised bed and entrained flow bed gasifiers [25–27], process design and variability studies for feed conditioning for methanol synthesis reactor, using heat integration strategy [7–9,28,29]. The effect of increased thermal efficiency of the gasifier is the reduction in mole fraction of hydrogen in the product gas from the gasifier, which can be compensated by exothermic water-gas shift reactor (alternatively supplied from water electrolysis), operating at lower temperatures. In addition to achieving the desired molar stoichiometric number (*SN*) of the feed gas to methanol synthesis reactor, the degree of water and carbon removal from the product gas by incorporation of appropriate technologies on the yield of methanol and plant efficiency has been analysed. Emphasis was given on total site CHP network synthesis and hot water recovery and thereby improving overall site energy efficiency. The objectives of this paper were thus to investigate technical and economic feasibility of bio-oil based methanol synthesis technologies with a view in commercial deployment over short-term future.

2. Process simulation and sensitivity studies

Two BOIG-MeOH process configurations with cryogenic ASU and water electrolyser that comprised of gasification, gas cleaning and processing, methanol synthesis and power generation are depicted in Figs. 1 and 2, respectively. The process operating variables specified in ASPEN Plus simulation are presented in Table 1.

Table 2 summarises the technology developers and capacities of the main units [30–33]. A single state-of-the-art pyrolyser unit of 200 t/d throughput of biomass produces 150 t/d of bio-oil [12]. A single train entrained flow gasifier [30] can process 2000 t/d of bio-oil from 14 such pyrolysis plants, to produce ~600 t/d of methanol. An oxygen-blown gasifier is opted since air will lower the heating value of the resulting product gas. The oxygen requirement for single train gasifier is 860 t/d, requiring one train cryogenic ASU unit [33]. A Lurgi methanol synthesis reactor [31] thus may produce 2270 t/d of methanol from 7290 t/d of bio-oil from 49 pyrolysis units, and 4 integrated gasification and ASU units, in a centralised 1350 MW (thermal input of bio-oil) BOIG-MEOH process.

Bio-oil was modelled using three representative components, i.e. acetic acid, acetol and guaiacol, indicated in Table 3, while RGibbs reactor (works on Gibbs free energy minimisation principles) was used to model the gasifier (Table 1). The simulation results of the bio-oil gasification were validated against literature results [34], with residual sum of square (RSS) obtained within an acceptable range (Table 3). Water electrolyser modelled as another RGibbs reactor (Table 1), is operated at 130 °C and 30 bar [34] (Fig. 2). Nitrogen generated from the cryogenic ASU (Fig. 1), modelled as a component separator, Sep (Table 1), can be used for purging the reactor vessels or can be sold.

A thermally neutral performance of the oxygen-blown entrained flow bio-oil gasifier (stream 1 to GASIFIER in Figs. 1 and 2) can be attained at ~1100 °C. This is achieved by preheating oxygen (stream 4) feed from ASU to a temperature of 630 °C [35] using very high pressure (VHP) steam generated by the heat recovery from the product gas of the gasifier. This way heat recovered at a lower level can be utilised in supplying endothermic heat of reforming reactions at a higher gasifier temperature. Bio-oil may not need to be preheated so as to prevent degradation and formation of char before entering the gasifier [26,36]. The product gas (stream 6) comprising of CO, CO_2, H_2 and H_2O as the main components, is likely to be free from tar, ash, nitrogen and sulphur, as bio-oil is relatively clean [12].

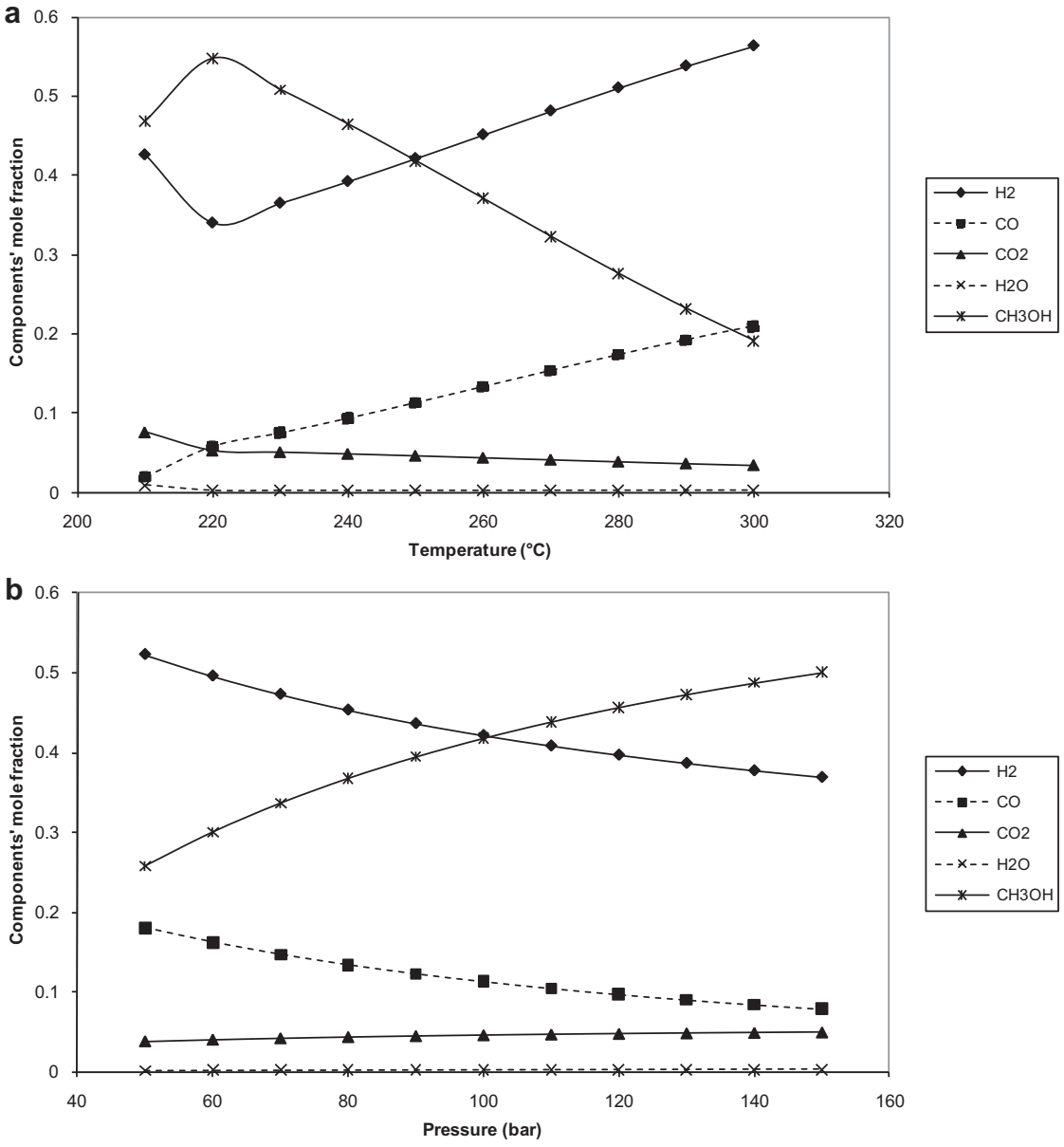

Fig. 3 – (a) Variation of components' mole fraction with temperature (pressure = 100 bar). (b) Variation of components' mole fraction with pressure (temperature = 250 °C).

Subsequently, heat from the product gas was recovered into the generation of VHP steam (SYNGCOOL). A water-gas shift reactor (WGS in Fig. 1) was needed prior to gas cooling for water removal in the ASU configuration. These are mainly to attain an appropriate molar stoichiometric number (*SN*): $(H_2 - CO_2)/(CO + CO_2) = 2$ [4,8] in the feed gas to the methanol synthesis reactor. In electrolyser configuration (Fig. 2), the stoichiometric ratio was met by supplying H_2 from the electrolyser, requiring no WGS reactor. In both configurations, the product gas was cooled to just above its dew point for water removal (H2OREM). The dry gas has a much enhanced performance in the methanol synthesis reactor, analysed later. The water removed can be sent to waste water treatment plant, comprising of physical, chemical or biological processes, and recovered as boiler feed water after 10% purge [37], the cost of which was considered

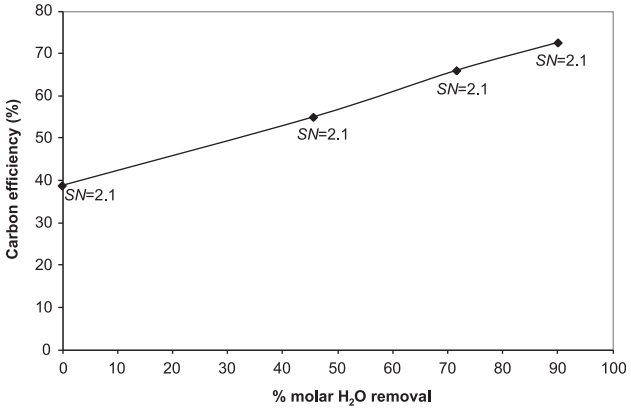

Fig. 4 – Effect of H_2O removal on carbon efficiency.

later. CO_2 in the product gas is removed using Sulfinol unit (combined physical and chemical solvent process) (CO2SEP) by 99% and 85% on molar basis, in electrolyser and ASU configurations respectively [38]. The CO_2 captured was compressed through CO2COMP to supercritical CO_2 at 80 bar, suitable for storage [39]. Subsequently, the clean syngas was compressed through SYNGCOMP to 100 bar prior to the methanol synthesis reactor (METHANOL).

A Lurgi isothermal and gaseous phase fixed bed methanol synthesis reactor can be suitable for the operating conditions provided in Table 1. The sensitivity analyses of methanol synthesis in terms of temperature and pressure conditions were performed, presented in the following section. The pressure of the gaseous product stream from METHANOL was brought down from 100 bar to 40 bar, by expanding through SYNGEXP (Figs. 1 and 2). The feed gas compressor and the product gas expander can be run on the same shaft. A minimum outlet pressure of 40 bar was achievable while keeping the outlet at gaseous phase. A flash column (METSEP) was further used to separate the gaseous and liquid products at 40 °C and 24 bar [29]. 98% recovery (molar basis) of methanol in the liquid product (stream 21) from METSEP can be achieved. The offgas containing unreacted gases such as H_2, CO, CH_4 etc. (stream 20) was fed to the gas turbine (GASTURB) for power generation.

A trace amount of natural gas (stream 22) was required for achieving a stable operating region and to refrain from modification of the gas turbine combustor [40]. The resulting Wobbe Index of the gas turbine (measure of interchangeability of fuel gases and for comparing the combustion energy among fuel gases with different compositions) was validated against industrial study by Shah et al. [41], in order to ensure that it was within ±10% of the stable combustion region. Air was supplied to the gas turbine combustor (GTCOMB), after compression to 14 bar via AIRCOMP. GTCOMB, operating at 1200 °C and 14 bar, did not require de-rating (reduction in burning temperature and compressor power ratio to allow a stable combustion), because the LHV of the gas feed into the combustor was found to be greater than 6 MJ/m^3 [38,40]. The exit temperature and pressure of the exhaust gas from the GASTURB are approximately 740 °C and 2 bar, respectively. The heat content of the exhaust gas from GASTURB was recovered into the generation of VHP steam in heat recovery steam generator (HRSG).

2.1. *Sensitivity studies of methanol synthesis reaction*

The principal reactions involved in the methanol synthesis reactor, modelled as a stoichiometric reactor (RStoic) in ASPEN Plus, are provided in Eqs. (1)–(3) [2]. Methanol synthesis reactors operate within 50–150 bar pressure and 230 °C–270 °C temperature, in the presence of Cu/Zn/Al catalyst [10].

$$CO + 2H_2 \leftrightarrow CH_3OH \quad \Delta H_R^\circ = -90.6\text{kJ/mol} \tag{1}$$

$$CO_2 + 3H_2 \leftrightarrow CH_3OH + H_2O \quad \Delta H_R^\circ = -49.7\text{kJ/mol} \tag{2}$$

$$CO + H_2O \leftrightarrow H_2 + CO_2 \quad \Delta H_R^\circ = -41.5\text{kJ/mol} \tag{3}$$

Low temperature and high pressure favour the reactions, according to Le Chatelier's principle. The temperature and pressure effects on the components' mole fractions are

Table 4 – Sensitivity analysis of operating conditions of WGS and CO2SEP on molar stoichiometric number (SN) of reactants in the methanol synthesis reactor in Fig. 1.

Temperature of WGS (°C)	Outlet of WGS						Outlet of CO2SEP											
	Components' molar flow rate (kmol/s)				SN	H_2/CO	SN						CO/CO_2					
	CO	CO_2	H_2	H_2O			99%	90%	**85%**	80%	75%	70%	99%	90%	**85%**	80%	75%	70%
200	0.24	1.13	1.70	0.03	0.41	7.06	6.70	4.49	3.73	3.16	2.71	2.35	21.35	2.13	1.42	1.07	0.85	0.71
250	0.28	1.09	1.66	0.07	0.41	5.95	5.69	4.00	3.39	2.91	2.52	2.21	25.72	2.57	1.71	1.29	1.03	0.86
300	0.33	1.04	1.61	0.12	0.41	4.87	4.69	3.47	3.00	2.62	2.30	2.03	32.15	3.22	2.14	1.61	1.29	1.07
350	0.39	0.98	1.55	0.18	0.41	3.97	3.85	2.99	2.63	2.33	2.07	1.86	40.48	4.05	2.70	2.02	1.62	1.35
400	0.45	0.92	1.48	0.25	0.41	3.28	3.20	2.58	2.30	2.07	1.87	1.69	50.52	5.05	3.37	2.53	2.02	1.68
450	**0.51**	**0.85**	**1.42**	**0.31**	**0.41**	**2.77**	2.71	2.24	**2.03**	1.85	1.69	1.54	62.09	6.21	**4.14**	3.10	2.48	2.07
500	0.57	0.79	1.36	0.37	0.41	2.38	2.33	1.98	1.81	1.66	1.53	1.41	75.00	7.50	5.00	3.75	3.00	2.50

Note: Outlet of WGS refers to stream 8 while outlet of CO2SEP refers to stream 12 in Fig. 1.

Table 5 – Data extracted from simulation and classification of heat utilisation and consumption for heat integration analysis. (a) ASU configuration. (b) Electrolyser configuration.

Process Unit	Supply Temperature (°C)	Target Temperature (°C)	Heat Duty (kW)			Heat supply /demand	Heat utilisation and consumption
			1 MW	675 MW	1350 MW		
(a)							
GASIFIER	1133	1133	0	11	20	neutral	
HE1	25	630	16	11026	22052	demand	supplied from VHP steam
HE2	450	50	82	55317	110662	supply	generate steam (MP)
HE3	130.8	35	4	2690	5381	supply	generate hot water
HE4	190.4	270	7	5007	10020	demand	supplied from VHP steam
HE5	169.9	40	32	21455	42944	supply	generate hot water
HRSG	737.2	100	236	95307	231116	supply	generate steam (VHP)
METHANOL	250	250	63	42714	85502	supply	generate steam (MP)
SYNGCOOL	1133	450	117	78949	157719	supply	generate steam (VHP)
WGS	450	450	27	17969	35924	supply	generate steam (MP)
(b)							
GASIFIER	1133	1133	0	11	20	neutral	
HE1	130	630	14	9249	18498	demand	supplied from VHP steam
HE2	188.5	35	3	2262	4529	supply	generate hot water
HE3	250	40	51	34726	69482	supply	generate hot water
HRSG	745.3	100	241	128448	256915	supply	generate steam (VHP)
METHANOL	250	250	112	75938	151937	supply	generate steam (MP)
SYNGCOOL	1133	100	213	143824	287475	supply	generate steam (VHP)

illustrated in Fig. 3(a) and (b), respectively. The efficiency is increased from 50 bar, 300 °C (20.9%) through 100 bar, 250 °C (48.3%) to 150 bar, 210 °C (67.4%). However, at a very low temperature the rate of reaction is very slow, while a very high pressure necessitates high compression energy and contemplation for equipment for safety reasons. Therefore, to attain the required rate of reaction and moderate compression energy, 250 °C and 100 bar are recommended [10].

The ideal value of *SN* is 2, however a *SN* of slightly higher than 2 is used in practice, in order to control the by-product formation [3]. *SN* greater than 2 is attained by higher hydrogen and lower CO_2 molar fractions in the syngas. The *SN* must be adjusted prior to the methanol synthesis reaction to ensure higher conversion and selectivity to methanol. A small amount of CO_2, 1–2%, that may act as a promoter for the primary reaction (Eq. (1)) and help in maintaining catalyst activity, is also required in the feed gas [8,10].

Water in the feed stream to methanol synthesis reactor is undesirable due to its dilution effect and facilitation of water-gas shift reaction (Eq. (3)), resulting in CO_2 instead of methanol. *SN* does not account for the molar ratio of water in the feed. Fig. 4 indicates that the removal of water from 0% to 90% on molar basis results in an increase in carbon efficiency, defined in Eq. (4), from 38.7% to 72.5%, while *SN* remains unchanged at 2.1. Thus, higher degree of water removal is desired alongside higher carbon efficiency, hence moles of methanol produced, whilst conforming to the specification of *SN*.

Furthermore, Table 4 presents a sensitivity analysis of the effect of temperature of WGS and the degree of CO_2 removal on *SN* for ASU configuration (Fig. 1). The water-gas shift reaction in Eq. (3) is favoured at low temperatures, thereby improving the H_2/CO molar ratio. A WGS operating temperature of 450 °C, which provides reasonable performance of its catalyst and reaction, and the removal of CO_2 by 85% on molar basis, can attain a *SN* of 2.03 and CO/CO_2 molar ratio of 4.14 in the feed gas.

3. CHP network design and energy efficiency

The supply and the target temperatures as well as the heat duties of the streams and process units were extracted from the integrated flowsheet simulations, shown in Table 5(a) and (b) for ASU and electrolyser cases in Figs. 1 and 2, respectively. Heat utilisation and consumption were classified based on the heat duties/temperature levels, in Table 5(a) and (b), respectively [42,43].

The VHP and MP steam that can be generated by the maximum recovery of the sensible heat from SYNGCOOL and HRSG and the product gas of WGS (HE2 in Fig. 1), was estimated using the composite curve analysis, within the specified minimum approach temperature, 20 °C [43,44]. The targeted steam main levels are VHP steam (100 bar, 650 °C superheated), MP steam (15 bar, 200 °C saturated) and LP steam (5 bar, 152 °C saturated), in line with industrial

$$\text{Carbon efficiency (\%)} = \frac{\text{moles of methanol produced}}{\text{moles of carbon oxides (CO + CO}_2\text{) in feed}} \times 100\% \quad (4)$$

processes [45]. The analysis is presented in Fig. 5(a), (b) and (c), respectively. Isothermal conditions in WGS and METHANOL were maintained by extracting their respective exothermic heat of reactions into MP steam generation (using enthalpy balance) on the shell side of the reactor.

The heat demands were placed by O_2 preheater (HE1), HE4 (in ASU configuration), Sulfinol unit and methanol distillation unit. The VHP steam was used in HE1 and HE4 for preheating based on composite curve analysis. The steam requirements by the Sulfinol and methanol distillation units, not simulated in ASPEN Plus, were estimated using industrial data, 1.42 kg of LP steam/kg of acid gas and 0.45 kg of LP steam/kg of methanol, respectively [46,47].

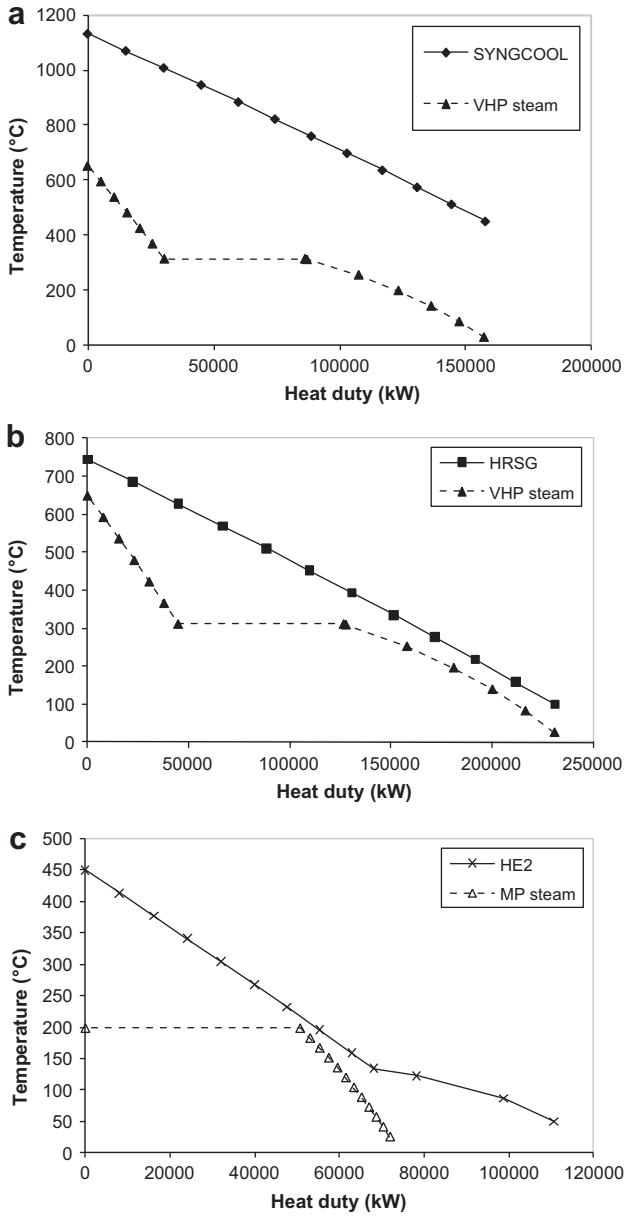

Fig. 5 – Composite curve analysis for determining the amount of steam generation from (a) SYNGCOOL, (b) HRSG and (c) HE2, in once-through 1350 MW BOIG-MeOH system with ASU configuration.

The CHP network is depicted in Fig. 6. The back-pressure steam turbines ST1 and ST2 are operated between VHP and LP steam levels and ST3 between MP and LP steam levels respectively. The condensing turbine, ST4 was further used to generate power after fulfilling the LP steam requirement by Sulfinol and methanol distillation units. 80% isentropic and 95% mechanical efficiencies were assumed.

The energy balance around two systems, comprising of the process site (Figs. 1 and 2) and the CHP network (e.g. Fig. 6), was analysed for 1 MW, 675 MW and 1350 MW capacities with once-through mode, and recycle mode (90%) for 1350 MW capacity, in Tables 6 and 7, respectively. The recycle mode refers to the recycling of the offgas from the methanol synthesis reactor (stream 20 in Figs. 1 and 2). It leads to higher production of methanol, in relation to the generation of power. The power requirement by the cryogenic ASU unit was estimated based on 235 kWh/t O_2 requirement by the site (Fig. 1) [48]. The power requirement by the water electrolyser unit was estimated to be 4049 kWh/t in ASPEN Plus simulation (Fig. 2).

The efficiency of an overall site was calculated based on the LHV of the bio-oil and the production of methanol and electricity, for both with and without the generation of low grade heat (Tables 6 and 7). The LHV of methanol was assumed to be 20 MJ/kg. In the ASU configuration in Fig. 1, the surplus low grade heat included the heat from HE3, HE5, excess heat from HE2 and heat released from the condenser (after condensing turbine ST4). The heat available from HE2, HE3, excess from SYNGCOOL (after the heat recovery using composite curve analysis) and condenser (after condensing turbine ST4) provided the low grade heat for the electrolyser configuration. The surplus low grade heat from the site can be recovered into hot water generation, which is particularly important in the current EU scenario where solar energy is targeted for domestic hot water generation. The electrolyser configuration consumes 3.6–5.3 times of power higher than the ASU configuration. Obviously, this is attributed to the high power requirement by the water electrolyser unit, 75–79% of the total power consumption on site, whilst the ASU only consumes 15.6–24.1%, respectively. The electrolyser configuration with recycle mode produces more methanol, compared to equivalent ASU cases; however at a cost of additional power requirement. The net energy efficiency of the sites increases with increasing capacity, due to higher proportional increment in power generation from syngas expander and gas and steam turbines from 0.14 MW through 117.4 MW–276.2 MW, for 1 MW, 675 MW and 1350 MW cases (ASU configuration), respectively.

The analysis of bio-oils derived from different biomass sources, poplar [34], miscanthus [49] and oilseed rape [50], is presented in Table 8(a). The heating values, chemical composition and moisture content have strong influence on the efficiency of BOIG-MeOH system. The efficiency increases from poplar (48.3%) through miscanthus (66.9%) to oilseed rape (68.2%), respectively (Table 8(b) presented for 1350 MW BOIG-MeOH with ASU configuration). The net energy efficiency is thus strongly influenced by their moisture contents, 30%, 10.1% and 9.5% more than their carbon and hydrogen wt%, 63%, 72.5% and 89.5%, respectively in Table 8(a).

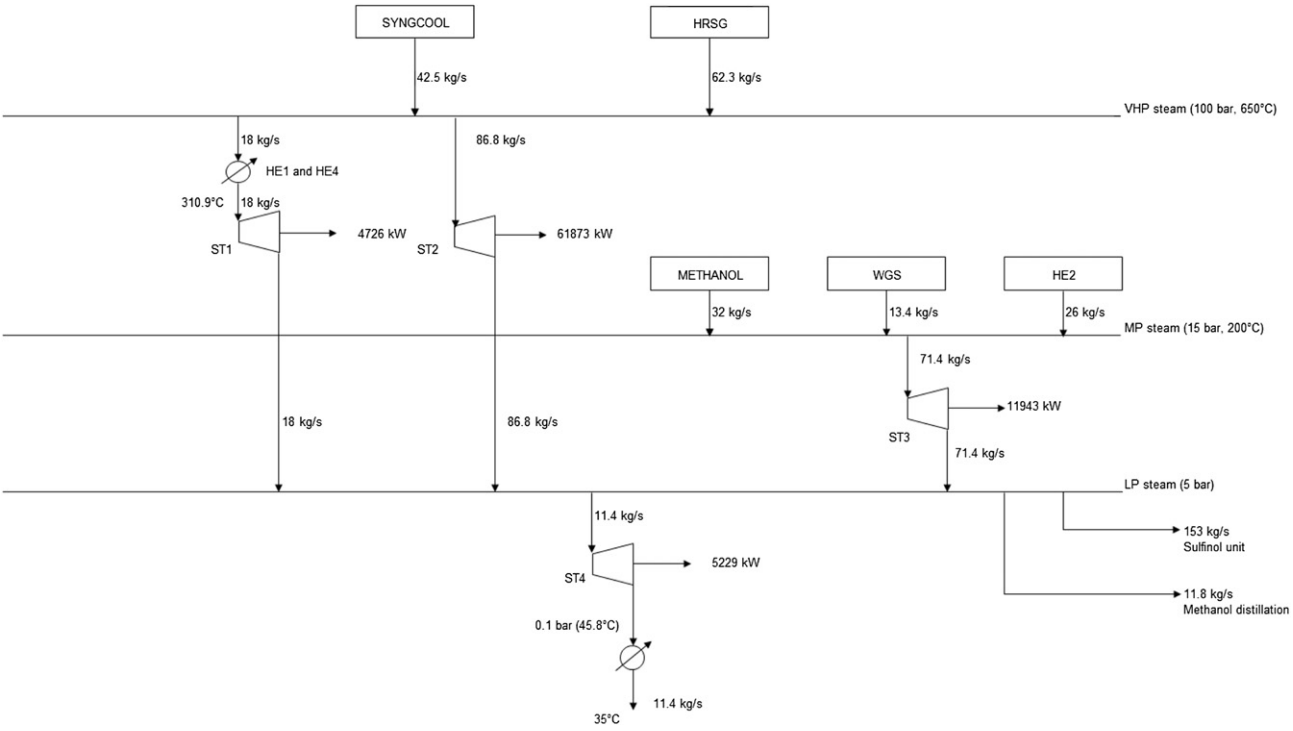

Fig. 6 – Heat and power network for once-through 1350 MW BOIG-MeOH system with ASU configuration.

4. Economic analysis

The objective of the detailed economic analysis was to evaluate the netback of the bio-oil feedstock and the COP of methanol, and their sensitivity with respect to the price fluctuation of certain components, capital, operating and transportation costs.

4.1. *Capital costs*

The capital cost of the processes under consideration (Figs. 1 and 2) has been evaluated in terms of the direct and indirect capital costs. The inside battery limit (ISBL) cost data, the base costs, scale factors and base scales, of the major process units, the outside battery limit (OSBL) costs and the indirect capital costs were estimated based on the works of Tijmensen et al. [38] and Hamelinck and Faaij [9], in Table 9. A scale factor, R was applied in the cost and size correlation in Eq. (5) [51], for evaluating various sizes of individual equipment, unless otherwise specified. Multiple units were considered if a desired capacity of a unit exceeds its maximum size, e.g. 400 MW HHV for the gasifier [38]. It was assumed that the Sulfinol unit accounted for 10% of the total capital cost, that is a proprietary information [38]. The cost of ASU was estimated based on the parameters provided in Table 9 (item 8) and using Eq. (5), while that of the water electrolyser was estimated based on 7500 SEK (Swedish Krona)/kW, Saxe and Alvfors [52], which is equivalent to 825 Euro/kW in 2007.

$$\frac{\mathrm{COST}_{\mathrm{size2}}}{\mathrm{COST}_{\mathrm{size1}}} = \left(\frac{\mathrm{SIZE}_2}{\mathrm{SIZE}_1}\right)^R \quad (5)$$

SIZE_1 and $\mathrm{COST}_{\mathrm{size1}}$ represent the capacity and the cost of a base unit, whilst SIZE_2 and $\mathrm{COST}_{\mathrm{size2}}$ represent the capacity and the cost of the unit after scaling up/down, respectively.

The capital costs of individual equipment were further levelised to year 2009 by applying a cost index (Eq. (6)), adopted from Chemical Engineering Plant Cost Index (CEPCI) [53].

$$\text{Present cost} = \text{Original cost} \times \left(\frac{\text{Index at present}}{\text{Index when original cost was obtained}}\right) \quad (6)$$

Fig. 7 illustrates the breakup of capital costs of individual equipment in a BOIG-MeOH configuration. The oxygen supply units remain one of the major contributors to the total capital cost, 18.6% and 52.5% for ASU and electrolyser configurations respectively. In addition to lower overall efficiency (albeit higher methanol production), the electrolyser configuration results in 65.2% higher capital cost than that of ASU configuration.

4.2. *Operating costs*

The fixed operating costs were estimated based on a percentage of the total indirect capital (TIC), given in Table 10. The cost of the personnel was estimated based on the study by Tijmensen et al. [54]. The fixed operating costs were evaluated according to the work of Sinnott [55]. Variable operating costs include the costs of natural gas [56] considered in all cases, electricity [56] in electrolyser configuration and steam [55] in 1350 MW, recycle mode ASU configuration, respectively. Finally, the percentage of miscellaneous cost was adopted from the work of Sinnott [55].

Table 6 – Energy balance for different capacities of BOIG-MeOH system with ASU configuration.

System mode	Once-through						Recycle (90%)	
System capacity	1 MW		675 MW		1350 MW		1350 MW	
	kW	kg/s	kW	kg/s	kW	kg/s	kW	kg/s
Heat recovery into steam generation	**372.1**	**0.115**	**270346.8**	**82.6**	**581501.1**	**176.2**	**453225.3**	**144.4**
SYNGCOOL (VHP, 100 bar)	111.1	0.030	78531.6	21.2	157433.6	42.5	157433.6	42.5
HRSG (VHP, 100 bar)	118.5	0.032	95201.0	25.7	230779.1	62.3	74827.3	20.2
METHANOL (MP, 15 bar)	63.0	0.024	42714.0	16.0	85502.0	32.0	113178.0	42.3
WGS (MP, 15 bar)	27.0	0.010	17969.0	6.7	35924.0	13.4	35924.0	13.4
HE2 (MP, 15 bar)	52.5	0.019	35931.2	13.0	71862.4	26.0	71862.4	26.0
Heat supplied to process units using generated steam	**280.2**	**0.135**	**189732.2**	**91.4**	**379451.0**	**182.8**	**389632.6**	**187.6**
HE1 and HE4	23.0	0.013	16033.0	9.0	32072.0	18.0	32072.0	18.0
Sulfinol unit	238.2	0.113	161262.0	76.5	322504.6	153.0	322504.6	153.0
Methanol distillation unit	19.0	0.009	12437.2	5.9	24874.4	11.8	35056.0	16.6
Surplus LP steam into condensing turbine ST4	**0.0**	**0.0**	**463.8**	**0.22**	**24031.2**	**11.4**	**−53121.6**	**−25.2**
Net heat generation	**65.4**		**44005.0**		**111664.6**		**65956.9**	
Power generation from site	**107.0**		**81922.0**		**192455.0**		**79628.0**	
GASTURB	101.0		77902.0		184411.0		60521.0	
SYNGEXP	6.0		4020.0		8044.0		19107.0	
Power generation from steam turbine	**35.0**		**35451.0**		**83771.0**		**47283.0**	
ST1	3.0		2364.0		4726.0		1750.0	
ST2	23.0		27016.0		61873.0		31863.0	
ST3	9.0		5970.0		11943.0		13670.0	
ST4	0.0		101.0		5229.0		0.0	
Power requirement on site	**81.8**		**64037.1**		**149526.9**		**101955.9**	
ASU	22.8		15430.1		30860.9		30860.9	
SYNGCOMP	13.0		8800.0		17613.0		34360.0	
CO2COMP	3.0		2288.0		4576.0		4576.0	
AIRCOMP	43.0		37519.0		96477.0		32159.0	
Net power generation	**60.2**		**53335.9**		**126699.1**		**24955.1**	
Production of methanol	388.0	0.019	262800.0	13.4	526000.0	26.3	739111.1	37.0
Efficiency based on LHV, (methanol + electricity)/bio-oil (%)	**44.8**		**46.8**		**48.3**		**56.6**	
Efficiency based on LHV, (methanol + electricity + net heat)/bio-oil (%)	**51.4**		**53.4**		**56.6**		**61.5**	

The bold numbers represent the sum of values within a specified category.

4.3. *Discounted cash flow, netback of bio-oil and cost of production of methanol analysis*

An instance of discounted cash flow analysis is presented that provides an annualised capital charge of 13% for a discount rate of 10% and 15 operating years. The start-up period is 2 years, with 25% and 75% of the total capital cost were distributed in the−1st and 0th year (0th year indicates the plant start-up year) [54].

The netback indicates the value of a feedstock obtained from selling its products at their market prices and is determined using expression (7) [43]. The netback thus sets the maximum acceptable buy-in price of a feedstock. The market price of the feedstock thus must be less than this price for an economic processing.

$$\text{Netback} = \text{Value from products} - (\text{Annualised capital cost} + \text{Annual operating cost}) \quad (7)$$

The contract price of methanol in the European region as posted by Methanex is 250 Euro/t (valid from 1st April to 30th June, 2010) [57]. The price of electricity was adopted from DECC [56], reported at 7.284 pence/kWh (2009) (equivalent to 80.12 Euro/MWh, assuming 1 GBP = 1.1 Euro), excluding the Climate Change Levy (CCL). The CCL only applies to industrial sectors where taxable supplies such as electricity, coal and petroleum are charged [58]. The full rate of CCL for the electricity is reported at 0.47 pence/kWh (equivalent to 5.17 Euro/MWh) [56]. A comparison of annualised capital charge, annual operating cost and the value of products and the netback of bio-oil (both, with and without CCL) between the ASU and electrolyser configurations for 1 MW, 675 MW and 1350 MW capacities is presented in Table 11. The COP [59] of methanol was calculated using Eq. (8), based on the price of bio-oil at 75 Euro/t [60], and the cost of electricity at 80.12 Euro/MWh in year 2009 [56].

$$\text{COP of methanol} = \frac{\text{Annualised capital cost} + \text{Annual operating cost} + \text{Cost of bio} - \text{oil} - \text{Cost of electricity generated}}{\text{Annual production of methanol}} \quad (8)$$

Table 7 – Energy balance for different capacities of BOIG-MeOH system with electrolyser configuration.

System mode	Once-through						Recycle (90%)	
System capacity	1 MW		675 MW		1350 MW		1350 MW	
	kW	kg/s	kW	kg/s	kW	kg/s	kW	kg/s
Heat recovery into steam generation	**419.4**	**0.125**	**327831.8**	**96.4**	**659428.9**	**193.8**	**523994.5**	**161.7**
SYNGCOOL (VHP, 100 bar)	185.2	0.050	125946.9	34.0	251893.8	68.0	251893.8	68.0
HRSG (VHP, 100 bar)	122.2	0.033	125946.9	34.0	255598.1	69.0	77790.7	21.0
METHANOL (MP, 15 bar)	112.0	0.042	75938.0	28.4	151937.0	56.8	194310.0	72.7
Heat supplied to process units using generated steam	**254.3**	**0.128**	**170932.6**	**85.7**	**342497.6**	**171.7**	**356621.2**	**178.4**
HE1	14.0	0.014	9249.0	9.0	18498.0	18.0	18498.0	18.0
Sulfinol unit	208.7	0.099	140392.8	66.6	281207.2	133.4	281207.2	133.4
Methanol distillation unit	31.6	0.015	21290.8	10.1	42792.4	20.3	56916.0	27.0
Surplus LP steam into condensing turbine ST4	**23.2**	**0.011**	**41316.8**	**19.6**	**84530.8**	**40.1**	**2677.2**	**1.27**
Net heat generation	**105.7**		**97100.1**		**196001.2**		**148096.2**	
Power generation from site	**114.0**		**108177.0**		**216382.0**		86960.0	
GASTURB	106.0		102539.0		205100.0		62921.0	
SYNGEXP	8.0		5638.0		11282.0		24039.0	
Power generation from steam turbine	**67.0**		**59574.0**		**120270.0**		**68196.0**	
ST1	6.0		3767.0		7534.0		4848.0	
ST2	49.0		42057.0		84826.0		50611.0	
ST3	7.0		4751.0		9501.0		12154.0	
ST4	5.0		8999.0		18409.0		583.0	
Power requirement on site	**525.7**		**336613.9**		**673255.2**		**619246.2**	
ELECTRO	393.7		265845.9		531702.2		531702.2	
SYNGCOMP	23.0		15826.0		31665.0		51622.0	
CO2COMP	2.0		1344.0		2691.0		2691.0	
AIRCOMP	43.0		53598.0		107197.0		33231.0	
Net power generation	**−280.7**		**−168862.9**		**−336603.2**		**−464090.2**	
Production of methanol	667.2	0.033	450800.0	22.5	902000.0	45.1	1200778.0	60.0
Efficiency based on LHV, (methanol + electricity)/bio-oil (%)	**38.7**		**41.8**		**41.9**		**54.6**	
Efficiency based on LHV, (methanol + electricity + net heat)/bio-oil (%)	**49.2**		**56.2**		**56.4**		**65.5**	

The bold numbers represent the sum of values within a specified category.

Higher netback (maximum acceptable buy-in price) of bio-oil and lower COP of methanol are desired. The netback of bio-oil for the best two cases, 1350 MW ASU configurations with and without recycle, is 45.2 Euro/t and 6.65 Euro/t, without the consideration of CCL, respectively. The COP of methanol from these two cases is 318.1 Euro/t and 469.3 Euro/t respectively. The inclusion of CCL has a negligible impact on economics, especially for the economically attractive cases, e.g. 0.4 Euro/t

Table 8 – (a) Proximate and ultimate analyses of bio-oils from various sources. (b) Comparison of performance analysis of once-through, 1350 MW BOIG-MeOH system with ASU configuration, between poplar wood, miscanthus and oilseed rape as feedstocks.

(a)

Source of bio-oil	Heating value (MJ/kg)	Proximate Analysis (wt%)		Ultimate Analysis (wt%)		
		Fixed Carbon and Volatiles	Moisture	C	H	O
Poplar	23.3	70.0	30.0	56.0	7.0	37.0
Miscanthus	30.7	89.9	10.1	64.2	8.3	27.5
Oilseed Rape	35.7	90.5	9.5	77.5	12.0	10.5

(b)

Type of bio-oil	Poplar	Miscanthus	Oilseed Rape
Net heat generation (MW)	111.7	23.5	17.7
Net power generation (MW)	126.7	116.3	117.8
Production of methanol (t/h)	94.7	141.6	144.5
LHV of methanol (MW)	526.0	786.9	802.9
Efficiency based on LHV, (methanol + electricity)/bio-oil (%)	48.3	66.9	68.2
Efficiency based on LHV, (methanol + electricity + net heat)/bio-oil (%)	56.6	68.6	69.5

Table 9 – Input data for capital cost evaluation.

Direct Capital Cost				
ISBL				
Item No.	Process unit	Base Cost (million Euro)	Scale factor, R	Base scale
1	Gasifier	25.5	0.7	400 MW HHV
2	Water-gas shift reactor	40.59	0.85	15.6 Mmol CO + H_2/h
3	Methanol reactor	7.7	0.6	87.5 t MeOH/h
4	Gas turbine	6.55	0.7	25 MW
5	Steam turbine (inc. condenser)	3.81	0.7	12.3 MW
6	HRSG	2.87	0.8	47.5 t/h
7	SYNGCOOL	2.87	0.8	47.5 t/h
8	Cryogenic ASU	19.6	0.75	24 t/h
9	Water electrolyser			825 Euro/kW
10	Compressor and expander	10.2	0.85	13.2 MW
OSBL				
Item No.	Specification	Cost estimation (% of ISBL)		
11	Instrumentation and control	5.0		
12	Buildings	1.5		
13	Grid connections	5.0		
14	Site preparation	0.5		
15	Civil works (inc. waste water treatment)	10.0		
16	Electronics	7.0		
17	Piping	4.0		
	Total Direct Capital (TDC)	ISBL + OSBL		
Indirect Capital Cost				
Item No.	Specification	Cost estimation (% of TDC)		
18	Engineering	15		
19	Contingency	10		
20	Fees/overheads/profits	10		
21	Start-up	5		
	Total Indirect Capital (TIC)			
	Total Capital Costs	TDC + TIC		

for 1350 MW ASU with recycle configuration. The generic trend is the increasing economic feasibility with increasing capacity and by the introduction of recycle mode. None of the electrolyser cases is economically feasible. The capital cost, operating cost and the cost of bio-oil (assuming price of bio-oil at 75 Euro/t, without incorporating transportation cost) contribute to 31.1%, 17.5% and 51.4%, respectively to the total annual investment of the economically attractive case, i.e. 1350 MW ASU with recycle configuration.

4.4. *Transportation cost of bio-oil*

The transportation cost of bio-oil is an important factor to analyse, when bio-oil produced from distributed pyrolysis plants needs to be transported to centralised BOIG-MeOH process. The data and analysis of bio-oil transportation from distributed pyrolysis plants to centralised sites, based on the studies by Bridgwater et al. [13], Rogers and Brammer [14] and Pootakham and Kumar [20], presented in Table 12 are applicable to the UK and EU contexts. The cost of transporting 303.75 t/h bio-oil (equivalent to 2.43 million t/y; or 2.24 million m^3/d; or 3.89 × 10^7 GJ/y) to 1350 MW BOIG-MeOH site was estimated using the distance rate [13,20] and zone costing approaches [14]. The results provided in Table 12 used both fixed and variable costs depending upon the distance or thermal value of bio-oil [13,14,20]. (Note: 1 USD = 0.8 Euro and 1 GBP = 1.1 Euro were assumed). The zone costing approach uses the number of round trips in a day within the distributed-centralised region as the basis to define a transport zone. Thus, zone 1 is the outermost zone where only one round trip is possible in a day, carrying the highest total cost amongst all zones, 64.2 million Euro/y or 26.42 Euro/t, compared to 8.6 million Euro/y or 3.54 Euro/t for zone 6 that implies 6 round trips in a day, respectively. It is hence beneficial to implement more round trips in a day so as to reduce the transportation cost. Tanker (truck) with load ranges of 24–44 tonnes and 60 m^3 per truck and pipeline capacity of 560 m^3/d were considered for a distance of 100 km between distributed pyrolysers and centralised BOIG-MeOH sites. The resulting transportation cost is 4.28–8.89 Euro/t (or 10.4–21.6 million Euro/y for 1350 MW case) that reduces the netback of bio-oil from 45.2 Euro/t (Table 11) to 40.9–36.3 Euro/t. In terms of COP of bio-oil, transportation adds 5.7–11.9% extra on 75 Euro/t.

By incorporating the transportation cost of bio-oil over a distance of 100 km, the netback of bio-oil in 1350 MW recycle and ASU configuration, would further be reduced to 40.9–36.3 Euro/t (compared to 45.2 Euro/t in Table 11) at the least, using the same basis.

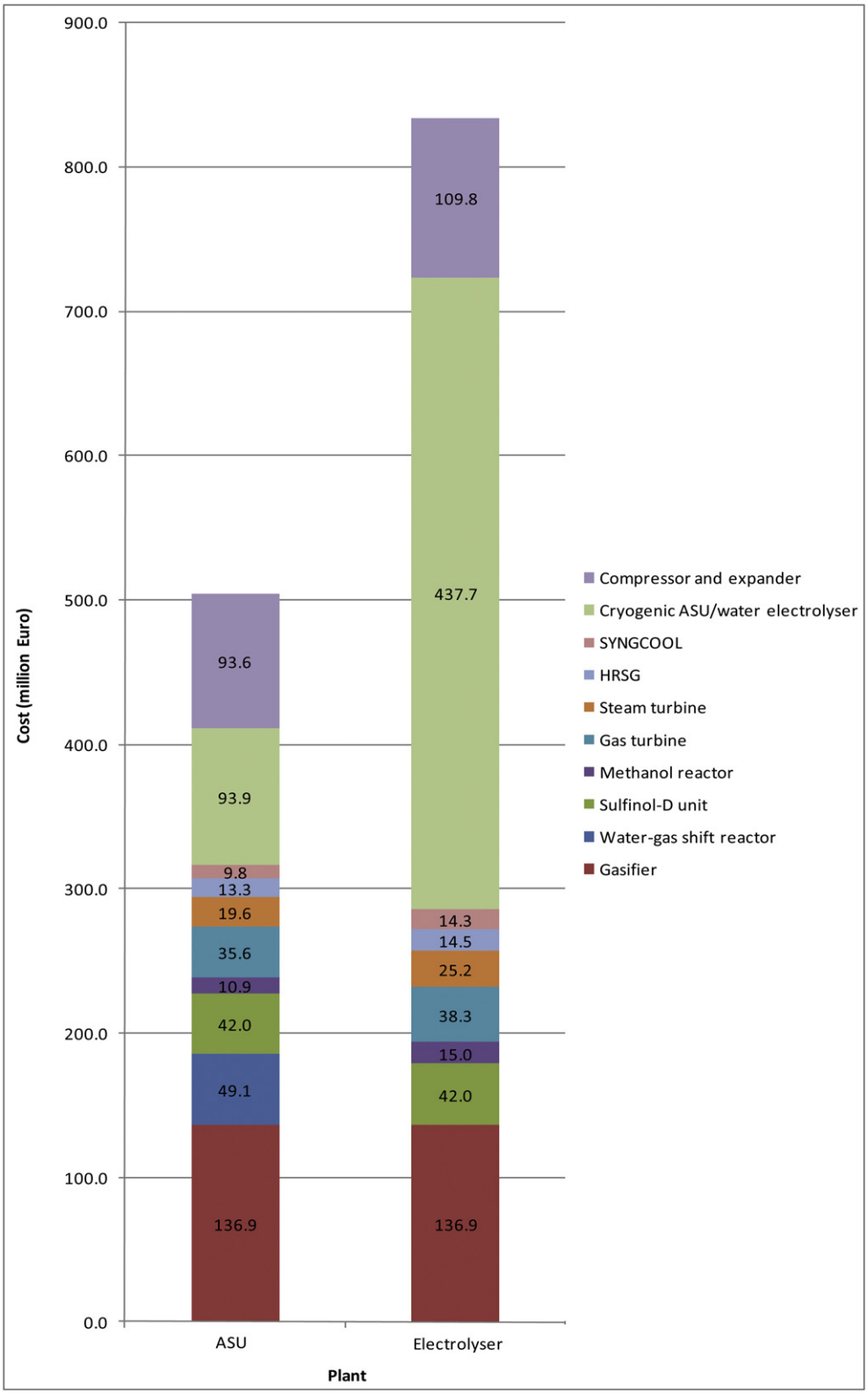

Fig. 7 – Comparison of capital cost for BOIG-MeOH system with capacity of 1350 MW, for ASU and electrolyser configuration. Cost breakdown of each process unit is provided within the chart.

4.5. *Analysis of economic feasibility*

The effect of market price of methanol on the netback of bio-oil was examined for the following prices of methanol, 106.7 Euro/t, 250 Euro/t and 299.6 Euro/t, and two sets of electricity price, 46.61 Euro/MWh (2005) and 80.12 Euro/MWh (2009) [56], for 1350 MW BOIG-MeOH system with ASU and recycle configuration, in Fig. 8(a). The estimated COP of methanol from natural

Table 10 – Input data for operating cost evaluation.

Item No.	Specification	Cost Estimation
Fixed Operating Cost		
1	Maintenance	10% of TIC
2	Personnel	0.595 million Euro/100 MW LHV
3	Laboratory costs	20% of (2)
4	Supervision	20% of (2)
5	Plant overheads	50% of (2)
6	Capital Charges	10% of TIC
7	Insurance	1% of TIC
8	Local taxes	2% of TIC
9	Royalties	1% of TIC
	Total Fixed Operating Cost (TFO)	
	Total Fixed Operating Cost per year	
Variable Operating Cost		
10	Natural gas	0.021 Euro/kWh
11	Electricity	0.080 Euro/kWh
12	Steam	10.5 Euro/t
	Total Variable Operating Cost (TVO)	
	Direct Production Cost (DPC) per year	TFO + TVO
Miscellaneous		
13	Sales expense, General overheads, Research and development	30% of DPC
	Total Operating Costs Per Year	DPC + Miscellaneous

gas is 4.7 Euro/GJ, which is equivalent to 106.7 Euro/t [61]. Hamelinck and Faaij [9] estimated the COP of methanol of 8.6–12 USD/GJ (equivalent to 214.7–299.6 Euro/t) from biomass. The maximum netback of bio-oil thus obtained is 66.9 Euro/t for the given maximum market prices of methanol and electricity. Based on the illustration in Fig. 8(a), the minimum price of methanol is 153.2 Euro/t and 146.9 Euro/t for the price of electricity of 46.61 Euro/MWh and 80.12 Euro/MWh, respectively, corresponding to zero netback of bio-oil.

Fig. 8(b) demonstrates the effect of the cost of bio-oil on the COP of methanol, for 0 Euro/t, 75 Euro/t and 150 Euro/t of the cost of bio-oil. The acceptable range of the cost of bio-oil is between 0–75 Euro/t; whilst 150 Euro/t of the cost of bio-oil may provide flexibility in the distance between distributed and centralised plants. An increase in the electricity price by 33.51 Euro/MWh from 2005 to 2009 can reduce the COP of methanol by 6.3 Euro/t. Escalation in the price of electricity and methanol from renewable resources in future can thus stimulate deployment of these systems.

If 5% reduction in the operating cost of BOIG-MeOH system is achieved, 0.9% lower COP of methanol than that reported in Table 11 can be attained. 20% reductions in operating cost result in 2.8% lower COP of methanol. Reduction in capital cost brings more significant improvements, e.g. 5% and 20% reductions in capital cost lower the COP of methanol by 1.6% and 5%, respectively. Following the assumptions in the works of Faaij et al. [51], the capital cost of 1350 MW ASU and recycle configuration can be reduced by 54.4% in the short-term, e.g. 2020, after 20th plant is built (838.2–382.4 million Euro/y), due to technological learning. After 100th plant is built, 69.1% reductions in capital cost or 242 Euro/t of COP of methanol compared to 318.1 Euro/t for the first plant are achievable. It

Table 11 – Summary of economic analysis, estimated netback of bio-oil and COP of methanol.

Configuration	ASU				Electrolyser			
Capacity (MW LHV)	1	675	1350	1350	1	675	1350	1350
Mode	Once-through			Recycle	Once-through			Recycle
Annualised capital charge (million Euro/y)	0.592	66.6	123.5	110.2	0.572	100.5	204.1	188.9
Annual operating cost (million Euro/y)	0.152	66.0	130.9	62.1	0.330	209.8	418.5	445.9
Value of products, exc. CCL (million Euro/y)	**0.226**	**128.8**	**270.6**	**282.1**	**0.240**	**162.3**	**324.7**	**432.3**
Value of products, inc. CCL (million Euro/y)	**0.232**	**131.0**	**275.8**	**283.1**				
a. Electricity, without CCL	0.087	34.2	81.2	16.0				
b. CCL for electricity	0.006	2.20	5.24	1.03				
c. Methanol	0.140	94.6	189.4	266.1	0.240	162.3	324.7	432.3
Bio-oil consumption (t/y)	1800	1214496	2430000	2430000	1800	1214496	2430000	2430000
Netback of bio-oil, exc. CCL (million Euro/y)	**−0.518**	**−3.89**	**16.15**	**109.8**	**−0.662**	**−148.0**	**−297.9**	**−202.6**
Netback of bio-oil, exc. CCL (Euro/t)	**−287.5**	**−3.20**	**6.65**	**45.2**	**−367.8**	**−121.9**	**−122.6**	**−83.4**
Netback of bio-oil, inc. CCL (million Euro/y)	**−0.512**	**−1.69**	**21.4**	**110.8**	**−0.671**	**−155.0**	**−311.8**	**−221.8**
Netback of bio-oil, inc. CCL (Euro/t)	**−284.4**	**−1.39**	**8.80**	**45.6**	**−372.8**	**−127.6**	**−128.3**	**−91.3**
Methanol production (t/y)	558.7	378400.0	757440.0	1064320.0	960.0	649152.4	1298880.0	1729086.4
Cost of bio-oil (million Euro/y)	0.135	91.1	182.3	182.3	0.135	91.1	182.3	182.3
COP of methanol, exc. CCL (million Euro/y)	**0.792**	**189.6**	**355.5**	**338.6**	**1.04**	**401.4**	**804.9**	**817.1**
COP of methanol, exc. CCL (Euro/t)	**1418.0**	**501.0**	**469.3**	**318.1**	**1080.2**	**618.3**	**619.7**	**472.6**
COP of methanol, inc. CCL (million Euro/y)	**0.787**	**187.4**	**350.2**	**337.5**	**1.05**	**408.4**	**818.8**	**836.3**
COP of methanol, inc. CCL (Euro/t)	**1408.0**	**495.2**	**462.4**	**317.1**	**1089.5**	**629.1**	**630.4**	**483.7**

The bold numbers represent the important economic results.

Table 12 – Cost of transporting bio-oil from distributed pyrolysis plants to centralised 1350 MW BOIG-MeOH system.

Researcher	Bridgwater et al., 2002 [13]		Rogers and Brammer, 2009 [14]		Pootakham and Kumar, 2010 [20]	
Method of transporting bio-oil	Tanker	Tanker	Tanker	Tanker	Tanker	Pipeline
Maximum load/capacity	30.5 t	24.0 t	44.0 t	44.0 t	60 m^3	560 m^3/d
Analysis approach	Distance rate	Distance rate	Zone costing	Zone costing	Distance rate	Distance rate
Cost estimating	Shell UK	Linkman	Zone 1	Zone 6		
Fixed cost	4.29 Euro/t		0.66 Euro/GJ	0.11 Euro/GJ	4.568 Euro/m^3	0.03384 Euro/m^3
Variable cost	0.039 Euro/t/km	0.043 Euro/t/km	0.99 Euro/GJ	0.11 Euro/GJ	0.04 Euro/m^3/km	0.09608 Euro/m^3/km
Distance assumed	100 km	100 km	96–224 km	0–11 km	100 km	100 km
Bio-oil transportation cost (million Euro/y)	19.9	10.4	64.2	8.6	19.2	21.6
Bio-oil transportation cost (Euro/t)	8.19	4.28	26.42	3.54	7.90	8.89

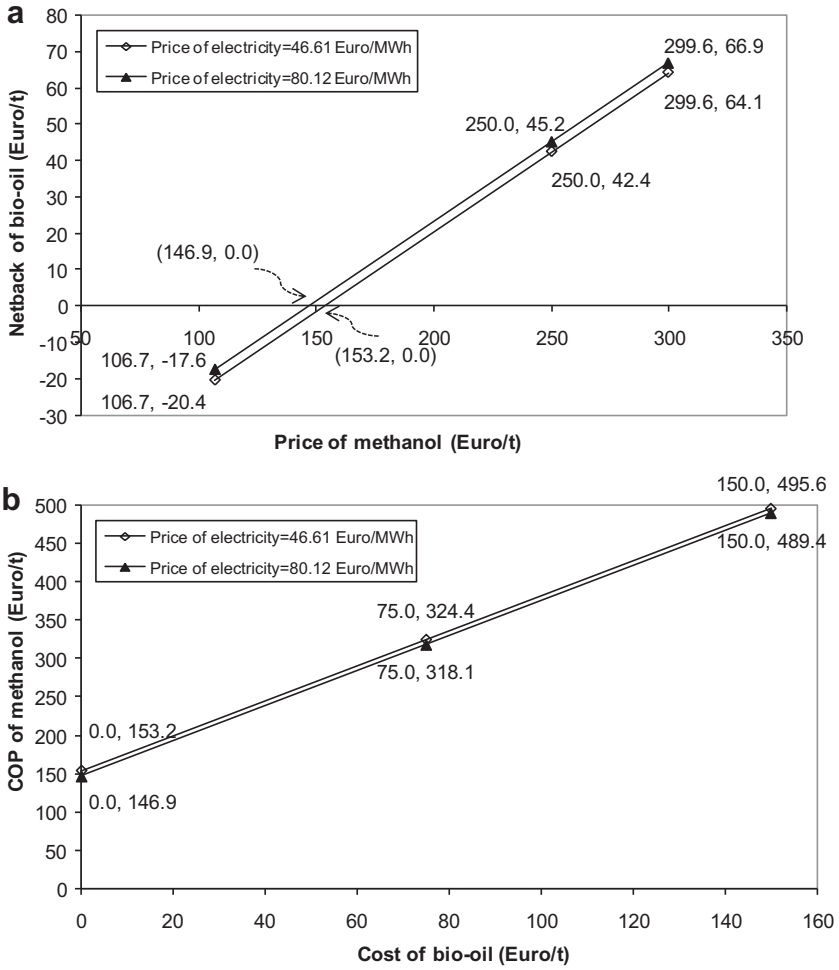

Fig. 8 – Sensitivity analysis of 1350 MW BOIG-MeOH system, recycle with ASU configuration on the (a) netback of bio-oil with variation in price of methanol and (b) cost of methanol with variation in cost of bio-oil, based on different prices of electricity without CCL.

may be noted that the learning effects imply projections based on today's value of a given currency.

5. Conclusions

The techno-economic feasibility of BOIG-MeOH system has been analysed using process variability and integration approaches. The performance of methanol synthesis reactor in terms of the yield of methanol was analysed with respect to the stoichiometric number in the feed gas and water removal, with the latter being very critical to achieve higher yield of methanol. The electrolyser configuration can achieve higher amount of methanol production compared to the ASU configuration. This is attributed to additional hydrogen supply from water dissociation, requiring no water-gas shift reaction,

however, at the cost of higher electricity and capital cost requirements by the water electrolyser unit. An energy efficient gasification process has been integrated in the context of overall CHP generation network that exploits heat recovery from the syngas cooler, HRSG, WGS and methanol synthesis reactor into the generation of surplus steam and thereby steam turbine power, oxygen preheating to avoid high temperature heat of reforming reactions within gasification and low grade heat recovery. The cost competitiveness and energy efficiency of the systems increase with increasing capacity and by the introduction of recycle. Between ASU and electrolyser configurations, the latter configuration is not economically feasible at this stage. The bio-oil gasification route provides more flexibility in terms of biomass selection and pyrolysis in distributed generations and processing of bio-oils using commercially available centralised scale gasification and methanol synthesis reactor, etc. technologies. This led to the performance analyses of centralised BOIG-MeOH system based on various biomass feedstocks, oilseed rape, miscanthus and poplar wood, resulting in highest to lowest energy efficiency obtained. These variations can be attributed to the characteristics of bio-oil, particularly the moisture content. The netback of bio-oil can be reduced with the incorporation of the transportation cost between the distributed pyrolysis and centralised BOIG-MeOH plants. A more competitive industrial scale process may be realised with rising price of electricity and reduction in capital and operating costs.

Acknowledgements

The authors would like to express their gratitude to The University of Manchester Alumni Fund and Process Integration Research Consortium for financial aid to support this research.

Nomenclature

R	Scale factor, Eq. (5)
SN	Stoichiometric number for the feed to methanol synthesis

REFERENCES

[1] Methanol Institute. Global methanol supply and demand [cited 22 March 2010]. Available from: www.methanol.org; 2010.
[2] Spath PL, Dayton DC. Preliminary screening—technical and economic assessment of synthesis gas to fuels and chemicals with emphasis on the potential for biomass-derived syngas. NREL/TP-510–34929. National Renewable Energy Laboratory (NREL); 2003.
[3] Dybkjaer I, Christensen TS. Syngas for large scale conversion of natural gas to liquid fuels. In: Studies in surface science and catalysis. Elsevier; 2001. p. 435–40.
[4] Olah GA, Goeppert A, Prakash GKS. Beyond oil and gas: the methanol economy. Weinheim: WILEY-VCH; 2006.
[5] Williams RH, Larson ED. A comparison of direct and indirect liquefaction technologies for making fluid fuels from coal. Energ Sustain Dev 2003;VII(4):103–29.
[6] Roan V, Betts D, Twining A, Dinh K, Wassink P, Simmons T. An investigation of the feasibility of coal-based methanol for application in transportation fuel cell systems. Georgetown University; 2004.
[7] Williams RH, Larson ED, Katofsky RE, Chen J. Methanol and hydrogen from biomass for transportation. Energ Sustain Dev 1995;1(5):18–34.
[8] Katofsky RE. The production of fluid fuels from biomass. Princeton University; 1993.
[9] Hamelinck CN, Faaij APC. Future prospects for production of methanol and hydrogen from biomass. J Power Sources 2002; 111(1):1–22.
[10] Hamelinck CN, Faaij APC. Future prospects for production of methanol and hydrogen from biomass. University Utrecht; 2001.
[11] Hamelinck C, Faaij A. System analysis of advanced biomass conversion concepts for production of methanol and hydrogen with Aspen-plus flowsheet modelling. University of Utrecht, Department of NW&S; 2000.
[12] Bridgwater AV. Technical and economic assessment of thermal processes for biofuels. Life cycle and techno-economic assessment of the Northeast biomass to liquid projects NNFCC project 08/018. COPE Ltd; 2009.
[13] Bridgwater AV, Toft AJ, Brammer JG. A techno-economic comparison of power production by biomass fast pyrolysis with gasification and combustion. Renew Sustain Energ Rev 2002;6(3):181–246.
[14] Rogers JG, Brammer JG. Analysis of transport costs for energy crops for use in biomass pyrolysis plant networks. Biomass Bioenerg 2009;33(10):1367–75.
[15] Brammer JG, Lauer M, Bridgwater AV. Opportunities for biomass-derived "bio-oil" in European heat and power markets. Energ Pol 2006;34(17):2871–80.
[16] Ringer M, Putsche V, Scahill J. Large-scale pyrolysis oil production: a technology assessment and economic analyses. NREL/TP-510–37779. National Renewable Energy Laboratory (NREL); 2006.
[17] Bradley D. European market study for biooil (Pyrolysis Oil); 2006 [Climate Change Solutions].
[18] BBC. Oil spill stories: the human impact of the Gulf of Mexico spill [cited 30 June 2010]. Available from: http://www.bbc.co.uk/worldservice/news/2010/06/100609_bresnahan_louisiana_wt_hs.shtml; 10 June 2010.
[19] Biomass to Liquid-BtL Implementation Report, Summary. Deutsche Energie-Agentur GmbH (dena), The German Energy Agency; 2006.
[20] Pootakham T, Kumar A. Bio-oil transport by pipeline: a techno-economic assessment. Bioresour Technol 2010;101(18):7137–43.
[21] Poplars, willows and peoples's wellbeings: synthesis of country progress reports - activities related to poplar and willow cultivation and utilization, 2004 through 2007. Working, Paper IPC/6. In: International poplar commission. Beijing, China: Food and Agriculture Organization of the United Nations (FAO); 2008.
[22] Williams FC, Thomas T. Some key issues concerning current poplar production and future marketing in the United Kingdom. New Forests 2006;31(3):343–59.
[23] Aylott MJ, Taylor G, Casella E, Smith P. TSEC-Biosys: yield and spatial supply of bioenergy poplar and willow short rotation coppice in the UK. In: Biomass role in the UK energy futures. London: The Royal Society; 2009, 28th–29th July.
[24] DEFRA. Experimental statistics: non-food crop areas United Kingdom. Department for Environment Food and Rural Affairs (DEFRA); 2009.
[25] Venderbosch RH, Prins W. Entrained Flow Gasification of Bio-Oil for Synthesis Gas. in 5th International Biomass

Conference of the Americas. 2001, September 17–21. Orlando, Florida, USA.
[26] van Rossum G, Kersten SRA, van Swaaij WPM. Catalytic and noncatalytic gasification of Pyrolysis Oil. Ind Eng Chem Res 2007;46(12):3959–67.
[27] Marda JR, DiBenedetto J, McKibben S, Evans RJ, Czernik S, French RJ, et al. Non-catalytic partial oxidation of bio-oil to synthesis gas for distributed hydrogen production. Int J Hydrogen Energy 2009;34(20):8519–34.
[28] Bludowsky T, Agar DW. Thermally integrated bio-syngas-production for biorefineries. Chem Eng Res Design 2009;87(9): 1328–39.
[29] Zhang Y, Xiao J, Shen L. Simulation of methanol production from biomass gasification in interconnected fluidized beds. Ind Eng Chem Res 2009;48(11):5351–9.
[30] Liu H, Chen C, Kojima T. Theoretical simulation of entrained flow IGCC gasifiers: effect of mixture fraction fluctuation on reaction owing to turbulent flow. Energy Fuel 2002;16(5): 1280–6.
[31] Kordabadi H, Jahanmiri A. A pseudo-dynamic optimization of a dual-stage methanol synthesis reactor in the face of catalyst deactivation. Chem Engg Processing Process Intensification 2007;46(12):1299–309.
[32] Hydrogenics. HySTAT™ A-Alkaline electrolyser [cited 3rd June 2010]. Available from: http://www.hydrogenics.com/.
[33] Universal Industrial Gases Inc. Cryogenic air separation plants and liquid plants producing nitrogen, oxygen and argon. Available from: http://www.uigi.com/new_cryo_plants.html [cited 3rd June 2010].
[34] MJvd Burgt. Chapter 12: entrained-flow gasification. In: Knoef HAM, editor. Handbook biomass gasification. Netherlands: BTG Biomass Technology Group; 2005. p. 248–58.
[35] Kakaras E, Doukelis A, Giannakopoulos D, Koumanakos A. Novel concepts for near zero-emissions IGCC power plants. Therm Sci 2006;10(3):81–92.
[36] Elliott DC, Hu J, Hart TR, Neuenschwander GG. Palladium catalyzed hydrogenation of bio-oils and organic compounds; 2009. US Patent 2009/0113787.
[37] Sadhukhan J, Ng KS, Shah N, Simons HJ. Heat integration strategy for economic production of combined heat and power from biomass waste. Energy Fuels 2009;23(10): 5106–20.
[38] Tijmensen MJ, Faaij AP, Hamelinck CN, Mv Hardeveid. The production of Fischer-Tropsch liquids and power through biomass gasification. Utrecht, Netherlands: Universiteit Utrecht, Science Technology Society; 2000.
[39] Williams E, Greenglass N, Ryals R. Carbon capture, pipeline and storage: a viable option for North Carolina utilities. Nicholas Institute for Environmental Policy Solutions and The Center on Global Change, Duke University; 2007.
[40] Rodrigues M, Walter A, Faaij A. Co-firing of natural gas and biomass gas in biomass integrated gasification/combined cycle systems. Energy 2003;28(11):1115–31.
[41] Shah M, Raybold T, Jamal A, Drnevich R, Bonaquist D, Jones R. IGCC: CO2 capture ready?. in Gasification Technology Conference. 2005. San Francisco.
[42] Ponton JW, Donaldson RAB. A fast method for the synthesis of optimal heat exchanger networks. Chem Eng Sci 1974;29: 2375–7.
[43] Ng KS, Lopez Y, Campbell GM, Sadhukhan J. Heat integration and analysis of decarbonised IGCC sites. Chem Eng Res Design 2010;88(2):170–88.
[44] Linnhoff B. Introduction to pinch technology. Linnhoff March Energy Service; 1998.
[45] El-Halwagi M, Harell D, Dennis Spriggs H. Targeting cogeneration and waste utilization through process integration. Appl Energy 2009;86(6):880–7.
[46] Kohl AL, Nielsen RB. Gas Purification. 5th ed. Elsevier; 1997.
[47] Uhde. Methanol [cited 29 April 2010]. Available from: http://www.uhde.eu/; 2008.
[48] Armstrong PA, Bennett DL, Foster EP, Stein VE. ITM oxygen: the new oxygen supply for the new IGCC market. in Gasification Technologies. 2005. San Francisco, California.
[49] Yorgun S, Yunus Emre S. Fixed-bed pyrolysis of *Miscanthus x giganteus*: product yields and bio-oil characterization. Energy Sourc Part A Recovery Utilization Environ Effects 2003;25(8): 779–90.
[50] Sensoz S, Angin D, Yorgun S, Kockar OM. Biooil production from an oilseed crop: fixed-bed pyrolysis of rapeseed (*Brassica napus* L.). Energy Sourc Part A Recovery Utilization Environ Effects 2000;22(10):891–900.
[51] Faaij A, Meuleman B, Rv Ree. Long term perspectives of Biomass Integrated Gasification/Combined Cycle (BIG/CC) technology: cost and electrical efficiency; 1998 [Utrecht, Netherlands].
[52] Saxe M, Alvfors P. Advantages of integration with industry for electrolytic hydrogen production. Energy 2007;32(1):42–50.
[53] Lozowski D. Economic indicators. Chem Eng 2010;117(3):63–4.
[54] Tijmensen MJA, Faaij APC, Hamelinck CN, van Hardeveld MRM. Exploration of the possibilities for production of Fischer Tropsch liquids and power via biomass gasification. Biomass Bioenerg 2002;23(2):129–52.
[55] Sinnott RK. Coulson & Richardson's chemical engineering design. 4th ed, vol. 6. , Oxford: Elsevier: Butterworth-Heinemann; 2006.
[56] DECC. Quarterly energy prices. Department of Energy and Climate Change (DECC); March 2010.
[57] Methanex. Methanol price [cited 30th September 2010]. Available from: www.methanex.com; 2010.
[58] HM Revenue and Customs. Climate change levy [cited 9th May 2010]. Available from: www.hmrc.gov.uk; 2010.
[59] Sadhukhan J, Mustafa MA, Misailidis N, Mateos-Salvador F, Du C, Campbell GM. Value analysis tool for feasibility studies of biorefineries integrated with value added production. Chem Eng Sci 2008;63(2):503–19.
[60] Bridgwater AV. An introduction to fast pyrolysis of biomass for fuels and chemicals. In: Bridgwater AV, Czernik S, Diebold J, Meier DOA, Peacocke C, Piskorz J, Radlein R, Fast pyrolysis of biomass: a Handbook, vol. 1. CPL Press; 1999. p. 1–13.
[61] Ohlstrom M, Makinen T, Laurikko J, Pipatti R. New concepts for biofuels in transportation. VTT Research Notes 2074. VTT Energy; 2001.

The Submitted Research Papers

PUBLICATION 3: Ng, K.S., Zhang, N., Sadhukhan, J., CO_2 abatement strategies for polygeneration systems: Process integration and analysis. *Chemical Engineering Research and Design.* Submitted (2011).

CO_2 Abatement Strategies for Polygeneration Systems: Process Integration and Analysis

Kok Siew Ng, Nan Zhang and Jhuma Sadhukhan*

Centre for Process Integration, School of Chemical Engineering and Analytical Science, University of Manchester, Manchester, M13 9PL, UK.

Abstract

Several decarbonised polygeneration systems exploiting carbon capture and storage (CCS) or CO_2 reuse technologies for the conversion of primary resources into clean fuels, chemicals, electricity and heat are systematically analysed for techno-economic feasibility. A simulation, heat integration and economic analysis based approach has been employed to arrive at a representative set of performance indicators for the trade-off analysis of polygeneration systems. These indicators include the effect of process configurations and operating conditions on the economic potential (*EP*), energetic efficiency, decarbonisation potential, economic risks and value of products and sensitivity in *EP* due to carbon taxations. The systems under consideration include coal gasification systems with cogeneration and polygeneration, integrated with various CO_2 abatement strategies. It has been recognised that transforming a CCS based polygeneration system (Scheme A) into an equivalent captured CO_2 reuse system (Scheme B) does not necessarily enhance energetic, economic and emission performances. On the other hand, upgrading a cogeneration system (Scheme C) into a polygeneration system (Scheme D) clearly improves all performance indicators. While bio-oil based polygeneration system (Scheme E) creates environmental incentives, its economic competitiveness is uncertain and can be enhanced by introducing credits on

product prices. Promising results in terms of improved energy efficiency from 36% in IGCC with CCS scheme to above 70% in polygeneration schemes, viable *EP* and a minimum of 75% of plant-wide CO_2 emission reduction demonstrate that the polygeneration Schemes A, D and E can become low carbon technologies of choice.

Keywords: chemical and transportation fuel production; CO_2 reuse and carbon capture and storage; clean coal technology; bioenergy and biorefinery; low carbon energy for developing economy; low carbon technology roadmap.

* Author/s to whom correspondence should be addressed:

E-mail: jhumasadhukhan@gmail.com

1. Introduction

Dwindling global oil reserves, environmental concerns and the need for domestic energy security have generated strong research and development focus in clean coal, natural gas and biomass based polygeneration systems (Adams and Barton, 2011). These primary resources can be converted into clean transportation fuels, chemicals, heat and electricity. Polygeneration systems incorporating carbon abatement technologies provide low plant emission, enhanced and flexible switching capability between a diverse range of feedstocks and products, energy security and economic drives (Li et al., 2010; Macdowell et al., 2010; Adams and Barton, 2011; Pires et al., 2011). CO_2 emission from coal is often problematic. Coal shares 25.6% of the total CO_2 emission by fuel in the UK, i.e. 531.8 million tonne of CO_2 in year 2008 (Prime et al., 2010). Development in decarbonised fossil energy production has mainly been focused around the integration of CCS into IGCC (Ng et al., 2010). The captured CO_2 can be compressed, transported through pipelines / ships, and stored in ocean (liquid storage),

geological formation (gaseous storage) and mineral carbonates (solid storage). However, the installation of CCS system into a power plant is notably an energy and cost intensive process requiring approximately 10-40% more energy than a plant without CCS, thereby reducing the overall plant efficiency to 31-33.6% (NETL, 2010). In addition, leakage may occur from the storage of CO_2. Recycling and reuse of CO_2 is a viable way of minimising plant CO_2 emission (Rihko-Struckmann et al., 2010). CO_2 can be reused for enhanced oil recovery in oil extraction process; microalgae production; production of urea, methanol, dimethyl ether, Fischer-Tropsch liquids, methane (Sabatier's reaction), syngas (tri-reforming process) and hydrogen (Song and Pan, 2004; Li et al., 2006; Barbarossa et al., 2009; Rihko-Struckmann et al., 2010). A recent breakthrough in the area of CO_2 reuse is the launching of the George Olah Plant in Iceland in 2010, for the production of methanol from captured CO_2 from industrial flue gases (CRI, 2010). Alternative to CCS and CO_2 reuse technologies, lignocellulosic biomass based polygeneration systems also have significant carbon reduction potential. Bio-oil, a higher energy density liquid, from biomass fast pyrolysis processes can be converted to methanol or liquid transportation fuels (diesel and gasoline) (Bridgwater, 2009; Venderbosch and Prins, 2010; Ng and Sadhukhan, 2011a, 2011b; Sadhukhan and Ng, 2011). The application of CO_2 abatement technology and alternative energy resources is a reality in minimising CO_2 emission.

The studies on polygeneration systems reveal that the production routes can be flexibly utilised according to market drives. Yet, enabling these technologies requires huge techno-economic barriers to overcome. One of the key challenges is the consensus between economic policy and environmental incentive. Adams and Barton (2011) have shown that rising CO_2 tax incentivises the production of more liquid fuels instead of

electricity due to the tax implication on the latter product. However, this production switch does not necessarily translate to low carbon life cycles. The authors have presented a transparent techno-economic approach for polygeneration systems. Higher efficiencies and economic incentives from the use of a combination of natural gas reforming and coal gasification for the production of syngas suitable for liquid fuel production have been achieved compared to a coal based system. The study by Rihko-Struckmann et al. (2010) evaluated the thermodynamic limitations, the energetic and exergetic efficiencies of a number of CO_2 usage routes for the storage of electrical energy into chemicals: methyl tertiary butyl ether, dimethyl carbonate, dimethyl ether, and via a number of processes, methanol to gasoline, Fischer-Tropsch, reverse water-gas shift, dry reforming, etc. With the fact that industrialisation will even be at a faster pace and that there will be an evolving phase for fully integrated environmental and economic policies, flexible CO_2 reuse into liquid fuel production can be regarded as an interim carbon reduction strategy, before 2020. Integration of bio-oil as a stable and cleaner intermediate energy carrier has also received a great deal of attention due to positive impact in a carbon-constrained world (Bridgwater, 2009; Ng and Sadhukhan, 2011a, 2011b; Sadhukhan and Ng, 2011). These studies have presented a comprehensive techno-economic performance analysis of a number of bio-oil based biofuel platforms, utilising indirect gasification route or direct upgrading route, for the production of methanol, Fischer-Tropsch liquids, gasoline and diesel alongside heat and electricity. Venderbosch and Prins (2010) have further studied characterisation of functionalities and chemical constituents of bio-oils based on target chemicals and biofuels to be generated. Their approach includes efficient heat integration, control and reliability analysis of a number of pyrolysis reactors, e.g. fluid bed, rotating cone and

vacuum pyrolysis at a demonstration scale and ablative and twin screw at a pilot scale, for the production and characterisation of bio-oils. The significance of CO_2 abatement technologies (CCS and / or CO_2 reuse) and biomass as a resource in polygeneration has clearly been recognised in these studies.

It is realised that the coal generation has a significant contribution to the security of electricity supply in the UK (ScottishPower, 2008). The ScottishPower has engaged into a demonstration project that uses Scottish coal and biomass co-firing technology integrated with advanced CCS options. A large scale co-processing plant planned in Scotland is an example of UK's energy security goals. Further, to restrict the temperature rise up to 2^oC over this century, the Annex I countries must switch to non-fossil resources or to fossil resources with CCS and in combination with other renewable resources. The Non-Annex I countries have also committed towards adaptation to alternative technologies to combat against climate change (UNFCCC, 2010). Considering the technologies of priority, the polygeneration schemes with CCS under consideration seem to offer low carbon technology solution for industrialised countries in the interim period (e.g. before 2020). Converting CO_2 into useful products is also a viable route at present to resolve the issues associated with the rising energy demand in the developing nations.

Converting a cogeneration system with CCS into a polygeneration system with CCS or reuse significantly increases energy efficiency and thereby reduces CO_2 emission. A comparative analysis between polygeneration systems either exploiting CCS or CO_2 reuse for the generation of similar set of products has been adopted in this paper. Schemes A and B with CCS and with CO_2 pre-combustion capture and reuse in

methane synthesis by Sabatier's reaction, respectively, are proposed to produce methanol, acetic acid, electricity and hydrogen. Further, Scheme C that includes coal IGCC system with CCS is transformed into a polygeneration Scheme D. In Scheme D, coal based post-combustion CO_2 from gas turbine (after hydrogen recovery) is tri-reformed using natural gas. The product gas from tri-reforming is conditioned by the addition of recovered hydrogen for the synthesis of methanol. Moreover, Scheme E using bio-oil as a feedstock in polygeneration Scheme A is also assessed considering its co-processing potential. Block flow diagrams for Schemes A-E are illustrated in Figure 1. All schemes exploit gasification based routes to provide clean products of choice.

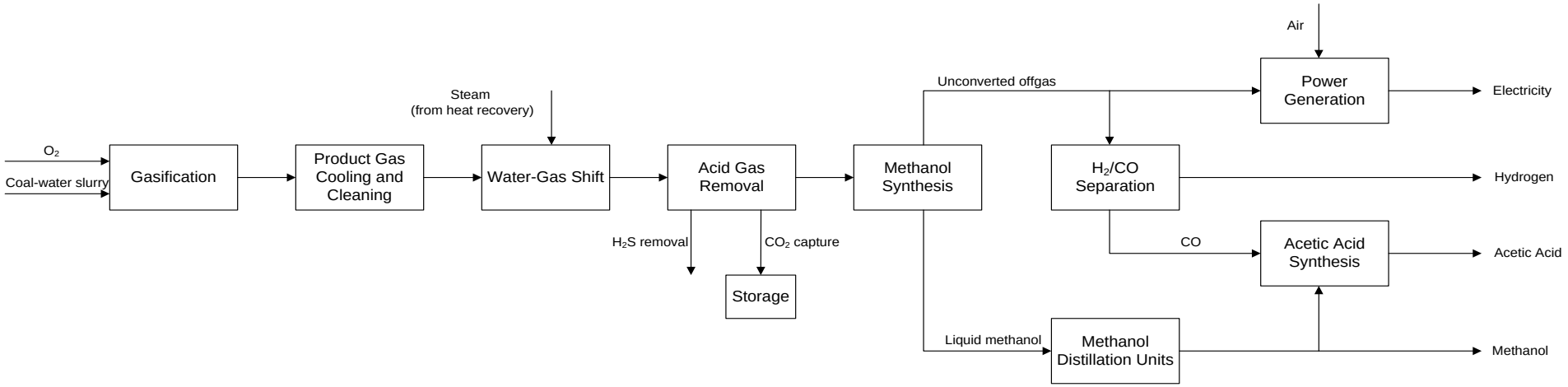
Air
Power Generation
Electricity
Unconverted offgas
Steam
(from heat recovery)
O_2
Coal-water slurry
Gasification
Product Gas Cooling and Cleaning
Water-Gas Shift
Acid Gas Removal
Methanol Synthesis
H_2/CO Separation
Hydrogen
CO
Acetic Acid Synthesis
Acetic Acid
H_2S removal
CO_2 capture
Storage
Liquid methanol
Methanol Distillation Units
Methanol

(a)

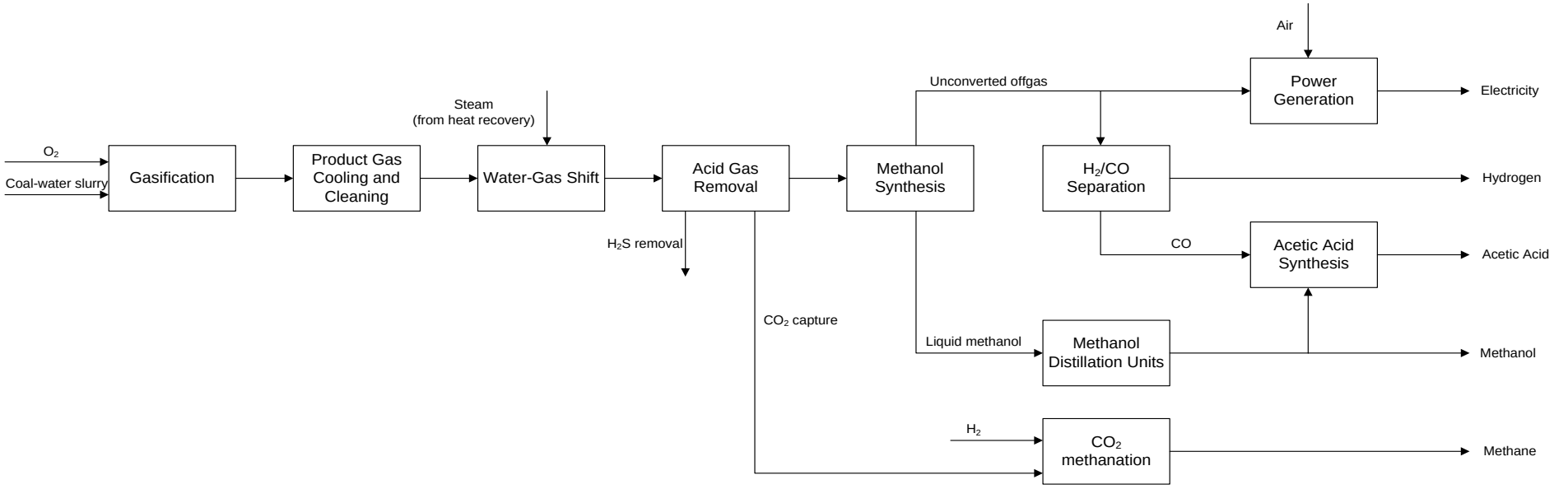
Air
Power Generation
Electricity
Unconverted offgas
Steam
(from heat recovery)
O_2
Coal-water slurry
Gasification
Product Gas Cooling and Cleaning
Water-Gas Shift
Acid Gas Removal
Methanol Synthesis
H_2/CO Separation
Hydrogen
CO
Acetic Acid Synthesis
Acetic Acid
H_2S removal
CO_2 capture
Liquid methanol
Methanol Distillation Units
Methanol
H_2
CO_2 methanation
Methane

(b)

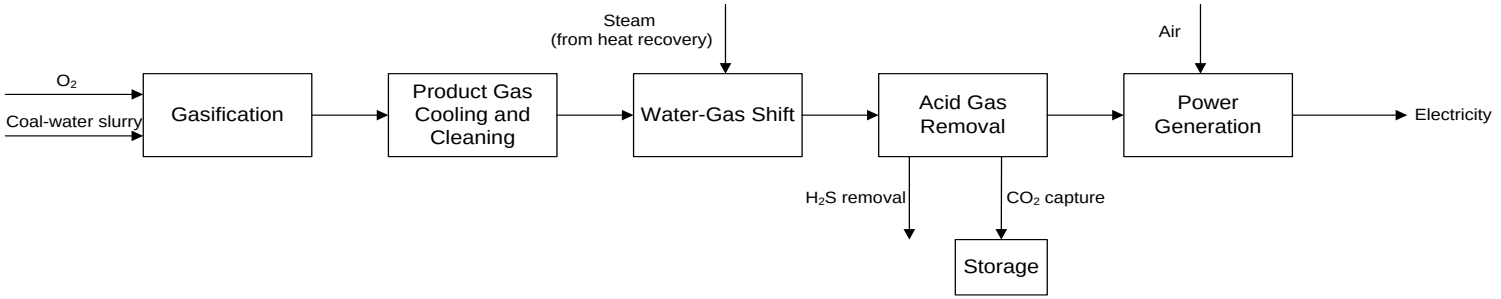
Steam
(from heat recovery)
Air
O_2
Coal-water slurry
Gasification
Product Gas Cooling and Cleaning
Water-Gas Shift
Acid Gas Removal
Power Generation
Electricity
H_2S removal
CO_2 capture
Storage

(c)

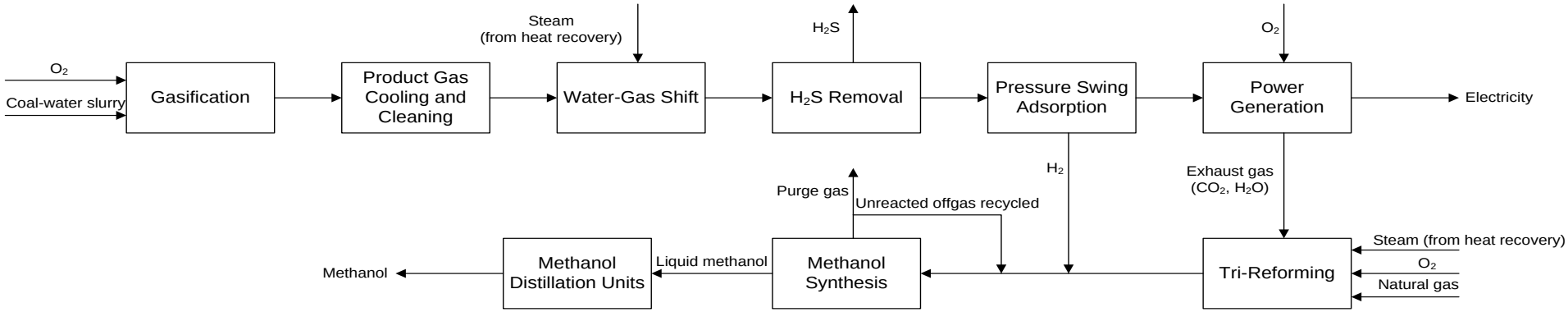
Steam
(from heat recovery)
H_2S
O_2
O_2
Coal-water slurry
Gasification
Product Gas Cooling and Cleaning
Water-Gas Shift
H_2S Removal
Pressure Swing Adsorption
Power Generation
Electricity
H_2
Exhaust gas
(CO_2, H_2O)
Purge gas
Unreacted offgas recycled
Steam (from heat recovery)
O_2
Natural gas
Methanol
Methanol Distillation Units
Liquid methanol
Methanol Synthesis
Tri-Reforming

(d)

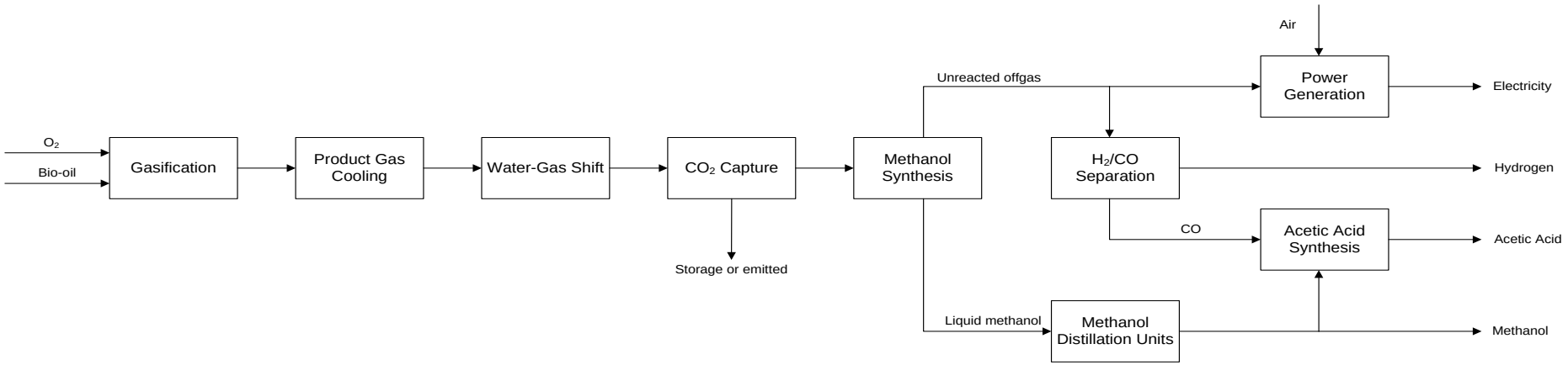

(e)

Figure 1: (a) Scheme A-Coal polygeneration with CCS. (b) Scheme B-Coal polygeneration with CO_2 methanation. (c) Scheme C-Coal IGCC with CCS. (d) Scheme D-Coal IGCC with tri-reforming and methanol synthesis. (e) Scheme E-Bio-oil polygeneration with CCS.

Development of polygeneration systems requires integrated production planning and process operations considering a wide range of market price fluctuation. Additionally, implication of the emission trading scheme and taxation (applicable to EU (Postnote, 2010)) on polygeneration system emission and economic performances must also be analysed. As the complexity in polygeneration system configurations and feedstock and product slate selections arises, arriving at an important and distinctive set of systems performance indicators becomes inherently challenging. This work takes the above challenges into consideration in suggesting a range of indicators for polygeneration systems trade-off analyses. These performance indicators include the effect of process configurations and operating conditions on the economic potential (*EP*), plant-wide decarbonisation potential, economic risks and product values and sensitivity in *EP* due to carbon taxations. Process integration tools provide efficient, low emission and marginally profitable designs. Related process integration works include heat integration (Smith, 2005), value analysis (Sadhukhan et al., 2004; Sadhukhan et al., 2008), biorefinery systems synthesis (Kokossis and Yang, 2010) and systems methodologies for CCS design (MacDowell et al., 2010) etc. Building upon process integration know-how, this work features the following tools for polygeneration systems trade-off analyses, discussed in the subsequent sections.

1. Process simulation considering variations in configurations and operating conditions.

2. Systematic energy integration and economic analysis framework.

3. Analysis of production portfolio and process operations for minimising economic risk due to price fluctuation of products, through classification by chances of occurrence.

4. Evaluation of product prices and carbon taxations for economic feasibility.

2. Methodology

The methodology comprising of process simulation in Aspen Plus, heat integration, economic analysis (including sensitivity analysis of price fluctuation of polygeneration products) is presented using coal polygeneration system with CCS, Scheme A, as an example (sections 2.1-2.3).

2.1 Process Simulation

Scheme A processing 2000 t/d of coal into methanol, acetic acid, electricity and hydrogen is simulated in ASPEN Plus, illustrated in Figure 2. The basis of modelling the process units is summarised in Table 1.

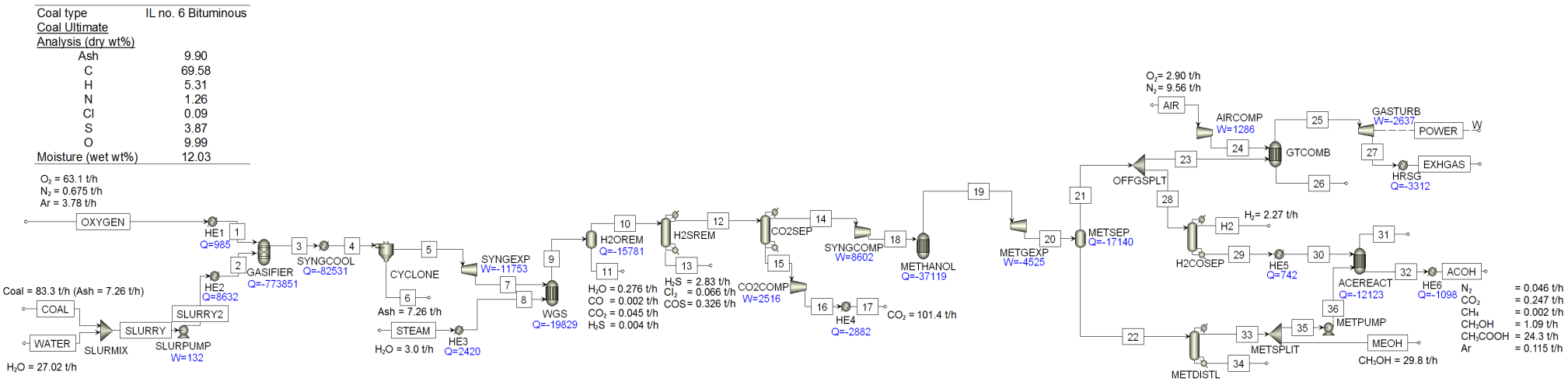

Q: kW
W: kW

Component Mole Fraction	Stream No.											
	3	9	18	19	21	22	23	EXHGAS	29	31	34	36
H_2	0.285	0.470	0.654	0.375	0.643	0.001	0.643				0.049	
H_2O	0.180	0.006	0.006	0.0005		0.001		0.232			0.058	
CO	0.421	0.223	0.311	0.142	0.239	0.006	0.239		0.669		0.255	
CO_2	0.084	0.272	0.004	0.018	0.026	0.007	0.026	0.096	0.073	0.211	0.322	
CH_4	0.0003	0.0003	0.0004	0.0007	0.001		0.001		0.003	0.010	0.003	
CH_3OH				0.418	0.014	0.983	0.014	0.005	0.041	0.023	0.227	1.000
CH_3COOH										0.075		
O_2								0.008				
N_2	0.007	0.007	0.009	0.017	0.029	0.0006	0.029	0.641	0.081	0.257	0.029	
Ar	0.011	0.011	0.015	0.028	0.048	0.001	0.048	0.017	0.134	0.425	0.056	
H_2S	0.010	0.010										
Cl_2	0.0001	0.0001										
COS	0.0006	0.0006										
Molar flow rates (kmol/s)	2.328	2.375	1.705	0.929	0.541	0.387	0.054	0.150	0.174	0.053	0.008	0.120

Figure 2: ASPEN Plus flowsheet model for coal polygeneration with CCS system (Scheme A).

Table 1: Coal polygeneration with CCS (Scheme A) process specification in ASPEN Plus simulation.

'Compr' = Compressor / turbine; 'Sep' = Component separator; 'RGibbs' = Gibbs reactor; 'REquil' = Equilibrium reactor; 'Flash2' = Two-outlet flash; 'Heater' = Heater; 'Mixer' = Stream mixer; 'SSplit' = Substream splitter; 'FSplit' = Stream splitter; 'Pump' = Pump.

Unit	ASPEN Plus model	Outlet Temperature (℃)	Pressure (bar)	Other Specification
ACEREACT	REquil	150	30	
AIRCOMP	Compr		14	Isentropic efficiency = 0.9
CO2COMP	Compr		80	Isentropic efficiency = 0.9
CO2SEP	Sep			CO_2 split fraction = 0.99
CYCLONE	SSplit			Ash split fraction = 1.0
GASIFIER	RGibbs	1371.1	75	
GASTURB	Compr		2	Isentropic efficiency = 0.9
GTCOMB	REquil	1200	14	
H2COSEP	Sep			H_2 split fraction = 1.0
H2OREM	Flash2	50	25	
H2SREM	Sep			H_2S, Cl_2, COS split fraction = 1.0
HE1	Heater	83.3	47	
HE2	Heater	121.1	42.4	
HE3	Heater	270	25	
HE4	Heater	35	80	
HE5	Heater	150	30	
HE6	Heater	30	30	
HRSG	Heater	100	1	
METDISTL	Sep			CH_3OH split fraction = 0.995
METGEXP	Compr		24	Isentropic efficiency = 0.9
METHANOL	REquil	250	100	
METPUMP	Pump		30	Pump efficiency = 0.9
METSEP	Flash2	40	24	
METSPLIT	FSplit			Flow to stream 35 = 0.12 kmol/s
OFFGSPLT	FSplit			Split fraction = 0.9
SLURMIX	Mixer		1	
SLURPUMP	Pump		42.4	Pump efficiency = 0.9
SYNGCOMP	Compr		100	Isentropic efficiency = 0.9
SYNGCOOL	Heater	430	75	
SYNGEXP	Compr		25	Isentropic efficiency = 0.9
WGS	Requil	250	25	

The coal-water slurry is gasified at 75 bar and 1371 ℃ in entrained flow gasifier (GASIFIER), using oxygen-enriched air (93.4% O_2, 1% N_2 and 5.6% Ar) as the gasification medium. The coal-water slurry and oxygen-enriched air are preheated to 121 ℃ and 83 ℃, respectively prior to gasification. The coal gasification model validated against literature results (Larson and Tingjin, 2003) is used in this study. The product gas (stream 3), containing a mixture of H_2, CO, CO_2, H_2O as major components with H_2/CO molar ratio of 0.7 is cooled down to 430 ℃ in SYNGCOOL, followed by ash removal in CYCLONE. The gas is further expanded in SYNGEXP in order to meet the operating conditions of water-gas shift (WGS) reaction, i.e. 25 bar and 250 ℃. The outlet temperature of the product gas from SYNGCOOL, operating conditions of WGS and the steam requirement by WGS are decided to achieve desired H_2/CO molar ratio of 2.1 in the product gas. Furthermore, numerous gas clean-up steps such as water (H2OREM), H_2S (H2SREM) and Rectisol process (Xie, 2001) for CO_2 removal (CO2SEP) processes are deployed to attain a target stoichiometric ratio of $(H_2-CO_2) / (CO+CO_2) = 2.07$ of the gas for methanol production (Ng and Sadhukhan, 2011a).

The clean product gas is compressed to 100 bar (SYNGCOMP) to meet the high operating pressure requirement by the methanol synthesis reactor (METHANOL). The methanol synthesis reactions in equations (1)-(3) take place in gaseous phase at 100 bar and 250 ℃ (Hamelinck and Faaij, 2002), with a CO conversion of 75%. The gaseous product from METHANOL is expanded to 24 bar in METGEXP. A flash column (METSEP) is further used to separate the gaseous and liquid products at 40 ℃ and 24 bar. 98% recovery (molar basis) of methanol from liquid stream 22 from METSEP is attained. The offgas containing unreacted gases such as H_2, CO, CH_4 etc. (stream 21) is utilised in power generation through gas turbine (GASTURB) and acetic acid

(ACEREACT) production. The offgas distribution can be adjusted through sensitivity analysis, discussed in section 2.3.1.

$$CO + 2H_2 \leftrightarrow CH_3OH \qquad \Delta H_R^{\circ} = -90.6\ \text{kJ/mol} \qquad (1)$$

$$CO_2 + 3H_2 \leftrightarrow CH_3OH + H_2O \qquad \Delta H_R^{\circ} = -49.7\ \text{kJ/mol} \qquad (2)$$

$$CO + H_2O \leftrightarrow H_2 + CO_2 \qquad \Delta H_R^{\circ} = -41.5\ \text{kJ/mol} \qquad (3)$$

Hydrogen is separated via a H_2/CO separation process (H2COSEP), such as cryogenic separation (technology developer such as Linde), e.g. partial condensation and liquid methane wash (Gunardson, 1998). Liquid methanol is sent to distillation units (METDISTL) to further recover 99.5% of methanol coming from METSEP (Uhde, 2008). A portion of the liquid methanol, depending on the availability of CO in the offgas after separation from the product gas, is used in acetic acid synthesis. The primary acetic acid synthesis route is via methanol carbonylation (equation (4)) at 150 ℃ and 30 bar (Yoneda et al., 2001). This process technology is available from BP, Monsanto, Chiyoda and UOP.

$$CH_3OH + CO \leftrightarrow CH_3COOH \qquad \Delta H_R^{\circ} = -136.6\ \text{kJ/mol} \qquad (4)$$

Three main products obtained are hydrogen (54.5 t/d, 75.7 MW, stream H2), acetic acid (583.7 t/d, 88.5 MW, stream ACOH) and methanol (716.2 t/d, 166.6 MW, stream MEOH). The site has a net deficit of power of 14.4 MW, even though the gas turbine produces 2.6 MW of power. Additional power can be generated through combined heat and power (CHP) production followed by heat recovery from

SYNGCOOL, heat recovery steam generator (HRSG) and reactors' cooling units, analysed in section 2.2.

2.2 Heat Integration

A systematic heat integration methodology for the recovery of maximum heat and power as a product enhancing the energy efficiency of an overall system is presented in Figure 3.

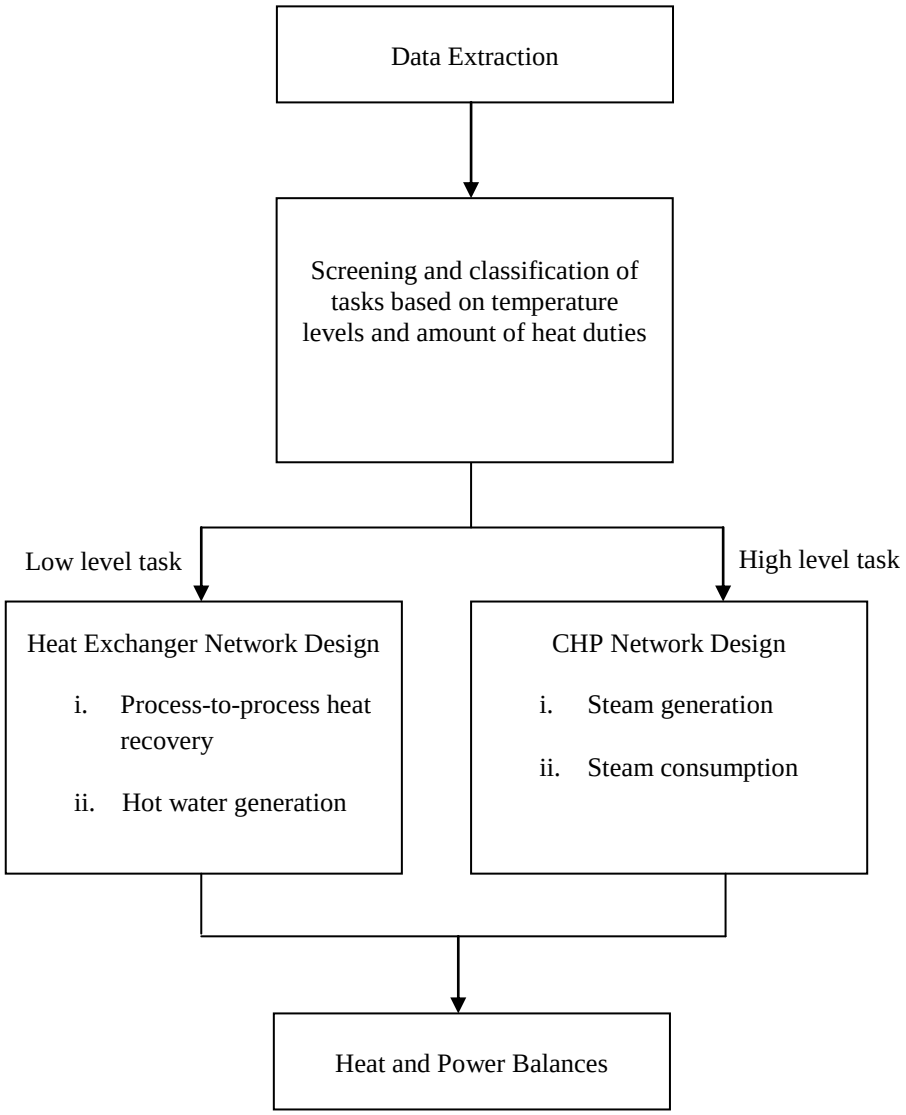

Figure 3: Heat integration strategy for polygeneration system.

Important data such as temperature and heat duties across process units are extracted from ASPEN Plus flowsheet simulation results in Figure 2, for screening and classification in high and low level heat integration tasks. The heat supply and demand of individual units are categorised in high and low level tasks based on the temperature levels and the amount of heat duties. The high level tasks involve CHP network design for steam generation and consumption based on composite curve and energy balance analyses, whilst the low level tasks indicate process-to-process heat exchanger network design based on pinch analysis (Smith, 2005; Ng et al., 2010). The low grade heat utilisation into hot water generation is also considered in heat exchanger network design.

The results of data extraction and classification of heat integration tasks in Scheme A (Figure 2) are summarised in Table 2. The heat from HRSG (3312 MW) though available at high temperature range (742 ℃-100 ℃) is negligible for steam generation (< 1 kg/s steam) and thus it is used for hot water generation, very relevant in the UK context. The heat demands by HE1, HE2 and HE5 at low temperature ranges are satisfied by the sensible heat available in H2OREM. The demand for LP steam (5 bar) is 4 MJ/kmol syngas by Rectisol (Xie, 2001) and 0.45 t/t methanol by METDISTL process (Uhde, 2008), respectively. The MP steam (14 bar) required by WGS is determined based on desired output condition of the product gas. Three levels of steam mains are considered according to the system requirement: VHP (80 bar, superheated to 500 ℃) that can be generated utilising exothermic heat of reaction from GASIFIER and sensible cooling duty of SYNGCOOL, MP (14 bar, superheated to 230 ℃) (sources are METHANOL and WGS reactors) and LP (5 bar and 152 ℃). It can be noted that the modelling of GASIFIER as RGibbs reactor (Table 1) may adequately present the product gas composition (Larson and Tingjin, 2003), but predict an optimistic amount

of exothermic heat of reaction due to the consideration of coal analysis at an elemental level. Therefore, Tables 2-3 highlight only the useful heat obtainable from GASIFIER, compared to the value presented in simulation Figure 2.

Table 2: Data extraction and classification for coal polygeneration system (Scheme A).

Process Unit	T_s **(℃)**	T_T **(℃)**	ΔH **(kW)**	**Heat Supply / Demand**	**Heat Utilisation / Source**
SYNGCOOL	1371	430	82531	Supply (High)	VHP steam generation (80 bar)
GASIFIER	1371.1	1371	464311	Supply (High) (Useful heat only)	VHP steam generation (80 bar)
WGS	250	249.9	19829	Supply (High)	MP steam generation (14 bar)
METHANOL	250	249.9	37119	Supply (High)	MP steam generation (14 bar)
HE4	147	35	2882	Supply (Low)	Process-to-process heating
HE6	149.9	30	1098	Supply (Low)	Process-to-process heating
H2OREM	249.9	50	15781	Supply (Low)	Process-to-process heating
METSEP	136.8	40	17140	Supply (Low)	Hot water generation
ACEREACT	150	149.9	12123	Supply (Low)	Hot water generation
HRSG	741.7	100	3312	Supply (Low)	Hot water generation
HE1	25	83.3	985	Demand (Low)	Process-to-process heating
HE2	27.73	121.1	8632	Demand (Low)	Process-to-process heating
HE5	40	150	742	Demand (Low)	Process-to-process heating

Steam Requirement	
Process Unit	**Mass flow rate of steam required (kg/s)**
Rectisol (5 bar)	4.5
Steam into WGS (HE3) (14 bar)	0.833
METDISTL (5 bar)	5.5

The steam generation and distribution are presented in CHP network diagram in Figure 4. The heat sources (SYNGCOOL, GASIFIER, WGS and METHANOL) provide steam to the steam mains and the heat sinks (WGS, Rectisol and METDISTL) consume steam from the steam mains. The remaining steam is expanded through steam turbines (ST1, ST2 and ST3) for power generation.

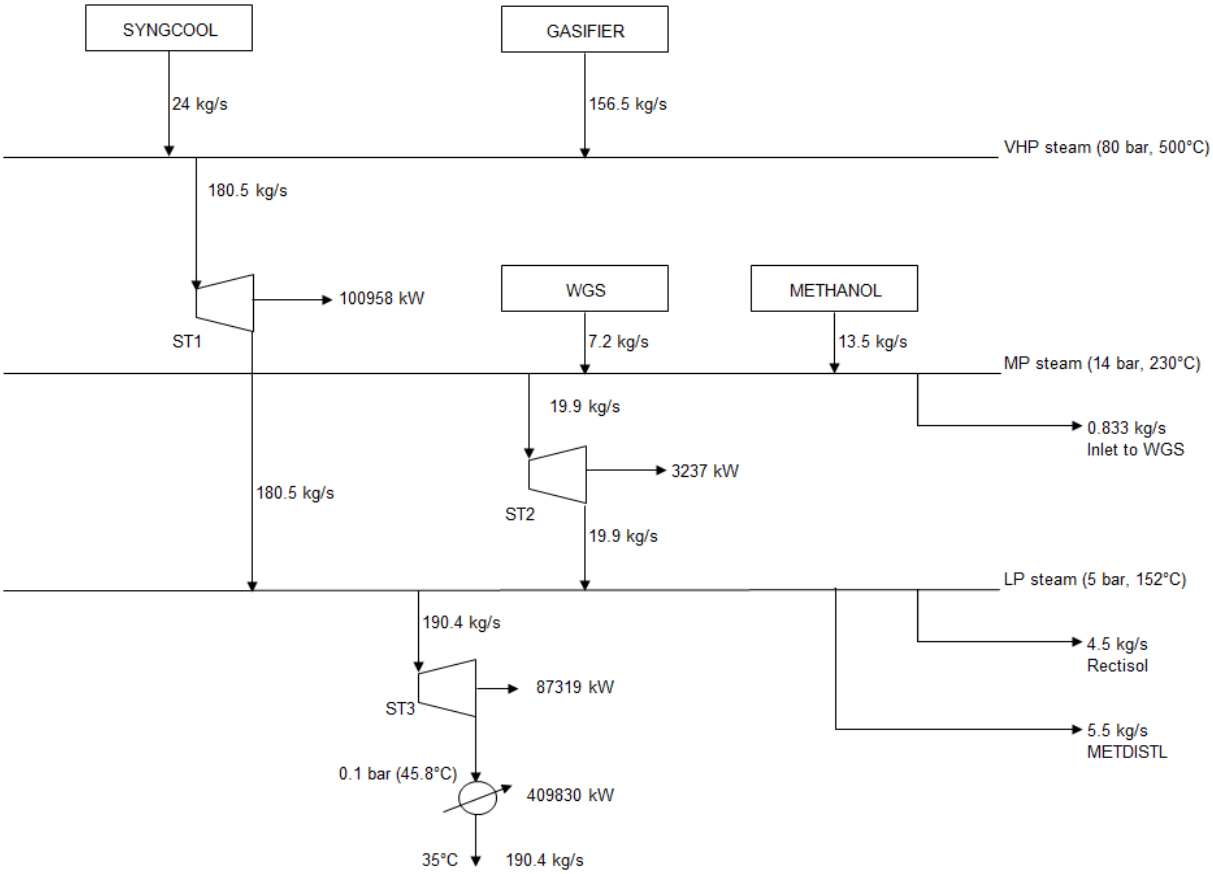

Figure 4: CHP network design for coal polygeneration with CCS system (Scheme A).

The heat and power balance of the overall system is presented in Table 3. The power requirements by the air separation unit (ASU) and the Rectisol unit are 235 kWh/t O_2 (Armstrong et al., 2005) and 5.89×10^{-4} MWh/kmol syngas (Xie, 2001), respectively. The net power generation is enhanced from a deficit of 14.4 MW previously obtained from process simulation in section 2.1 to 177 MW after heat integration. As a result, the net energy efficiency is increased to 78%, based on 648 MW of LHV of coal. This is in comparison to only 36% of energy efficiency achievable from a coal IGCC plant with CCS (Scheme C) under consideration (NETL, 2010).

Table 3: Heat and power balance for Scheme A.

	kg/s	kW
Steam generation	**305.6**	**911844.5**
SYNGCOOL (VHP, 80 bar)	24.0	81045.5
GASIFIER (VHP, 80 bar)	156.5	464310.6
WGS (MP, 14 bar)	7.2	19829.0
METHANOL (MP, 14 bar)	13.5	37119.0
Steam requirement	**10.8**	**23436.5**
Rectisol (LP, 5 bar)	4.5	9479.7
Inlet to WGS (MP, 14 bar)	0.8	2389.1
METDISTL (LP, 5 bar)	5.5	11567.7
Hot water generation	**178.3**	**41977.0**
METSEP	74.2	17140.0
ACEREACT	52.5	12123.0
HRSG	14.3	3312.0
Heat exchangers	37.3	9402.0
Power generation from steam turbine		**191514.0**
ST1		100958.0
ST2		3237.0
ST3		87319.0
Power generation on site		**18915.0**
GASTURB		2637.0
METGEXP		4525.0
SYNGEXP		11753.0
Power requirement on site		**33297.8**
ASU		15871.9
CO2COMP		2516.0
SYNGCOMP		8602.0
Rectisol		5021.9
AIRCOMP		1286.0
Net power generation (kW)		**177131.2**

2.3 Economic Analysis

The economic analysis of decarbonised polygeneration systems and the sensitivity analyses of the offgas distribution and conversion to methanol synthesis on the overall system performance are presented in section 2.3.1. The sensitivity analysis of price fluctuation of products is included in section 2.3.2.

2.3.1 Economic Potential (EP) Analysis

EP of polygeneration systems is determined using equation (5).

$$EP = H \sum_{i=1}^{i=NP} r_i p_i - CC - OC \tag{5}$$

H is the total number of operating hours per year; r_i and p_i are the production rate and unit price of product i, respectively; NP is the total number of products; CC and OC are annual capital cost and annual operating cost, respectively.

The capital cost is evaluated in terms of the direct (ISBL and OSBL) and indirect capital costs. The ISBL comprises of the cost of equipment which can be estimated using cost and size correlation, in equation (6). The parameters such as base cost, base scale and scale factor θ (Hamelinck and Faaij, 2002; Denton, 2003; IPCC, 2005; Larson et al., 2005; Zhu and Jones, 2009) are given in Appendix A. Each cost is levelised to the current cost using equation (7), where Chemical Engineering Plant Cost Index (CEPCI) is applied. The parameters for the estimation of the OSBL and the indirect capital cost (Hamelinck and Faaij, 2002) are also provided in Appendix A. The discounted cash flow method is applied for determining the annual charge for the capital investment, i.e. 11% using the following assumptions:

- Discount rate: 10%
- Plant life: 15 years
- Start-up period: 3 years (20%, 45%, 35%)

$$\frac{\mathrm{COST}_{\mathrm{size2}}}{\mathrm{COST}_{\mathrm{size1}}} = \left(\frac{\mathrm{SIZE}_2}{\mathrm{SIZE}_1} \right)^{\theta} \tag{6}$$

SIZE_1 and $\mathrm{COST}_{\mathrm{size1}}$ represent the capacity and the cost of a base unit, whilst SIZE_2 and $\mathrm{COST}_{\mathrm{size2}}$ represent the capacity and the cost of the unit after scaling up/down, respectively.

$$\text{Present cost} = \text{Original cost} \times \left(\frac{\text{Index at present}}{\text{Index when original cost was obtained}} \right) \tag{7}$$

The operating cost comprising of the fixed and variable costs is evaluated. The parameters for estimating the operating costs (Tijmensen et al., 2002; Sinnott, 2006; DECC, 2010) are given in Appendix A. The economic assumptions are as follows:

- Operating hours per year (*H*): 8000 hours
- Current CEPCI: 555.2 (April, 2010)

The current market prices / estimated cost of production are identified for evaluating the total value of the products, i.e. electricity (74.14 Euro/MWh (DECC, 2010)), hydrogen (1104 Euro/t (Stiegel and Ramezan, 2006)), acetic acid (550 Euro/t (ICIS Pricing, 2010)) and methanol (255 Euro/t (Methanex, 2010)).

The offgas from methanol synthesis reaction can be distributed into electricity, hydrogen and acetic acid production. The effect of split fractions of 0.9, 0.5 and 0.1 of stream 28 in Figure 2 on overall *EP* prior to the heat integration is presented in Table 4(a). A split fraction of 0.9 means 90% of the offgas is used for hydrogen and acetic acid production while 10% is used for power generation through gas turbine. The scenario with a split fraction of 0.9 is the most economically favourable case, *EP* = 33.7 million Euro/y. The other two scenarios with split fractions of 0.5 (*EP* = −6.6 million Euro/y) and 0.1 (*EP* = −46.8 million Euro/y) are not economically viable. There is no net electricity generation from all these scenarios. Lowering the split fraction of the offgas from 0.9 to 0.1 increases the electricity generation from the gas turbine. This in turn reduces the plant's operating cost by 10%. However, the value of products is reduced significantly by 87% due to the reduction in the split fraction. Thus, overall a higher level of diversion into added value production is desired. High added value production is however accompanied with a higher level of economic risk, discussed in section 2.3.2.

Two different values of conversion of CO in methanol synthesis, 75% and 50%, after heat integration and for an offgas split fraction of 0.9, producing 43.7 t/h and 28 t/h of methanol, respectively, are also taken into consideration to select preferred operating scenario in terms of *EP* (Table 4(b)). The trends suggest that lower conversion of CO in methanol synthesis reaction results in higher *EP*, 211.7 million Euro/y at 50% conversion and 139.9 million Euro/y at 75% conversion, respectively. This is primarily due to the higher value acetic acid production, 49.9 t/h at 50% conversion compared to 24.3 t/h at 75% conversion, respectively. A portion of methanol, 27.1 t/h for 50%

conversion and 13.8 t/h for 75% conversion, respectively is utilised in carbonylation process for the formation of acetic acid (equation (4)).

The sensitivity studies of the distribution of the offgas from the methanol synthesis reactor as well as the conversion in methanol synthesis reaction explain the importance of manipulation of operating conditions on polygeneration system performance. The manipulation of these operating conditions serves as a low cost modification option for the mitigation of moderate level of economic risks, discussed in section 2.3.2. The increased *EP* presented in Table 4(a) and (b) also demonstrates the importance of energy integration and efficiency studies. The power generating from gas and steam turbines is sufficient for the whole system supply, leading to a considerable reduction in operating cost by 19% and an increase in product value by 56%.

Table 4: (a) Sensitivity analysis of the effect of split fraction of offgas on the economic potential. (b) Sensitivity analysis of the effect of conversion of methanol synthesis reaction on the economic potential.

Note: All costs in million Euro/y.

(a)

OFFGSPLT split fraction	**0.9**	**0.5**	**0.1**
Capital cost	71.1	72.0	72.4
Operating cost	83.1	78.9	74.6
Value of products	187.9	144.4	100.2
Hydrogen	20.0	11.1	2.2
Acetic Acid	107.0	59.4	11.9
Methanol	60.9	73.8	86.0
Economic potential	**33.7**	**−6.6**	**−46.8**

(b)

Conversion of CO in METHANOL (%)	**75**	**50**
Capital cost	85.7	83.4
Operating cost	67.4	67.2
Value of products	293.0	362.3
Electricity	105.1	105.7
Hydrogen	20.0	35.2
Acetic Acid	107.0	219.6
Methanol	60.9	1.8
Economic potential	**139.9**	**211.7**

2.3.2 Sensitivity Analysis of Price Fluctuation of Polygeneration Products

Uncertainty in price of chemicals is due to instability in supply and demand, oil prices and unforeseen circumstances such as natural disaster and oil spill etc. Further complication arises particularly in a polygeneration plant wherein there are competing productions. Therefore, the effect of price fluctuations of products on *EP*, through classification by chances of occurrence has been introduced as follows.

There are four products under consideration: electricity, hydrogen, acetic acid and methanol. The unit prices of products, p_w, p_x, p_y and p_z, respectively, are considered as variables. Three sets of prices are assumed for each product: base price ($p_{i,0}$), a price lower than the base price by a difference of Δ% ($p_{i,-\Delta\%}$) and a price higher than the base price by a difference of Δ% ($p_{i,+\Delta\%}$). Based on Counting Principle, there are 81 (n) combinations due to three sets of prices for four individual products ($3\times3\times3\times3$), (equation (8)).

$$\underset{n\times 4}{\begin{bmatrix} p_{w,0} & p_{x,0} & p_{y,0} & p_{z,0} \\ p_{w,-\Delta\%} & p_{x,-\Delta\%} & p_{y,-\Delta\%} & p_{z,-\Delta\%} \\ p_{w,+\Delta\%} & p_{x,+\Delta\%} & p_{y,+\Delta\%} & p_{z,+\Delta\%} \\ \text{M} & \text{M} & \text{M} & \text{M} \end{bmatrix}} \underset{4\times 1}{\begin{bmatrix} r_w \\ r_x \\ r_y \\ r_z \end{bmatrix}} = \underset{n\times 1}{\begin{bmatrix} r_w p_{w,0} + r_x p_{x,0} + r_y p_{y,0} + r_z p_{z,0} \\ r_w p_{w,-\Delta\%} + r_x p_{x,-\Delta\%} + r_y p_{y,-\Delta\%} + r_z p_{z,-\Delta\%} \\ r_w p_{w,+\Delta\%} + r_x p_{x,+\Delta\%} + r_y p_{y,+\Delta\%} + r_z p_{z,+\Delta\%} \\ \text{M} \end{bmatrix}} \tag{8}$$

The *EP* (equation (5)) due to the market price combinations for a constant Δ% and variable Δ% in equation (8) is predicted in Matlab environment. The *CC* and *OC* are 85.7 million Euro/y and 67.4 million Euro/y, respectively. The value of products and *EP* of the base case in Figure 2 on a basis of 8000 operating hours per year are 293.0 million Euro/y and 139.9 million Euro/y, respectively (Table 4(b)). By assuming that

the system results in an acceptable *EP* at the current market scenario, any variation in *EP* due to price fluctuation may lead to an economic risk. An "economic risk" refers to a loss in revenue due to any event (a combination of product prices). It is important to predict and classify the potential economic risk in various ranges, e.g. ≥ 0%, 0% to −20%, −20% to −50% and < −50% (− indicates reduction in revenue compared to the base case revenue). The frequency of having a particular class of economic risk (e.g. ≥ 0%) is determined by counting the number of events resulted into the given class of economic risk. The probability of occurrence of a particular class of economic risk is obtained by the ratio of the frequency of events resulting into the given class of economic risk to the total number of events.

Case 1: Constant Δ%

Table 5(a) summarises the classification of economic risks, the frequency of events resulting into each class of economic risk, probability of occurrence of each event and the decision to be taken, based on 50% variation in individual product price fluctuation. All scenarios with positive variation in *EP* are in safe *EP* region, and the probability of having such scenario is approximately 51%. Thus, the probability of having moderate to critical economic risk is significant.

Case 2: Variable Δ%

Table 5(b) takes account of individual product price fluctuations over a certain period discussed as follows, in order to assess the economic risk, frequency of events within each class of economic risk, probability of occurrence of each event and the modification requirement.

Table 5: (a) Constant variation in price fluctuation. (b) Non-constant variation in price fluctuation.

(a)

Classes of economic risks	Frequency	Probability (%)	Decision
≥ 0% variation	41	50.6	No potential economic risk. Modification is not required.
within 0% to −20% variation	11	13.6	Moderate economic risk. Low cost modification may be required.
within −20% to −50% variation	15	18.5	High economic risk. Moderate to high cost modification is required.
< −50% variation	14	17.3	Critical economic risk. Major retrofitting of the plant is required.
Total number of events	81		

(b)

Classes of economic risks	Frequency	Probability (%)	Decision
≥ 0% variation	52	64.2	No potential economic risk. Modification is not required.
within 0% to −20% variation	9	11.1	Moderate economic risk. Low cost modification may be required.
within −20% to −50% variation	14	17.3	High economic risk. Moderate to high cost modification is required.
< −50% variation	6	7.4	Critical economic risk. Major retrofitting of the plant is required.
Total number of events	81		

The contract price of methanol from January 2006 to September 2010 (Methanex, 2010) is presented in Figure 5(a). The price fluctuation of acetic acid is not published, and thus the price fluctuation of methanol is used as a benchmark for its price. The price of hydrogen is often kept proprietarily by organisation. The price fluctuation of hydrogen is thus inferred from the price of natural gas (DECC, 2010) (Figure 5(b)). The price of electricity (Figure 5(b)) is also obtained from DECC (2010). Table 6 presents the percentage price variation from the base case unit price of products.

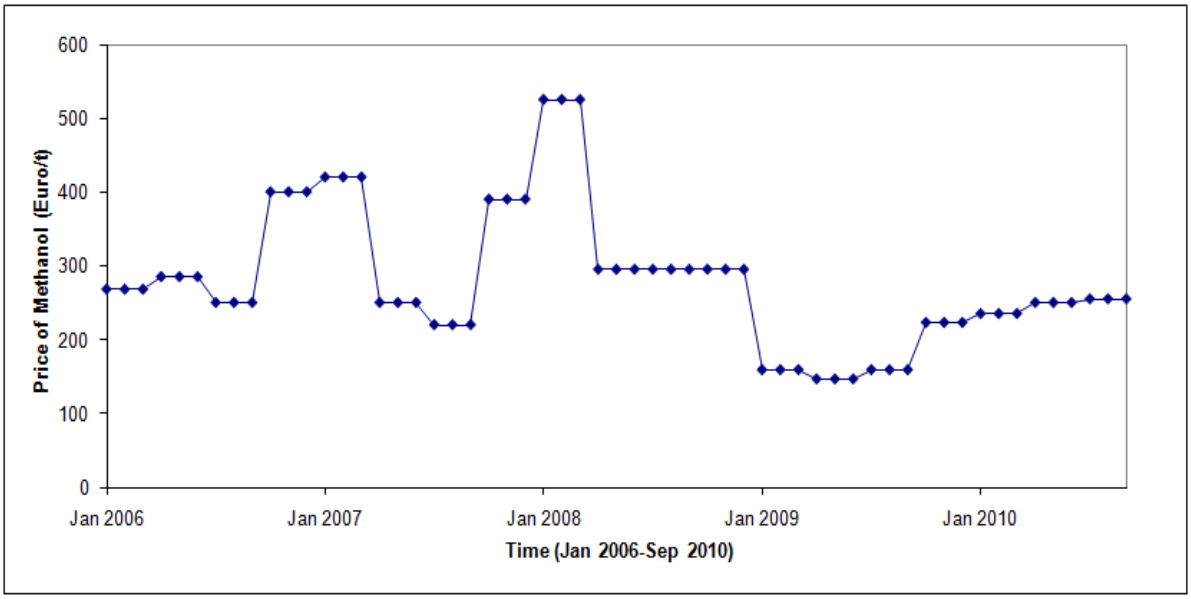

(a)

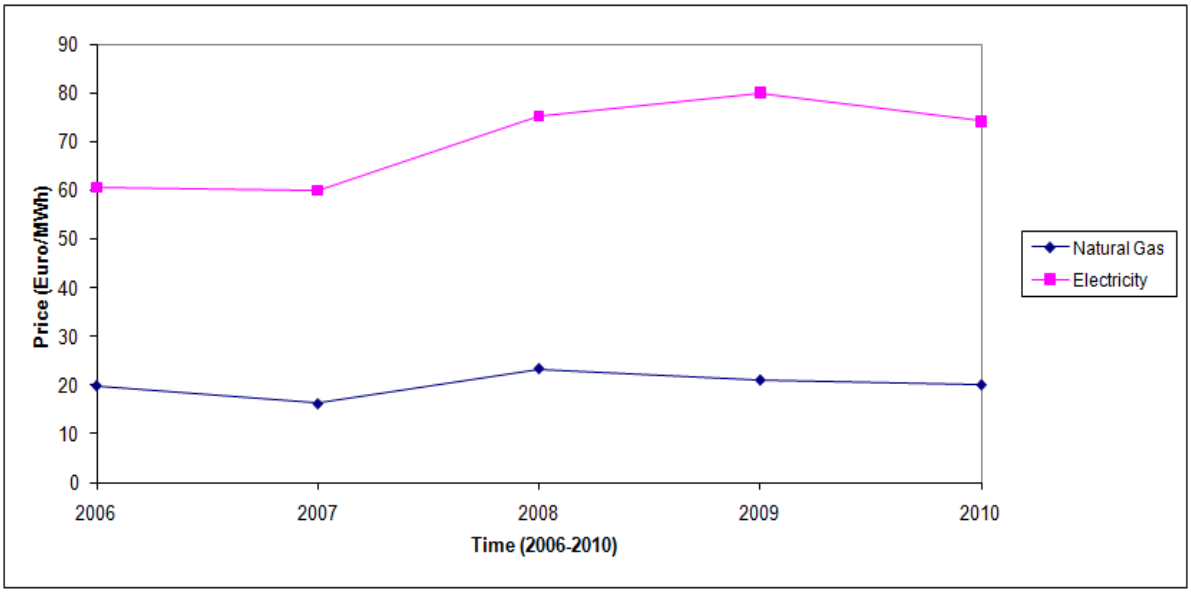

(b)

Figure 5: (a) Price fluctuation of methanol (Jan 2006-Sep 2010). (b) Price fluctuation of natural gas and electricity (2006-2010).

Table 6: Variation in prices of products.

Product (i)	Variation, Δ (%)			Price, p_i (Euro/MWh * or Euro/t **)		
	min	base	max	min	base	max
Electricity * (w)	−10	0	+35	66.7	74.14	100.1
Hydrogen * (x)	−20	0	+45	883.2	1104	1600.8
Acetic acid** (y)	−50	0	+110	275.0	550	1155.0
Methanol ** (z)	−50	0	+110	127.5	255	535.5

It is evident that 41 events in case of constant Δ% and 52 events in case of variable Δ% out of a total of 81 events (combinations of prices) result in higher *EP* or no economic risk. Table 5(b) indicates 64% probability of having no economic risk and 7% probability of having critical economic risk. However, the probability of having moderate to high economic risks is also within a range of 28% and comparable to 32% probability in the constant Δ% case. This suggests that a significant reduction in revenue due to product price fluctuation may be encountered, and hence, various levels of cost modification strategies must be analysed as a part of detailed system design exercise. To mitigate moderate to high economic risk, the low to high cost modification in Table 5 may be achieved by diversion to lower impact (generally lower value) products (e.g. by the manipulation of operating conditions) discussed in section 2.3.1, while the critical economic risk may only be mitigated by plant retrofitting. The product with the highest market price fluctuation is likely to result in the highest economic risk and vice versa. Thus the sequence of the highest to the lowest impact products (or the reverse order of preference in terms of product diversion) in Table 6 is as follows, acetic acid / methanol > hydrogen > electricity. Polygeneration framework provides flexibility in product diversion and thereby ways of mitigating various levels of economic risks.

3. CO_2 Emission Minimisation through Process Modification

The simulation of other polygeneration schemes is outlined in section 3.1. The thermodynamic efficiency, *EP* and environmental impact of the various process schemes are presented in section 3.2. The CO_2 mitigation options and future deployment potential of polygeneration systems are discussed in section 3.3.

3.1 Simulation of Polygeneration Schemes

All schemes, A-E, under consideration have the same coal or bio-oil input processing capacity, i.e. 648 MW. Schemes A-D have a throughput of 2000 t/d of coal, while 3102 t/d of bio-oil is used in Scheme E to achieve 648 MW (LHV of bio-oil is 18 MJ/kg). Additional operating parameters of Schemes C-E used in ASPEN Plus simulation are given in Appendix B. Heat integration strategy illustrated in Figure 3 is undertaken for all systems under consideration.

Scheme B-Coal polygeneration with CO_2 methanation (Figure 1(b))

CCS is included in Scheme A in order (i) to obtain a suitable stoichiometric ratio in the product gas for methanol production; (ii) to reduce CO_2 emission from the system. Whilst carbon capture unit is essential, storage is optional, however. CO_2 captured can be utilised into other chemical production, such as methane, benzene, methanol etc. An alternative process Scheme B that utilises CO_2 into methane production in Sabatier's reaction (equation (9)) is introduced. The operating condition of the Sabatier's reaction is set at 2 bar and 300 ℃ (Barbarossa et al., 2009). 2.56 kmol/s of hydrogen is required and 96% conversion of CO_2 by mole is achieved for the production of 35.5 t/h of methane. CO_2 is released with the exhaust gas from gas turbine and unreacted gases

from acetic acid synthesis and Sabatier's reactions. The Sabatier's reaction has been successful in space-based applications. These include production of water in International Space Station and the In-Situ Resource Utilisation for space exploration to Mars by NASA (Curie, 2010).

$$CO_2 + 4H_2 \leftrightarrow CH_4 + 2H_2O \qquad \Delta H_R^{\circ} = -167\ \text{kJ/mol} \qquad (9)$$

Scheme C-Coal IGCC with CCS (Figure 1(c))

In this scheme, coal is gasified into syngas and heat and power, with CCS in pre-combustion process (Ng et al., 2010). CO_2 may be emitted with the exhaust gas from the gas turbine.

Scheme D-Coal IGCC with tri-reforming and methanol synthesis (Figure 1(d))

The cost of CCS and the degree of decarbonisation pose an important trade-off in coal IGCC system with CCS (Ng et al., 2010). Scheme D producing methanol by the reuse of CO_2 generated from the gas turbine in tri-reforming process (equations (10)-(12)) (Song and Pan, 2004) can potentially replace the cogeneration Scheme C. Tri-reforming of methane using CO_2 for the production of valuable syngas with desired ratio and reduction of carbon formation on catalyst was first implemented by Song and Pan (2004). The tri-reforming process fed with CH_4, CO_2, H_2O and O_2 with a molar ratio of 1: 0.475: 0.475: 0.1 is operated at 1 bar and 850 ℃ (Song and Pan, 2004). The product gas contains H_2 to CO at a molar ratio of 1.68.

$$CH_4 + CO_2 \leftrightarrow 2CO + 2H_2 \qquad \Delta H_R^{\circ} = +247.3\ \text{kJ/mol} \qquad (10)$$

$$CH_4 + H_2O \leftrightarrow CO + 3H_2 \qquad \Delta H_R^{\circ} = +206.3\ \text{kJ/mol} \qquad (11)$$

$$CH_4 + 0.5O_2 \leftrightarrow CO + 2H_2 \qquad \Delta H_R^{\circ} = -35.6\,\text{kJ/mol} \qquad (12)$$

98% H_2 (1.5 kmol/s in this case) is separated from the product gas from gasification using pressure swing adsorption (PSA), which is then combined with the product gas from tri-reforming process. The remaining CO enriched gas from PSA is sent to gas turbine for electricity generation. A small amount of natural gas is needed to maintain an acceptable Wobbe Index for the gas turbine (Ng et al., 2010). Oxygen is used in an oxy-fuel gas turbine combustor, avoiding dilution of the fuel gas with nitrogen, and thereby reducing nitrogen in the downstream tri-reforming and methanol synthesis processes. A highly concentrated CO_2 stream is resulted from gas turbine combustion. The exhaust gas from gas turbine is then routed to the tri-reforming process. 95% of the unreacted offgas from methanol synthesis are recycled to enhance the production of methanol, while the rest is purged. The proposed integrated scheme meets the desired H_2/CO molar stoichiometric ratio in the feed gas to the methanol synthesis without any use of CCS.

Scheme E-Bio-oil polygeneration with CCS (Figure 1(e))

Bio-oil derived from fast pyrolysis of poplar wood is used as a feedstock in polygeneration Scheme E (similar to Scheme A that uses coal). The bio-oil is modelled using acetic acid, acetol and guaiacol. The results of bio-oil gasification performance were validated elsewhere (Ng and Sadhukhan, 2011a, 2011b). The operating conditions of some of the process units in Scheme A are adjusted to tailor for the bio-oil system. These include the temperature and pressure of the gasifier set at 1112 ℃ and 30 bar. This is to attain thermally neutral gasification reaction condition. The product gas from the gasification contains 31% H_2, 25% H_2O, 32% CO and 12% CO_2 by mole. Steam is

not required in WGS due to high water content in the product gas attributed to the high moisture content in bio-oil. The gas cleaning process excluded cyclone and H_2S removal units since bio-oil is free from contaminants. Pre-combustion CCS is used to capture 85% of CO_2 in order to attain a stoichiometric ratio $(H_2-CO_2) / (CO+CO_2) = 2.05$, desired for high yield of methanol (Ng and Sadhukhan, 2011a).

3.2 Polygeneration Scheme Performance Trade-offs

The analyses of process schemes A-E in terms of thermodynamic efficiency and net plant-wide emission and *EP* are presented in Table 7 and Table 8, respectively.

Table 7: Thermodynamic efficiency and emission analyses of various process schemes.

Process Scheme	Coal polygeneration with CCS (Scheme A)	Coal polygeneration with CO_2 methanation (Scheme B)	Coal IGCC with CCS (Scheme C)	Coal IGCC with tri-reforming and methanol synthesis (Scheme D)	Bio-oil polygeneration with CCS (Scheme E)
Thermodynamic Efficiency Analysis					
Product	LHV (MW)				
1. Electricity	177.1	191.7	237.0	123.4	14.3
2. Hydrogen	75.7	0.0	0.0	0.0	107.6
3. Acetic Acid	88.5	88.5	0.0	0.0	48.4
4. Methanol	166.6	166.6	0.0	2852.8	178.3
5. Methane	0.0	494.0	0.0	0.0	0.0
Total LHV of products	**507.9**	**940.8**	**237.0**	**2976.2**	**348.6**
Feed	LHV (MW)				
Main feedstock	Coal	Coal	Coal	Coal	Bio-oil
LHV of main feedstock	648.0	648.0	648.0	648.0	648.0
Additional feedstock	-	Hydrogen	-	Natural gas	Natural gas
LHV of additional	-	619.8	-	2802.6	22.7
Total LHV of feedstock	**648.0**	**1267.8**	**648.0**	**3450.6**	**670.7**
Thermal efficiency based on LHV of feedstock (%)	**78.4**	**74.2**	**36.6**	**86.3**	**52.0**
Emission Analysis					
Net CO_2 emission (t/h)	4.7	8.7	44.7	52.1	-
CO_2 captured / reused (t/h)	101.4 (captured)	97.4 (reused)	141.9 (captured)	216.8 (reused)	-
CO_2 reduction (%)	95.6	91.8	76.0	80.6	-
CO_2 emission per unit product (t CO_2/GWh)	7.7	8.3	127.8	16.9	-
CO_2 emission per unit feedstock (t CO_2/GWh)	7.3	6.8	68.9	15.1	-

Note: LHV of coal = 28 MJ/kg; bio-oil = 18 MJ/kg; hydrogen = 120.1 MJ/kg; acetic acid = 13.1 MJ/kg; methanol = 20.1 MJ/kg; methane = 50.1 MJ/kg; natural gas = 47.1 MJ/kg.

Table 8: Economic analysis of various process schemes.

Process Scheme	Coal polygeneration with CCS (Scheme A)	Coal polygeneration with CO_2 methanation (Scheme B)	Coal IGCC with CCS (Scheme C)	Coal IGCC with tri-reforming and methanol synthesis (Scheme D)	Bio-oil polygeneration with CCS (Scheme E)
Capital cost (million Euro/y)	85.7	89.2	86.2	142.9	66.9
Operating cost (million Euro/y)	67.4	255.2	67.4	655.4	12.2
Value of products (million Euro/y)	293.0	360.6	140.6	1115.5	160.6
1. Electricity	105.1	113.7	140.6	73.2	8.5
2. Hydrogen	20.0	0.0	0.0	0.0	28.5
3. Acetic Acid	107.0	107.0	0.0	0.0	58.5
4. Methanol	60.9	60.9	0.0	1042.3	65.2
5. Methane	0.0	79.0	0.0	0.0	0.0
Economic potential (million Euro/y)	**139.9**	**16.2**	**−13.1**	**317.2**	**81.6***
Economic potential (Euro/GJ)	**9.5**	**0.6**	**−1.9**	**3.6**	**8.1***

Note: Unit price of electricity = 74.14 Euro/MWh (DECC, 2010); hydrogen = 1104 Euro/t (Stiegel and Ramezan, 2006); acetic acid = 550 Euro/t (ICIS Pricing, 2010); methanol = 255 Euro/t (Methanex, 2010); methane = 20 Euro/MWh (DECC, 2010).

* The economic potential for Scheme E should be lower because the current value only reflects the netback of bio-oil, since the cost of bio-oil has not been accounted in the operating cost.

A comparison between Schemes A and B (polygeneration with CCS and with reuse, respectively) demonstrates that increasing the total value of products does not necessarily enhance an overall systems performance. Numerous trade-offs need to be considered. The total LHV of the products from Scheme B is 85% higher than that from Scheme A (on the basis of Scheme A product LHV), due to the additional production of methane from captured CO_2. In spite of this, the energy efficiency of Scheme B is lower than that in Scheme A attributed to the hydrogen requirement in the Sabatier's reaction (equation (9)) (Table 7). Scheme B has higher CO_2 emission per unit product than Scheme A, 8.3 t CO_2/GWh compared to 7.7 t CO_2/GWh, respectively (Table 7). The on-

site generation of hydrogen in Scheme B is not sufficient to meet the entire requirement and thus additional hydrogen is imported. This leads to 3.8 times higher operating cost for Scheme B compared to Scheme A, on the basis of a price of hydrogen of 1104 Euro/t (Stiegel and Ramezan, 2006). Compared to the operating cost, the product value due to methane production in Scheme B is only increased by 1.2 times from Scheme A. As a result, the *EP* of Scheme B is lower than that of Scheme A, 16.2 million Euro/y and 139.9 million Euro/y, respectively (Table 8). Scheme A would thus be more desirable in terms of energetic and emission performance improvement. If the value of methane increases to 51.3 Euro/MWh, both schemes would be cost-competitive (on the basis of 139.9 million Euro/y).

The negative *EP* from Scheme C suggests that the value of electricity generated does not offset the cost of CCS (Table 8). A price of 81 Euro/MWh of electricity has been estimated in order to achieve an economically viable Scheme C (*EP* > 0). Modification of a cogeneration system Scheme C into a polygeneration system Scheme D is likely to improve systems performances. The CO_2 emission per unit product from Scheme D (17 t CO_2/GWh) is lower than that from Scheme C (128 t CO_2/GWh) (Table 7). The advantage of Scheme D is that a substantial amount of methanol is produced by the integration of the post-combustion flue gas and natural gas in the tri-reforming process, increasing the overall value of the products that can compensate for the increased operating cost. There is a prominent improvement in the *EP*, from −13.1 million Euro/y in Scheme C to 317.2 million Euro/y in Scheme D (Table 8). As also observed from the study of Adams and Barton (2011), diverting captured CO_2 into liquid product is energetically more efficient and economically more favourable under

the current policy context, though the CO_2 reuse schemes do not save the total emission across life cycle, because eventually the products are consumed.

Scheme E, bio-oil polygeneration into methanol, acetic acid, hydrogen and electricity, is less efficient compared to analogous Scheme A using coal. This is primarily due to the lower LHV of bio-oil of 18 MJ/kg than 28 MJ/kg of coal and higher moisture content, i.e. 30 wt% of bio-oil and 12 wt% of coal, respectively (Larson and Tingjin, 2003; Ng and Sadhukhan, 2011a). Due to the thermal neutrality of the bio-oil gasification process, no excess steam is available for power production. Scheme E results in higher methanol production (CO conversion of 82%) (Ng and Sadhukhan, 2011a) than that from Scheme A (75%), however the acetic acid production from Scheme E is only half of that from Scheme A. Considering carbon sequestration during biomass growth, 66 t CO_2/GWh emission from Scheme E can be eliminated. The netback of bio-oil in Scheme E, that indicates the maximum buy-in price of bio-oil (81.6 million Euro/y or 8.1 Euro/GJ), is lower than the *EP* of Scheme A (139.9 million Euro/y) (Table 8). The bio-oil polygeneration system may still compete with the coal based schemes, if renewable products from bio-oil are given credits. The overall bio-oil based product value must at least be increased by 5.8 Euro/GJ, for cost-competitive performance against coal. Banding of price structure at various levels is introduced under the Renewables Obligation in the UK. This is to ensure that the technologies at a demonstration stage receive support and incentives for further exploitation at a larger scale (DECC, 2011). Our previous studies have also indicated mechanisms to create economic incentives for bio-oil based polygeneration systems (Ng and Sadhukhan, 2011a, 2011b; Sadhukhan and Ng, 2011).

3.3 Ranking of Polygeneration Schemes

Which design is superior? Capture and store, capture and reuse or reuse without capturing CO_2?

Based on the performance analyses of Schemes A-D (Figure 1) detailed in section 3.2, the following ranking in the order of preference for these schemes can be established.

Highest to lowest thermodynamic efficiency: D > A > B > C

Lowest to highest emission: A < B < D < C

Highest to lowest *EP* per unit output energy: A > D > B > C

The analyses suggest that modification of a cogeneration system into a polygeneration system is likely to boost the systems performances, whilst revamping a polygeneration system by adding more products does not necessarily relate to a significant improvement.

The CO_2 reuse cases, i.e. Schemes B and D represent the direct and indirect utilisation of CO_2, respectively. Scheme D, wherein post-combustion CO_2 without capture is converted into methanol through syngas platform has a more flexible configuration compared to Scheme B (polygeneration with CO_2 capture and reuse). It provides flexibility in syngas conditioning for the generation of other products, e.g. Fischer-Tropsch liquid, dimethyl ether etc. Most of the CO_2 reuse processes require hydrogen. A CO_2 reuse system self-sufficient in cost-effective hydrogen supply (without requiring any import or without including expensive hydrogen production technique) is highly envisaged, as demonstrated in Scheme D. The plant-wide emissions

from reuse Schemes B and D are lower than that from CCS Schemes A and C. However, from whole system life cycle perspectives, reuse schemes can only slow down CO_2 release to the atmosphere. In contrast, 96% and 76% of CO_2 from Schemes A and C (Table 7), respectively, are captured and stored underground, where the CO_2 life cycle can be prolonged. Considering all these aspects, Scheme A is regarded as the 'winner' attributed to its high efficiency, low CO_2 emission from a whole system life cycle perspective and high *EP* per unit output energy.

The impact of carbon tax

Based on the emission analysis of Schemes A-D (Figure 1) in Table 7, the order of sensitivity of *EP* to carbon tax can be established as follows (from the lowest to the highest slope in Figure 6(a)).

Lowest to highest sensitivity to carbon tax: A < B < D < C

Scheme A is able to withstand higher carbon tax rate, due to its high *EP* and low CO_2 emission. The *EP* only reduces to 102 million Euro/y for as high a carbon tax as 1000 Euro/t. Although less sensitive to carbon tax, levying carbon tax poses a great impact on Scheme B in view of its low *EP* that reduces to zero for a carbon tax of 235 Euro/t. Scheme D is more sensitive to carbon taxation than Schemes A and B, due to its higher CO_2 emission rate at 52.1 t/h compared to 8.7 t/h and 4.7 t/h from Schemes B and A, respectively. The carbon tax rate should be as high as 468 Euro/t, in order for Scheme D (best performance in reuse cases) to compete against Scheme A (best performance in CCS cases). At this point, the *EP* vs. carbon tax lines for Schemes A and D intercept, providing an *EP* of 122 million Euro/y. Negative *EP* for Scheme D is incurred above 762 Euro/t of carbon tax. There is no direct economic competition due to

carbon tax between reuse Schemes B and D, unless the tax rate is as high as 900 Euro/t. It is recognised that based on the consideration of both the sensitivity to carbon tax as well as *EP*, a scheme with low *EP* and with high environmental emission can be penalised by carbon tax (e.g. Scheme B). Broadly speaking, schemes with low *EP* and low emission are more likely to be susceptible to carbon tax than schemes with high *EP* and high emission (e.g. Scheme D). Obviously, schemes with high *EP* and low emission are the best options (Scheme A).

The maximum limit on CO_2 emission for $EP = 0$ for various carbon tax rates is investigated, using Scheme D as the base case, in Figure 6(b). The maximum limit on the CO_2 emission decreases exponentially from 32 million t/y to 6 million t/y with increasing carbon tax rate from 10 Euro/t to 50 Euro/t. Thus higher carbon tax rate lowers the total CO_2 emission and the economics of a system. Nevertheless, higher carbon tax rate at 40-50 Euro/t has shown 25% difference in the maximum limit, and it is expected that the difference will eventually become insignificant beyond carbon tax rate of 50 Euro/t due to the flattening of the exponential function. This forms a bottleneck with no further possibility of CO_2 emission reduction, even when the carbon tax rate is increased and thus carbon taxation essentially receded into the background.

The capital intensive CCS is likely to be realisable in industrialised nations. Annex I countries (UNFCCC, 2011) with high energy consumption per capita, stringent emission target, carbon tax and trading uncertainties, may opt for CCS in polygeneration schemes, such as Scheme A, whilst the reuse polygeneration schemes can become technologies of choice for developing economy in the interim period.

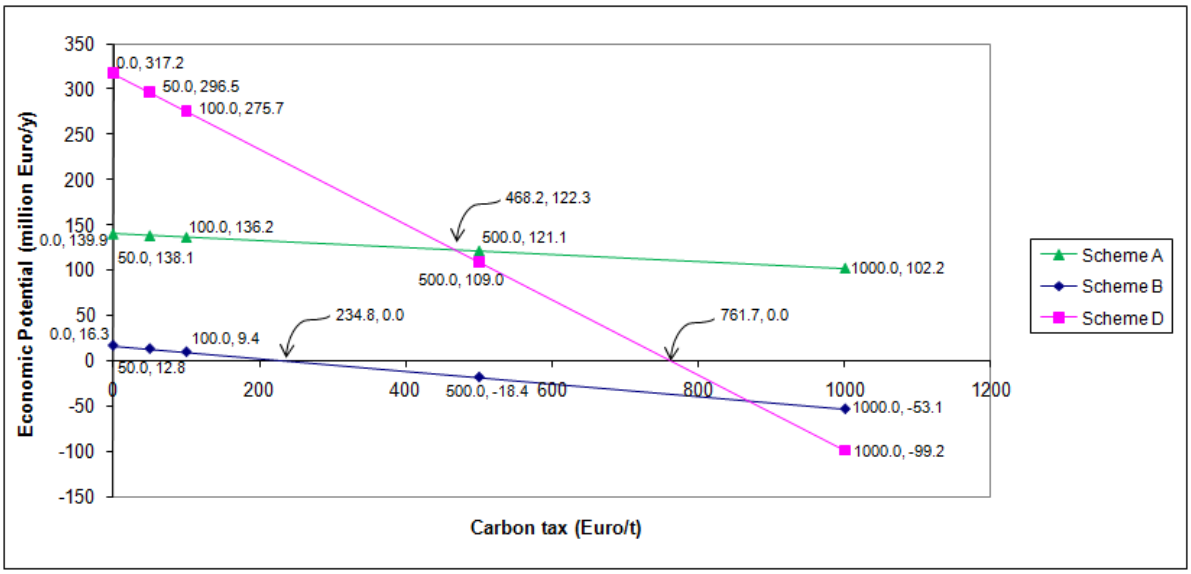

(a)

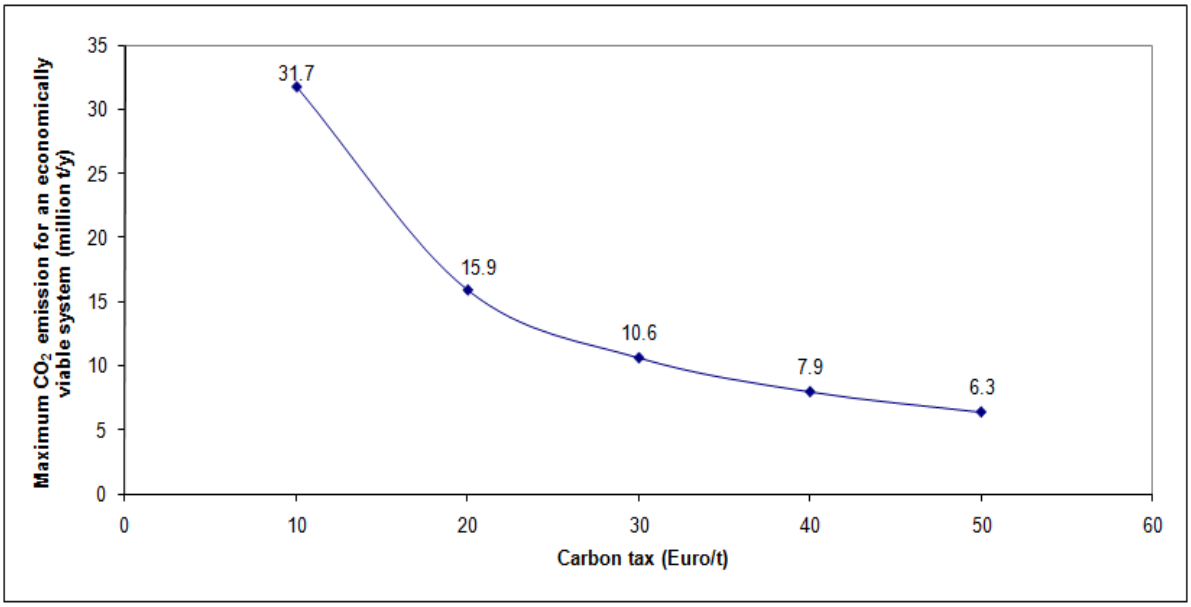

(b)

Figure 6: (a) Effect of variation in carbon tax rate on the economic potential of system. (b) Maximum CO_2 emission at different carbon tax rate for an economically viable system (Scheme D).

Bioenergy with carbon capture and storage

The integration of carbon capture and storage in the biomass based energy systems, known as bioenergy carbon capture and storage technology, has recently generated significant interest (IPCC, 2005; Rhodes and Keith, 2008; McGlashan et al., 2010). Such a technology is capable of producing useful product while achieving negative net atmospheric carbon emissions and hence generating more carbon credits. However, the prospect of this technology is unforeseeable due to a number of reasons such as the potential of utilisation of biomass in large scale production of fuels, chemicals and power; lack of experience and analysis (IPCC, 2005). In this study, Scheme E presents such an example. This scheme uses bio-oil instead of biomass as the feedstock. It has been found that Scheme E is less compelling compared to Scheme A with respect to the efficiency and the economic performance (Table 7 and Table 8). This imposes a greater challenge on the potential of bio-oil in substituting fossil fuels. However, by comparing between a conventional coal IGCC system (Scheme C) and a bio-oil polygeneration system (Scheme E), the latter can be beneficial, provided that the cost of bio-oil can be reduced to a significant extent.

One may argue that CO_2 storage is not necessary since biomass is regarded as carbon neutral source, because the CO_2 emitted can be re-captured by plants and crops. This is true as long as the rate of absorption of CO_2 by biomass crops is almost equal to the rate of emission of CO_2, and assuming that the amount of crops is more than sufficient to absorb the CO_2. This could be difficult if biomass crops within a particular area are largely harvested for the utilisation in a large scale system, and the plantation of biomass crops is not rapid enough to cope with the emission of CO_2 from large scale polygeneration systems. IPCC pointed out that bioenergy with carbon capture and

storage technology is realisable once the economies of scale are improved, via three possibilities (IPCC, 2005):

- Nearby CO_2 pipeline is available
- Co-processing of biomass with coal
- Scaling up the biomass energy plant for larger production

4. Conclusions

Process integration based performance analysis indicators for techno-economic feasibility of several decarbonised polygeneration systems are presented. The approach embraced simulation of polygeneration systems in ASPEN Plus; heat integration strategies for maximum heat recovery and power generation; economic analysis and economic risk assessment using classification by chances of occurrence of product prices. This study presents alternative coal and bio-oil based polygeneration schemes in the light of exploring various CO_2 emission minimisation pathways. These include capture and storage through CCS (Schemes A and C), capture and reuse (Scheme B) as well as reuse without capture (Scheme D). An additional polygeneration system utilising bio-oil (Scheme E) has also been presented. The performance of a cogeneration system can be improved by converting it into a polygeneration system. However, modification of an existing polygeneration system by including more products may not always create economic incentives. The performances of all schemes are compared with respect to the thermodynamic efficiency, emission, economic potential and economic sensitivity to carbon tax. Furthermore, different polygeneration schemes may be suitable for different countries depending upon emission reduction measures. Given that

industrialisation will even be at a faster pace and that there will be an unmet need for fully integrated environmental and economic policies in the interim phase, flexible CO_2 reuse into liquid fuels has potential as an interim carbon reduction strategy, while CCS based polygeneration systems are proven to exhibit long term benefits.

Nomenclatures

CC	Annual capital cost
EP	Economic potential
H	Total number of operating hours per year
ΔH_R°	Standard enthalpy change of reaction
N	Number of events derived from Counting Principle
NP	Total number of products
OC	Annual operating cost
p_i	Unit price of product i
r_i	Production rate of product i
θ	Scale factor, equation (6)

Appendix A

The economic parameters required for evaluating capital and operating costs are presented in Table A.1 and Table A.2, respectively.

Table A.1: Capital cost parameters.

ISBL					
No.	Process unit	Base Cost (million USD)	Scale factor, θ	Base scale	Scale unit
1	Coal handling [a]	29.58	0.67	2367	t/d coal input
2	Gasifier (GE type) [a]	62.92	0.67	716	MW coal input
3	Cyclone [a]	0.91	0.7	68.7	m^3/s gas feed
4	Water-gas shift reactor [a]	12.24	0.67	1377	MW LHV coal input
5	Rectisol [b, i]	54.1	0.7	9909	kmol CO_2/h
6	CO_2 transport and storage [c]	5.6 Euro/t CO_2			
7	Methanol reactor [b]	7	0.6	87.5	t MeOH/h
8	Methanol separation [b]	15.1	0.7	87.5	t MeOH/h
9	Acetic acid reactor and purification[d]	2 times of [(7) + (8)]			
10	H_2/CO separation [ii] or PSA [b]	28	0.7	9600	kmol/h feed
11	Gas turbine [a]	56	0.75	266	MW
12	Steam turbine (inc. condenser) [a]	45.5	0.67	136	MW
13	HRSG [a]	41.2	1	355	MW heat duty
14	SYNGCOOL [a]	25.4	0.6	77	MW heat duty
15	ASU [a]	35.6	0.5	76.6	t O_2/h
16	Compressor [a]	4.83	0.67	10	MW
17	Expander [a]	2.41	0.67	10	MW
18	Tri-reformer/ Methanator [b, iii]	9.4	0.6	1390	kmol/h feed
OSBL [b]					
No.	Specification	Cost estimation (% of ISBL)			
19	Instrumentation and control	5			
20	Buildings	1.5			
21	Grid connections	5			
22	Site preparation	0.5			
23	Civil works	10			
24	Electronics	7			
25	Piping	4			
	Total Direct Capital (TDC)	**ISBL + OSBL**			
Indirect Capital Cost [b]					
No.	Specification	Cost estimation (% of TDC)			
26	Engineering	15			
27	Contingency	10			
28	Fees/overheads/profits	10			
29	Start-up	5			
	Total Indirect Capital (TIC)				
	Total Capital Cost	**TDC+TIC**			

Note:

[a] Larson et al., 2005. Economic parameters taken from year 2003. Assume 1USD = 0.9 Euro (2003).

[b] Hamelinck and Faaij, 2002. Economic parameters taken from year 2001. Assume 1 USD = 1.1 Euro (2001).

[c] IPCC, 2005. Cost of CO_2 transport: 0-5 USD/t CO_2; Cost of CO_2 storage: 0.6-8.3 USD/t CO_2. Average values of CO_2 transport and storage are taken. Assume 1 USD = 0.8 Euro (2010).

[d] Cost of acetic acid reactor and purification is estimated based on 2 times of the cost of methanol reactor and distillation units, as suggested by Zhu and Jones, 2009.

[i] Cost of Rectisol is assumed to be 2 times of Selexol, as suggested by Denton, 2003.

[ii] Cost of H_2/CO separation unit is estimated based on the cost of PSA.

[iii] Costs of tri-reformer and methanator are assumed to be the same as the cost of steam reformer.

CEPCI: 2001= 394.3; 2003=402.0; 2010 (April)=555.2

Table A.2: Operating cost parameters.

Fixed Operating Cost [a]		
No.	Specification	Cost Estimation
1	Maintenance	10 % of indirect capital cost
2	Personnel	0.595 million Euro/100 MWth LHV
3	Laboratory costs	20% of (2)
4	Supervision	20% of (2)
5	Plant overheads	50% of (2)
6	Capital Charges	10% of indirect capital cost
7	Insurance	1% of indirect capital cost
8	Local taxes	2% of indirect capital cost
9	Royalties	1% of indirect capital cost
Variable Operating Cost [b]		
No.	Specification	Cost estimation
10	Natural Gas	20 Euro/MWh
11	Coal	2.4 Euro/GJ
12	Electricity	74.14 Euro/MWh
	Direct Production Cost (DPC)	**Variable + Fixed Operating Costs**
Miscellaneous [a]		
No.	Specification	Cost estimation
13	Sales expense, general overheads, research and development	30% of DPC
	Total OPEX per year	**DPC + Miscellaneous**

Note:
[a] The parameters except personnel are taken from Sinnott, 2006. Estimation for personnel is taken from Tijmensen et al., 2002.
[b] The variable operating costs for various feedstocks are taken from DECC, 2010.

Appendix B

Additional data are provided for modelling systems in Schemes C, D and E in ASPEN Plus, summarised in Table B.1.

Table B.1 : Additional data / results for Schemes C, D and E in ASPEN Plus modelling.

Process units and specification	Scheme C	Scheme D	Scheme E
Water-gas shift reactor			
• Steam flow rate (t/h)	20	35	-
• Temperature (℃)	370 (HTWGS [i]); 200 (LTWGS [i])	200	450
• Pressure (bar)	15 (HTWGS); 15 (LTWGS)	15	30
Gas turbine			
• Air / oxygen [ii] to gas turbine combustion chamber (kmol/s)	4	0.87	0.45
• Natural gas to gas turbine combustion chamber (kmol/s)	-	0.4	0.03
• Exhaust gas flow rate (kmol/s)	4.9	2.5	0.5
• Exhaust gas composition (mole fraction)			
CO_2	0.06	0.64	0.09
H_2O	0.28	0.34	0.21
Unreacted gas (O_2, N_2, Ar)	0.66	0.02	0.70
Tri-reformer			
• Feed flow rate (kmol/s)			
Steam		0.73	
Oxygen		0.33	
Natural gas		3.31	
• Product gas flow rate (kmol/s)		13.0	
• Product gas composition (mole fraction)			
H_2		0.59	
H_2O		0.03	
CO		0.36	
CO_2		0.02	

Note:
[i] There are high temperature and low temperature water-gas shift reactors for the system in Scheme C, i.e. HTWGS and LTWGS, respectively.
[ii] Air consists of 21 mol% oxygen and 79% nitrogen. Pure oxygen is used for gas turbine combustion in Scheme D.

Acknowledgement

The authors express their gratitude to The University of Manchester Alumni Fund and Process Integration Research Consortium for financial aid to support this research.

References

Adams, T. A. II, Barton, P. I., 2011. Combining coal gasification and natural gas reforming for efficient polygeneration. Fuel Process. Technol. 92(3), 639-655.

Armstrong, P. A., Bennett, D. L., Foster, E. P., Stein, V. E., 2005. ITM oxygen: the new oxygen supply for the new IGCC market. In *Gasification Technologies*, San Francisco, California, 9-12 October.

Barbarossa, V., Capriccioli, A., Sardella, B., Tosti, S., 2009. Carbon dioxide utilisation for methane production by renewable energy sources. In *Sustainable Fossil Fuel for Future Energy*, Rome, 8-11 July.

Bridgwater, A. V., 2009. Technical and economic assessment of thermal processes for biofuels, NNFCC project 08/018, COPE Ltd.

Carbon Recycling International (CRI), 2010. CRI breaks ground for the George Olah Renewable Methanol Plant. http://www.carbonrecycling.is/ (accessed 10 June 2011).

Curie, M., 2010. International space station water system successfully activated, 26th October. NASA. http://www.nasa.gov/home/hqnews/2010/oct/HQ_10-275_Sabatier_prt.htm (accessed 10 June 2011).

Department of Energy and Climate Change (DECC), 2010. Quarterly energy prices: June 2010. http://www.decc.gov.uk/ (accessed 30 September 2010)

Department of Energy and Climate Change (DECC). Renewables Obligation. http://www.decc.gov.uk/ (accessed 10 June 2011).

Denton, D. L., 2003. Coal gasification–today's technology of choice and tomorrow's bright promise. In *AIChE*, East Tennessee Section.

Gunardson, H., 1998. Industrial gases in petrochemical processes. Marcel Dekker, Inc., New York.

Hamelinck, C. N., Faaij, A. P. C., 2002. Future prospects for production of methanol and hydrogen from biomass. J. Power Sources. 111(1), 1-22.

ICIS Pricing, 2010. http://www.icispricing.com/il_shared/Samples/SubPage95.asp (accessed 30 September 2010).

Intergovernmental Panel on Climate Change (IPCC), 2005. IPCC special report on carbon dioxide capture and storage, http://www.ipcc.ch/publications_and_data/publications_and_data_reports.shtml (accessed 10 June 2011)

Kokossis, A. C., Yang, A., 2010. On the use of systems technologies and a systematic approach for the synthesis and the design of future biorefineries. Comput. Chem. Eng. 34(9), 1397-1405.

Larson, E. D., Tingjin, R., 2003. Synthetic fuel production by indirect coal liquefaction. Energy for Sustainable Development. 7(4), 79-102.

Larson, E. D., Jin, H., Celik, F. E., 2005. Gasification-based fuels and electricity production from biomass, without and with carbon capture and storage, Princeton Environmental Institute, Princeton University.
http://www.princeton.edu/pei/energy/publications/texts/ (accessed 30 September 2010)

Li, Y., Markley, B., Mohan, A. R., Rodriguez-Santiago, V., Thompson, D., Niekerk, D. V., 2006. Utilization of carbon dioxide from coal-fired power plant for the production of value-added products, Penn State College of Earth and Mineral Sciences.
http://www.ems.psu.edu/~elsworth/courses/egee580/Utilization_final_report.pdf
(accessed 10 June 2011)

Li, Z., Gao, D., Chang, L., Liu, P., Pistikopoulos, E. N., 2010. Coal-derived methanol for hydrogen vehicles in China: Energy, environment, and economic analysis for distributed reforming. Chem. Eng. Res. Des. 88(1), 73-80.

MacDowell, N., Florin, N., Buchard, A., Hallett, J., Galindo, A., Jackson, G., Adjiman, C. S., Williams, C. K., Shah, N., Fennell, P., 2010. An overview of CO_2 capture technologies. Energy & Environmental Science. 3(11), 1645-1669.

McGlashan, N., Shah, N., Workman M., 2010. The potential for the deployment of negative emissions technologies in the UK. Work stream 2, Report 18 of the AVOID programme (AV/WS2/D1/R18). www.avoid.uk.net (accessed 10 June 2011)

Methanex, 2010. Methanol price. www.methanex.com (accessed 30 September 2010).

National Energy Technology Laboratory (NETL), 2010. Cost and performance baseline for fossil energy plants volume 1: bituminous coal and natural gas to electricity, DOE/NETL-2010/1397.

Ng, K. S., Lopez, Y., Campbell, G. M., Sadhukhan, J., 2010. Heat integration and analysis of decarbonised IGCC sites. Chem. Eng. Res. Des. 88(2), 170-188.

Ng, K. S., Sadhukhan, J., 2011a. Process integration and economic analysis of bio-oil platform for the production of methanol and combined heat and power. Biomass Bioenergy. 35(3), 1153-1169.

Ng, K. S., Sadhukhan, J., 2011b. Techno-economic performance analysis of bio-oil based Fischer-Tropsch and CHP synthesis platform. Biomass Bioenergy, Accepted.

Pires, J. C. M., Martins, F. G., Alvim-Ferraz, M. C. M., Simões, M., 2011. Recent developments on carbon capture and storage: An overview. Chem. Eng. Res. Des., Accepted.

Postnote, 2010. Global carbon trading, Number 354. Parliament Office of Science and Technology. http://www.parliament.uk/documents/documents/upload/postpn354.pdf (accessed 10 June 2011)

Prime, J.; Mackintosh, J.; Chan, J., 2010. Special feature - carbon dioxide emissions: Carbon dioxide emissions and energy consumption in the UK. BERR, UK. http://www.berr.gov.uk/files/file50671.pdf (accessed 10 June 2011)

Rhodes, J., Keith, D., 2008. Biomass with capture: negative emissions within social and environmental constraints: an editorial comment. Climatic Change 87(3), 321-328.

Rihko-Struckmann, L. K., Peschel, A., Hanke-Rauschenbach, R., Sundmacher, K., 2010. Assessment of methanol synthesis utilizing exhaust CO_2 for chemical storage of electrical energy. Ind. Eng. Chem. Res. 49 (21), 11073-11078.

Sadhukhan, J., Zhang, N., Zhu, X. X., 2004. Analytical optimisation of industrial systems and applications to refineries, petrochemicals. Chem. Eng. Sci. 59 (20), 4169-4192.

Sadhukhan, J., Mustafa, M. A., Misailidis, N., Mateos-Salvador, F., Du, C., Campbell, G. M., 2008. Value analysis tool for feasibility studies of biorefineries integrated with value added production. Chem. Eng. Sci. 63(2), 503-519.

Sadhukhan, J., Ng, K. S., 2011. Economic and European Union environmental sustainability criteria assessment of bio-oil based biofuel systems: refinery integration cases. Ind. Eng. Chem. Res., Accepted.

ScottishPower, 2008. ScottishPower announces major coal contract with Scottish coal. http://www.scottishpower.com/PressReleases_1725.htm (accessed 10 June 2011).

Sinnott, R. K., 2006. Coulson & Richardson's chemical engineering design volume 6, 4th ed. Butterworth-Heinemann, Oxford.

Song, C., Pan, W., 2004. Tri-reforming of methane: a novel concept for catalytic production of industrially useful synthesis gas with desired H_2/CO ratios. Catal. Today 98(4), 463-484.

Smith, R., 2005. Chemical process design and integration. John Wiley and Sons Ltd., Chichester, UK.

Stiegel, G. J., Ramezan, M., 2006. Hydrogen from coal gasification: an economical pathway to a sustainable energy future. Int. J. Coal. Geol. 65(3-4), 173-190.

Tijmensen, M. J. A., Faaij, A. P. C., Hamelinck, C. N., van Hardeveld, M. R. M., 2002. Exploration of the possibilities for production of Fischer-Tropsch liquids and power via biomass gasification. Biomass Bioenergy 23(2), 129-152.

Uhde, 2008. Methanol. http://www.uhde.eu/ (accessed 10 June 2011).

United Nations Framework Convention on Climate Change (UNFCCC). Parties & Observers. http://unfccc.int/parties_and_observers/items/2704.php (accessed 10 June 2011).

United Nations Framework Convention on Climate Change (UNFCCC), 2010. Report of the conference of the parties on its fifteenth session. Part two: action taken by the conference of the parties, FCCC/CP/2009/11/Add.1.
http://unfccc.int/resource/docs/2009/cop15/eng/11a01.pdf (accessed 10 June 2011)

Venderbosch, R. H., Prins, W., 2010. Fast pyrolysis technology development. Biofuels, Bioproducts and Biorefining 4(2), 178-208.

Xie, C., 2001. Modeling the performance and emissions of integrated gasification combined cycle based Lurgi ammonia synthesis system. North Carolina State University, US. http://repository.lib.ncsu.edu/ir/handle/1840.16/1837 (accessed 10 June 2011)

Yoneda, N., Kusano, S., Yasui, M., Pujado, P., Wilcher, S., 2001. Recent advances in processes and catalysts for the production of acetic acid. Appl. Catal. A. 221(1-2), 253-265.

Zhu, Y., Jones, S., 2009. Techno-economic analysis for the thermochemical conversion of lignocellulosic biomass to ethanol via acetic acid synthesis, PNNL-18483, US DOE.

PUBLICATION 4: Ng, K.S., Zhang, N., Sadhukhan, J., A graphical CO_2 emission treatment intensity assessment for energetic and economic analyses of integrated decarbonised energy systems. *Computers & Chemical Engineering.* Submitted (2011).

A Graphical CO_2 Emission Treatment Intensity Assessment for Energetic and Economic Analyses of Integrated Decarbonised Energy Systems

Kok Siew Ng, Nan Zhang and Jhuma Sadhukhan*

Centre for Process Integration, School of Chemical Engineering and Analytical Science, University of Manchester, Manchester, M13 9PL, UK.

Abstract

Design of clean energy systems is highly complex due to the existence of a variety of CO_2 abatement and integration options. In this study, an effective decision-making methodology has been developed for facilitating the selection of lowest energy and cost intensity systems, from a portfolio of flowsheet configurations with different decarbonisation strategies. The fundamental aspect of the proposed methodology lies in thermodynamic feasibility assessment as well as quantification of CO_2 emission treatment intensity using a graphical approach (CO_2 emission balance diagram) for energetic and economic performance analyses of integrated decarbonised systems. The relationship between the graphical representation and performances is established using Blocks and Boundaries on integrated systems. The effectiveness of the methodology has been demonstrated through a range of coal gasification based polygeneration and cogeneration systems, incorporating either of carbon capture and storage (CCS) or CO_2 reuse options.

Keywords: clean coal technology; coal to liquid fuel synthesis; CO_2 reuse; polygeneration; carbon capture and storage; process integration

* Author/s to whom correspondence should be addressed:

E-mail: jhumasadhukhan@gmail.com

1. Introduction

CO_2 abatement system in the context of clean energy production has received considerable attention in recent times. Stringent environmental regulation has been enforced as an essential measure in mitigating greenhouse gases and tackling global warming. The implementation of carbon tax in industrialised countries directly affects the economic performances of fossil fuel plants. CO_2 abatement system consists of a capture process with links to storage or reuse system. Carbon capture and storage (CCS) technologies in pre-combustion, post-combustion and oxy-combustion routes are the leading CO_2 abatement systems. The captured CO_2 is subsequently transported and stored underground (IPCC, 2005). CCS has been commercialised but has not yet been widely employed attributed to the high infrastructural cost. Chemical looping is an emerging CO_2 capture technology (Fan et al., 2008). The concept involves conversion of gaseous carbonaceous fuels via redox (reduction-oxidation) reactions, by using metal oxide composite particles. The technology has been broadly practised in combustion processes for power generation and thus known as chemical looping combustion (Jerndal et al., 2006). In light of the advantages of capturing CO_2 effectively and avoiding the use of expensive air separation unit, the chemical looping concept enables clean coal gasification processes without any significant reduction in energy efficiency. Thus it can be further extended into syngas chemical looping process, producing hydrogen, electricity as well as transportation fuels (Gupta et al., 2007; Tomlinson et al., 2007). Another alternative route for mitigating CO_2 is via reusing CO_2 into the

production of other useful chemicals or fuels. This route is still under explored due to uncertainties in thermodynamic and economic feasibility with respect to the conversion of highly stable CO_2.

The two most prevalent process integration techniques, i.e. heat integration (Linnhoff et al., 1994; Smith, 2005) and mass integration (El-Halwagi, 1997) have widely been adopted in the fields of energy savings and pollution reduction. The combined heat and mass integration analyses into targeting power cogeneration potential as well as utilisation of combustible waste have been studied by El-Halwagi et al. (2009). El-Halwagi et al. (2003) devised a material reuse strategy using effective graphical targeting approaches to minimise the consumption of fresh resources. Linnhoff and Dhole (1993) proposed a CO_2 emission targeting approach for total site, with the consideration of trade-offs between process fuel and steam, between steam, site fuel and cogeneration and fuel mix. Tan and Foo (2007) developed a new application of graphical pinch analysis for carbon-constrained energy sector planning, known as "carbon emission pinch analysis (CEPA)", extending the scopes to a wider context, i.e. from an industrial site to a regional or national energy sector. Zhelev and Ridolfi (2006) presented a holistic decision-making tool for resource management by utilising combined emergy (considering environmental and economic values) and pinch concepts (considering thermodynamic aspect). Klemeš et al. (2007) presented a whole system techno-economic modelling approach to assess the cost of carbon capture in coal-fired power station. Friedler et al. (1993) introduced a P-graph methodology for systematic synthesis of process networks with an aim of obtaining optimum structures based on economic benefits. Friedler (2010) provided a comprehensive review of the early stage and state-of-the art process integration techniques for solving energy and pollution

related problems. In their works, process economics are a key consideration in the implementation of CO_2 abatement strategies into an energy system. A variety of CO_2 abatement options are possible, leading to various complex flowsheet configurations. In addition, their application on a full scale is uncertain due to potential thermodynamic and economic implications. It is widely recognised that an effective however shortcut methodology is imperative for analysing the feasibility of integration of CO_2 abatement options, embracing CO_2 reuse or CCS into coal gasification system. The proposed effective and shortcut methodology for the selection, decision-making and integration of CO_2 abatement processes into an energy system can be used for grassroots as well as retrofit designs. Screening is an important aspect in the context of the above primary objectives of the methodology. This requires comparison of distinctive thermodynamic and economic features between various flowsheet configurations. Consequently, the energetic and economic performances of integrated CO_2 abatement and energy systems are built upon the interpretation of CO_2 treatment intensity standpoint.

Five coal gasification process schemes with various CO_2 abatement strategies are exemplified to demonstrate a fundamental relationship between an integrated system performance and its emission treatment intensity index (ETII). The systems under consideration as follows: polygeneration with CCS system (Case A); polygeneration with CO_2 reuse into methanation process (Case B); integrated gasification combined cycle (IGCC) with CCS (Case C); modified IGCC with CO_2 reuse into syngas generation via tri-reforming process and further into methanol synthesis (Case D); syngas chemical looping (Case E), are illustrated in Appendix A. The paper contributes to the following tools:

- A shortcut methodology comprising of thermodynamic and economic feasibility assessment.

- A systematic graphical representation that features the generation and removal of CO_2 of all the concerning process units within a system, coined as “Emission balance diagram (EBD)” for the quantification of the treatment intensity of CO_2 abatement system, ETII.

- Block and Boundary concept, combined with shortcut energy auditing and economic evaluation approaches for deriving the relationship between ETII and plant performances.

2. Methodology

CCS and CO_2 reuse are the two main CO_2 abatement strategies. The selection of an appropriate CO_2 abatement strategy for an energy system remains a great challenge since numerous CO_2 conversion pathways and their integration synergies with the parent system exist. Within the consideration of CO_2 reuse route, there are numerous CO_2 conversion pathways leading to an exhaustive number of design configurations. This section presents an overview of the methodology using thermodynamic screening based on Gibbs energy assessment and EBD and ETII for ranking of integrated options according to cost and energy intensities.

2.1 Overview of Methodology

Figure 1 presents a shortcut approach for investigating the impact of integration of CO_2 abatement facility (CCS or CO_2 reuse) to a system. This methodology allows flexibility in product generation and CO_2 conversion pathways, not necessarily driven by market values of products, but also by thermodynamic and CO_2 treatment intensities. It uses distinctive thermodynamic and economic performance features with an acceptable level of accuracy for screening and decision-making amongst various integrated systems. The selected flowsheet can further be analysed using simulation modelling, mass and heat integration and detailed economic assessment.

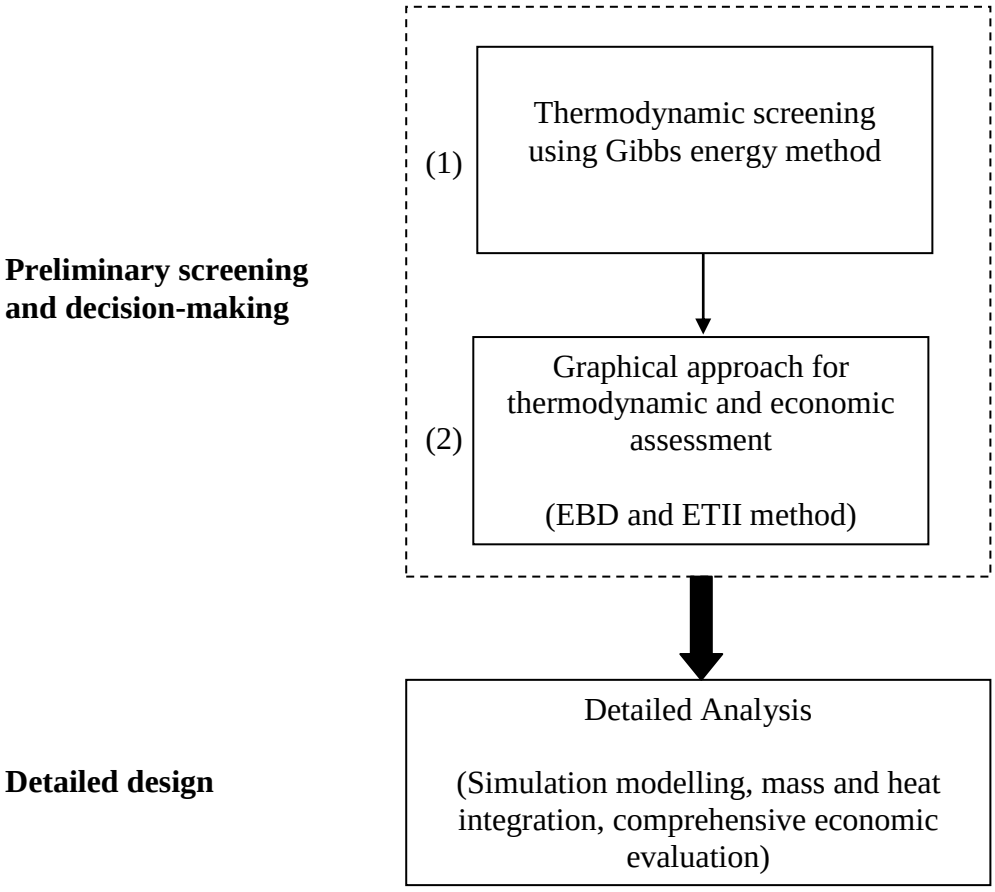

Figure 1: Overview of proposed shortcut methodology as the preliminary screening and decision-making of integrated CO_2 abatement systems.

To enhance the selection procedure and effective decision-making of which design is more appropriate, the proposed methodology comprises of the following two steps:

(1) The Gibbs energy method is used to screen out the thermodynamically non-favourable CO_2 conversion pathways. (section 2.2)

(2) EBD is constructed featuring the mass fraction and mass load of CO_2 generated / consumed. A mass and energy balance or a basic simulation model for the mass and energy balance of integrated flowsheets is developed. ETII is predicted to estimate the plant performances of integrated decarbonised systems. (section 2.3)

The relationship between ETII and the energy and cost intensities of integrated CO_2 abatement systems is established using Block and Boundary concept, detailed in section 3. This leads to the investigation of a range of coal gasification systems with different CO_2 abatement strategies in section 3. The proposed shortcut methodology is capable of screening thermodynamically and economically favourable CO_2 abatement routes in order for feeding these configurations into detailed process integration and optimisation studies.

2.2 Thermodynamic Screening Assessment using Gibbs Energy Method

CO_2 is a highly stable component and most of the reactions converting CO_2 are energetically unfavourable (Xu and Moulijn, 1996). Therefore, Gibbs energy method is adopted for evaluating thermodynamic spontaneity of CO_2 conversion pathways (Kondepudi, 2008). In this study, four illustrative reactions in equations (1)-(4) in Table 1 have been selected for thermodynamic screening. The thermodynamic data required

for estimating the enthalpy change and Gibbs energy change of reactions are given in Appendix B. These reactions encompass the production of methane (equation (1)), methanol (equation (2)), formic acid (equation (3)) and syngas (equation (4), dry reforming process) utilising CO_2.

Table 1: Standard enthalpy change and Gibbs energy change for the selected CO_2 reaction pathways.

Reaction	ΔH_R° (kJ/mol)	ΔG_R° (kJ/mol)	Equation
CO_2 (*g*) + $4H_2$ (*g*) → CH_4 (*g*) + $2H_2O$ (*l*)	−253.0	−130.6	(1)
CO_2 (*g*) + $3H_2$ (*g*) → CH_3OH (*l*) + H_2O (*l*)	−131.0	−9.0	(2)
CO_2 (*g*) + H_2 (*g*) → HCOOH (*l*)	−31.2	+33.0	(3)
CO_2 (*g*) + CH_4 (*g*) → 2CO (*g*) + $2H_2$ (*g*)	+247.3	+170.7	(4)

The standard enthalpy change of reaction, ΔH_R° is estimated using equation (5). The change in the standard Gibbs energy of reaction, ΔG_R° is estimated using equations (6) and (7), under STP condition (i.e. 298.15 K and 1 atm).

$$\Delta H_R^\circ = \sum \Delta H_{f,products}^\circ - \sum \Delta H_{f,reactants}^\circ \quad (5)$$

$$\Delta G_R^\circ = \sum \Delta G_{f,products}^\circ - \sum \Delta G_{f,reactants}^\circ \quad (6)$$

$$\Delta G_f^\circ = \Delta H_f^\circ - T\Delta S_f^\circ \quad (7)$$

$\Delta H_{f,products}^\circ$ and $\Delta H_{f,reactants}^\circ$ are the standard enthalpy change of formation of products and reactants, respectively. $\Delta G_{f,products}^\circ$ and $\Delta G_{f,reactants}^\circ$ are the changes in the Gibbs energy of formation of products and reactants, respectively. ΔG_f°, ΔH_f° and ΔS_f° represent the change in the standard Gibbs energy of formation, standard enthalpy of formation and standard entropy of formation of substances. *T* is the temperature in K.

According to the results summarised in Table 1, the reactions in equations (1)-(3) are exothermic and the reaction in equation (4) is endothermic. For a reaction to proceed spontaneously, the Gibbs free energy should decrease ($\Delta G_R^{\circ} < 0$) at constant temperature and pressure, alongside an increase in entropy change ΔS. The methane production in equation (1) is energetically favourable due to strong negative ΔG_R°. The methanol production in equation (2) is thermodynamically less favourable since the reaction has a lower negative ΔG_R°. The formic acid formation reactions in equation (3) and dry reforming reaction in equation (4) are not thermodynamically spontaneous due to positive ΔG_R°.

The change in Gibbs energy is a function of temperature (T) and pressure (p), in equation (8). The relationship between the change in the Gibbs energy and temperature at constant pressure is expressed in equation (9), implying that an increase in entropy (S) favours a spontaneous reaction, i.e. decrease in ΔG. Equation (10) demonstrates the Gibbs energy change with respect to pressure at constant temperature as a function of volume (V).

$$dG = Vdp - SdT \tag{8}$$

$$\left(\frac{dG}{dT}\right)_p = -S \tag{9}$$

$$\left(\frac{dG}{dp}\right)_T = V \tag{10}$$

The sensitivity analyses are carried out to assess the temperature dependency of the Gibbs free energy. The feasibility of a reaction within a range of operating temperatures is thus predicted. Since the reuse of CO_2 often involves liquid product

formations, variation in Gibbs energy with respect to pressure may not be significant. Equation (9) can further be derived to associate the temperature dependency of the Gibbs free energy change with the enthalpy change, demonstrated by Gibbs-Helmholtz equation (11) (Kondepudi, 2008). Equation (12) shows the integrated form derived from the differential form of equation (11) for estimating the ΔG_R at a specific temperature, assuming that ΔH_R has negligible variation with temperature. The variation in ΔG_R with respect to T is illustrated in Figure 2. Figure 2 provides information regarding the range of operating temperature where a reaction may occur (constant pressure is assumed at 1 atm). The reactions in equations (2) and (3) are not likely to proceed at any temperature since ΔG_R is always in the positive region. A temperature lower than 610 K favours the reaction in equation (1), while a temperature greater than 960 K helps the reaction in equation (4) to proceed spontaneously. The differential form of equation (10) can be integrated into equation (13), assuming ideal gas law, to predict ΔG_R at a particular pressure.

$$\left(\frac{\partial\left(\Delta G_R / T\right)}{\partial T}\right)_p = -\frac{\Delta H_R}{T^2} \tag{11}$$

$$\left(\frac{\Delta G_R}{T}\right)_{T_2} = \left(\frac{\Delta G_R}{T}\right)_{T_1} + \Delta H_R\left(\frac{1}{T_2} - \frac{1}{T_1}\right) \tag{12}$$

$$\Delta G_R\left(p_2\right) = \Delta G_R\left(p_1\right) + nRT\ln\left(\frac{p_2}{p_1}\right) \tag{13}$$

where T_1 and T_2 are the initial and final temperatures; p_1 and p_2 are the initial and final pressures, respectively. n is the number of mole. R is the universal gas constant (0.008314 kJ/mol-K).

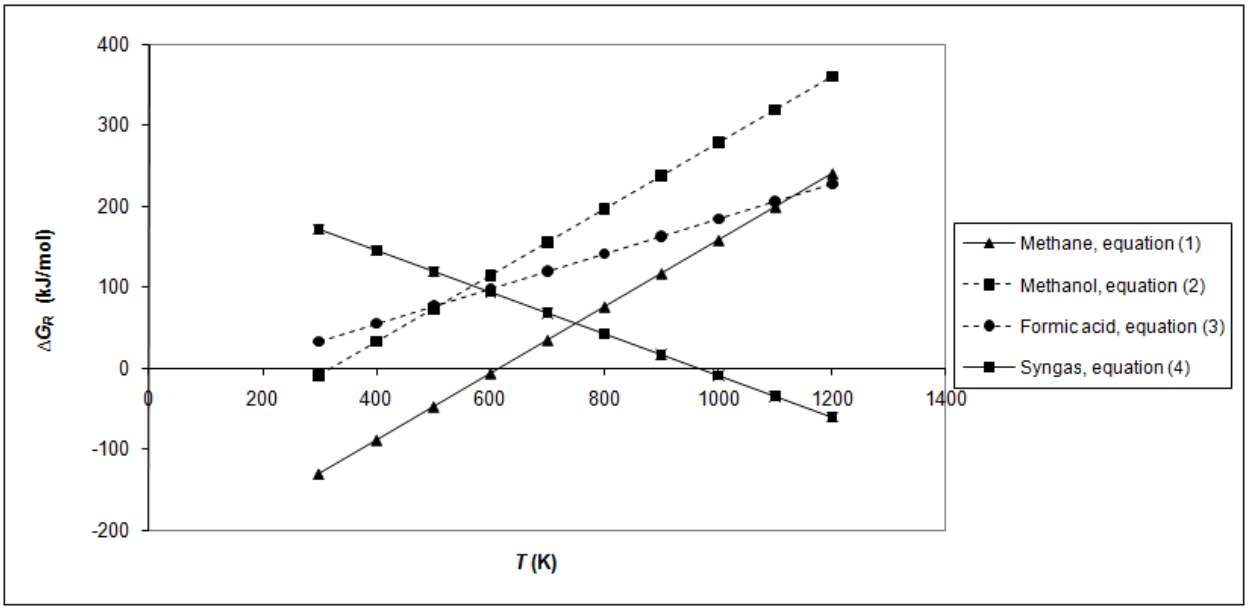

Figure 2: Effect of temperature on Gibbs energy of reaction.

In conclusion, the conversion of CO_2 into the formation of methanol (equation (2)) and formic acid (equation (3)) formation are not thermodynamically favourable under the investigated temperature conditions. The formation of methane (equation (1)) is thermodynamically spontaneous at a lower temperature range of 298 - 610 K, while syngas production from CO_2 (equation (4)) is energetically favourable provided that it is carried out at a high temperature range of 960 - 1200 K.

2.3 Emission Balance Diagram and Emission Treatment Intensity Index

A systematic graphical representation, EBD, is proposed for analysing the CO_2 generation and removal from every process unit within a system. EBD of CO_2 comprises of two profiles, CO_2 generation and CO_2 removal profiles. The mass fraction of CO_2 is plotted against the mass load of CO_2, resulting in a step-down chart. A general EBD is illustrated in Figure 3.

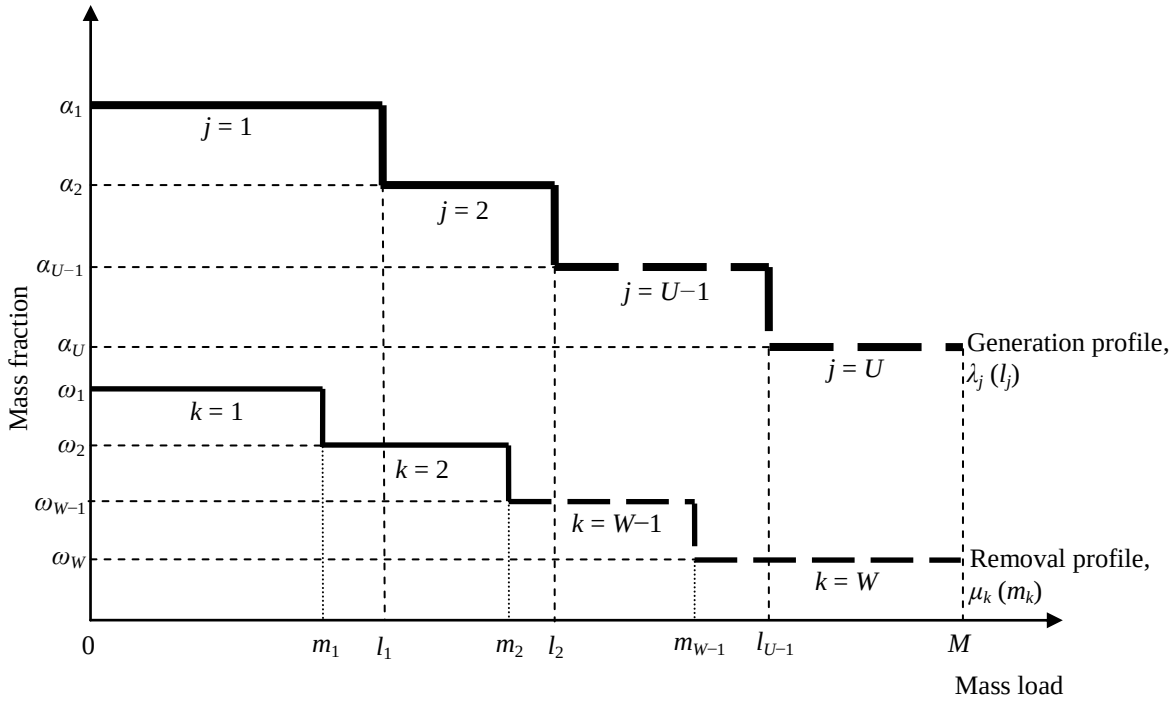

Figure 3: Emission balance diagram showing generation and removal profiles.

The concept behind construction and usefulness of EBD is as follows.

1. The generation and removal profiles are presented by horizontal steps in the order of decreasing mass fraction of emission component and cumulative mass loads. The mass fraction of the emission component at the outlet gaseous streams from the generation (from reaction) or removal (stored / emitted / reused) processes is plotted against its corresponding mass load. Both profiles should end at the same point in abscissa as their total mass loads are the same thus achieving CO_2 mass balance within a process plant. The method is built upon the 'path diagram' introduced by El-Halwagi (1997) where the flow of a species in each stream is tracked through a path. The EBD however concerns with the points where there are changes in the amount and concentration of emission component due to generation or removal.

2. This diagram can be used in targeting for emission minimisation such as through manipulation of related process operating conditions. Furthermore, it can be used for analysing the CO_2 treatment intensity within a process plant, discussed as follows.

ETII is introduced as a quantitative parameter for classifying emission treatment processes, i.e. CO_2 treatment in this context, based on the area confined between the generation and removal profiles. The derivation of ETII is demonstrated as follows:

Let the functions of the generation and removal profiles be $\lambda_j(l_j)$ and $\mu_k(m_k)$, respectively. l_j and m_k represent the mass loads of CO_2 within a step, j or k in the generation and removal profiles, respectively. U and W are the total number of steps in the generation and removal profiles, respectively.

$$\begin{aligned}
&\text{Area between the generation and removal profiles} \\
&= \text{Area under generation profile } A(\lambda) - \text{Area under removal profile } A(\mu) \\
&= \sum_{j=1}^{U} \int_{l_{j-1}}^{l_j} \lambda_j(l_j)\, dl_j - \sum_{k=1}^{W} \int_{m_{k-1}}^{m_k} \mu_k(m_k)\, dm_k \\
&= \left[\alpha_1(l_1 - 0) + \alpha_2(l_2 - l_1) + \mathrm{K} + \alpha_U(M - l_{U-1})\right] - \left[(\omega_1(m_1 - 0) + \omega_2(m_2 - m_1) + \mathrm{K} + \omega_W(M - m_{W-1}))\right]
\end{aligned} \tag{14}$$

α and ω are the mass fractions of CO_2 in the generation and removal profiles, respectively. M is the total mass load of CO_2 shown as the final point on the profile.

Assuming that the generation profile lies above the removal profile, the area between the two profiles, defined in equation (14) should have a value greater than zero. Transforming equation (14) into a dimensionless form, equation (15) can be obtained.

$$\frac{\sum_{j=1}^{U}\int_{l_{j-1}}^{l_j} \lambda_j(l_j)\, dl_j - \sum_{k=1}^{W}\int_{m_{k-1}}^{m_k} \mu_k(m_k)\, dm_k}{\sum_{k=1}^{W}\int_{m_{k-1}}^{m_k} \mu_k(m_k)\, dm_k} = \frac{A(\lambda) - A(\mu)}{A(\mu)} = \frac{A(\lambda)}{A(\mu)} - 1 > 0 \qquad (15)$$

ETII is defined as the ratio between the area under the generation profile, $A(\lambda)$ and the area under the removal profile, $A(\mu)$, shown in equation (16).

$$ETII = \frac{A(\lambda)}{A(\mu)} \qquad (16)$$

Therefore, if the generation profile is placed above the removal profile (CO_2 reuse case), ETII should have a value greater than 1. If there is a case where the generation profile lies below the removal profile (storage case), then ETII should be less than 1. Higher ETII for CO_2 reuse cases is desirable and vice versa for storage cases. Both directions imply to lower total plant investment (TPI) and higher overall net energy, explained later in section 3.4.

3. Derivation of the Relationship between Emission Treatment Intensity Index and Plant Performances

3.1 Block and Boundary Concept

A block and boundary concept is introduced for the design prioritisation and scoping analysis between similar plant types (e.g. coal gasification) with different production routes and process configurations. In this approach a process flowsheet is divided into key blocks, each comprising of a group of processes dedicated to perform a task or to achieve an objective, e.g. syngas generation, gas cleaning, CO_2 reduction, etc. The philosophy is to compare thermodynamic and economic performances between

similar functioning blocks, though containing different process configurations, in different flowsheets. Thus, a number of similar functioning blocks and boundaries in various flowsheets are identified. Typically, a coal decarbonised polygeneration plant has 4 key blocks, syngas generation and cleanup, CO_2 separation, CO_2 disposal (storage / reuse) and production (cogeneration / polygeneration), respectively illustrated in Figure 4. It is recommended that the number of blocks within a system should be kept to a minimum number to avoid losing practicability of the screening approach.

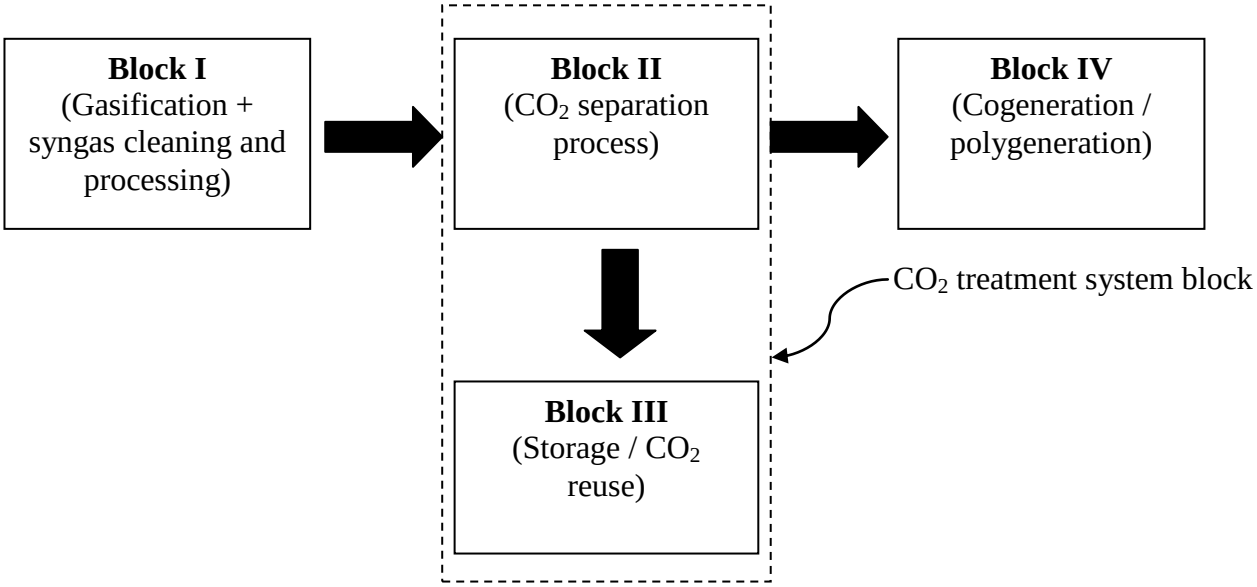

Figure 4: Block representation of coal polygeneration system.

3.2 Case Studies

The ASPEN Plus simulation flowsheets of five coal gasification Cases A-E with different CO_2 abatement integration synergies are illustrated in Figure 5(a)-(e). The process descriptions are provided in Appendix A.

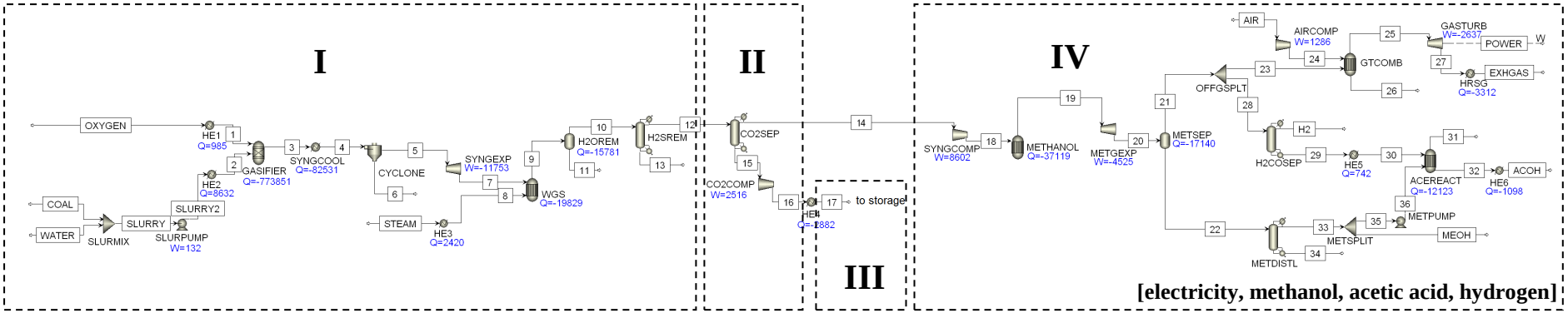
I
II
III
IV
OXYGEN
COAL
WATER
SLURRY
SLURRY2
SLURMIX
SLURPUMP
W=132
HE1
Q=985
HE2
Q=8632
GASIFIER
Q=-773851
SYNGCOOL
Q=-82531
CYCLONE
STEAM
HE3
Q=2420
SYNGEXP
W=-11753
WGS
Q=-19829
H2OREM
Q=-15781
H2SREM
CO2SEP
CO2COMP
W=2516
HE4
Q=-1882
to storage
SYNGCOMP
W=8602
METHANOL
Q=-37119
METGEXP
W=-4525
METSEP
Q=-17140
AIR
AIRCOMP
W=1286
GTCOMB
GASTURB
W=-2637
POWER
W
EXHGAS
HRSG
Q=-3312
OFFGSPLT
H2
H2COSEP
HE5
Q=742
ACEREACT
Q=-12123
ACOH
HE6
Q=-1098
METPUMP
METSPLIT
MEOH
METDISTL
[electricity, methanol, acetic acid, hydrogen]

(a)

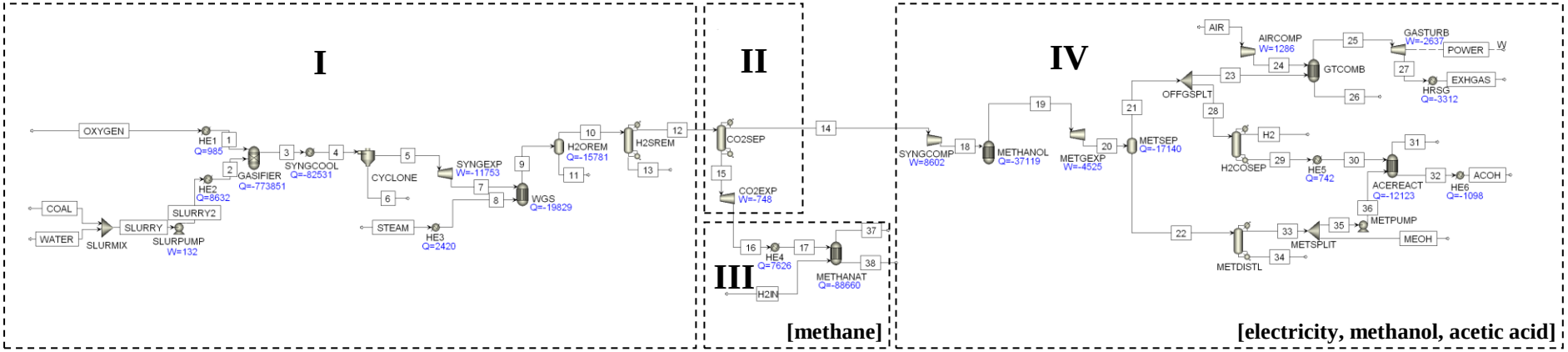
I
II
III
IV
OXYGEN
COAL
WATER
SLURRY
SLURRY2
SLURMIX
SLURPUMP
W=132
HE1
Q=985
HE2
Q=8632
GASIFIER
Q=-773851
SYNGCOOL
Q=-82531
CYCLONE
STEAM
HE3
Q=2420
SYNGEXP
W=-11753
WGS
Q=-19829
H2OREM
Q=-15781
H2SREM
CO2SEP
CO2EXP
W=-748
HE4
Q=7626
H2IN
METHANAT
Q=-88660
[methane]
SYNGCOMP
W=8602
METHANOL
Q=-37119
METGEXP
W=-4525
METSEP
Q=-17140
AIR
AIRCOMP
W=1286
GTCOMB
GASTURB
W=-2637
POWER
W
EXHGAS
HRSG
Q=-3312
OFFGSPLT
H2
H2COSEP
HE5
Q=742
ACEREACT
Q=-12123
ACOH
HE6
Q=-1098
METPUMP
METSPLIT
MEOH
METDISTL
[electricity, methanol, acetic acid]

(b)

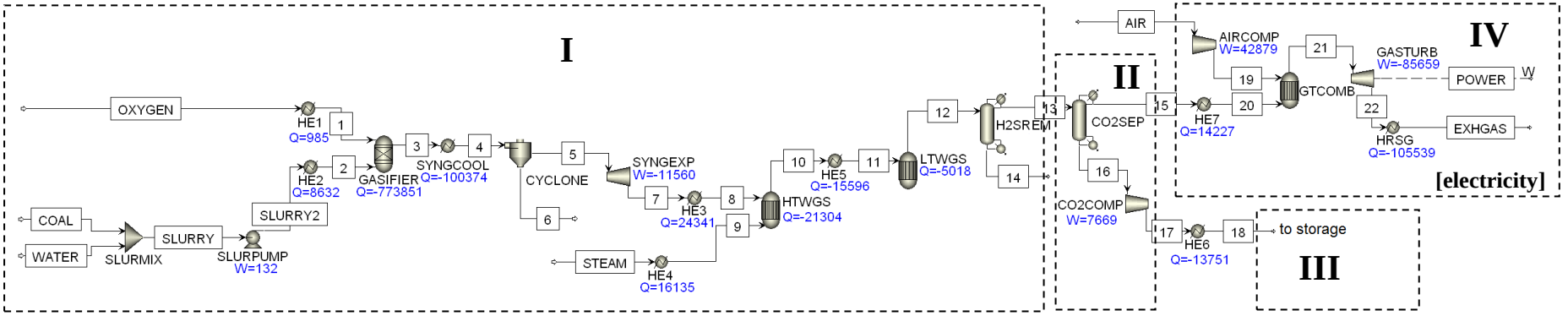
I
II
III
IV
OXYGEN
HE1
Q=985
1
2
HE2
Q=8632
GASIFIER
Q=-773851
3
SYNGCOOL
Q=-100374
4
CYCLONE
5
6
SYNGEXP
W=-11560
7
HE3
Q=24341
8
9
HTWGS
Q=-21304
10
HE5
Q=-15596
11
LTWGS
Q=-5018
12
H2SREM
13
14
CO2SEP
15
16
CO2COMP
W=7669
17
HE6
Q=-13751
18
to storage
AIR
AIRCOMP
W=42879
19
20
HE7
Q=14227
21
GTCOMB
22
GASTURB
W=-85659
POWER
W
HRSG
Q=-105539
EXHGAS
[electricity]
COAL
WATER
SLURRY
SLURMIX
SLURPUMP
W=132
SLURRY2
STEAM
HE4
Q=16135

(c)

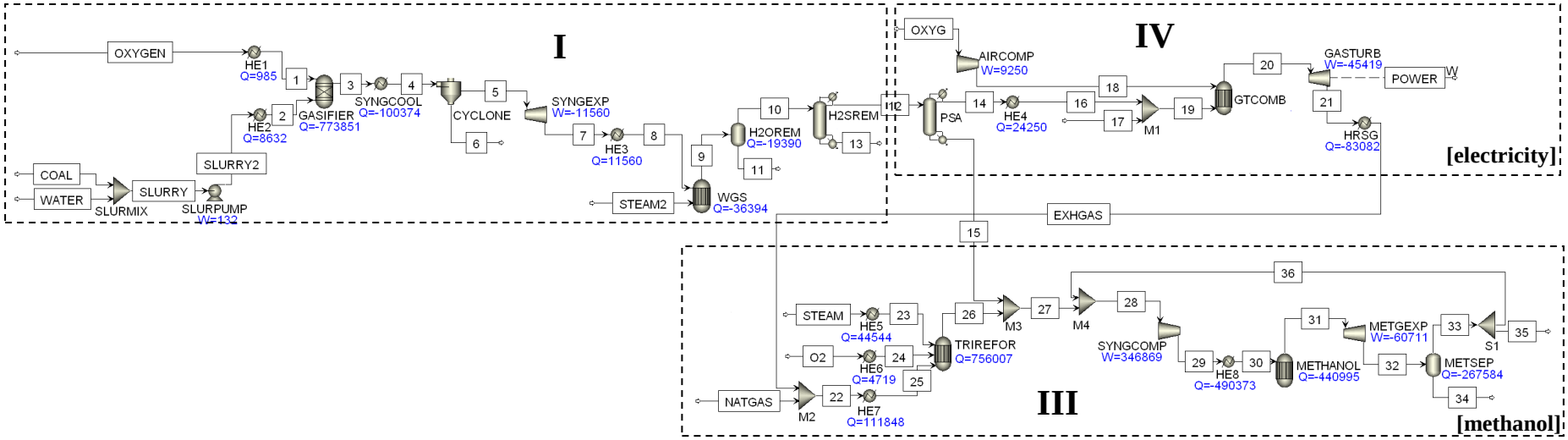
I
III
IV
OXYGEN
HE1
Q=985
1
2
HE2
Q=8632
GASIFIER
Q=-773851
3
SYNGCOOL
Q=-100374
4
CYCLONE
5
6
SYNGEXP
W=-11560
7
HE3
Q=11560
8
9
WGS
Q=-36394
10
H2OREM
Q=-19390
11
H2SREM
12
13
COAL
WATER
SLURRY
SLURMIX
SLURPUMP
W=132
SLURRY2
STEAM2
OXYG
AIRCOMP
W=9250
PSA
14
HE4
Q=24250
16
17
M1
18
19
GTCOMB
20
GASTURB
W=-45419
POWER
W
21
HRSG
Q=-83082
[electricity]
EXHGAS
15
STEAM
HE5
Q=44544
23
O2
HE6
Q=4719
24
25
TRIREFOR
Q=756007
26
M3
27
M4
28
SYNGCOMP
W=346869
29
HE8
Q=-490373
30
31
METHANOL
Q=-440995
32
METEXP
W=-60711
33
METSEP
Q=-267584
34
S1
35
36
NATGAS
M2
22
HE7
Q=111848
[methanol]

(d)

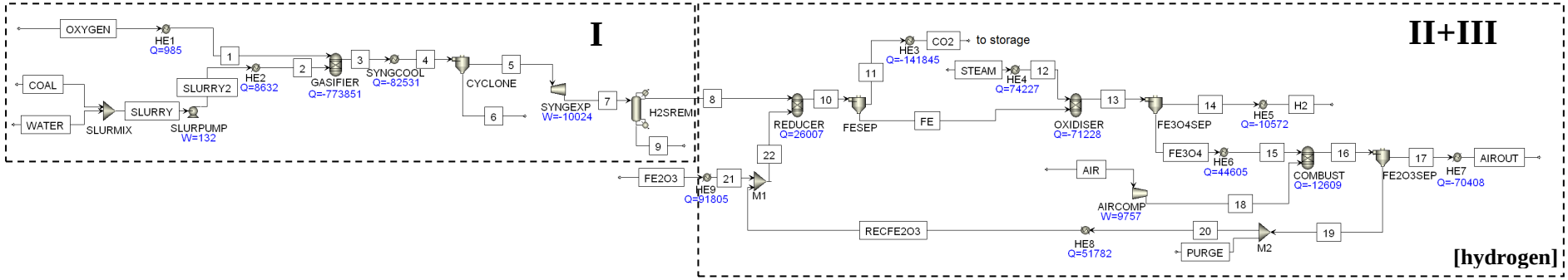

(e)

Figure 5: Block and boundary for (a) coal polygeneration system with CCS (Case A); (b) coal polygeneration system with CO_2 capture and reuse for methane production (Case B); (c) IGCC with CCS (Case C) (d) Modified IGCC with polygeneration through reuse of CO_2 via tri-reforming and methanol synthesis (Case D); (e) coal gasification system with syngas chemical looping system for CO_2 capture and hydrogen production (Case E).

Note: The main product(s) in a block is(are) represented in square bracket.

Figure 5(a) presents a coal polygeneration system with CCS, Case A, producing electricity, hydrogen, acetic acid and methanol. Figure 5(b) is a modification of Case A, wherein captured CO_2 is reused into methanation process (Case B). The blocks and boundaries I to IV across processes that exhibit similar functionality are classified for each flowsheet. Block I encompasses the GASIFIER, CYCLONE, water-gas shift (WGS) reactor, water (H2OREM) and H_2S removal (H2SREM) processes. CO_2 capture system (CO2SEP) is contained in block II. Block III represents the CO_2 storage / reuse process. Block IV encapsulates all production routes mainly consisting of reaction and separation processes. After grouping similar functional processes into individual blocks in a flowsheet, it is clear that only block III is different between Cases A and B. Blocks II and III can further be combined into one block (Figure 4). Cases A and B thus differ by only one block.

A more complicated example of distinctive and significant system modification can also be analysed using Block and Boundary concept. Figure 5(c) shows a coal integrated gasification combined cycle (IGCC) system (Case C). The coal cogeneration system producing combined heat and power (CHP) can be revamped into a polygeneration system producing methanol as an additional product to CHP (Case D), illustrated in Figure 5(d). The modified design comprises of the reuse of CO_2 from the flue gas of gas turbine into syngas generation via tri-reforming process, followed by methanol synthesis reaction. The design in Case D is without a capture system, hence block II is eliminated. Thus, block I in Cases C and D is almost similar, while blocks II, III and IV are distinctive in configuration.

Figure 5(e) shows the integration of syngas chemical looping system into a coal gasification plant with hydrogen production (Case E). The processes within the flowsheet have been divided into only three blocks, with no polygeneration site (block IV) in this case, according to the convention presented in Figure 4.

After defining the blocks and boundaries for processes within a system, the net energy requirement / generation and economic performances are assessed for each block. They constitute the two most essential impact criteria for integration of a particular block into a system. Since the whole purpose is to compare the performances between different flowsheets, a detailed energy and economic evaluation is not needed, provided that the parameters involved in the estimation are set on a consistent basis with valid assumptions and the results ought to achieve a satisfactory confidence level.

3.2.1 Shortcut Energy Auditing

A shortcut energy auditing is undertaken to account for the energy requirement and generation by important processes within blocks that are dissimilar in configuration between various flowsheets. The energy intensity of each distinct block can thus be determined. The energy requirement and generation in the form of heat duties and power are extracted from a flowsheet. Since this is a shortcut method primarily aimed at effective screening, evaluation and decision making, the energy implication of common activities need not to be taken into account. These include the low grade heat generation and energy requirement for coal preparation, ash and sulphur removal etc. The power requirement of ASU is 235 kWh/t O_2 (Armstrong et al. 2005). The steam and electricity consumption of CO_2 capture process (Rectisol is assumed) is 4 MJ/kmol syngas and 5.89×10^{-4} MWh/kmol syngas, respectively (Xie, 2001). A summary of results

comparing the energy requirement and generation by each block between Cases A and B is presented in Table 2. Note that a negative sign with a net energy implies energy requirement by a block and vice versa signifies energy generation, respectively. The most crucial result in Table 2 is the difference in the net energy requirement by the CO_2 treatment block II+III between Cases A and B. Case B (CO_2 reuse into methane production) is more energy intensive than Case A (CCS) due to the CO_2 treatment block.

Results of similar shortcut energy auditing performed on Cases C and D are presented in Table 3. The values of intermediate streams such as syngas and hydrogen exiting the boundary of a block and entering another block are not accounted, since these values would be cancelled out in the overall analysis. Block I results in a discrepancy of approximately 1.3% between Cases C and D. The CO_2 treatment system in Case D is more energy intensive than that in Case C, evident from the net energy requirement of 771.24 MW (block III) in Case D compared to 23.64 MW (block II+IIII) in Case C, respectively. Block IV in Case C generates 88% more energy compared to in Case D. However, the net product energy values need to be accounted for in the overall net energy value calculations discussed in section 3.4.

Table 4 presents the energy requirement and generation of Case E. The results manifest that Case E has low energy intensities amongst all cases studied.

Table 2: Energy auditing using block analysis method for Cases A and B.

Case	Case A			Case B		
Block	I	II+III	IV	I	II+III	IV
Energy Requirement (MW)						
1. Steam requirement for WGS	2.42			2.42		
2. Oxygen production (ASU)	14.83			14.83		
3. Steam requirement in CO_2 capture system (Rectisol)		9.40			9.40	
4. Electricity requirement in CO_2 capture system (Rectisol)		4.98			4.98	
5. CO_2 compressor		2.52				
6. Steam requirement for heating CO_2 feed into methanator					7.63	
7. Air and syngas compressor			9.89			9.89
Sub-total	**17.25**	**16.90**	**9.89**	**17.25**	**22.01**	**9.89**
Energy Generation (MW)						
1. Gasification and syngas cooler	846.77			846.77		
2. Syngas expander	11.75			11.75		
3. CO_2 expander					0.75	
4. Gas turbine			2.64			2.64
5. HRSG			3.31			3.31
6. METHANOL and ACEREACT			49.24			49.24
Sub-total	**858.52**	**0.00**	**55.19**	**858.52**	**0.75**	**55.19**
Net Energy (MW)	**841.27**	**−16.90**	**45.30**	**841.27**	**−21.26**	**45.30**

Table 3: Energy auditing using block analysis method for Cases C and D.

Case	Case C			Case D		
Block	I	II+III	IV	I	III	IV
Energy Requirement (MW)						
1. Steam requirement for WGS	16.48			27.50		
2. Oxygen production (ASU)	14.83			14.83	8.96	23.55
3. Steam requirement in CO_2 capture system (Rectisol)		10.44				
4. Electricity requirement in CO_2 capture system (Rectisol)		5.53				
5. CO_2 compressor		7.67				
6. Energy required for tri-reforming process					917.12	
7. Air compressor / syngas compressor			42.88		346.87	9.25
8. Energy for heating feed into GTCOMB.			14.23			24.25
Sub-total	**31.31**	**23.64**	**57.11**	**42.33**	**1272.95**	**57.05**
Energy Generation (MW)						
1. Gasification and syngas cooler	864.61			864.61		
2. Syngas expander	11.56			11.56		
3. Methanol gas expander					60.71	
4. METHANOL					441.00	
5. Gas turbine			85.66			45.4
6. HRSG			105.54			83.1
Sub-total	**876.17**	**0.00**	**191.2**	**876.17**	**501.71**	**128.5**
Net Energy (MW)	**844.86**	**−23.64**	**134.09**	**833.84**	**−771.24**	**71.45**

Table 4: Energy auditing using block analysis method for Case E.

Case	Case E	
Block	I	II+III
Energy Requirement (MW)		
1. Oxygen production (ASU)	14.83	
2. Steam requirement for oxidiser		74.23
3. Air compressor		9.78
4. Heat duty for heating Fe_2O_3 (make-up and recycle)		56.37
5. Endothermic heat of reducer		26.01
6. Heat duty for heating Fe_3O_4		44.61
Sub-total	**14.83**	**211.0**
Energy Generation (MW)		
1. Gasification and syngas cooler	846.77	
2. Syngas expander	10.02	
3. CO_2 cooling		141.85
4. H_2 cooling		10.57
5. Exothermic heat of oxidiser		71.23
6. Exothermic heat of combustor		12.61
7. Air cooler		70.41
Sub-total	**856.79**	**306.67**
Net Energy (MW)	**841.96**	**95.67**

3.2.2 Shortcut Economic Evaluation

Likewise a shortcut economic evaluation by taking the capital cost, operating cost and value of products into consideration is performed to assess the cost intensity of individual blocks within systems. The capital cost evaluation is simplified by taking the equipment cost solely into account, while the operating cost only includes the cost of raw materials (8000 operating hours per year is assumed). The costs of auxiliary equipment such as heat exchanger, mixer, splitter, pump etc. that are common in individual blocks between systems can be omitted for the purpose of comparative analysis. The costs of utility such as steam and electricity are not considered at this stage since rigorous heat integration analysis on overall systems would reveal actual utility costs. All costs of equipment are estimated using power law method (cost and size correlation) (Peters et al., 2003; Ng and Sadhukhan, 2011) and levelised to the current year value (or to a recent most consistent year) using the Chemical Engineering Plant Cost Index (CEPCI), e.g. current CEPCI = 556.8 (November 2010). The economic data are given in Appendix C. The discounted cash flow analysis is adopted to determine an annualised capital charge of 11% based on the following assumptions.

- Discount rate: 10%
- Plant life: 15 years
- Start-up period: 3 years (20%, 45%, 35%)

A shortcut economic evaluation of each block for Cases A and B is summarised in Table 5. Note that a negative economic value indicates that the product value is lower than the capital and operating costs involved and vice versa. Blocks I and IV have the same cost implications, henceforth, a comparison of economic performances between

the two cases is based on the cost implication of block II+III. Clearly, the CO_2 treatment system (block II+III) in Case B is highly cost intensive compared to that in Case A, indicated by a TPI of 173.0 million Euro/year in Case B compared to 7.5 million Euro/year in Case A, respectively. Although methane generated as an additional product by the reuse of CO_2 adds 71.1 million Euro/year in Case B, it is also associated with the cost of hydrogen purchased or produced, 164.1 million Euro/year. The resulting net economic value is −101.9 million Euro/year in Case B compared to −7.5 million Euro/year in Case A, respectively.

Table 6 provides the economic evaluation for Cases C and D. The results have shown that Case D has higher cost intensity than Case C, demonstrated by the high TPI of mainly blocks II+III and IV, under consideration. The economic value from block IV in Case D is −35.3 million Euro/year compared to 41.5 million Euro/year in Case C, respectively. The TPI of block III in Case D (403.0 million Euro/year) is 40 times higher than block II+III in Case C (9.8 million Euro/year). However, due to the higher production of high value methanol in Case D leading to an economic value of 843.7 million Euro/year compared to −9.8 million Euro/year in Case C, the option of reusing CO_2 seems to be more appealing than CCS. In this case, the economic value of methanol is more than the value required to offset the energy cost caused by thermodynamic infeasibility.

The integration of chemical looping system into the coal gasification system incurs a relatively low TPI of 9.4 million Euro/year. It also results in a relatively high economic value of 82.0 million Euro/year, attributed to hydrogen generation from block II+III, presented in Table 7.

Table 5: Economic evaluation using block analysis method for Cases A and B.

Case	Case A			Case B		
Block	I	II+III	IV	I	II+III	IV
Capital Cost (million Euro)						
1. GASIFIER	73.4			73.4		
2. WGS	9.2			9.2		
3. SYNGCOOL	33.0			33.0		
4. ASU	40.3			40.3		
5. Expander	3.3			3.3	0.5	
6. Rectisol		61.0			61.0	
7. CO_2 transport and storage		4.5				
8. Compressor		2.4	6.0			6.0
9. Methanator					19.8	
10. Gas turbine			2.2			2.2
11. HRSG			0.5			0.5
12. Methanol reactor			7.3			7.3
13. Acetic acid reactor			14.6			14.6
14. H_2/CO separation			13.2			13.2
Sub-total (million Euro)	**159.2**	**67.9**	**43.7**	**159.2**	**81.3**	**43.7**
Annualised capital cost (million Euro/year)	**17.5**	**7.5**	**4.8**	**17.5**	**8.9**	**4.8**
Operating Cost (million Euro/year)						
1. Coal	53.4			53.4		
2. Hydrogen					164.1	
Sub-total (million Euro/year)	**53.4**	**0.0**	**0.0**	**53.4**	**164.1**	**0.0**
Value of Products (million Euro/year)						
1. Electricity			1.5			1.5
2. Methanol			72.8			72.8
3. Acetic acid			107.0			107.0
4. Hydrogen			20.0			20.0
5. Methane					71.1	
Sub-total (million Euro/year)	**0.0**	**0.0**	**201.3**	**0.0**	**71.1**	**201.3**
Economic Value (million Euro/year) [value of product – (capital cost + operating cost)]	**−70.9**	**−7.5**	**196.5**	**−70.9**	**−101.9**	**196.5**
Total Plant Investment (million Euro/year) [(capital cost + operating cost)]	**70.9**	**7.5**	**4.8**	**70.9**	**173.0**	**4.8**

Table 6: Economic evaluation using block analysis method for Cases C and D.

Case	Case C			Case D		
Block	I	II+III	IV	I	III	IV
Capital Cost (million Euro)						
1. GASIFIER	73.4			73.4		
2. WGS	18.4			9.2		
3. SYNGCOOL	37.1			37.1		
4. ASU	40.3			40.3	31.3	50.8
5. Expander	3.3			3.3	10.1	
6. Rectisol		77.1				
7. CO_2 transport and storage		6.4				
8. Compressor		5.0	16.0		64.8	5.7
9. Tri-reformer					43.4	
10. Gas turbine			29.8			18.5
11. HRSG			15.3			12.0
12. Methanol reactor					31.8	
13. PSA						44.7
Sub-total (million Euro)	**172.5**	**88.5**	**61.1**	**163.3**	**181.4**	**131.7**
Annualised capital cost (million Euro/year)	**19.0**	**9.8**	**6.7**	**18.0**	**20.0**	**14.5**
Operating Cost (million Euro/year)						
1. Coal	53.4			53.4		
2. Natural gas					383.0	46.3
Sub-total (million Euro/year)	**53.4**	**0.0**	**0.0**	**53.4**	**383.0**	**46.3**
Value of Products (million Euro/year)						
1. Electricity			48.2			25.5
2. Methanol					1246.7	
Sub-total (million Euro/year)	**0.0**	**0.0**	**48.2**	**0.0**	**1246.7**	**25.5**
Economic Value (million Euro/year) [value of product – (capital cost + operating cost)]	**−72.4**	**−9.8**	**41.5**	**−71.4**	**843.7**	**−35.3**
Total Plant Investment (million Euro/year) [(capital cost + operating cost)]	**72.4**	**9.8**	**6.7**	**71.4**	**403.0**	**60.8**

Table 7: Economic evaluation using block analysis method for Case E.

Case	Case E	
Block	I	II+III
Capital Cost (million Euro)		
1. GASIFIER	73.4	
2. SYNGCOOL	33.0	
3. ASU	40.3	
4. Expander	3.0	
5. Chemical looping system		70.6
6. CO_2 transport and storage		8.3
7. Compressor		5.9
Sub-total (million Euro)	**149.7**	**84.8**
Annualised capital cost (million Euro/year)	**16.5**	**9.4**
Operating Cost (million Euro/year)		
1. Coal	53.4	
Sub-total (million Euro/year)	**53.4**	**0.0**
Value of Products (million Euro/year)		
1. Hydrogen		91.4
Sub-total (million Euro/year)	**0.0**	**91.4**
Economic Value (million Euro/year) [value of product – (capital cost + operating cost)]	**−69.9**	**82.0**
Total Plant Investment (million Euro/year) [(capital cost + operating cost)]	**69.9**	**9.4**

3.3 Emission Balance Diagram and Emission Treatment Intensity Index Analyses

A mass and energy balance or a basic simulation model for the mass and energy balance of integrated flowsheets (e.g. in Figure 5 and discussed in Appendix A) is used to develop EBD of various cases. Figure 6(a) and (b) illustrate the EBD for Cases A (Figure 5 (a)) and B (Figure 5 (b)), respectively. The removal profile in Figure 6(a) shows that a mass load of 28.2 kg/s of CO_2 at a mass fraction of 1.0 is removed by CO2SEP through stream 17 and transported into storage facilities. The remaining CO_2 is emitted from different points in the system such as exhaust gas from gas turbine etc. to the atmosphere. CO_2 of a mass load of 19.9 kg/s at a mass fraction of 0.59 and a mass load of 8.6 kg/s at a mass fraction of 0.18 generated from WGS and GASIFIER, respectively, primarily constitutes the generation profile. Other sources of CO_2 include GTCOMB and METHANOL units. The generation profile in Case B shown in Figure 6(b) is exactly the same as in Case A shown in Figure 6(a). However, the removal profile in Case B is under the generation profile that differs from Case A. This is attributed to a low mass fraction of CO_2 of 0.033 for a mass load of 27.1 kg/s consumed by the methanation process.

The EBD for Cases C and D are depicted in Figure 6(c) and (d), respectively. The sources of CO_2 generation in Case C include gasifier, high and low temperature water-gas shift reactors. A mass load of 39.4 kg/s of CO_2 at mass fraction of 1.0 is captured and stored whilst a mass load of 12.4 kg/s at a mass fraction of 0.1 is emitted. CO_2 in Case D is generated from WGS, GTCOMB, METHANOL and GASIFIER. A total of 80.4% of CO_2 (60.2 kg/s) is consumed by the tri-reforming reaction, while the remaining CO_2 is emitted from METSEP.

The EBD for Case E is depicted in Figure 6(e). CO_2 is generated from GASIFIER, 8.6 kg/s at a mass fraction of 0.71 and REDUCER, 43.1 kg/s at a mass fraction of 0.18. A total mass load of CO_2 of 51.7 kg/s at a mass fraction of 0.71 is removed and stored after being separated from FESEP.

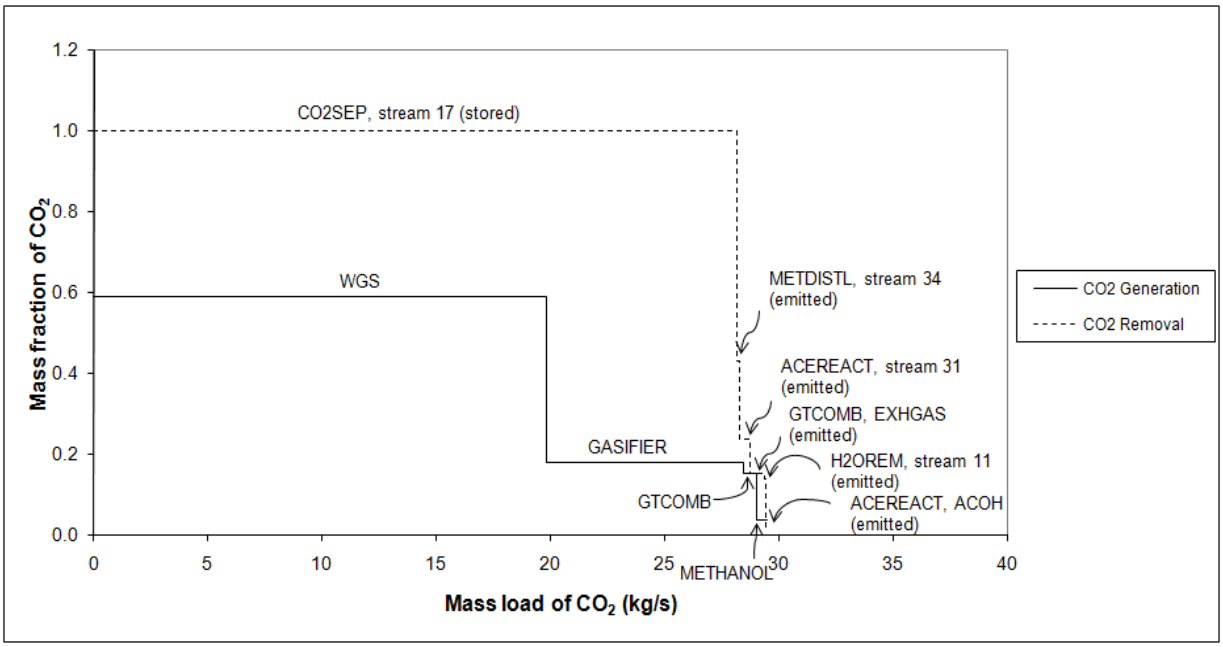

(a)

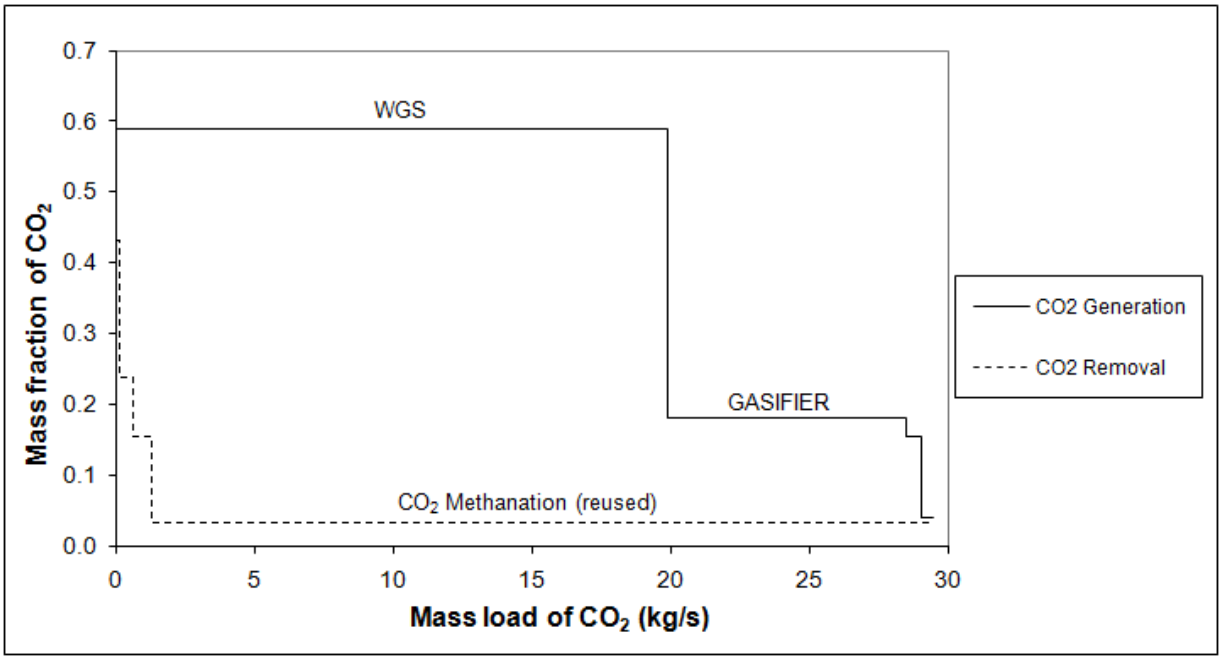
0.7
0.6
0.5
0.4
0.3
0.2
0.1
0.0
Mass fraction of CO_2
WGS
GASIFIER
CO_2 Methanation (reused)
0
5
10
15
20
25
30
Mass load of CO_2 (kg/s)
CO2 Generation
CO2 Removal

(b)

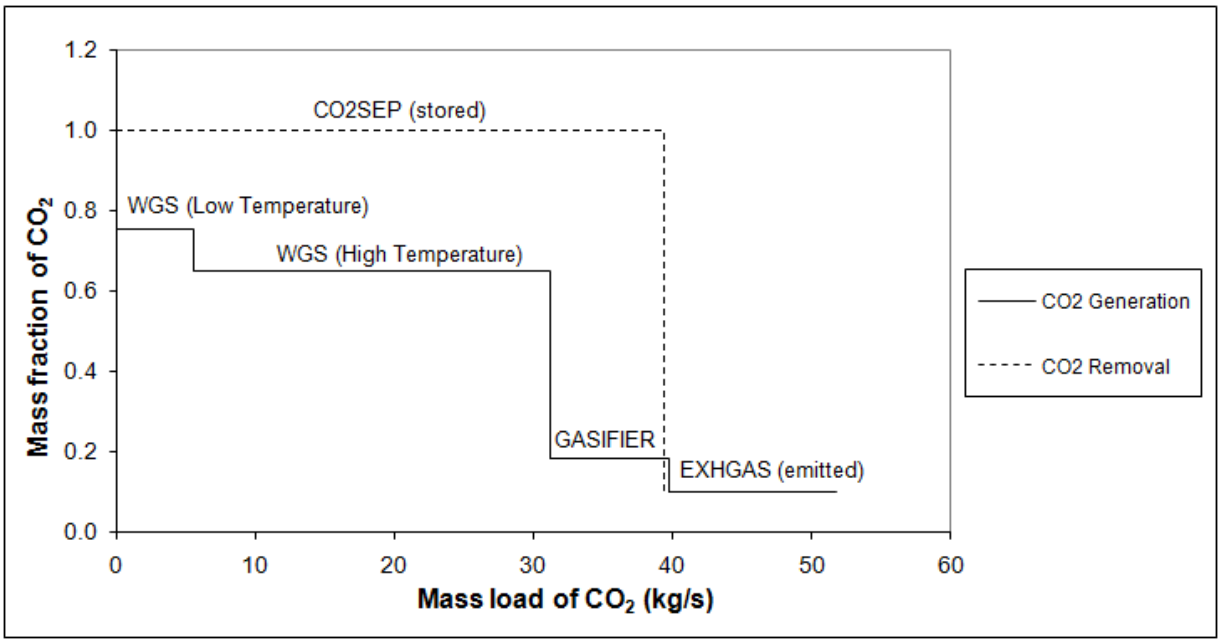
1.2
1.0
0.8
0.6
0.4
0.2
0.0
Mass fraction of CO_2
CO2SEP (stored)
WGS (Low Temperature)
WGS (High Temperature)
GASIFIER
EXHGAS (emitted)
0
10
20
30
40
50
60
Mass load of CO_2 (kg/s)
CO2 Generation
CO2 Removal

(c)

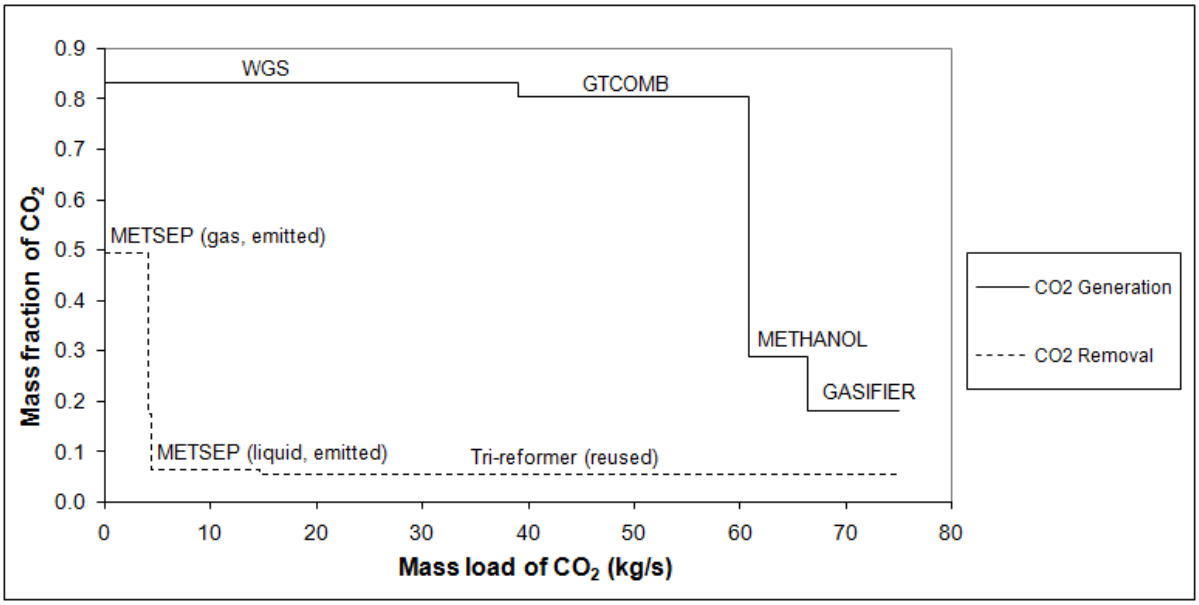

(d)

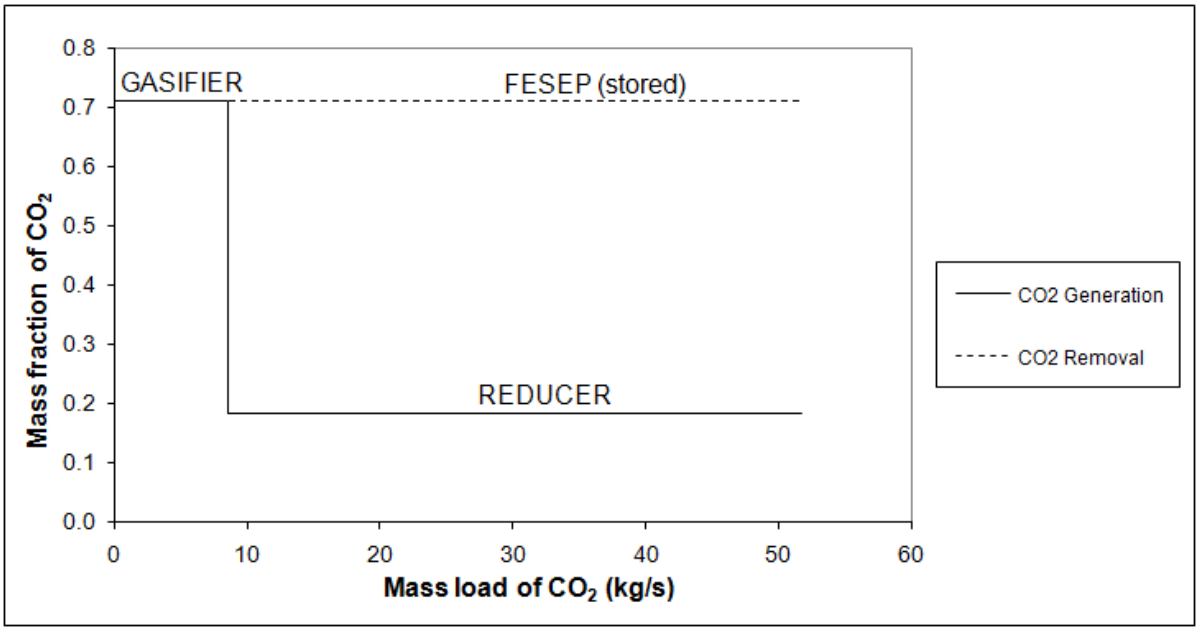

(e)

Figure 6: CO_2 emission balance diagrams for (a) Case A; (b) Case B; (c) Case C; (d) Case D and (e) Case E.

The ETII is evaluated for Cases A-E using equation (16), 0.47, 11.19, 0.58, 8.74 and 0.38, respectively. The ETII of systems incorporating a given category of CO_2 disposal system must only be compared with each other because they use the same basis. In this study, two classes of CO_2 disposal system are considered storage system (after capture or through other concentrating processes) and reuse system (CO_2 is converted into other form of chemical or fuel with or without capture). Thus ETII of Case A must be compared against that of Cases C and E while the ETII of Case B should be compared against that of Case D, respectively. The longest horizontal line at the lowest mass fraction on the CO_2 removal profiles of Cases B and D represents CO_2 reuse (Figure 6(b) and (d)), while the longest horizontal line at the highest mass fraction on the CO_2 removal profiles of Cases A, C and E indicates CO_2 removal by CCS (Figure 6(a), (c) and (e)). Thus, CCS cases result in ETII of less than 1 (the removal profile is above the generation profile), whilst the reuse cases have ETII of greater than 1 (the generation profile is above the removal profile). For ETII < 1, the energy intensity of a CCS based system increases with increasing ETII (increasing ratio of area under the generation profile and area under the removal profile). In the contrary, for ETII > 1, the energy intensity of a CO_2 reuse system increases with decreasing ETII (decreasing ratio of area under the generation profile and area under the removal profile). From here, EBD can thus be used as an initial prediction / indicator of the treatment intensity between these two classes of CO_2 disposal system (storage or reuse) based on the position of the generation and removal profiles, further discussed in section 3.4.

3.4 Establishing the Relationship between Emission Treatment Intensity Index and Plant Performances

The CO_2 capture system and / or reuse system is expected to be integrated to coal gasification systems generating clean syngas, i.e. block I. Intuitively, there is only one way interaction from block I to block II+III+IV. This implies that any modification in block II+III+IV will not have any effect on block I. Applying the Block and Boundary concept, block II+III+IV are now grouped together and block I and block II+III+IV are analysed separately in Table 8.

As evident, all the energy and economic criteria of block I have negligible variations between cases, once a uniform basis for the coal throughput, a heating value of 648 MW, is considered. On the other hand, the overall net energy and TPI of block II+III+IV vary depending upon ETII. The energy generation / consumption by process units has been estimated in Tables 2-4 and the resulting energy values of streams is estimated from the difference between LHV of products (methanol, acetic acid etc.) and additional feeds (e.g. hydrogen in Case B and natural gas in Case D). The overall net energy from block II+III+IV is the total energy available from process units (Tables 2-4) and streams (Table 8), on the basis of LHV of feedstock (i.e. syngas connecting block I and block II+III+IV). Similarly, TPI are given on the basis of LHV of syngas. The overall net energy and TPI are strongly dependent on ETII for block II+III+IV. As hypothesised in section 3.3, ETII should be analysed for a given CO_2 disposal category. Thus, the dependency of the overall net energy and TPI on ETII must also be interpreted for a given CO_2 disposal category.

Table 8: Summary results of ETII, energy and cost evaluations for Cases A to E.

Case	A	B	C	D	E
	Polygeneration with CCS	Polygeneration with methanation	Cogeneration with CCS	Polygeneration with tri-reforming	Chemical Looping
ETII	**0.47**	**11.19**	**0.58**	**8.74**	**0.38**
Block I					
Coal (MW)	648.1	648.1	648.1	648.1	648.1
Net energy from process units (MW)	841.3	841.3	844.9	833.8	842.0
Overall Net Energy (MW/MW coal)	**1.30**	**1.30**	**1.30**	**1.29**	**1.30**
Total Plant Investment (million Euro/year)	70.9	70.9	72.4	71.4	69.9
Total Plant Investment (Euro/MWh coal)	**13.7**	**13.7**	**14.0**	**13.8**	**13.5**
Block II+III+IV					
Syngas LHV (MW)	412.6	412.6	405.7	400.9	424.7
Additional feed LHV (MW)	0.0	619.8	0.0	2802.6	0.0
Product LHV (MW)	330.8	749.1	0.0	2852.8	345.4
Net energy from process units (MW)	28.4	24.0	110.4	−699.8	95.7
Net energy from streams (product – additional feed) (MW)	330.8	129.3	0.0	50.2	345.4
Overall Net Energy (MW/MW syngas)	**0.87**	**0.37**	**0.27**	**−1.62**	**1.04**
Total Plant Investment (million Euro/year)	12.3	177.9	16.5	463.8	9.4
Total Plant Investment (Euro/MWh syngas)	**3.7**	**53.9**	**5.1**	**144.6**	**2.8**

The overall net energy of a system implies its energy intensity. Higher the overall net energy of a system, lower is its energy intensity. The storage Cases A, C and E with ETII < 1, the overall net energy decreases (energy intensity increases) with increasing ETII (section 3.3). Thus, the sequence of cases with the highest to the lowest overall net energy is as follows: Case E > A > C (Table 8). The syngas chemical looping case is also considered as one of the CCS cases as it achieves a high level of decarbonisation (hence, high purity CO_2). Analogically, the overall net energy increases with decreasing energy intensity hence increasing ETII for CO_2 reuse cases with ETII > 1 (Case B has higher overall net energy than Case D).

TPI indicates the cost intensity of a system, i.e. higher TPI implies higher cost intensity of a system. As obvious, for storage Cases A, C and E with ETII < 1, TPI increases with increasing ETII (increasing cost intensity) (Case C > A > E) and TPI decreases with increasing ETII (decreasing cost intensity) for CO_2 reuse cases with ETII > 1 (Case D has higher TPI than Case B).

Higher overall net energy and lower TPI of a system are desirable. This requires higher ETII in reuse case and lower ETII in storage case, respectively. For the storage cases the maximum value of ETII = 1, while for the reuse cases the minimum value of ETII is 1. Thus both cases meet at an ETII value of 1.0 (equation (15) and (16)). EBD and ETII are thus an effective way of assessing energy and economics of integrated CO_2 abatement systems.

4. Conclusions

A shortcut methodology has been developed for analysing the performance of integrated decarbonised coal gasification systems. This methodology also serves as a decision-making tool to be conveniently used for selecting energetically and economically favourable systems at preliminary design stage. The proposed methodology comprises of two steps: preliminary screening using Gibbs energy method; this is followed by the analysis of graphical emission balance diagram (EBD) and emission treatment intensity index (ETII) for plant energetic and economic performances. The relationship between ETII and plant performance is derived using shortcut energy auditing and economic evaluation aided by Block and Boundary concept on plant flowsheets. ETII applicable to individual categories of CO_2 disposal systems (storage or CO_2 reuse) is related to the energy and cost intensities of integrated CO_2 abatement and energy systems. Coal with CCS systems considered are: polygeneration into methanol, acetic acid, hydrogen and electricity (Case A); cogeneration into heat and electricity (Case C); and syngas chemical looping for high purity hydrogen production (Case E). Coal with CO_2 reuse systems under consideration include: similar polygeneration system as Case A with methanation (Case B); and tri-reforming process and methanol synthesis Case D. Amongst the CCS options, coal syngas chemical looping (Case E) is the most energy efficient and least cost intensive; this is followed by coal polygeneration with CCS (Case A); and coal cogeneration with CCS (Case C), respectively. Case D is energetically and economically more intensive than Case B.

Nomenclatures

A	Area under generation / removal profile on emission balance diagram
ETII	Emission Treatment Intensity Index
G	Gibbs energy
$\Delta G^{o}_{f,products}$	Change of Gibbs energy of formation of products
$\Delta G^{o}_{f,reactants}$	Change of Gibbs energy of formation of reactants
$\Delta H^{o}_{f,products}$	Standard enthalpy change of formation of products
$\Delta H^{o}_{f,reactants}$	Standard enthalpy change of formation of reactants
ΔH^{o}_{R}	Standard enthalpy change of reaction
l_j	Mass load of CO_2 within a step j
m_k	Mass load of CO_2 within a step k
M	Total mass load of CO_2 shown as the final point on the profile
n	Number of moles
p	Pressure
R	Universal gas constant
S	Entropy
ΔS°_{f}	Standard entropy change of formation of substances
T	Temperature
TPI	Total plant investment
U	Total number of steps in the generation profile
V	Volume
W	Total number of steps in the removal profile

α	Mass fraction of CO_2 in the generation profile
λ_j	Function of generation profile with steps *j*
μ_k	Function of removal profile with steps *k*
ω	Mass fraction of CO_2 in the removal profile

Appendix A

Process descriptions for Cases A-E are provided as follows:

Case A-Coal polygeneration with CCS (Figure 5(a))

Electricity, hydrogen, methanol and acetic acid are the products generated from this polygeneration system. Coal-water slurry is gasified (GASIFIER) using oxygen-enriched air as the gasification medium to produce syngas (stream 3), containing a mixture of H_2, CO, CO_2, H_2O as major components. Subsequently, the syngas is cooled in a syngas cooler (SYNGCOOL), and undergoes a series of gas conditioning and cleaning processes, comprising ash removal in CYCLONE, water removal (H2OREM), H_2S removal (H2SREM) and CO_2 separation (CO2SEP) processes. A target stoichiometric ratio of $(H_2-CO_2) / (CO+CO_2) = 2$ of syngas for methanol synthesis (METHANOL) is attained (Ng and Sadhukhan, 2011). A flash column (METSEP) is used to separate the gaseous and liquid products. The offgas containing unreacted gases such as H_2, CO, CH_4 etc. (stream 21) is utilised in power generation through gas turbine (GASTURB) and acetic acid (ACEREACT) production. Hydrogen is separated via H_2/CO separation process (H2COSEP) as a product. Liquid methanol (stream 22) is sent to distillation units (METDISTL) to further recover methanol coming from METSEP. A portion of the liquid methanol (stream 35), depending on the availability of CO in the offgas after separation from the product gas, is used in acetic acid synthesis.

Case B-Coal polygeneration with CO_2 methanation (Figure 5(b))

Electricity, methanol, acetic acid and methane are the products generated from this polygeneration system. This case only differs from Case A in terms of the CO_2 disposal step. In this case, CO_2 is reused into methane production in METHANAT through Sabatier's reaction, instead of storage in Case A. All the hydrogen produced from the system is utilised in methane production and a part of the hydrogen required by the process is imported.

Case C-Coal IGCC with CCS (Figure 5(c))

The main products from this cogeneration system are heat and electricity. In this case, coal is gasified into syngas for the production of heat and power. The syngas is conditioned through high and low temperature water-gas shift reactors (HTWGS and LTWGS) and is cleaned through H_2S removal (H2SREM) and CO_2 removal (CO2SEP). CO_2 is captured and stored. The clean syngas is then used into gas turbine (GASTURB) for the generation of electricity.

Case D-Coal IGCC with tri-reforming and methanol synthesis (Figure 5(d))

Methanol and electricity are the main products from this system. Case D is a modification of Case C. In Case D, CO_2 in the exhaust gas (EXHGAS) from gas turbine (GASTURB) is reused in tri-reforming process (TRIREFOR) for the production of methanol. Tri-reforming of methane (Song and Pan, 2004) uses CO_2, steam and oxygen for the production of valuable syngas with desired ratio and for the reduction of carbon formation on catalyst. Hydrogen (stream 15) is separated from the syngas from gasification using pressure swing adsorption (PSA). Hydrogen recovered is then

combined with the syngas from tri-reforming process (stream 26). The remaining CO enriched gas (stream 14) from PSA is sent to gas turbine for electricity generation. A highly concentrated CO_2 stream is resulted from gas turbine combustion. The exhaust gas from gas turbine (EXHGAS) is then routed to the tri-reforming process. The unreacted offgas (stream 36) from methanol synthesis are recycled to enhance the production of methanol, while the rest is purged (stream 35). The proposed integrated system meets the desired H_2/CO molar stoichiometric ratio in the feed gas to the methanol synthesis without any use of CCS.

Scheme E-Coal syngas chemical looping (Figure 5(e))

Hydrogen is the sole product from this system. Syngas is generated in the same way as in all other cases. Case E considers the integration of syngas chemical looping concept into a coal gasification system, with an aim of producing high purity CO_2 (REDUCER) and hydrogen (OXIDISER) simultaneously. The metal oxide (Fe_2O_3) can be recovered through combustor (COMBUST) using air, and recycled back to REDUCER.

The syngas chemical looping concept (Tomlinson et al., 2007; Fan et al., 2008) is featured in Figure A.1. Firstly, the syngas generated from gasifier consisting of CO, H_2 and light hydrocarbons is introduced into a reducer, where it is reacted with Fe_2O_3. Fe_2O_3 is reduced to form Fe during the reaction, whilst CO_2 and H_2O are the main products formed according to equations (A.1) and (A.2). Equation (A.3) presents the generic reaction applicable to CO, H_2 as well as other hydrocarbons, occurring in the reducer. MO and M represent different metal oxide phases. In the next stage, Fe is reacted with steam to produce H_2 (equation (A.4)), while Fe is oxidised to Fe_3O_4.

Finally, Fe_3O_4 is regenerated into Fe_2O_3 via combustion with air and recycled back to the reducer, provided in equation (A.5).

Reducer: (Tomlinson et al. 2007)

$$3\ CO + Fe_2O_3 \leftrightarrow 3\ CO_2 + 2\ Fe \quad \text{(A.1)}$$

$$3\ H_2 + Fe_2O_3 \leftrightarrow 3\ H_2O + 2\ Fe \quad \text{(A.2)}$$

$$C_xH_yO_z + (2x + y/2 - z)\ MO \leftrightarrow (2x + y/2 - z)\ M + x\ CO_2 + (y/2)\ H_2O \quad \text{(A.3)}$$

Oxidiser: (Tomlinson et al. 2007)

$$3\ Fe + 4\ H_2O \leftrightarrow Fe_3O_4 + 4\ H_2 \quad \text{(A.4)}$$

Combustor: (Tomlinson et al. 2007)

$$4\ Fe_3O_4 + O_2 \leftrightarrow 6\ Fe_2O_3 \quad \text{(A.5)}$$

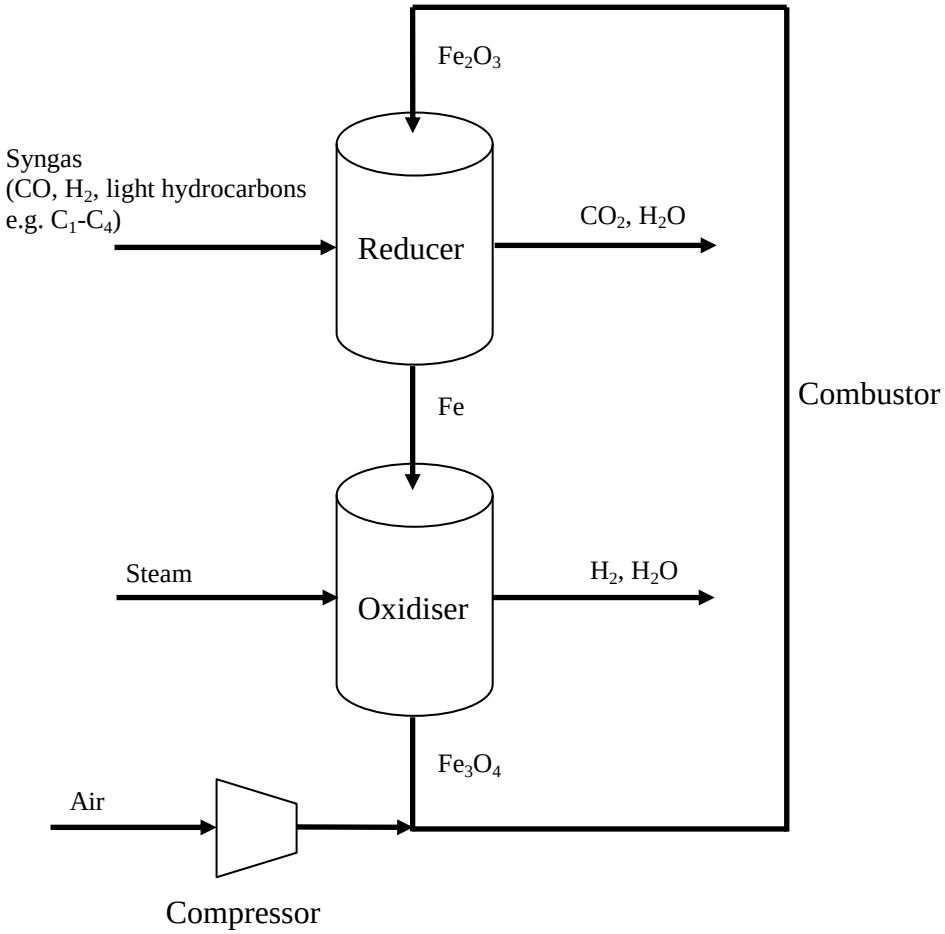

Figure A.1: Syngas chemical looping scheme.

Appendix B

The thermodynamic data (Atkins and Paula, 2005) required for estimating the standard enthalpy change of reaction and standard Gibbs energy of reaction is provided in Table B.1.

Table B.1: Standard heat of formation and standard Gibbs energy of formation for various components. (Atkins and Paula, 2005)

Component	Standard heat of formation at 298.15 K, ΔH_f° (kJ/mol)	Standard Gibbs energy of formation at 298.15 K, ΔG_f° (kJ/mol)
CO_2 (*g*)	−393.51	−394.36
H_2 (*g*)	0	0
CH_3OH (*l*)	−238.66	−166.27
H_2O (*l*)	−285.83	−237.13
CH_4 (*g*)	−74.81	−50.72
HCOOH (*l*)	−424.72	−361.35
CO (*g*)	−110.53	−137.17

Appendix C

The economic data (Hamelinck and Faaij, 2002; Denton, 2003; IPCC, 2005; Larson et al., 2005; Stiegel and Ramezan, 2006; Zhu and Jones, 2009; DECC, 2010; ICIS Pricing, 2010; Methanex, 2011) required for evaluating capital cost, operating cost and value of products are provided in Table C.1.

Table C.1: Economic parameters for evaluating capital cost, operating costs and value of products.

Capital cost					
No.	Process unit	Base Cost (million USD)	Scale factor	Base scale	Scale unit
1	Gasifier (GE type) [a]	62.92	0.67	716	MW coal input
2	Water-gas shift reactor [a]	12.24	0.67	1377	MW LHV coal input
3	Rectisol [b, i]	54.1	0.7	9909	kmol CO_2/h
4	CO_2 transport and storage [c]	5.6 Euro/t CO_2			
5	Methanol reactor [b]	7	0.6	87.5	t MeOH/h
6	Acetic acid reactor [d]	2 times of (5)			
7	H_2/CO separation [b, ii]	28	0.7	9600	kmol/h feed
8	Gas turbine [a]	56	0.75	266	MW
9	HRSG [a]	41.2	1	355	MW heat duty
10	SYNGCOOL [a]	25.4	0.6	77	MW heat duty
11	ASU [a]	35.6	0.5	76.6	t O_2/h
12	Compressor [a]	4.83	0.67	10	MW
13	Expander [a]	2.41	0.67	10	MW
14	Tri-reformer/ Methanator [b, iii]	9.4	0.6	1390	kmol/h feed

Operating cost		
No.	Raw material	Cost Estimation
1	Natural Gas [e]	18 Euro/MWh
2	Coal [e]	2.86 Euro/GJ
3	Hydrogen [f]	1104 Euro/t

Market price		
No.	Product	Price
1	Electricity [e]	70.29 Euro/MWh
2	Methanol [g]	305 Euro/t
3	Acetic acid [h]	550 Euro/t
4	Hydrogen [f]	1104 Euro/t
5	Methane [e]	18 Euro/MWh

Note:

[a] Larson et al., 2005. Economic parameters taken from year 2003. Assume 1USD = 0.9 Euro (2003).

[b] Hamelinck and Faaij, 2002. Economic parameters taken from year 2001. Assume 1 USD = 1.1 Euro (2001).

[c] IPCC, 2005. Cost of CO_2 transport: 0-5 USD/t CO_2; Cost of CO_2 storage: 0.6-8.3 USD/t CO_2. Average values of CO_2 transport and storage are taken. Assume 1 USD = 0.8 Euro (2010).

[d] Cost of acetic acid reactor is estimated based on 2 times of the cost of methanol reactor, as suggested by Zhu and Jones, 2009.

[e] DECC, 2010.

[f] Stigel and Ramezan, 2006.

[g] Methanex, 2011. Contract price valid from April to June 2011.

[h] ICIS pricing, 2010.

[i] Cost of Rectisol is assumed to be 2 times of Selexol, as suggested by Denton, 2003.

[ii] Cost of H_2/CO separation unit is estimated based on the cost of PSA.

[iii] Costs of tri-reformer and methanator are assumed to be the same as the cost of steam reformer.

CEPCI

2001= 394.3; 2003=402.0; 2010 (November)=556.8

Acknowledgement

The authors express their gratitude to The University of Manchester Alumni Fund and Process Integration Research Consortium for financial aid to support this research.

References

Armstrong PA, Bennett DL, Foster EP, Stein VE. ITM oxygen: the new oxygen supply for the new IGCC market. In *Gasification Technologies*. 2005, 9-12 October. San Francisco, California.

Atkins P, Paula J. The elements of physical chemistry. 4th ed. Oxford: Oxford University Press; 2005.

Department of Energy and Climate Change (DECC). Quarterly energy prices: December 2010, 2010. [cited 11 May 2010]. Available from: www.decc.gov.uk.

Denton DL. Coal gasification–today's technology of choice and tomorrow's bright promise. In *AIChE*. 2003, 29 October. East Tennessee Section.

El-Halwagi MM, Pollution prevention though process integration. Academic Press; 1997.

El-Halwagi MM, Gabriel F, Harell D, Rigorous graphical targeting for resource conservation via material recycle / reuse networks. Ind. Eng. Chem. Res. 2003; 42(19): p. 4319-28.

El-Halwagi MM, Harell D, Spriggs HD. Targeting cogeneration and waste utilization through process integration. Appl. Energ. 2009; 86(6): p. 880-7.

Fan L, Li F, Ramkumar S. Utilization of chemical looping strategy in coal gasification processes. Particuology. 2008; 6(3): p. 131-42.

Friedler F, Tarjan K, Huang YW, Fan LT, Graph-theoretic approach to process synthesis: polynomial algorithm for maximal structure generation. Comput. Chem. Eng. 1993; 17(9): p. 929-42.

Friedler F, Process integration, modelling and optimisation for energy saving and pollution reduction. Appl. Therm. Eng. 2010; 30(16), p. 2270-80.

Gupta P, Velazquez-Vargas LG, Fan L-S. Syngas redox (SGR) process to produce hydrogen from Coal Derived Syngas. Energy Fuels. 2007; 21(5): p. 2900-8.

Hamelinck CN, Faaij APC. Future prospects for production of methanol and hydrogen from biomass. J. Power Sources. 2002; 111(1): p. 1-22.

ICIS Pricing. 2010. [cited 18 March 2011]. Available from: http://www.icispricing.com/il_shared/Samples/SubPage95.asp.

Intergovernmental Panel on Climate Change (IPCC). IPCC special report on carbon dioxide capture and storage. 2005. [cited 10 June 2011]. Available from: http://www.ipcc.ch/publications_and_data/publications_and_data_reports.shtml

Jerndal E, Mattisson T, Lyngfelt A. Thermal analysis of chemical-looping combustion. Chem. Eng. Res. Des. 2006; 84(9): p. 795-806.

Klemeš J, Bulatov I, Cockerill T, Techno-economic modelling and cost functions of CO_2 capture processes. Comput. Chem. Eng. 2007; 31(5-6): p. 445-55.

Kondepudi D, Introduction to modern thermodynamics. Chichester: Wiley; 2008.

Larson ED, Jin H, Celik FE. Gasification-based fuels and electricity production from biomass, without and with carbon capture and storage. 2005. Princeton Environmental Institute, Princeton University.

Linnhoff B, Dhole VR. Targeting for CO_2 emissions for total sites. Chem. Eng. Technol. 1993; 16(4): p. 252-9.

Linnhoff B, Townsend DW, Boland D. A user guide on process integration for the efficient use of energy. 1994, IChemE.

Methanex. Methanol price, 2011. [cited 1 May 2011]. Available from: www.methanex.com.

Ng KS, Sadhukhan J. Process integration and economic analysis of bio-oil platform for the production of methanol and combined heat and power. Biomass Bioenergy. 2011; 35(3): p. 1153-69.

Peters MS, Timmerhaus KD, West RE. Plant design and economics for chemical engineers. 5th ed. New York, US: McGraw-Hill; 2003.

Smith R, Chemical process design and integration. Chichester,UK: John Wiley and Sons Ltd.; 2005.

Song C, Pan W. Tri-reforming of methane: a novel concept for catalytic production of industrially useful synthesis gas with desired H_2/CO ratios. 2004; Catal. Today 98(4): p. 463-484.

Stiegel GJ, Ramezan M. Hydrogen from coal gasification: an economical pathway to a sustainable energy future. Int. J. Coal. Geol. 2006; 65(3-4): p. 173-90.

Tan RR, Foo DCY. Pinch analysis approach to carbon-constrained energy sector planning. Energy. 2007; 32(8): p. 1422-9.

Tomlinson G, Gray D, White C, Chemical looping process in a coal-to-liquids configuration. USDOE/NETL-2008/1307, 2007. National Energy Technology Laboratory.

Xie C, Modeling the performance and emissions of integrated gasification combined cycle based Lurgi ammonia synthesis system. 2001, North Carolina State University, US. [cited 10 June 2011]. Available from: http://repository.lib.ncsu.edu/ir/handle/1840.16/1837.

Xu X, Moulijn JA. Mitigation of CO_2 by chemical conversion: plausible chemical reactions and Promising Products. Energy Fuels. 1996; 10(2): p. 305-25.

Zhelev TK, Ridolfi R. Energy recovery and environmental concerns addressed through emergy-pinch analysis. Energy. 2006; 31(13): p. 2486-98.

Zhu Y, Jones S. Techno-economic Analysis for the thermochemical conversion of lignocellulosic biomass to ethanol via acetic acid synthesis. PNNL-18483, 2009. US DOE.

Appendix 1

ASPEN Plus Process Simulation Flowsheets

and Stream Results

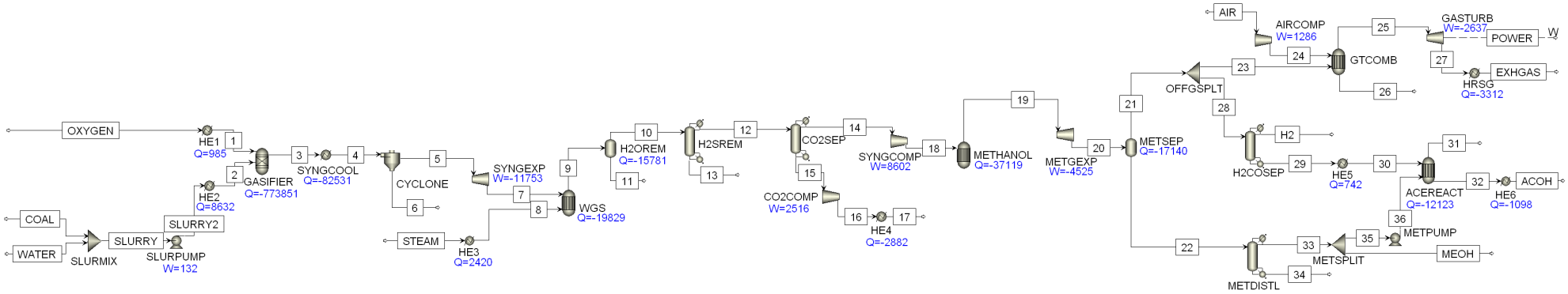

Q: Heat duty (kW)
W: Power (kW)

Figure A1.1: Coal polygeneration system with CCS (Case / Scheme A)

Table A1.1: Stream results for Case / Scheme A.

Stream No.	1	2	3	4	5	6	7	8	9	10	11	12	13	14	15
Phase	VAPOUR	MIXED	VAPOUR	VAPOUR	VAPOUR	SOLID	VAPOUR	VAPOUR	VAPOUR	VAPOUR	LIQUID	MIXED	VAPOUR	MIXED	VAPOUR
Substream: MIXED															
Mole Flow (kmol/s)															
S	0	0.025	1.03E-07	1.03E-07	1.03E-07	0	1.03E-07	0	1.03E-07	2.29E-12	1.03E-07	0	2.29E-12	0	0
O_2	0.548	0.064	1.50E-12	1.50E-12	1.50E-12	0	1.50E-12	0	1.50E-12	1.50E-12	7.35E-17	1.50E-12	0	1.50E-12	0
N_2	0.007	0.009	0.016	0.016	0.016	0	0.016	0	0.016	0.016	6.44E-07	0.016	0	0.016	0
H_2	0	0.537	0.664	0.664	0.664	0	0.664	0	1.115	1.115	3.76E-06	1.115	0	1.115	0
H_2O	0	0.571	0.420	0.420	0.420	0	0.420	0.046	0.015	0.011	0.004	0.011	0	0.011	0
CO	0	0	0.981	0.981	0.981	0	0.981	0	0.530	0.530	2.30E-05	0.530	0	0.530	0
CO_2	0	0	0.195	0.195	0.195	0	0.195	0	0.647	0.646	2.87E-04	0.646	0	0.006	0.640
H_2S	0	0	0.023	0.023	0.023	0	0.023	0	0.023	0.023	3.16E-05	0	0.023	0	0
C	0	1.179	2.78E-18	2.78E-18	2.78E-18	0	2.78E-18	0	0	0	0	0	0	0	0
CH_4	0	0	6.31E-04	6.31E-04	6.31E-04	0	6.31E-04	0	6.31E-04	6.31E-04	6.28E-08	6.31E-04	0	6.31E-04	0
CH_3OH	0	0	9.57E-08	9.57E-08	9.57E-08	0	9.57E-08	0	9.57E-08	9.13E-08	4.43E-09	9.13E-08	0	9.13E-08	0
Cl_2	0	2.58E-04	2.58E-04	2.58E-04	2.58E-04	0	2.58E-04	0	2.58E-04	2.58E-04	8.60E-07	0	2.58E-04	0	0
COS	0	0	0.002	0.002	0.002	0	0.002	0	0.002	0.002	3.24E-06	0	0.002	0	0
Ar	0.026	0	0.026	0.026	0.026	0	0.026	0	0.026	0.026	1.25E-06	0.026	0	0.026	0
CH_3COOH	0	0	3.12E-10	3.12E-10	3.12E-10	0	3.12E-10	0	3.12E-10	1.90E-10	1.22E-10	1.90E-10	0	1.90E-10	0
Total Flow (kmol/s)	0.581	2.385	2.328	2.328	2.328	0	2.328	0.046	2.375	2.370	0.005	2.345	0.025	1.705	0.640
Total Flow (t/h)	67.5	103.1	170.6	170.6	170.6	0	170.6	3.000	173.6	173.3	0.329	170.1	3.219	68.7	101.4
Total Flow (m^3/s)	0.366	0.485	4.244	1.815	1.815	0	4.253	0.084	4.132	2.547	9.26E-05	2.521	0.027	1.830	0.688
Temperature (°C)	83.3	121.1	1371.1	430.0	430.0		276.0	270.0	250.0	50.0	50.0	50.0	50.0	50.0	50.0
Pressure (bar)	47.0	42.4	75.0	75.0	75.0		25.0	25.0	25.0	25.0	25.0	25.0	25.0	25.0	25.0
Vapor Fraction	1.000	0.256	1.000	1.000	1.000		1.000	1.000	1.000	1.000	0	1.000	1.000	0.999	1.000
Liquid Fraction	0	0.744	0	0	0		0	0	0	0	1.000	1.46E-05	0	0.001	0
Solid Fraction	0	0	0	0	0		0	0	0	0	0	0	0	0	0
Enthalpy (J/kg)	5.25E+04	2.09E+07	-3.75E+06	-5.44E+06	-5.44E+06		-5.68E+06	-1.30E+07	-6.22E+06	-6.53E+06	-1.45E+07	-6.64E+06	-7.47E+05	-3.29E+06	-8.92E+06
Entropy (J/kg-K)	-762.9	3.28E+04	3138.9	1630.8	1630.8		1681.8	-2796.4	1114.0	340.0	-7288.0	309.5	665.4	861.0	-470.8
Density (kg/m^3)	51.2	59.1	11.2	26.1	26.1		11.1	9.973	11.7	18.9	987.1	18.7	33.5	10.4	41.0
Average Molecular Weight	32.3	12.0	20.4	20.4	20.4		20.4	18.0	20.3	20.3	19.8	20.1	36.0	11.2	44.0
Liquid Volumetric Flow 60°F (m^3/s)	0.031	0.052	0.110	0.110	0.110	0	0.110	8.35E-04	0.127	0.127	9.57E-05	0.125	0.001	0.091	0.034
Substream: TOTAL															
Total Flow (t/h)	67.5	110.4	177.9	177.9	170.6	7.257	170.6	3.000	173.6	173.3	0.329	170.1	3.219	68.7	101.4
Enthalpy (kW)	985.5	5.97E+05	-1.76E+05	-2.59E+05	-2.58E+05	-895.9	-2.69E+05	-1.08E+04	-3.00E+05	-3.14E+05	-1326.5	-3.14E+05	-668.0	-6.27E+04	-2.51E+05
Substream: NCPSD															
Mass Flow (t/h)															
Ash	0	7.257	7.257	7.257	0	7.257	0	0	0	0	0	0	0	0	0
Mass Fraction															
Ash	0	1.000	1.000	1.000	0	1.000	0	0	0	0	0	0	0	0	0
Total Flow (t/h)	0	7.257	7.257	7.257	0	7.257	0	0	0	0	0	0	0	0	0
Temperature (°C)		121.1	1371.1	430.0		430.0									
Pressure (bar)	47.0	42.4	75.0	75.0		75.0	25.0	25.0		25.0	25.0	25.0	25.0	25.0	25.0
Vapor Fraction		0	0	0		0									
Liquid Fraction		0	0	0		0									
Solid Fraction		1.000	1.000	1.000		1.000									

Table A1.1 (con't)

Stream No.	16	17	18	19	20	21	22	23	24	25	26	27	28	29	30
Phase	VAPOUR	VAPOUR	VAPOUR	VAPOUR	MIXED	VAPOUR	LIQUID	VAPOUR	VAPOUR	VAPOUR		VAPOUR	VAPOUR	MIXED	VAPOUR
Substream: MIXED															
Mole Flow (kmol/s)															
S	0	0	0	0	0	0	0	0	0	0	0	0	0	0	0
O_2	0	0	1.50E-12	1.50E-12	1.50E-12	1.47E-12	2.78E-14	1.47E-13	0.025	0.001	0	0.001	1.32E-12	1.32E-12	1.32E-12
N_2	0	0	0.016	0.016	0.016	0.016	2.41E-04	0.002	0.095	0.096	0	0.096	0.014	0.014	0.014
H_2	0	0	1.115	0.349	0.349	0.348	4.14E-04	0.035	0	1.37E-07	0	1.37E-07	0.313	0	0
H_2O	0	0	0.011	4.94E-04	4.94E-04	3.33E-06	4.90E-04	3.33E-07	0	0.035	0	0.035	3.00E-06	3.00E-06	3.00E-06
CO	0	0	0.530	0.132	0.132	0.129	0.002	0.013	0	1.39E-07	0	1.39E-07	0.116	0.116	0.116
CO_2	0.640	0.640	0.006	0.017	0.017	0.014	0.003	0.001	0	0.014	0	0.014	0.013	0.013	0.013
H_2S	0	0	0	0	0	0	0	0	0	0	0	0	0	0	0
C	0	0	0	0	0	0	0	0	0	0	0	0	0	0	0
CH_4	0	0	6.31E-04	6.31E-04	6.31E-04	6.07E-04	2.38E-05	6.07E-05	0	0	0	0	5.47E-04	5.47E-04	5.47E-04
CH_3OH	0	0	9.13E-08	0.388	0.388	0.008	0.381	7.84E-04	0	7.84E-04	0	7.84E-04	0.007	0.007	0.007
Cl_2	0	0	0	0	0	0	0	0	0	0	0	0	0	0	0
COS	0	0	0	0	0	0	0	0	0	0	0	0	0	0	0
Ar	0	0	0.026	0.026	0.026	0.026	4.70E-04	0.003	0	0.003	0	0.003	0.023	0.023	0.023
CH_3COOH	0	0	1.90E-10	1.90E-10	1.90E-10	2.97E-13	1.90E-10	2.97E-14	0	2.97E-14	0	2.97E-14	2.67E-13	2.67E-13	2.67E-13
Total Flow (kmol/s)	0.640	0.640	1.705	0.929	0.929	0.541	0.387	0.054	0.120	0.150	0	0.150	0.487	0.174	0.174
Total Flow (t/h)	101.4	101.4	68.7	68.7	68.7	24.0	44.7	2.403	12.5	14.9	0	14.9	21.6	19.4	19.4
Total Flow (m^3/s)	0.279	0.205	0.700	0.404	1.309	0.587	0.016	0.059	0.468	1.315	0	6.363	0.529	0.184	0.204
Temperature (°C)	147.0	35.0	220.5	250.0	136.8	40.0	40.0	40.0	383.9	1200.0		745.4	40.0	40.0	150.0
Pressure (bar)	80.0	80.0	100.0	100.0	24.0	24.0	24.0	24.0	14.0	14.0	14.0	2.000	24.0	24.0	30.0
Vapor Fraction	1.000	1.000	1.000	1.000	0.992	1.000	0	1.000	1.000	1.000		1.000	1.000	0.972	1.000
Liquid Fraction	0	0	0	0	0.008	0	1.000	0	0	0		0	0	0.028	0
Solid Fraction	0	0	0	0	0	0	0	0	0	0		0	0	0	0
Enthalpy (J/kg)	-8.83E+06	-8.93E+06	-2.83E+06	-4.78E+06	-5.02E+06	-3.18E+06	-7.39E+06	-3.18E+06	3.72E+05	-1.93E+06		-2.57E+06	-3.18E+06	-3.61E+06	-3.47E+06
Entropy (J/kg-K)	-449.3	-731.7	953.7	-2312.5	-2248.2	257.4	-7221.2	257.4	206.3	1115.5		1187.0	257.4	1150.1	1477.5
Density (kg/m^3)	100.8	137.4	27.3	47.3	14.6	11.4	772.8	11.4	7.393	3.141		0.649	11.4	29.3	26.3
Average Molecular Weight	44.0	44.0	11.2	20.6	20.6	12.3	32.1	12.3	28.9	27.5		27.5	12.3	30.9	30.9
Liquid Volumetric Flow 60°F (m^3/s)	0.034	0.034	0.091	0.045	0.045	0.029	0.016	0.003	0.006	0.007	0	0.007	0.026	0.009	0.009
Substream: TOTAL															
Total Flow (t/h)	101.4	101.4	68.7	68.7	68.7	24.0	44.7	2.403	12.5	14.9	0	14.9	21.6	19.4	19.4
Enthalpy (kW)	-2.49E+05	-2.52E+05	-5.41E+04	-9.12E+04	-9.57E+04	-2.12E+04	-9.16E+04	-2123.1	1286.4	-7975.0	0	-1.06E+04	-1.91E+04	-1.94E+04	-1.87E+04
Substream: NCPSD															
Mass Flow (t/h)															
Ash	0	0	0	0	0	0	0	0	0	0	0	0	0	0	0
Mass Fraction															
Ash	0	0	0	0	0	0	0	0	0	0	0	0	0	0	0
Total Flow (t/h)	0	0	0	0	0	0	0	0	0	0	0	0	0	0	0
Temperature (°C)															
Pressure (bar)	80.0	80.0	100.0		24.0	24.0	24.0	24.0	14.0			2.000	24.0	24.0	30.0
Vapor Fraction															
Liquid Fraction															
Solid Fraction															

Table A1.1 (con't)

Stream No.	31	32	33	34	35	36	ACOH	AIR	COAL	EXHGAS	H2	MEOH	OXYGEN	SLURRY	SLURRY2	STEAM	WATER
Phase	VAPOUR	LIQUID	LIQUID	MIXED	LIQUID	LIQUID	LIQUID	VAPOUR	MIXED	VAPOUR	VAPOUR	LIQUID	VAPOUR	LIQUID	LIQUID	LIQUID	LIQUID
Substream: MIXED																	
Mole Flow (kmol/s)																	
S	0	0	0	0	0	0	0	0	0.025	0	0	0	0	0.025	0.025	0	0
O_2	1.28E-12	4.64E-14	0	2.78E-14	0	0	4.64E-14	0.025	0.064	0.001	0	0	0.548	0.064	0.064	0	0
N_2	0.014	4.55E-04	0	2.41E-04	0	0	4.55E-04	0.095	0.009	0.096	0	0	0.007	0.009	0.009	0	0
H_2	0	0	0	4.14E-04	0	0	0	0	0.537	1.37E-07	0.313	0	0	0.537	0.537	0	0
H_2O	2.05E-07	2.79E-06	0	4.90E-04	0	0	2.79E-06	0	0.155	0.035	0	0	0	0.571	0.571	0.046	0.417
CO	7.96E-10	2.76E-11	0	0.002	0	0	2.76E-11	0	0	1.39E-07	0	0	0	0	0	0	0
CO_2	0.011	0.002	0	0.003	0	0	0.002	0	0	0.014	0	0	0	0	0	0	0
H_2S	0	0	0	0	0	0	0	0	0	0	0	0	0	0	0	0	0
C	0	0	0	0	0	0	0	0	1.179	0	0	0	0	1.179	1.179	0	0
CH_4	5.14E-04	3.24E-05	0	2.38E-05	0	0	3.24E-05	0	0	0	0	0	0	0	0	0	0
CH_3OH	0.001	0.009	0.379	0.002	0.120	0.120	0.009	0	0	7.84E-04	0	0.259	0	0	0	0	0
Cl_2	0	0	0	0	0	0	0	0	2.58E-04	0	0	0	0	2.58E-04	2.58E-04	0	0
COS	0	0	0	0	0	0	0	0	0	0	0	0	0	0	0	0	0
Ar	0.022	8.00E-04	0	4.70E-04	0	0	8.00E-04	0	0	0.003	0	0	0.026	0	0	0	0
CH_3COOH	0.004	0.113	0	1.90E-10	0	0	0.113	0	0	2.97E-14	0	0	0	0	0	0	0
Total Flow (kmol/s)	0.053	0.125	0.379	0.008	0.120	0.120	0.125	0.120	1.968	0.150	0.313	0.259	0.581	2.385	2.385	0.046	0.417
Total Flow (t/h)	7.378	25.8	43.7	0.991	13.8	13.8	25.8	12.5	76.1	14.9	2.274	29.8	67.5	103.1	103.1	3.000	27.0
Total Flow (m^3/s)	0.062	0.008	0.016	0.006	0.005	0.005	0.007	2.937	15.0	4.662	0.340	0.011	14.2	0.029	0.029	8.39E-04	0.008
Temperature (°C)	150.0	150.0	40.0	40.0	40.0	40.3	30.0	25.0	25.0	100.0	40.0	40.0	25.0	26.2	27.7	25.0	25.0
Pressure (bar)	30.0	30.0	24.0	24.0	24.0	30.0	30.0	1.013	1.013	1.000	24.0	24.0	1.013	1.000	42.4	1.013	1.013
Vapor Fraction	1.000	0	0	0.680	0	0	0	1.000	0.311	1.000	1.000	0	1.000	0	0	0	0
Liquid Fraction	0	1.000	1.000	0.320	1.000	1.000	1.000	0	0.689	0	0	1.000	0	1.000	1.000	1.000	1.000
Solid Fraction	0	0	0	0	0	0	0	0	0	0	0	0	0	0	0	0	0
Enthalpy (J/kg)	-3.00E+06	-7.40E+06	-7.40E+06	-6.85E+06	-7.40E+06	-7.40E+06	-7.55E+06	1.77E-10	3.35E+07	-3.37E+06	2.14E+05	-7.40E+06	-1.05E-10	2.06E+07	2.06E+07	-1.59E+07	-1.59E+07
Entropy (J/kg-K)	-602.7	-3894.6	-7362.5	-1445.1	-7362.5	-7359.9	-4067.9	148.2	6.21E+04	166.3	-1.24E+04	-7362.5	63.6	4.22E+04	4.20E+04	-9030.5	-9030.5
Density (kg/m^3)	33.1	870.5	774.8	43.8	774.8	774.5	1041.0	1.179	1.411	0.886	1.858	774.8	1.320	999.2	998.2	993.5	993.5
Average Molecular Weight	38.8	57.5	32.0	32.8	32.0	32.0	57.5	28.9	10.7	27.5	2.016	32.0	32.3	12.0	12.0	18.0	18.0
Liquid Volumetric Flow 60°F (m^3/s)	0.003	0.007	0.015	4.06E-04	0.005	0.005	0.007	0.006	0.045	0.007	0.017	0.010	0.031	0.052	0.052	8.35E-04	0.008
Substream: TOTAL																	
Total Flow (t/h)	7.378	25.8	43.7	0.991	13.8	13.8	25.8	12.5	83.3	14.9	2.274	29.8	67.5	110.4	110.4	3.000	27.0
Enthalpy (kW)	-6149.9	-5.31E+04	-8.98E+04	-1886.7	-2.84E+04	-2.84E+04	-5.42E+04	6.12E-13	7.07E+05	-1.39E+04	135.5	-6.13E+04	-1.97E-12	5.88E+05	5.88E+05	-1.32E+04	-1.19E+05
Substream: NCPSD																	
Mass Flow (t/h)																	
Ash	0	0	0	0	0	0	0	0	7.257	0	0	0	0	7.257	7.257	0	0
Mass Fraction																	
Ash	0	0	0	0	0	0	0	0	1.000	0	0	0	0	1.000	1.000	0	0
Total Flow (t/h)	0	0	0	0	0	0	0	0	7.257	0	0	0	0	7.257	7.257	0	0
Temperature (°C)									25.0					26.2	27.7		
Pressure (bar)			24.0	24.0	24.0	30.0	30.0	1.013	1.013	1.000	24.0	24.0	1.013	1.000	42.4	1.013	1.013
Vapor Fraction									0					0	0		
Liquid Fraction									0					0	0		
Solid Fraction									1.000					1.000	1.000		

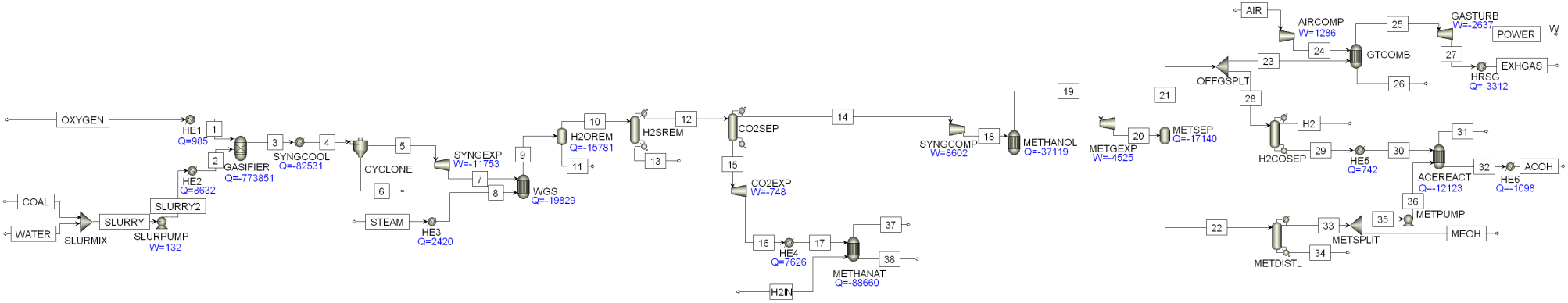

Q: Heat duty (kW)
W: Power (kW)

Figure A1.2: Coal polygeneration system with CO_2 reused into methanation (Case / Scheme B).

Table A1.2: Stream results for Case / Scheme B.

Stream No.	1	2	3	4	5	6	7	8	9	10	11	12	13	14	15	16	17	18
Phase	VAPOUR	MIXED	VAPOUR	VAPOUR	VAPOUR	SOLID	VAPOUR	VAPOUR	VAPOUR	VAPOUR	LIQUID	MIXED	VAPOUR	MIXED	VAPOUR	VAPOUR	VAPOUR	VAPOUR
Substream: MIXED																		
Mole Flow (kmol/s)																		
S	0	0.025	1.03E-07	1.03E-07	1.03E-07	0	1.03E-07	0	1.03E-07	2.29E-12	1.03E-07	0	2.29E-12	0	0	0	0	0
O_2	0.548	0.064	1.50E-12	1.50E-12	1.50E-12	0	1.50E-12	0	1.50E-12	1.50E-12	7.35E-17	1.50E-12	0	1.50E-12	0	0	0	1.50E-12
N_2	0.007	0.009	0.016	0.016	0.016	0	0.016	0	0.016	0.016	6.44E-07	0.016	0	0.016	0	0	0	0.016
H_2	0	0.537	0.664	0.664	0.664	0	0.664	0	1.115	1.115	3.76E-06	1.115	0	1.115	0	0	0	1.115
H_2O	0	0.571	0.420	0.420	0.420	0	0.420	0.046	0.015	0.011	0.004	0.011	0	0.011	0	0	0	0.011
CO	0	0	0.981	0.981	0.981	0	0.981	0	0.530	0.530	2.30E-05	0.530	0	0.530	0	0	0	0.530
CO_2	0	0	0.195	0.195	0.195	0	0.195	0	0.647	0.646	2.87E-04	0.646	0	0.006	0.640	0.640	0.640	0.006
H_2S	0	0	0.023	0.023	0.023	0	0.023	0	0.023	0.023	3.16E-05	0	0.023	0	0	0	0	0
C	0	1.179	2.78E-18	2.78E-18	2.78E-18	0	2.78E-18	0	0	0	0	0	0	0	0	0	0	0
CH_4	0	0	6.31E-04	6.31E-04	6.31E-04	0	6.31E-04	0	6.31E-04	6.31E-04	6.28E-08	6.31E-04	0	6.31E-04	0	0	0	6.31E-04
CH_3OH	0	0	9.57E-08	9.57E-08	9.57E-08	0	9.57E-08	0	9.57E-08	9.13E-08	4.43E-09	9.13E-08	0	9.13E-08	0	0	0	9.13E-08
Cl_2	0	2.58E-04	2.58E-04	2.58E-04	2.58E-04	0	2.58E-04	0	2.58E-04	2.58E-04	8.60E-07	0	2.58E-04	0	0	0	0	0
COS	0	0	0.002	0.002	0.002	0	0.002	0	0.002	0.002	3.24E-06	0	0.002	0	0	0	0	0
Ar	0.026	0	0.026	0.026	0.026	0	0.026	0	0.026	0.026	1.25E-06	0.026	0	0.026	0	0	0	0.026
CH_3COOH	0	0	3.12E-10	3.12E-10	3.12E-10	0	3.12E-10	0	3.12E-10	1.90E-10	1.22E-10	1.90E-10	0	1.90E-10	0	0	0	1.90E-10
Total Flow (kmol/s)	0.581	2.385	2.328	2.328	2.328	0	2.328	0.046	2.375	2.370	0.005	2.345	0.025	1.705	0.640	0.640	0.640	1.705
Total Flow (t/h)	67.5	103.1	170.6	170.6	170.6	0	170.6	3.000	173.6	173.3	0.329	170.1	3.219	68.7	101.4	101.4	101.4	68.7
Total Flow (m^3/s)	0.366	0.485	4.244	1.815	1.815	0	4.253	0.084	4.132	2.547	9.26E-05	2.521	0.027	1.830	0.688	1.036	15.2	0.700
Temperature (°C)	83.3	121.1	1371.1	430.0	430.0		276.0	270.0	250.0	50.0	50.0	50.0	50.0	50.0	50.0	19.0	300.0	220.5
Pressure (bar)	47.0	42.4	75.0	75.0	75.0		25.0	25.0	25.0	25.0	25.0	25.0	25.0	25.0	25.0	15.0	2.000	100.0
Vapor Fraction	1.000	0.256	1.000	1.000	1.000		1.000	1.000	1.000	1.000	0	1.000	1.000	0.999	1.000	1.000	1.000	1.000
Liquid Fraction	0	0.744	0	0	0		0	0	0	0	1.000	1.46E-05	0	0.001	0	0	0	0
Solid Fraction	0	0	0	0	0		0	0	0	0	0	0	0	0	0	0	0	0
Enthalpy (J/kg)	5.25E+04	2.09E+07	-3.75E+06	-5.44E+06	-5.44E+06		-5.68E+06	-1.30E+07	-6.22E+06	-6.53E+06	-1.45E+07	-6.64E+06	-7.47E+05	-3.29E+06	-8.92E+06	-8.95E+06	-8.68E+06	-2.83E+06
Entropy (J/kg-K)	-762.9	3.28E+04	3138.9	1630.8	1630.8		1681.8	-2796.4	1114.0	340.0	-7288.0	309.5	665.4	861.0	-470.8	-460.6	561.3	953.7
Density (kg/m^3)	51.2	59.1	11.2	26.1	26.1		11.1	9.973	11.7	18.9	987.1	18.7	33.5	10.4	41.0	27.2	1.847	27.3
Average Molecular Weight	32.3	12.0	20.4	20.4	20.4		20.4	18.0	20.3	20.3	19.8	20.1	36.0	11.2	44.0	44.0	44.0	11.2
Liquid Volumetric Flow 60°F (m^3/s)	0.031	0.052	0.110	0.110	0.110	0	0.110	8.35E-04	0.127	0.127	9.57E-05	0.125	0.001	0.091	0.034	0.034	0.034	0.091
Substream: TOTAL																		
Total Flow (t/h)	67.5	110.4	177.9	177.9	170.6	7.257	170.6	3.000	173.6	173.3	0.329	170.1	3.219	68.7	101.4	101.4	101.4	68.7
Enthalpy (kW)	985.5	5.97E+05	-1.76E+05	-2.59E+05	-2.58E+05	-895.9	-2.69E+05	-1.08E+04	-3.00E+05	-3.14E+05	-1326.5	-3.14E+05	-668.0	-6.27E+04	-2.51E+05	-2.52E+05	-2.44E+05	-5.41E+04
Substream: NCPSD																		
Mass Flow (t/h)																		
Ash	0	7.257	7.257	7.257	0	7.257	0	0	0	0	0	0	0	0	0	0	0	0
Mass Fraction																		
Ash	0	1.000	1.000	1.000	0	1.000	0	0	0	0	0	0	0	0	0	0	0	0
Total Flow (t/h)	0	7.257	7.257	7.257	0	7.257	0	0	0	0	0	0	0	0	0	0	0	0
Temperature (°C)		121.1	1371.1	430.0		430.0												
Pressure (bar)	47.0	42.4	75.0	75.0		75.0	25.0	25.0		25.0	25.0	25.0	25.0	25.0	25.0	15.0	2.000	100.0
Vapor Fraction		0	0	0		0												
Liquid Fraction		0	0	0		0												
Solid Fraction		1.000	1.000	1.000		1.000												

Table A1.2 (con't)

Stream No.	19	20	21	22	23	24	25	26	27	28	29	30	31	32	33	34	35	36
Phase	VAPOUR	MIXED	VAPOUR	LIQUID	VAPOUR	VAPOUR	VAPOUR		VAPOUR	VAPOUR	MIXED	VAPOUR	VAPOUR	LIQUID	LIQUID	MIXED	LIQUID	LIQUID
Substream: MIXED																		
Mole Flow (kmol/s)																		
S	0	0	0	0	0	0	0	0	0	0	0	0	0	0	0	0	0	0
O_2	1.50E-12	1.50E-12	1.47E-12	2.78E-14	1.47E-13	0.025	0.001	0	0.001	1.32E-12	1.32E-12	1.32E-12	1.28E-12	4.64E-14	0	2.78E-14	0	0
N_2	0.016	0.016	0.016	2.41E-04	0.002	0.095	0.096	0	0.096	0.014	0.014	0.014	0.014	4.55E-04	0	2.41E-04	0	0
H_2	0.349	0.349	0.348	4.14E-04	0.035	0	1.37E-07	0	1.37E-07	0.313	0	0	0	0	0	4.14E-04	0	0
H_2O	4.94E-04	4.94E-04	3.33E-06	4.90E-04	3.33E-07	0	0.035	0	0.035	3.00E-06	3.00E-06	3.00E-06	2.05E-07	2.79E-06	0	4.90E-04	0	0
CO	0.132	0.132	0.129	0.002	0.013	0	1.39E-07	0	1.39E-07	0.116	0.116	0.116	7.96E-10	2.76E-11	0	0.002	0	0
CO_2	0.017	0.017	0.014	0.003	0.001	0	0.014	0	0.014	0.013	0.013	0.013	0.011	0.002	0	0.003	0	0
H_2S	0	0	0	0	0	0	0	0	0	0	0	0	0	0	0	0	0	0
C	0	0	0	0	0	0	0	0	0	0	0	0	0	0	0	0	0	0
CH_4	6.31E-04	6.31E-04	6.07E-04	2.38E-05	6.07E-05	0	0	0	0	5.47E-04	5.47E-04	5.47E-04	5.14E-04	3.24E-05	0	2.38E-05	0	0
CH_3OH	0.388	0.388	0.008	0.381	7.84E-04	0	7.84E-04	0	7.84E-04	0.007	0.007	0.007	0.001	0.009	0.379	0.002	0.120	0.120
Cl_2	0	0	0	0	0	0	0	0	0	0	0	0	0	0	0	0	0	0
COS	0	0	0	0	0	0	0	0	0	0	0	0	0	0	0	0	0	0
Ar	0.026	0.026	0.026	4.70E-04	0.003	0	0.003	0	0.003	0.023	0.023	0.023	0.022	8.00E-04	0	4.70E-04	0	0
CH_3COOH	1.90E-10	1.90E-10	2.97E-13	1.90E-10	2.97E-14	0	2.97E-14	0	2.97E-14	2.67E-13	2.67E-13	2.67E-13	0.004	0.113	0	1.90E-10	0	0
Total Flow (kmol/s)	0.929	0.929	0.541	0.387	0.054	0.120	0.150	0	0.150	0.487	0.174	0.174	0.053	0.125	0.379	0.008	0.120	0.120
Total Flow (t/h)	68.7	68.7	24.0	44.7	2.403	12.5	14.9	0	14.9	21.6	19.4	19.4	7.378	25.8	43.7	0.991	13.8	13.8
Total Flow (m^3/s)	0.404	1.309	0.587	0.016	0.059	0.468	1.315	0	6.363	0.529	0.184	0.204	0.062	0.008	0.016	0.006	0.005	0.005
Temperature (°C)	250.0	136.8	40.0	40.0	40.0	383.9	1200.0		745.4	40.0	40.0	150.0	150.0	150.0	40.0	40.0	40.0	40.3
Pressure (bar)	100.0	24.0	24.0	24.0	24.0	14.0	14.0	14.0	2.000	24.0	24.0	30.0	30.0	30.0	24.0	24.0	24.0	30.0
Vapor Fraction	1.000	0.992	1.000	0	1.000	1.000	1.000		1.000	1.000	0.972	1.000	1.000	0	0	0.680	0	0
Liquid Fraction	0	0.008	0	1.000	0	0	0		0	0	0.028	0	0	1.000	1.000	0.320	1.000	1.000
Solid Fraction	0	0	0	0	0	0	0		0	0	0	0	0	0	0	0	0	0
Enthalpy (J/kg)	-4.78E+06	-5.02E+06	-3.18E+06	-7.39E+06	-3.18E+06	3.72E+05	-1.93E+06		-2.57E+06	-3.18E+06	-3.61E+06	-3.47E+06	-3.00E+06	-7.40E+06	-7.40E+06	-6.85E+06	-7.40E+06	-7.40E+06
Entropy (J/kg-K)	-2312.5	-2248.2	257.4	-7221.2	257.4	206.3	1115.5		1187.0	257.4	1150.1	1477.5	-602.7	-3894.6	-7362.5	-1445.1	-7362.5	-7359.9
Density (kg/m^3)	47.3	14.6	11.4	772.8	11.4	7.393	3.141		0.649	11.4	29.3	26.3	33.1	870.5	774.8	43.8	774.8	774.5
Average Molecular Weight	20.6	20.6	12.3	32.1	12.3	28.9	27.5		27.5	12.3	30.9	30.9	38.8	57.5	32.0	32.8	32.0	32.0
Liquid Volumetric Flow 60°F (m^3/s)	0.045	0.045	0.029	0.016	0.003	0.006	0.007	0	0.007	0.026	0.009	0.009	0.003	0.007	0.015	4.06E-04	0.005	0.005
Substream: TOTAL																		
Total Flow (t/h)	68.7	68.7	24.0	44.7	2.403	12.5	14.9	0	14.9	21.6	19.4	19.4	7.378	25.8	43.7	0.991	13.8	13.8
Enthalpy (kW)	-9.12E+04	-9.57E+04	-2.12E+04	-9.16E+04	-2123.1	1286.4	-7975.0	0	-1.06E+04	-1.91E+04	-1.94E+04	-1.87E+04	-6149.9	-5.31E+04	-8.98E+04	-1886.7	-2.84E+04	-2.84E+04
Substream: NCPSD																		
Mass Flow (t/h)																		
Ash	0	0	0	0	0	0	0	0	0	0	0	0	0	0	0	0	0	0
Mass Fraction																		
Ash	0	0	0	0	0	0	0	0	0	0	0	0	0	0	0	0	0	0
Total Flow (t/h)	0	0	0	0	0	0	0	0	0	0	0	0	0	0	0	0	0	0
Temperature (°C)																		
Pressure (bar)		24.0	24.0	24.0	24.0	14.0			2.000	24.0	24.0	30.0			24.0	24.0	24.0	30.0
Vapor Fraction																		
Liquid Fraction																		
Solid Fraction																		

Table A1.2 (con't)

Stream No.	37	38	ACOH	AIR	COAL	EXHGAS	H2	H2IN	MEOH	OXYGEN	SLURRY	SLURRY2	STEAM	WATER
Phase	VAPOUR		LIQUID	VAPOUR	MIXED	VAPOUR	VAPOUR	VAPOUR	LIQUID	VAPOUR	LIQUID	LIQUID	LIQUID	LIQUID
Substream: MIXED														
Mole Flow (kmol/s)														
S	0	0	0	0	0.025	0	0	0	0	0	0.025	0.025	0	0
O_2	0	0	4.64E-14	0.025	0.064	0.001	0	0	0	0.548	0.064	0.064	0	0
N_2	0	0	4.55E-04	0.095	0.009	0.096	0	0	0	0.007	0.009	0.009	0	0
H_2	0.100	0	0	0	0.537	1.37E-07	0.313	2.560	0	0	0.537	0.537	0	0
H_2O	1.230	0	2.79E-06	0	0.155	0.035	0	0	0	0	0.571	0.571	0.046	0.417
CO	0	0	2.76E-11	0	0	1.39E-07	0	0	0	0	0	0	0	0
CO_2	0.025	0	0.002	0	0	0.014	0	0	0	0	0	0	0	0
H_2S	0	0	0	0	0	0	0	0	0	0	0	0	0	0
C	0	0	0	0	1.179	0	0	0	0	0	1.179	1.179	0	0
CH_4	0.615	0	3.24E-05	0	0	0	0	0	0	0	0	0	0	0
CH_3OH	0	0	0.009	0	0	7.84E-04	0	0	0.259	0	0	0	0	0
Cl_2	0	0	0	0	2.58E-04	0	0	0	0	0	2.58E-04	2.58E-04	0	0
COS	0	0	0	0	0	0	0	0	0	0	0	0	0	0
Ar	0	0	8.00E-04	0	0	0.003	0	0	0	0.026	0	0	0	0
CH_3COOH	0	0	0.113	0	0	2.97E-14	0	0	0	0	0	0	0	0
Total Flow (kmol/s)	1.970	0	0.125	0.120	1.968	0.150	0.313	2.560	0.259	0.581	2.385	2.385	0.046	0.417
Total Flow (t/h)	120.0	0	25.8	12.5	76.1	14.9	2.274	18.6	29.8	67.5	103.1	103.1	3.000	27.0
Total Flow (m^3/s)	46.9	0	0.007	2.937	15.0	4.662	0.340	63.5	0.011	14.2	0.029	0.029	8.39E-04	0.008
Temperature (°C)	300.0		30.0	25.0	25.0	100.0	40.0	25.0	40.0	25.0	26.2	27.7	25.0	25.0
Pressure (bar)	2.000	2.000	30.0	1.013	1.013	1.000	24.0	1.000	24.0	1.013	1.000	42.4	1.013	1.013
Vapor Fraction	1.000		0	1.000	0.311	1.000	1.000	1.000	0	1.000	0	0	0	0
Liquid Fraction	0		1.000	0	0.689	0	0	0	1.000	0	1.000	1.000	1.000	1.000
Solid Fraction	0		0	0	0	0	0	0	0	0	0	0	0	0
Enthalpy (J/kg)	-9.99E+06		-7.55E+06	1.77E-10	3.35E+07	-3.37E+06	2.14E+05	1.85E-09	-7.40E+06	-1.05E-10	2.06E+07	2.06E+07	-1.59E+07	-1.59E+07
Entropy (J/kg-K)	-1614.1		-4067.9	148.2	6.21E+04	166.3	-1.24E+04	54.3	-7362.5	63.6	4.22E+04	4.20E+04	-9030.5	-9030.5
Density (kg/m^3)	0.710		1041.0	1.179	1.411	0.886	1.858	0.081	774.8	1.320	999.2	998.2	993.5	993.5
Average Molecular Weight	16.9		57.5	28.9	10.7	27.5	2.016	2.016	32.0	32.3	12.0	12.0	18.0	18.0
Liquid Volumetric Flow 60°F (m^3/s)	0.062	0	0.007	0.006	0.045	0.007	0.017	0.137	0.010	0.031	0.052	0.052	8.35E-04	0.008
Substream: TOTAL														
Total Flow (t/h)	120.0	0	25.8	12.5	83.3	14.9	2.274	18.6	29.8	67.5	110.4	110.4	3.000	27.0
Enthalpy (kW)	-3.33E+05	0	-5.42E+04	6.12E-13	7.07E+05	-1.39E+04	135.5	9.54E-12	-6.13E+04	-1.97E-12	5.88E+05	5.88E+05	-1.32E+04	-1.19E+05
Substream: NCPSD														
Mass Flow (t/h)														
Ash	0	0	0	0	7.257	0	0	0	0	0	7.257	7.257	0	0
Mass Fraction														
Ash	0	0	0	0	1.000	0	0	0	0	0	1.000	1.000	0	0
Total Flow (t/h)	0	0	0	0	7.257	0	0	0	0	0	7.257	7.257	0	0
Temperature (°C)					25.0						26.2	27.7		
Pressure (bar)			30.0	1.013	1.013	1.000	24.0	1.000	24.0	1.013	1.000	42.4	1.013	1.013
Vapor Fraction					0						0	0		
Liquid Fraction					0						0	0		
Solid Fraction					1.000						1.000	1.000		

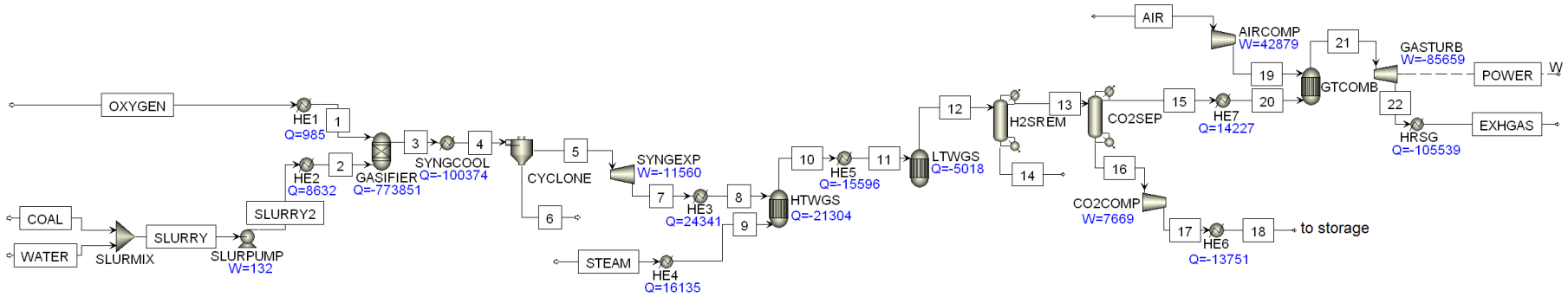

Q: Heat duty (kW)
W: Power (kW)

Figure A1.3: Coal IGCC system with CCS (Case / Scheme C).

Table A1.3: Stream results for Case / Scheme C.

Stream No.	1	2	3	4	5	6	7	8	9	10	11	12	13	14	15
Phase	VAPOUR	MIXED	VAPOUR	VAPOUR	VAPOUR	SOLID	MIXED	VAPOUR	VAPOUR	VAPOUR	VAPOUR	VAPOUR	VAPOUR	VAPOUR	VAPOUR
Substream: MIXED															
Mole Flow (kmol/s)															
S	0	0.025	1.03E-07	1.03E-07	1.03E-07	0	1.03E-07	1.03E-07	0	1.03E-07	1.03E-07	1.03E-07	0	1.03E-07	0
O_2	0.548	0.064	1.50E-12	1.50E-12	1.50E-12	0	1.50E-12	1.50E-12	0	1.50E-12	1.50E-12	1.50E-12	1.50E-12	0	1.50E-12
N_2	0.007	0.009	0.016	0.016	0.016	0	0.016	0.016	0	0.016	0.016	0.016	0.016	0	0.016
H_2	0	0.537	0.664	0.664	0.664	0	0.664	0.664	0	1.248	1.248	1.373	1.373	0	1.373
H_2O	0	0.571	0.420	0.420	0.420	0	0.420	0.420	0.308	0.145	0.145	0.019	0.019	0	0.019
CO	0	0	0.981	0.981	0.981	0	0.981	0.981	0	0.398	0.398	0.272	0.272	0	0.272
CO_2	0	0	0.195	0.195	0.195	0	0.195	0.195	0	0.779	0.779	0.905	0.905	0	0.009
H_2S	0	0	0.023	0.023	0.023	0	0.023	0.023	0	0.023	0.023	0.023	0	0.023	0
C	0	1.179	2.78E-18	2.78E-18	2.78E-18	0	2.78E-18	2.78E-18	0	0	0	0	0	0	0
CH_4	0	0	6.31E-04	6.31E-04	6.31E-04	0	6.31E-04	6.31E-04	0	6.31E-04	6.31E-04	6.31E-04	6.31E-04	0	6.31E-04
Cl_2	0	2.58E-04	2.58E-04	2.58E-04	2.58E-04	0	2.58E-04	2.58E-04	0	2.58E-04	2.58E-04	2.58E-04	0	2.58E-04	0
COS	0	0	0.002	0.002	0.002	0	0.002	0.002	0	0.002	0.002	0.002	0	0.002	0
Ar	0.026	0	0.026	0.026	0.026	0	0.026	0.026	0	0.026	0.026	0.026	0.026	0	0.026
Total Flow (kmol/s)	0.581	2.385	2.328	2.328	2.328	0	2.328	2.328	0.308	2.637	2.637	2.637	2.612	0.025	1.716
Total Flow (t/h)	67.5	103.1	170.6	170.6	170.6	0	170.6	170.6	20.0	190.6	190.6	190.6	187.4	3.224	45.5
Total Flow (m^3/s)	0.366	0.485	4.244	1.221	1.221	0	4.755	8.301	0.557	9.400	4.149	6.916	6.850	0.065	4.502
Temperature (°C)	83.3	121.1	1371.1	200.0	200.0		119.1	370.0	270.0	370.0	200.0	200.0	200.0	200.0	200.0
Pressure (bar)	47.0	42.4	75.0	75.0	75.0		15.0	15.0	25.0	15.0	25.0	15.0	15.0	15.0	15.0
Vapor Fraction	1.000	0.256	1.000	1.000	1.000		0.939	1.000	1.000	1.000	1.000	1.000	1.000	1.000	1.000
Liquid Fraction	0	0.744	0	0	0		0.061	0	0	0	0	0	0	0	0
Solid Fraction	0	0	0	0	0		0	0	0	0	0	0	0	0	0
Enthalpy (J/kg)	5.25E+04	2.09E+07	-3.75E+06	-5.80E+06	-5.80E+06		-6.05E+06	-5.53E+06	-1.30E+07	-6.71E+06	-7.01E+06	-7.10E+06	-7.21E+06	-5.96E+05	-2.34E+06
Entropy (J/kg-K)	-762.9	3.28E+04	3138.9	999.3	999.3		1068.5	2143.1	-2796.4	1314.2	571.5	615.1	583.2	1165.4	1381.7
Density (kg/m^3)	51.2	59.1	11.2	38.8	38.8		9.968	5.710	9.973	5.633	12.8	7.657	7.599	13.7	2.809
Average Molecular Weight	32.3	12.0	20.4	20.4	20.4		20.4	20.4	18.0	20.1	20.1	20.1	19.9	36.0	7.367
Liquid Volumetric Flow 60°F (m^3/s)	0.031	0.052	0.110	0.110	0.110	0	0.110	0.110	0.006	0.136	0.136	0.141	0.139	0.001	0.091
Substream: TOTAL															
Total Flow (t/h)	67.5	110.4	177.9	177.9	170.6	7.257	170.6	170.6	20.0	190.6	190.6	190.6	187.4	3.224	45.5
Enthalpy (kW)	985.5	5.97E+05	-1.76E+05	-2.76E+05	-2.75E+05	-1330.9	-2.87E+05	-2.62E+05	-7.20E+04	-3.56E+05	-3.71E+05	-3.76E+05	-3.76E+05	-534.2	-2.96E+04
Substream: NCPSD															
Mass Flow (t/h)															
Ash	0	7.257	7.257	7.257	0	7.257	0	0	0	0	0	0	0	0	0
Mass Fraction															
Ash	0	1.000	1.000	1.000	0	1.000	0	0	0	0	0	0	0	0	0
Total Flow (t/h)	0	7.257	7.257	7.257	0	7.257	0	0	0	0	0	0	0	0	0
Temperature (°C)		121.1	1371.1	200.0		200.0									
Pressure (bar)	47.0	42.4	75.0	75.0		75.0	15.0	15.0	25.0		25.0		15.0	15.0	15.0
Vapor Fraction		0	0	0		0									
Liquid Fraction		0	0	0		0									
Solid Fraction		1.000	1.000	1.000		1.000									

Table A1.3 (con't)

Stream No.	16	17	18	19	20	21	22	AIR	COAL	EXHGAS	OXYGEN	SLURRY	SLURRY2	STEAM
Phase	VAPOUR	VAPOUR	VAPOUR	VAPOUR	VAPOUR	VAPOUR	VAPOUR	VAPOUR	MIXED	VAPOUR	VAPOUR	LIQUID	LIQUID	LIQUID
Substream: MIXED														
Mole Flow (kmol/s)														
S	0	0	0	0	0	0	0	0	0.025	0	0	0.025	0.025	0
O_2	0	0	0	0.840	1.50E-12	0.016	0.016	0.840	0.064	0.016	0.548	0.064	0.064	0
N_2	0	0	0	3.160	0.016	3.176	3.176	3.160	0.009	3.176	0.007	0.009	0.009	0
H_2	0	0	0	0	1.373	8.52E-06	8.52E-06	0	0.537	8.52E-06	0	0.537	0.537	0
H_2O	0	0	0	0	0.019	1.394	1.394	0	0.155	1.394	0	0.571	0.571	0.308
CO	0	0	0	0	0.272	4.25E-06	4.25E-06	0	0	4.25E-06	0	0	0	0
CO_2	0.896	0.896	0.896	0	0.009	0.282	0.282	0	0	0.282	0	0	0	0
H_2S	0	0	0	0	0	0	0	0	0	0	0	0	0	0
C	0	0	0	0	0	0	0	0	1.179	0	0	1.179	1.179	0
CH_4	0	0	0	0	6.31E-04	0	0	0	0	0	0	0	0	0
CH_3OH	0	0	0	0	9.57E-08	9.57E-08	9.57E-08	0	0	9.57E-08	0	0	0	0
Cl_2	0	0	0	0	0	0	0	0	2.58E-04	0	0	2.58E-04	2.58E-04	0
COS	0	0	0	0	0	0	0	0	0	0	0	0	0	0
Ar	0	0	0	0	0.026	0.026	0.026	0	0	0.026	0.026	0	0	0
CH_3COOH	0	0	0	0	3.12E-10	3.12E-10	3.12E-10	0	0	3.12E-10	0	0	0	0
Total Flow (kmol/s)	0.896	0.896	0.896	4.000	1.716	4.894	4.894	4.000	1.968	4.894	0.581	2.385	2.385	0.308
Total Flow (t/h)	141.9	141.9	141.9	415.4	45.5	461.0	461.0	415.4	76.1	461.0	67.5	103.1	103.1	20.0
Total Flow (m^3/s)	2.349	0.612	0.287	15.6	4.299	42.8	206.2	97.9	15.0	151.8	14.2	0.029	0.029	0.006
Temperature (°C)	200.0	384.9	35.0	383.9	480.0	1200.0	740.2	25.0	25.0	100.0	25.0	26.2	27.7	25.0
Pressure (bar)	15.0	80.0	80.0	14.0	25.0	14.0	2.000	1.013	1.013	1.000	1.013	1.000	42.4	1.013
Vapor Fraction	1.000	1.000	1.000	1.000	1.000	1.000	1.000	1.000	0.311	1.000	1.000	0	0	0
Liquid Fraction	0	0	0	0	0	0	0	0	0.689	0	0	1.000	1.000	1.000
Solid Fraction	0	0	0	0	0	0	0	0	0	0	0	0	0	0
Enthalpy (J/kg)	-8.78E+06	-8.58E+06	-8.93E+06	3.72E+05	-1.22E+06	-1.92E+06	-2.59E+06	1.77E-10	3.35E+07	-3.41E+06	-1.05E-10	2.06E+07	2.06E+07	-1.59E+07
Entropy (J/kg-K)	-16.6	13.4	-731.7	206.3	2671.9	1037.4	1112.7	148.2	6.21E+04	63.6	63.6	4.22E+04	4.20E+04	-9030.5
Density (kg/m^3)	16.8	64.3	137.4	7.393	2.941	2.991	0.621	1.179	1.411	0.843	1.320	999.2	998.2	993.5
Average Molecular Weight	44.0	44.0	44.0	28.9	7.367	26.2	26.2	28.9	10.7	26.2	32.3	12.0	12.0	18.0
Liquid Volumetric Flow 60°F (m^3/s)	0.048	0.048	0.048	0.214	0.091	0.213	0.213	0.214	0.045	0.213	0.031	0.052	0.052	0.006
Substream: TOTAL														
Total Flow (t/h)	141.9	141.9	141.9	415.4	45.5	461.0	461.0	415.4	83.3	461.0	67.5	110.4	110.4	20.0
Enthalpy (kW)	-3.46E+05	-3.38E+05	-3.52E+05	4.29E+04	-1.54E+04	-2.45E+05	-3.31E+05	2.04E-11	7.07E+05	-4.37E+05	-1.97E-12	5.88E+05	5.88E+05	-8.81E+04
Substream: NCPSD														
Mass Flow (t/h)														
Ash	0	0	0	0	0	0	0	0	7.257	0	0	7.257	7.257	0
Mass Fraction														
Ash	0	0	0	0	0	0	0	0	1.000	0	0	1.000	1.000	0
Total Flow (t/h)	0	0	0	0	0	0	0	0	7.257	0	0	7.257	7.257	0
Temperature (°C)									25.0			26.2	27.7	
Pressure (bar)	15.0	80.0	80.0	14.0	25.0		2.000	1.013	1.013	1.000	1.013	1.000	42.4	1.013
Vapor Fraction									0			0	0	
Liquid Fraction									0			0	0	
Solid Fraction									1.000			1.000	1.000	

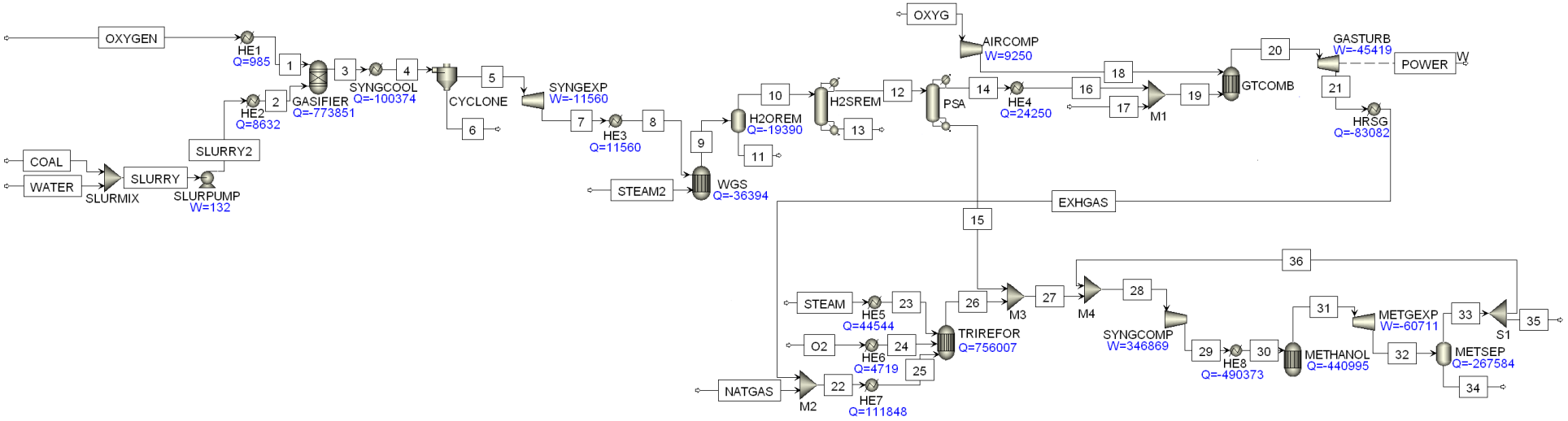

Q: Heat duty (kW)
W: Power (kW)

Figure A1.4: Coal polygeneration system with tri-reforming and methanol synthesis (Case / Scheme D).

Table A1.4: Stream results for Case / Scheme D.

Stream No.	1	2	3	4	5	6	7	8	9	10	11	12	13	14	15	16	17
Phase	VAPOUR	MIXED	VAPOUR	VAPOUR	VAPOUR	SOLID	MIXED	VAPOUR	VAPOUR	VAPOUR	LIQUID	MIXED	VAPOUR	MIXED	VAPOUR	VAPOUR	VAPOUR
Substream: MIXED																	
Mole Flow (kmol/s)																	
S	0	0.025	1.03E-07	1.03E-07	1.03E-07	0	1.03E-07	1.03E-07	1.03E-07	5.34E-14	1.03E-07	0	5.34E-14	0	0	0	0
O_2	0.548	0.064	1.50E-12	1.50E-12	1.50E-12	0	1.50E-12	1.50E-12	1.50E-12	1.50E-12	7.09E-16	1.50E-12	0	1.50E-12	0	1.50E-12	0
N_2	0.007	0.009	0.016	0.016	0.016	0	0.016	0.016	0.016	0.016	6.03E-06	0.016	0	0.016	0	0.016	0
H_2	0	0.537	0.664	0.664	0.664	0	0.664	0.664	1.550	1.550	4.21E-05	1.550	0	0.031	1.519	0.031	0
H_2O	0	0.571	0.420	0.420	0.420	0	0.420	0.420	0.074	0.007	0.067	0.007	0	0.007	0	0.007	0
CO	0	0	0.981	0.981	0.981	0	0.981	0.981	0.096	0.096	3.92E-05	0.096	0	0.096	0	0.096	0
CO_2	0	0	0.195	0.195	0.195	0	0.195	0.195	1.081	1.075	0.006	1.075	0	1.075	0	1.075	0
H_2S	0	0	0.023	0.023	0.023	0	0.023	0.023	0.023	0.023	3.91E-04	0	0.023	0	0	0	0
C	0	1.179	2.78E-18	2.78E-18	2.78E-18	0	2.78E-18	2.78E-18	0	0	0	0	0	0	0	0	0
CH_4	0	0	6.31E-04	6.31E-04	6.31E-04	0	6.31E-04	6.31E-04	6.31E-04	6.31E-04	6.32E-07	6.31E-04	0	6.31E-04	0	6.31E-04	0.400
CH_3OH	0	0	9.57E-08	9.57E-08	9.57E-08	0	9.57E-08	9.57E-08	9.57E-08	4.59E-08	4.98E-08	4.59E-08	0	4.59E-08	0	4.59E-08	0
Cl_2	0	2.58E-04	2.58E-04	2.58E-04	2.58E-04	0	2.58E-04	2.58E-04	2.58E-04	2.48E-04	1.09E-05	0	2.48E-04	0	0	0	0
COS	0	0	0.002	0.002	0.002	0	0.002	0.002	0.002	0.001	4.00E-05	0	0.001	0	0	0	0
Ar	0.026	0	0.026	0.026	0.026	0	0.026	0.026	0.026	0.026	1.19E-05	0.026	0	0.026	0	0.026	0
CH_3COOH	0	0	3.12E-10	3.12E-10	3.12E-10	0	3.12E-10	3.12E-10	3.12E-10	2.04E-11	2.91E-10	2.04E-11	0	2.04E-11	0	2.04E-11	0
Total Flow (kmol/s)	0.581	2.385	2.328	2.328	2.328	0	2.328	2.328	2.868	2.795	0.073	2.771	0.024	1.252	1.519	1.252	0.400
Total Flow (t/h)	67.5	103.1	170.6	170.6	170.6	0	170.6	170.6	205.6	200.3	5.313	197.2	3.165	186.1	11.0	186.1	23.1
Total Flow (m^3/s)	0.366	0.485	4.244	1.221	1.221	0	4.755	6.107	7.522	4.697	0.001	4.656	0.041	2.095	2.552	3.136	9.916
Temperature (°C)	83.3	121.1	1371.1	200.0	200.0		119.1	200.0	200.0	30.0	30.0	30.0	30.0	30.0	30.0	480.0	25.0
Pressure (bar)	47.0	42.4	75.0	75.0	75.0		15.0	15.0	15.0	15.0	15.0	15.0	15.0	15.0	15.0	25.0	1.000
Vapor Fraction	1.000	0.256	1.000	1.000	1.000		0.939	1.000	1.000	1.000	0	1.000	1.000	0.996	1.000	1.000	1.000
Liquid Fraction	0	0.744	0	0	0		0.061	0	0	0	1.000	8.37E-06	0	0.004	0	0	0
Solid Fraction	0	0	0	0	0		0	0	0	0	0	0	0	0	0	0	0
Enthalpy (J/kg)	5.25E+04	2.09E+07	-3.75E+06	-5.80E+06	-5.80E+06		-6.05E+06	-5.80E+06	-7.66E+06	-7.83E+06	-1.45E+07	-7.95E+06	-7.65E+05	-8.42E+06	7.14E+04	-7.95E+06	-4.65E+06
Entropy (J/kg-K)	-762.9	3.28E+04	3138.9	999.3	999.3		1068.5	1656.6	247.7	-481.8	-7329.6	-522.5	720.9	-203.5	-1.09E+04	628.2	-5017.1
Density (kg/m^3)	51.2	59.1	11.2	38.8	38.8		9.968	7.762	7.594	11.8	1020.1	11.8	21.4	24.7	1.200	16.5	0.647
Average Molecular Weight	32.3	12.0	20.4	20.4	20.4		20.4	20.4	19.9	19.9	20.2	19.8	36.0	41.3	2.016	41.3	16.0
Liquid Volumetric Flow 60°F (m^3/s)	0.031	0.052	0.110	0.110	0.110	0	0.110	0.110	0.151	0.149	0.002	0.148	0.001	0.067	0.081	0.067	0.021
Substream: TOTAL																	
Total Flow (t/h)	67.5	110.4	177.9	177.9	170.6	7.257	170.6	170.6	205.6	200.3	5.313	197.2	3.165	186.1	11.0	186.1	23.1
Enthalpy (kW)	985.5	5.97E+05	-1.76E+05	-2.76E+05	-2.75E+05	-1330.9	-2.87E+05	-2.75E+05	-4.38E+05	-4.36E+05	-2.13E+04	-4.35E+05	-672.8	-4.36E+05	218.6	-4.11E+05	-2.98E+04
Substream: NCPSD																	
Mass Flow (t/h)																	
Ash	0	7.257	7.257	7.257	0	7.257	0	0	0	0	0	0	0	0	0	0	0
Mass Fraction																	
Ash	0	1.000	1.000	1.000	0	1.000	0	0	0	0	0	0	0	0	0	0	0
Total Flow (t/h)	0	7.257	7.257	7.257	0	7.257	0	0	0	0	0	0	0	0	0	0	0
Temperature (°C)		121.1	1371.1	200.0		200.0											
Pressure (bar)	47.0	42.4	75.0	75.0		75.0	15.0	15.0		15.0	15.0	15.0	15.0	15.0	15.0	25.0	1.000
Vapor Fraction		0	0	0		0											
Liquid Fraction		0	0	0		0											
Solid Fraction		1.000	1.000	1.000		1.000											

Table A1.4 (con't)

Stream No.	18	19	20	21	22	23	24	25	26	27	28	29	30	31	32	33	34
Phase	VAPOUR	VAPOUR	VAPOUR	VAPOUR	VAPOUR	VAPOUR	VAPOUR	VAPOUR	VAPOUR	VAPOUR	VAPOUR	VAPOUR	VAPOUR	VAPOUR	VAPOUR	VAPOUR	LIQUID
Substream: MIXED																	
Mole Flow (kmol/s)																	
S	0	0	0	0	0	0	0	0	0	0	0	0	0	0	0	0	0
O_2	0.870	1.50E-12	0.005	0.005	0.005	0	0.331	0.005	0	0	0	0	0	0	0	0	0
N_2	0	0.016	0.016	0.016	0.016	0	0	0.016	0.016	0.016	0.272	0.272	0.272	0.272	0.272	0.270	0.002
H_2	0	0.031	6.24E-06	6.24E-06	6.24E-06	0	0	6.24E-06	7.691	9.210	17.9	17.9	17.9	9.195	9.195	9.189	0.006
H_2O	0	0.007	0.839	0.839	0.839	0.732	0	0.839	0.369	0.369	0.371	0.371	0.371	0.245	0.245	0.002	0.243
CO	0	0.096	2.88E-05	2.88E-05	2.88E-05	0	0	2.88E-05	4.613	4.613	5.450	5.450	5.450	0.889	0.889	0.881	0.008
CO_2	0	1.075	1.572	1.572	1.572	0	0	1.572	0.203	0.203	2.012	2.012	2.012	2.137	2.137	1.904	0.233
H_2S	0	0	0	0	0	0	0	0	0	0	0	0	0	0	0	0	0
C	0	0	0	0	0	0	0	0	0	0	0	0	0	0	0	0	0
CH_4	0	0.401	0	0	3.309	0	0	3.309	0.065	0.065	0.912	0.912	0.912	0.912	0.912	0.892	0.020
CH_3OH	0	4.59E-08	4.59E-08	4.59E-08	4.59E-08	0	0	4.59E-08	4.59E-08	4.59E-08	0.106	0.106	0.106	4.541	4.541	0.111	4.429
Cl_2	0	0	0	0	0	0	0	0	0	0	0	0	0	0	0	0	0
COS	0	0	0	0	0	0	0	0	0	0	0	0	0	0	0	0	0
Ar	0	0.026	0.026	0.026	0.026	0	0	0.026	0.026	0.026	0.441	0.441	0.441	0.441	0.441	0.436	0.004
Total Flow (kmol/s)	0.870	1.652	2.459	2.459	5.768	0.732	0.331	5.768	13.0	14.5	27.5	27.5	27.5	18.6	18.6	13.7	4.947
Total Flow (t/h)	100.2	209.2	309.5	309.5	500.6	47.5	38.1	500.6	586.2	597.2	1178.2	1178.2	1178.2	1178.2	1178.2	611.6	566.6
Total Flow (m^3/s)	3.323	5.913	21.5	114.5	158.6	1.177	20.7	361.2	1212.4	1259.5	78.6	24.3	12.0	8.104	17.0	14.4	0.198
Temperature (°C)	370.0	372.5	1200.0	847.3	57.5	500.0	480.0	480.0	850.0	771.4	414.3	791.7	250.0	250.0	165.9	30.0	30.0
Pressure (bar)	14.0	15.0	14.0	2.000	1.000	40.0	1.000	1.000	1.000	1.000	20.0	100.0	100.0	100.0	40.0	24.0	24.0
Vapor Fraction	1.000	1.000	1.000	1.000	1.000	1.000	1.000	1.000	1.000	1.000	1.000	1.000	1.000	1.000	1.000	1.000	0
Liquid Fraction	0	0	0	0	0	0	0	0	0	0	0	0	0	0	0	0	1.000
Solid Fraction	0	0	0	0	0	0	0	0	0	0	0	0	0	0	0	0	0
Enthalpy (J/kg)	3.32E+05	-7.59E+06	-7.98E+06	-8.51E+06	-7.63E+06	-1.25E+07	4.46E+05	-6.83E+06	-2.17E+06	-2.13E+06	-3.79E+06	-2.73E+06	-4.23E+06	-5.58E+06	-5.76E+06	-5.50E+06	-7.75E+06
Entropy (J/kg-K)	53.1	150.1	1205.5	1258.8	-1647.5	-2289.3	901.4	-121.6	6224.2	6299.9	2038.7	2140.0	185.8	-2115.7	-2068.2	-1339.2	-6960.5
Density (kg/m^3)	8.378	9.830	3.996	0.751	0.877	11.2	0.511	0.385	0.134	0.132	4.164	13.4	27.4	40.4	19.2	11.8	796.7
Average Molecular Weight	32.0	35.2	35.0	35.0	24.1	18.0	32.0	24.1	12.5	11.4	11.9	11.9	11.9	17.6	17.6	12.4	31.8
Liquid Volumetric Flow 60°F (m^3/s)	0.047	0.088	0.102	0.102	0.279	0.013	0.018	0.279	0.682	0.764	1.458	1.458	1.458	0.929	0.929	0.731	0.198
Substream: TOTAL																	
Total Flow (t/h)	100.2	209.2	309.5	309.5	500.6	47.5	38.1	500.6	586.2	597.2	1178.2	1178.2	1178.2	1178.2	1178.2	611.6	566.6
Enthalpy (kW)	9249.7	-4.41E+05	-6.86E+05	-7.32E+05	-1.06E+06	-1.65E+05	4719.3	-9.49E+05	-3.53E+05	-3.53E+05	-1.24E+06	-8.93E+05	-1.38E+06	-1.82E+06	-1.89E+06	-9.34E+05	-1.22E+06
Substream: NCPSD																	
Mass Flow (t/h)																	
Ash	0	0	0	0	0	0	0	0	0	0	0	0	0	0	0	0	0
Mass Fraction																	
Ash	0	0	0	0	0	0	0	0	0	0	0	0	0	0	0	0	0
Total Flow (t/h)	0	0	0	0	0	0	0	0	0	0	0	0	0	0	0	0	0
Temperature (°C)																	
Pressure (bar)	14.0	15.0		2.000	1.000	40.0	1.000	1.000		1.000	20.0	100.0	100.0		40.0	24.0	24.0
Vapor Fraction																	
Liquid Fraction																	
Solid Fraction																	

Table A1.4 (con't)

Stream No.	35	36	COAL	EXHGAS	NATGAS	O2	OXYG	OXYGEN	SLURRY	SLURRY2	STEAM	STEAM2	WATER
Phase	VAPOUR	VAPOUR	MIXED	VAPOUR	VAPOUR	VAPOUR	VAPOUR	VAPOUR	LIQUID	LIQUID	LIQUID	VAPOUR	LIQUID
Substream: MIXED													
Mole Flow (kmol/s)													
S	0	0	0.025	0	0	0	0	0	0.025	0.025	0	0	0
O_2	0	0	0.064	0.005	0	0.331	0.870	0.548	0.064	0.064	0	0	0
N_2	0.013	0.256	0.009	0.016	0	0	0	0.007	0.009	0.009	0	0	0
H_2	0.459	8.729	0.537	6.24E-06	0	0	0	0	0.537	0.537	0	0	0
H_2O	8.75E-05	0.002	0.155	0.839	0	0	0	0	0.571	0.571	0.732	0.540	0.417
CO	0.044	0.837	0	2.88E-05	0	0	0	0	0	0	0	0	0
CO_2	0.095	1.808	0	1.572	0	0	0	0	0	0	0	0	0
H_2S	0	0	0	0	0	0	0	0	0	0	0	0	0
C	0	0	1.179	0	0	0	0	0	1.179	1.179	0	0	0
CH_4	0.045	0.847	0	0	3.309	0	0	0	0	0	0	0	0
CH_3OH	0.006	0.106	0	4.59E-08	0	0	0	0	0	0	0	0	0
Cl_2	0	0	2.58E-04	0	0	0	0	0	2.58E-04	2.58E-04	0	0	0
COS	0	0	0	0	0	0	0	0	0	0	0	0	0
Ar	0.022	0.414	0	0.026	0	0	0	0.026	0	0	0	0	0
Total Flow (kmol/s)	0.684	13.0	1.968	2.459	3.309	0.331	0.870	0.581	2.385	2.385	0.732	0.540	0.417
Total Flow (t/h)	30.6	581.0	76.1	309.5	191.1	38.1	100.2	67.5	103.1	103.1	47.5	35.0	27.0
Total Flow (m^3/s)	0.719	13.7	15.0	76.3	82.0	8.205	21.3	14.2	0.029	0.029	0.013	1.677	0.008
Temperature (°C)	30.0	30.0	25.0	100.0	25.0	25.0	25.0	25.0	26.2	27.7	25.0	250.0	25.0
Pressure (bar)	24.0	24.0	1.013	1.000	1.000	1.000	1.013	1.013	1.000	42.4	1.000	14.0	1.013
Vapor Fraction	1.000	1.000	0.311	1.000	1.000	1.000	1.000	1.000	0	0	0	1.000	0
Liquid Fraction	0	0	0.689	0	0	0	0	0	1.000	1.000	1.000	0	1.000
Solid Fraction	0	0	0	0	0	0	0	0	0	0	0	0	0
Enthalpy (J/kg)	-5.50E+06	-5.50E+06	3.35E+07	-9.48E+06	-4.65E+06	-1.16E-10	-1.16E-10	-1.05E-10	2.06E+07	2.06E+07	-1.59E+07	-1.30E+07	-1.59E+07
Entropy (J/kg-K)	-1339.2	-1339.2	6.21E+04	37.4	-5017.1	3.420	0.064	63.6	4.22E+04	4.20E+04	-9030.5	-2602.9	-9030.5
Density (kg/m^3)	11.8	11.8	1.411	1.127	0.647	1.291	1.308	1.320	999.2	998.2	993.5	5.798	993.5
Average Molecular Weight	12.4	12.4	10.7	35.0	16.0	32.0	32.0	32.3	12.0	12.0	18.0	18.0	18.0
Liquid Volumetric Flow 60°F (m^3/s)	0.037	0.695	0.045	0.102	0.177	0.018	0.047	0.031	0.052	0.052	0.013	0.010	0.008
Substream: TOTAL													
Total Flow (t/h)	30.6	581.0	83.3	309.5	191.1	38.1	100.2	67.5	110.4	110.4	47.5	35.0	27.0
Enthalpy (kW)	-4.67E+04	-8.87E+05	7.07E+05	-8.15E+05	-2.47E+05	-1.23E-12	-3.24E-12	-1.97E-12	5.88E+05	5.88E+05	-2.09E+05	-1.26E+05	-1.19E+05
Substream: NCPSD													
Mass Flow (t/h)													
Ash	0	0	7.257	0	0	0	0	0	7.257	7.257	0	0	0
Mass Fraction													
Ash	0	0	1.000	0	0	0	0	0	1.000	1.000	0	0	0
Total Flow (t/h)	0	0	7.257	0	0	0	0	0	7.257	7.257	0	0	0
Temperature (°C)			25.0						26.2	27.7			
Pressure (bar)	24.0		1.013	1.000	1.000	1.000	1.013	1.013	1.000	42.4	1.000	14.0	1.013
Vapor Fraction			0						0	0			
Liquid Fraction			0						0	0			
Solid Fraction			1.000						1.000	1.000			

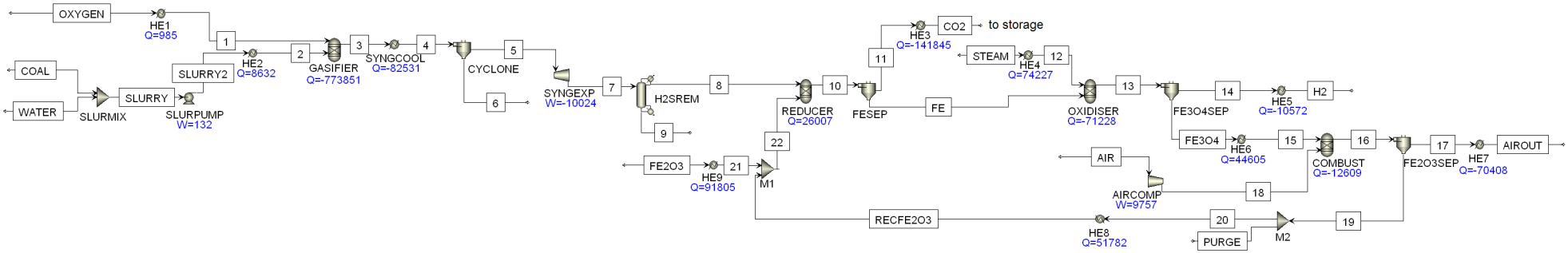

Q: Heat duty (kW)
W: Power (kW)

Figure A1.5: Coal gasification with syngas chemical looping (Case E).

Table A1.5: Stream results for Case E.

Stream No.	1	2	3	4	5	6	7	8	9	10	11	12
Phase	VAPOUR	MIXED	VAPOUR	VAPOUR	VAPOUR	SOLID	VAPOUR	VAPOUR	VAPOUR	VAPOUR	VAPOUR	VAPOUR
Substream: MIXED												
Mole Flow (kmol/s)												
S	0	0.025	1.03E-07	1.03E-07	1.03E-07	0	1.03E-07	0	0	0	0	1.03E-07
O_2	0.548	0.064	1.50E-12	1.50E-12	1.50E-12	0	1.50E-12	1.50E-12	0	0	0	0
N_2	0.007	0.009	0.016	0.016	0.016	0	0.016	0.016	0	0.016	0.016	0
H_2	0	0.537	0.664	0.664	0.664	0	0.664	0.664	0	0	0	0
H_2O	0	0.571	0.420	0.420	0.420	0	0.420	0.420	1.456	1.081	1.081	0
CO	0	0	0.981	0.981	0.981	0	0.981	0.981	0	0	0	0
CO_2	0	0	0.195	0.195	0.195	0	0.195	0.195	0	1.175	1.175	0
H_2S	0	0	0.023	0.023	0.023	0	0.023	0	0	0	0	0.023
C	0	1.179	2.78E-18	2.78E-18	2.78E-18	0	2.78E-18	0	0	0	0	0
CH_4	0	0	6.31E-04	6.31E-04	6.31E-04	0	6.31E-04	6.31E-04	0	0.002	0.002	0
Cl_2	0	2.58E-04	2.58E-04	2.58E-04	2.58E-04	0	2.58E-04	0	0	0	0	2.58E-04
COS	0	0	0.002	0.002	0.002	0	0.002	0	0	0	0	0.002
Ar	0.026	0	0.026	0.026	0.026	0	0.026	0.026	0	0.026	0.026	0
Total Flow (kmol/s)	0.581	2.385	2.328	2.328	2.328	0	2.328	2.304	1.456	2.301	2.301	0.025
Total Flow (t/h)	67.5	103.1	170.6	170.6	170.6	0	170.6	167.4	94.4	261.8	261.8	3.224
Total Flow (m^3/s)	0.366	0.485	4.244	1.815	1.815	0	3.692	3.653	2.124	7.798	7.798	0.039
Temperature (°C)	83.3	121.1	1371.1	430.0	430.0		299.0	299.0	232.2	950.0	950.0	299.0
Pressure (bar)	47.0	42.4	75.0	75.0	75.0		30.0	30.0	28.8	30.0	30.0	30.0
Vapor Fraction	1.000	0.256	1.000	1.000	1.000		1.000	1.000	1.000	1.000	1.000	1.000
Liquid Fraction	0	0.744	0	0	0		0	0	0	0	0	0
Solid Fraction	0	0	0	0	0		0	0	0	0	0	0
Enthalpy (J/kg)	5.25E+04	2.09E+07	-3.75E+06	-5.44E+06	-5.44E+06		-5.65E+06	-5.75E+06	-1.30E+07	-8.67E+06	-8.67E+06	-4.91E+05
Entropy (J/kg-K)	-762.9	3.28E+04	3138.9	1630.8	1630.8		1672.4	1656.8	-3003.8	581.7	581.7	1207.4
Density (kg/m^3)	51.2	59.1	11.2	26.1	26.1		12.8	12.7	12.3	9.326	9.326	22.7
Average Molecular Weight	32.3	12.0	20.4	20.4	20.4		20.4	20.2	18.0	31.6	31.6	36.0
Liquid Volumetric Flow 60°F (m^3/s)	0.031	0.052	0.110	0.110	0.110	0	0.110	0.108	0.026	0.085	0.085	0.001
Substream: TOTAL												
Total Flow (t/h)	67.5	110.4	177.9	177.9	170.6	7.257	170.6	167.4	94.4	482.4	261.8	3.224
Enthalpy (kW)	985.5	5.97E+05	-1.76E+05	-2.59E+05	-2.58E+05	-895.9	-2.68E+05	-2.67E+05	-3.42E+05	-6.01E+05	-6.31E+05	-439.9
Substream: CIPSD												
Mole Flow (kmol/s)												
Fe_2O_3	0	0	0	0	0	0	0	0	0	0.002	0	0
Fe	0	0	0	0	0	0	0	0	0	1.093	0	0
Fe_3O_4	0	0	0	0	0	0	0	0	0	0	0	0
Total Flow (kmol/s)	0	0	0	0	0	0	0	0	0	1.094	0	0
Total Flow (t/h)	0	0	0	0	0	0	0	0	0	220.6	0	0
Temperature (°C)										950.0		
Pressure (bar)	47.0	42.4		75.0			30.0	30.0	28.8	30.0		30.0
Vapor Fraction										0		
Liquid Fraction										0		
Solid Fraction										1.000		
Enthalpy (J/kg)										4.83E+05		
Entropy (J/kg-K)										739.6		
Density (kg/m^3)										7514.1		
Average Molecular Weight										56.0		
Substream: NCPSD												
Mass Flow (t/h)												
Ash	0	7.257	7.257	7.257	0	7.257	0	0	0	0	0	0
Mass Fraction												
Ash	0	1.000	1.000	1.000	0	1.000	0	0	0	0	0	0
Total Flow (t/h)	0	7.257	7.257	7.257	0	7.257	0	0	0	0	0	0
Temperature (°C)		121.1	1371.1	430.0		430.0						
Pressure (bar)	47	42.4	75	75		75	30	30	28.8			30
Vapor Fraction		0	0	0		0						
Liquid Fraction		0	0	0		0						
Solid Fraction		1	1	1		1						

Table A1.5 (con't)

Stream No.	13	14	15	16	17	18	19	20	21	22	AIR	AIROUT
Phase	VAPOUR	VAPOUR	SOLID	VAPOUR	SOLID	VAPOUR	SOLID	SOLID	SOLID	SOLID	VAPOUR	VAPOUR
Substream: MIXED												
Mole Flow (kmol/s)												
S	0	0	0	0	0	0	0	0	0	0	0	0
O_2	0	0	0	0.020	0.020	0.126	0	0	0	0	0.126	0.020
N_2	0	0	0	0.474	0.474	0.474	0	0	0	0	0.474	0.474
H_2	1.427	1.427	0	0	0	0	0	0	0	0	0	0
H_2O	0.029	0.029	0	0	0	0	0	0	0	0	0	0
CO	0	0	0	0	0	0	0	0	0	0	0	0
CO_2	0	0	0	0	0	0	0	0	0	0	0	0
H_2S	0	0	0	0	0	0	0	0	0	0	0	0
C	0	0	0	0	0	0	0	0	0	0	0	0
CH_4	0	0	0	0	0	0	0	0	0	0	0	0
Cl_2	0	0	0	0	0	0	0	0	0	0	0	0
COS	0	0	0	0	0	0	0	0	0	0	0	0
Ar	0	0	0	0	0	0	0	0	0	0	0	0
Total Flow (kmol/s)	1.456	1.456	0	0.494	0.494	0.600	0	0	0	0	0.600	0.494
Total Flow (t/h)	12.3	12.3	0	50.1	50.1	62.3	0	0	0	0	62.3	50.1
Total Flow (m^3/s)	2.111	2.111	0	1.645		1.259	0	0	0	0	14.7	0.415
Temperature (°C)	250.0	250.0		1049.4	527.1	559.7					25.0	30.0
Pressure (bar)	30.0	30.0	30.0	33.0	30.0	33.0		30.0	30.0	30.0	1.013	30.0
Vapor Fraction	1.000	1.000		1.000	0	1.000					1.000	1.000
Liquid Fraction	0	0		0	0	0					0	0
Solid Fraction	0	0		0	1.000	0					0	0
Enthalpy (J/kg)	7.33E+05	7.33E+05		1.15E+06	5.07E+06	5.64E+05					1.77E-10	5171.0
Entropy (J/kg-K)	-5046.2	-5046.2		655.0	9320.2	218.0					148.2	-933.1
Density (kg/m^3)	1.613	1.613		8.455		13.7					1.179	33.5
Average Molecular Weight	2.338	2.338		28.2	28.2	28.9					28.9	28.2
Liquid Volumetric Flow 60°F (m^3/s)	0.077	0.077	0	0.026	0.026	0.032	0	0	0	0	0.032	0.026
Substream: TOTAL												
Total Flow (t/h)	315.1	12.3	302.8	365.1	50.1	62.3	315.0	299.3	315.0	315.0	62.3	50.1
Enthalpy (kW)	-3.83E+05	2497.0	-3.41E+05	-3.44E+05	7.05E+04	9756.5	-4.15E+05	-3.94E+05	-3.60E+05	-3.60E+05	3.06E-12	71.9
Substream: CIPSD												
Mole Flow (kmol/s)												
Fe_2O_3	0	0	0	0.548	0	0	0.548	0.521	0.548	0.548	0	0
Fe	0.022	0	0.022	0	0	0	0	0	0	0	0	0
Fe_3O_4	0.358	0	0.358	0	0	0	0	0	0	0	0	0
Total Flow (kmol/s)	0.380	0	0.380	0.548	0	0	0.548	0.521	0.548	0.548	0	0
Total Flow (t/h)	302.8	0	302.8	315.0	0	0	315.0	299.3	315.0	315.0	0	0
Temperature (°C)	250.0		800.0	1049.4			527.1	527.1	1049.4	1049.8		
Pressure (bar)	30.0		30.0	33.0		33.0	30.0	30.0	30.0	30.0	1.013	30.0
Vapor Fraction	0		0	0			0	0	0	0		
Liquid Fraction	0		0	0			0	0	0	0		
Solid Fraction	1.000		1.000	1.000			1.000	1.000	1.000	1.000		
Enthalpy (J/kg)	-4.59E+06		-4.06E+06	-4.11E+06			-4.74E+06	-4.74E+06	-4.11E+06	-4.11E+06		
Entropy (J/kg-K)	-1050.2		-351.3	-319.7			-908.7	-908.7	-319.7	-319.3		
Density (kg/m^3)	5226.8		5225.5	1037.3			3139.2	3139.2	1037.3	1035.7		
Average Molecular Weight	221.2		221.2	159.7			159.7	159.7	159.7	159.7		
Substream: NCPSD												
Mass Flow (t/h)												
Ash	0	0	0	0	0	0	0	0	0	0	0	0
Mass Fraction												
Ash	0	0	0	0	0	0	0	0	0	0	0	0
Total Flow (t/h)	0	0	0	0	0	0	0	0	0	0	0	0
Temperature (°C)												
Pressure (bar)			30			33		30	30	30	1.013	30
Vapor Fraction												
Liquid Fraction												
Solid Fraction												

Table A1.5 (con't)

Stream No.	COAL	CO2	FE	FE2O3	FE3O4	H2	OXYGEN	PURGE	RECFE2O3	SLURRY	SLURRY2	STEAM	WATER
Phase	MIXED	MIXED	SOLID	SOLID	SOLID	MIXED	VAPOUR	SOLID	SOLID	LIQUID	LIQUID	LIQUID	LIQUID
Substream: MIXED													
Mole Flow (kmol/s)													
S	0.025	0	0	0	0	0	0	0	0	0.025	0.025	0	0
O_2	0.064	0	0	0	0	0	0.548	0	0	0.064	0.064	0	0
N_2	0.009	0.016	0	0	0	0	0.007	0	0	0.009	0.009	0	0
H_2	0.537	0	0	0	0	1.427	0	0	0	0.537	0.537	0	0
H_2O	0.155	1.081	0	0	0	0.029	0	0	0	0.571	0.571	1.456	0.417
CO	0	0	0	0	0	0	0	0	0	0	0	0	0
CO_2	0	1.175	0	0	0	0	0	0	0	0	0	0	0
H_2S	0	0	0	0	0	0	0	0	0	0	0	0	0
C	1.179	0	0	0	0	0	0	0	0	1.179	1.179	0	0
CH_4	0	0.002	0	0	0	0	0	0	0	0	0	0	0
Cl_2	2.58E-04	0	0	0	0	0	0	0	0	2.58E-04	2.58E-04	0	0
COS	0	0	0	0	0	0	0	0	0	0	0	0	0
Ar	0	0.026	0	0	0	0	0.026	0	0	0	0	0	0
Total Flow (kmol/s)	1.968	2.301	0	0	0	1.456	0.581	0	0	2.385	2.385	1.456	0.417
Total Flow (t/h)	76.1	261.8	0	0	0	12.3	67.5	0	0	103.1	103.1	94.4	27.0
Total Flow (m^3/s)	15.0	0.499	0	0	0	1.201	14.2	0	0	0.029	0.029	0.026	0.008
Temperature (°C)	25.0	30.0		25.0		30.0	25.0			26.2	27.7	25.0	25.0
Pressure (bar)	1.013	30.0		30.0		30.0	1.013	30.0	30.0	1.000	42.4	28.8	1.013
Vapor Fraction	0.311	0.234		0		0.981	1.000			0	0	0	0
Liquid Fraction	0.689	0.766		0		0.019	0			1.000	1.000	1.000	1.000
Solid Fraction	0	0		1.000		0	0			0	0	0	0
Enthalpy (J/kg)	3.35E+07	-1.06E+07				-2.37E+06	-1.05E-10			2.06E+07	2.06E+07	-1.59E+07	-1.59E+07
Entropy (J/kg-K)	6.21E+04	-2812.2				-1.29E+04	63.6			4.22E+04	4.20E+04	-9030.5	-9030.5
Density (kg/m^3)	1.411	145.8				2.835	1.320			999.2	998.2	993.5	993.5
Average Molecular Weight	10.7	31.6		53.1		2.338	32.3			12.0	12.0	18.0	18.0
Liquid Volumetric Flow 60°F (m^3/s)	0.045	0.085	0	0	0	0.077	0.031	0	0	0.052	0.052	0.026	0.008
Substream: TOTAL													
Total Flow (t/h)	83.3	261.8	220.6	315.0	302.8	12.3	67.5	15.8	299.3	110.4	110.4	94.4	27.0
Enthalpy (kW)	7.07E+05	-7.73E+05	2.96E+04	-4.52E+05	-3.86E+05	-8075.2	-1.97E-12	-2.07E+04	-3.42E+05	5.88E+05	5.88E+05	-4.16E+05	-1.19E+05
Substream: CIPSD													
Mole Flow (kmol/s)													
Fe_2O_3	0	0	0.002	0.548	0	0	0	0.027	0.521	0	0	0	0
Fe	0	0	1.093	0	0.022	0	0	0	0	0	0	0	0
Fe_3O_4	0	0	0	0	0.358	0	0	0	0	0	0	0	0
Total Flow (kmol/s)	0	0	1.094	0.548	0.380	0	0	0.027	0.521	0	0	0	0
Total Flow (t/h)	0	0	220.6	315.0	302.8	0	0	15.8	299.3	0	0	0	0
Temperature (°C)			950.0	25.0	250.0			527.1	1049.4				
Pressure (bar)	1.013	30.0	30.0	30.0	30.0	30.0	1.013	30.0	30.0	1.000	42.4	28.8	1.013
Vapor Fraction			0	0	0			0	0				
Liquid Fraction			0	0	0			0	0				
Solid Fraction			1.000	1.000	1.000			1.000	1.000				
Enthalpy (J/kg)			4.83E+05	-5.16E+06	-4.59E+06			-4.74E+06	-4.11E+06				
Entropy (J/kg-K)			739.6	-1721.3	-1050.2			-908.7	-319.7				
Density (kg/m^3)			7514.1	5159.8	5226.8			3139.2	1037.3				
Average Molecular Weight			56.0	159.7	221.2			159.7	159.7				
Substream: NCPSD													
Mass Flow (t/h)													
Ash	7.257	0	0	0	0	0	0	0	0	7.257	7.257	0	0
Mass Fraction													
Ash	1.000	0	0	0	0	0	0	0	0	1.000	1.000	0	0
Total Flow (t/h)	7.257	0	0	0	0	0	0	0	0	7.257	7.257	0	0
Temperature (°C)	25.0									26.2	27.7		
Pressure (bar)	1.013	30		30		30	1.013	30	30	1	42.4	28.8	1.013
Vapor Fraction	0									0	0		
Liquid Fraction	0									0	0		
Solid Fraction	1									1	1		

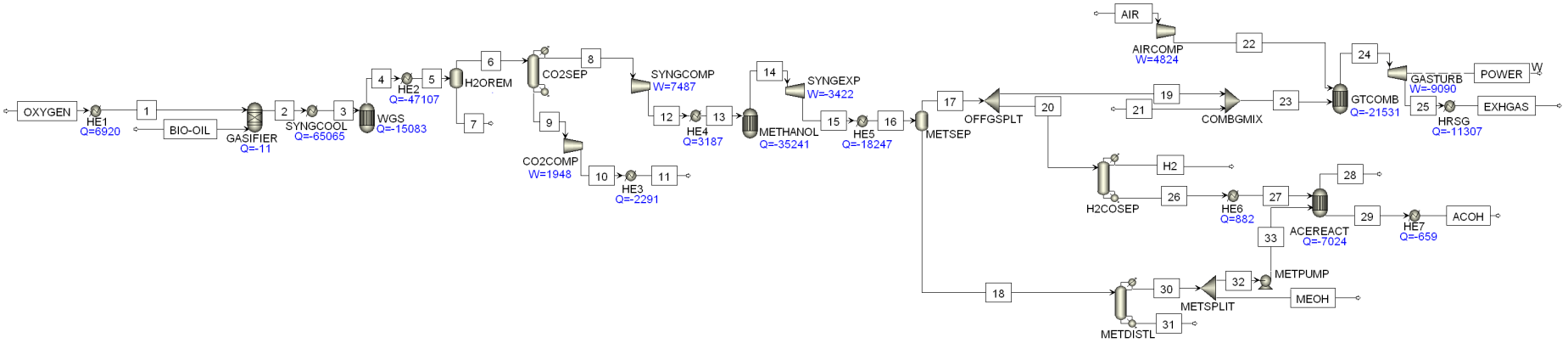

Q: Heat duty (kW)
W: Power (kW)

Figure A1.6: Bio-oil polygeneration system with CCS (Scheme E).

Table A1.6: Stream results for Scheme E.

Stream No.	1	2	3	4	5	6	7	8	9	10	11	12	13	14
Phase	VAPOUR	VAPOUR	VAPOUR	VAPOUR	MIXED	VAPOUR	LIQUID	MIXED	VAPOUR	VAPOUR	VAPOUR	VAPOUR	VAPOUR	VAPOUR
Substream: MIXED														
Mole Flow (kmol/s)														
CH_3COOH / acetic acid	0	2.66E-10	2.66E-10	2.66E-10	2.66E-10	5.61E-12	2.61E-10	5.61E-12	0	0	0	5.61E-12	5.61E-12	5.61E-12
$CH_3C(O)CH_2OH$ / acetol	0	1.12E-17	1.12E-17	0	0	0	0	0	0	0	0	0	0	0
$C_6H_4(OH)(OCH_3)$ / guaiacol	0	0	0	0	0	0	0	0	0	0	0	0	0	0
O_2	0.485	7.56E-15	7.56E-15	7.56E-15	7.56E-15	7.53E-15	2.68E-17	7.53E-15	0	0	0	7.53E-15	7.53E-15	7.53E-15
N_2	0	0	0	0	0	0	0	0	0	0	0	0	0	0
H_2	0	0.808	0.808	1.209	1.209	1.209	2.95E-04	1.209	0	0	0	1.209	1.209	0.494
H_2O	0	0.663	0.663	0.262	0.262	0.009	0.253	0.009	0	0	0	0.009	0.009	0.008
CO	0	0.838	0.838	0.437	0.437	0.435	0.001	0.435	0	0	0	0.435	0.435	0.076
CO_2	0	0.327	0.327	0.728	0.728	0.705	0.023	0.106	0.5991576	0.599	0.599	0.106	0.106	0.107
C	0	6.25E-22	6.25E-22	0	0	0	0	0	0	0	0	0	0	0
CH_4	0	0.002	0.002	0.002	0.002	0.002	1.21E-05	0.002	0	0	0	0.002	0.002	0.002
CH_3OH	0	6.28E-08	6.28E-08	6.28E-08	6.28E-08	1.38E-08	4.90E-08	1.38E-08	0	0	0	1.38E-08	1.38E-08	0.358
Total Flow (kmol/s)	0.485	2.637	2.637	2.637	2.637	2.360	0.277	1.761	0.599	0.599	0.599	1.761	1.761	1.045
Total Flow (t/h)	55.9	185.2	185.2	185.2	185.2	165.0	20.1	70.1	94.9	94.9	94.9	70.1	70.1	70.1
Total Flow (m^3/s)	1.013	10.1	5.285	5.285	2.119	2.114	0.006	1.575	0.537	0.252	0.192	0.679	0.766	0.454
Temperature (°C)	480.0	1112.0	450.0	450.0	50.0	50.0	50.0	50.0	50.0	130.8	35.0	190.4	250.0	250.0
Pressure (bar)	30.0	30.0	30.0	30.0	30.0	30.0	30.0	30.0	30.0	80.0	80.0	100.0	100.0	100.0
Vapor Fraction	1.000	1.000	1.000	1.000	0.895	1.000	0	0.999	1.000	1.000	1.000	1.000	1.000	1.000
Liquid Fraction	0	0	0	0	0.105	0	1.000	0.001	0	0	0	0	0	0
Solid Fraction	0	0	0	0	0	0	0	0	0	0	0	0	0	0
Enthalpy (J/kg)	4.46E+05	-5.43E+06	-6.70E+06	-6.99E+06	-7.91E+06	-7.11E+06	-1.45E+07	-4.66E+06	-8.92E+06	-8.85E+06	-8.93E+06	-4.28E+06	-4.11E+06	-5.92E+06
Entropy (J/kg-K)	17.6	2742.3	1509.3	1196.6	-764.9	7.698	-7098.2	246.4	-505.3	-486.8	-731.7	330.6	662.7	-2403.0
Density (kg/m^3)	15.3	5.081	9.732	9.732	24.3	21.7	993.3	12.4	49.1	104.8	137.4	28.7	25.4	42.9
Average Molecular Weight	32.0	19.5	19.5	19.5	19.5	19.4	20.2	11.1	44.0	44.0	44.0	11.1	11.1	18.6
Liquid Volumetric Flow 60°F (m^3/s)	0.026	0.118	0.118	0.132	0.132	0.126	0.006	0.094	0.032	0.032	0.032	0.094	0.094	0.051
Substream: TOTAL														
Total Flow (t/h)	55.9	185.2	185.2	185.2	185.2	165.0	20.1	70.1	94.9	94.9	94.9	70.1	70.1	70.1
Enthalpy (kW)	6920.0	-2.80E+05	-3.45E+05	-3.60E+05	-4.07E+05	-3.26E+05	-8.09E+04	-9.08E+04	-2.35E+05	-2.33E+05	-2.36E+05	-8.33E+04	-8.01E+04	-1.15E+05

Table A1.6 (con't)

Stream No.	15	16	17	18	19	20	21	22	23	24	25	26	27	28
Phase	VAPOUR	MIXED	VAPOUR	LIQUID	VAPOUR	VAPOUR	VAPOUR	VAPOUR	VAPOUR	VAPOUR	VAPOUR	MIXED	VAPOUR	VAPOUR
Substream: MIXED														
Mole Flow (kmol/s)														
CH_3COOH / acetic acid	5.61E-12	5.61E-12	1.14E-14	5.60E-12	1.14E-15	1.03E-14	0	0	1.14E-15	1.14E-15	1.14E-15	1.03E-14	1.03E-14	0.006
$CH_3C(O)CH_2OH$ / acetol	0	0	0	0	0	0	0	0	0	0	0	0	0	0
$C_6H_4(OH)(OCH_3)$ / guaiacol	0	0	0	0	0	0	0	0	0	0	0	0	0	0
O_2	7.53E-15	7.53E-15	7.43E-15	1.09E-16	7.43E-16	6.68E-15	0	0.095	7.43E-16	0.006	0.006	6.68E-15	6.68E-15	6.60E-15
N_2	0	0	0	0	0	0	0	0.356	0	0.356	0.356	0	0	0
H_2	0.494	0.494	0.494	4.58E-04	0.049	0.444	0	0	0.049	3.66E-07	3.66E-07	0	0	0
H_2O	0.008	0.008	6.54E-05	0.008	6.54E-06	5.88E-05	0	0	6.54E-06	0.110	0.110	5.88E-05	5.88E-05	1.07E-05
CO	0.076	0.076	0.075	9.71E-04	0.008	0.068	0	0	0.008	3.86E-07	3.86E-07	0.068	0.068	8.81E-10
CO_2	0.107	0.107	0.093	0.014	0.009	0.084	0	0	0.009	0.047	0.047	0.084	0.084	0.080
C	0	0	0	0	0	0	0	0	0	0	0	0	0	0
CH_4	0.002	0.002	0.002	4.97E-05	1.63E-04	0.001	0.03	0	0.030	0	0	0.001	0.001	0.001
CH_3OH	0.358	0.358	0.009	0.349	9.31E-04	0.008	0	0	9.31E-04	9.31E-04	9.31E-04	0.008	0.008	0.003
Total Flow (kmol/s)	1.045	1.045	0.673	0.372	0.067	0.606	0.030	0.450	0.097	0.519	0.519	0.161	0.161	0.091
Total Flow (t/h)	70.1	70.1	27.1	43.0	2.709	24.4	1.733	46.7	4.442	51.2	51.2	21.2	21.2	14.5
Total Flow (m^3/s)	0.962	0.746	0.730	0.015	0.073	0.657	0.734	1.756	0.178	4.539	21.9	0.167	0.189	0.106
Temperature (°C)	169.9	40.0	40.0	40.0	40.0	40.0	25.0	383.9	34.8	1200.0	742.1	40.0	150.0	150.0
Pressure (bar)	40.0	24.0	24.0	24.0	24.0	24.0	1.013	14.0	14.0	14.0	2.000	24.0	30.0	30.0
Vapor Fraction	1.000	0.644	1.000	0	1.000	1.000	1.000	1.000	1.000	1.000	1.000	0.952	1.000	1.000
Liquid Fraction	0	0.356	0	1.000	0	0	0	0	0	0	0	0.048	0	0
Solid Fraction	0	0	0	0	0	0	0	0	0	0	0	0	0	0
Enthalpy (J/kg)	-6.10E+06	-7.04E+06	-6.20E+06	-7.56E+06	-6.20E+06	-6.20E+06	-4.65E+06	3.72E+05	-5.59E+06	-1.66E+06	-2.30E+06	-7.22E+06	-7.07E+06	-8.57E+06
Entropy (J/kg-K)	-2358.5	-4599.4	-859.0	-6955.1	-859.0	-859.0	-5023.8	206.3	-2371.0	1120.8	1192.7	273.6	643.3	-584.6
Density (kg/m^3)	20.2	26.1	10.3	781.8	10.3	10.3	0.656	7.393	6.932	3.132	0.649	35.2	31.0	37.8
Average Molecular Weight	18.6	18.6	11.2	32.2	11.2	11.2	16.0	28.9	12.7	27.4	27.4	36.4	36.4	44.3
Liquid Volumetric Flow 60°F (m^3/s)	0.051	0.051	0.036	0.015	0.004	0.032	0.002	0.024	0.005	0.024	0.024	0.009	0.009	0.005
Substream: TOTAL														
Total Flow (t/h)	70.1	70.1	27.1	43.0	2.709	24.4	1.733	46.7	4.442	51.2	51.2	21.2	21.2	14.5
Enthalpy (kW)	-1.19E+05	-1.37E+05	-4.66E+04	-9.04E+04	-4663.9	-4.20E+04	-2235.6	4823.9	-6899.5	-2.36E+04	-3.27E+04	-4.24E+04	-4.15E+04	-3.44E+04

Table A1.6 (con't)

Stream No.	29	30	31	32	33	ACOH	AIR	BIO-OIL	EXHGAS	H2	MEOH	OXYGEN
Phase	LIQUID	LIQUID	MIXED	LIQUID	LIQUID	LIQUID	VAPOUR	LIQUID	VAPOUR	VAPOUR	LIQUID	VAPOUR
Substream: MIXED												
Mole Flow (kmol/s)												
CH_3COOH / acetic acid	0.062	0	5.60E-12	0	0	0.062	0	0.097	1.14E-15	0	0	0
$CH_3C(O)CH_2OH$ / acetol	0	0	0	0	0	0	0	0.097	0	0	0	0
$C_6H_4(OH)(OCH_3)$ / guaiacol	0	0	0	0	0	0	0	0.097	0	0	0	0
O_2	0	0	0	0	0	0	0.095	0	0.006	0	0	0.485
N_2	0	0	0	0	0	0	0.356	0	0.356	0	0	0
H_2	0	0	4.58E-04	0	0	0	0	0	3.66E-07	0.444	0	0
H_2O	4.81E-05	0	0.008	0	0	4.81E-05	0	0.600	0.110	0	0	0
CO	1.03E-11	0	9.71E-04	0	0	1.03E-11	0	0	3.86E-07	0	0	0
CO_2	0.004	0	0.014	0	0	0.004	0	0	0.047	0	0	0
C	0	0	0	0	0	0	0	0	0	0	0	0
CH_4	3.06E-05	0	4.97E-05	0	0	3.06E-05	0	0	0	0	0	0
CH_3OH	0.008	0.347	0.002	0.070	0.070	0.008	0	0	9.31E-04	0	0.277	0
Total Flow (kmol/s)	0.073	0.347	0.025	0.070	0.070	0.073	0.450	0.892	0.519	0.444	0.277	0.485
Total Flow (t/h)	14.8	40.0	2.999	8.075	8.075	14.8	46.7	129.3	51.2	3.225	31.9	55.9
Total Flow (m^3/s)	0.005	0.014	0.014	0.003	0.003	0.004	11.0	0.033	15.9	0.482	0.011	12.0
Temperature (°C)	150.0	40.0	40.0	40.0	40.3	30.0	25.0	25.0	100.0	40.0	40.0	25.0
Pressure (bar)	30.0	24.0	24.0	24.0	30.0	30.0	1.013	1.013	1.013	24.0	24.0	1.000
Vapor Fraction	0	0	0.498	0	0	0	1.000	0	1.000	1.000	0	1.000
Liquid Fraction	1.000	1.000	0.502	1.000	1.000	1.000	0	1.000	0	0	1.000	0
Solid Fraction	0	0	0	0	0	0	0	0	0	0	0	0
Enthalpy (J/kg)	-7.49E+06	-7.40E+06	-9.78E+06	-7.40E+06	-7.40E+06	-7.65E+06	1.77E-10	-7.98E+06	-3.10E+06	2.14E+05	-7.40E+06	-1.16E-10
Entropy (J/kg-K)	-3832.9	-7362.5	-2130.9	-7362.5	-7359.9	-4026.7	148.2	-5731.8	176.0	-1.24E+04	-7362.5	3.420
Density (kg/m^3)	859.6	774.8	60.8	774.8	774.5	1032.0	1.179	1085.8	0.895	1.858	774.8	1.291
Average Molecular Weight	56.3	32.0	33.7	32.0	32.0	56.3	28.9	40.3	27.4	2.016	32.0	32.0
Liquid Volumetric Flow 60°F (m^3/s)	0.004	0.014	0.001	0.003	0.003	0.004	0.024	0.034	0.024	0.024	0.011	0.026
Substream: TOTAL												
Total Flow (t/h)	14.8	40.0	2.999	8.075	8.075	14.8	46.7	129.3	51.2	3.225	31.9	55.9
Enthalpy (kW)	-3.07E+04	-8.22E+04	-8148.0	-1.66E+04	-1.66E+04	-3.14E+04	2.30E-12	-2.86E+05	-4.40E+04	192.1	-6.56E+04	-1.81E-12